



HAL
open science

Effectors of selectivity in laccase catalyzed reactions

Lu Ren

► **To cite this version:**

Lu Ren. Effectors of selectivity in laccase catalyzed reactions. Catalysis. Ecole Centrale Marseille, 2019. English. NNT: 2019ECDM0013 . tel-03080959

HAL Id: tel-03080959

<https://theses.hal.science/tel-03080959>

Submitted on 18 Dec 2020

HAL is a multi-disciplinary open access archive for the deposit and dissemination of scientific research documents, whether they are published or not. The documents may come from teaching and research institutions in France or abroad, or from public or private research centers.

L'archive ouverte pluridisciplinaire **HAL**, est destinée au dépôt et à la diffusion de documents scientifiques de niveau recherche, publiés ou non, émanant des établissements d'enseignement et de recherche français ou étrangers, des laboratoires publics ou privés.

École Doctorale – Sciences Chimiques ED250
Institut des sciences moléculaires de Marseille (iSm2)-BiosCienc

THÈSE DE DOCTORAT

pour obtenir le grade de
DOCTEUR de l'ÉCOLE CENTRALE de MARSEILLE

Discipline : Chimie

TITRE DE LA THÈSE :

Effectors of selectivity in laccase catalyzed reactions

Par

REN Lu

Directeur de thèse : Thierry TRON

Co-Directeur de thèse: Dr. Pierre ROUSSELOT-PAILLEY

Soutenue le 17 décembre 2019

devant le jury composé de :

Mme. Belèn ALBELA	Maître de conférences (École normale supérieure de Lyon)	Rapporteur
Mme. Christine CAVAZZA	Directrice de recherche (CEA Grenoble)	Rapporteur
Mme. Ling PENG	Directeur de Recherche CNRS (Aix-Marseille Université)	Examineur
M. Thierry TRON	Directeur de Recherche CNRS (Aix-Marseille Université)	Directeur de thèse
Mme. Karine HEUZE	Chargé de recherche CNRS (Université de Bordeaux)	Invitée
M. Pierre ROUSSELOT-PAILLEY	Chargé de recherche CNRS (Aix-Marseille Université)	Co-directeur de thèse, Invitée

To my motherland,

Much distress regenerates a nation,

May we defeat the 2019 novel coronavirus soon.

École Doctorale – Sciences Chimiques ED250
Institut des sciences moléculaires de Marseille (iSm2)-BiosCiencs

THÈSE DE DOCTORAT

pour obtenir le grade de
DOCTEUR de l'ÉCOLE CENTRALE de MARSEILLE

Discipline : Chimie

TITRE DE LA THÈSE :

Effectors of selectivity in laccase catalyzed reactions

Par

REN Lu

Directeur de thèse : Thierry TRON

Co-Directeur de thèse: Dr. Pierre ROUSSELOT-PAILLEY

Soutenue le 17 décembre 2019

devant le jury composé de :

Mme. Belèn ALBELA	Maître de conférences (École normale supérieure de Lyon)	Rapporteur
Mme. Christine CAVAZZA	Directrice de recherche (CEA Grenoble Center)	Rapporteur
Mme. Ling PENG	Directeur de Recherche CNRS (Aix-Marseille Université)	Examineur
M. Thierry TRON	Directeur de Recherche CNRS (Aix-Marseille Université)	Directeur de thèse
Mme. Karine HEUZE	Chargé de recherche CNRS (Université de Bordeaux)	Invitée
M. Pierre ROUSSELOT-PAILLEY	Chargé de recherche CNRS (Aix-Marseille Université)	Co-directeur de thèse, Invitée

ACKNOWLEDGEMENTS

The completion of the challenge for a doctoral degree, apart from my personal endeavor, would not be possible without the continuous help and encouragement from the people mentally or spatially around me. I would like to express my gratitude to them.

First, I would like to give my great thanks to professor Marius REGLIER. About four years ago, he seriously forwarded my email about PhD position inquiry to professor Thierry TRON, which indirectly gave me the opportunity to work in *Institute des Sciences Moléculaires de Marseille* (ISM2). And it is the beginning of all the story.

I also owe my deepest gratitude to my supervisor, professor Thierry TRON. I thank him for his professional advice and guidance during my research. Throughout these three years, he encouraged me countless times when I did not obtain the desired experiment results and doubted myself. I am especially grateful for him in believing in me, motivating me to be a real scientist.

My sincere gratitude extends to my co-supervisor Dr. Pierre Rousselot-PAILLEY, for his important help during the whole process of my PhD. He actively helped me solving the problems I encountered in the project and trained me with great patience in the experimental operation, I really appreciated his tolerance and kindness to me.

I would like to express my sincere thanks to Dr. Yasmina MEKMOUCHE and Dr. Simeng ZHOU, for their active participation in the discussions of my topic and providing valuable advice to my research. They shared me with their energy, which made me never give up.

Many thanks and greetings to my colleagues in the lab ISM2 BiosCiences. I particularly thank Dr. MARESCA Marc for his advice on ELISA; thank Dr. FAURE Bruno for his technical support of the FTIR machine and other equipment, thank Dr. Viviane ROBERT, Ms. Agnes AMOURIC, Ms. Elise COURVOISIER-DEZORD and Ms. Yolande CHARMASSON for helping me in the culture of *Pichia pastoris* during *AtDIR6* production, thank Dr. Michael LAFOND and Dr. Christophe DECROOS for their guidance and discussions on the purification of *AtDIR6*, as well as the use of FPLC, Maybe I can't list here all the people and the good things they have done for me, but I will always remember their selfless and patient help.

My thanks also go to my officemates for the friendship and enjoyment they provided to me. Especially Ms. Alessia MUNZONE, she was always willing to help me either in the specialist area or in life with pressure, I regard her as one of my best friends.

I acknowledge the hospitality of Dr. Karine HEUZE during my stay in Bordeaux. I thank her and her PhD student Mr. HongTao JI for their help in providing magnetic particles for my experiment and helping us to do a series of characterizations of the particles.

Sincere appreciation is also acknowledged to my thesis committee: Professor Christine CAVAZZA, Professor Belèn ALBELA, Professor Ling PENG, for their insightful comments and kind encouragement.

The deepest gratitude to my most loyal friends around me in France, including Mr. Jie ZHANG, Ms. Dan FENG, Ms. Fangfang YANG, Ms. Xiaoxi PAN, Ms. Wenjing YANG, Ms. Lan YANG, Ms. Qi WANG, Mr. Rui LIU, Mr. Lingyu KONG, Mr. Guochao GAO, Mr. Jian YANG and forth. They have offered me invaluable help both in my academic and casual life, we shared the joys and sorrows in Marseille. I am thankful to their companion and encouragement, tolerance and patience along the way. The days we struggle together will be remembered forever.

My PhD study would not be possible without the unconditional support of my loved families, I really thank them for understanding my will to pursue my dream, and for forgiving me for being absent in each of the full moon days for three years, while these special days, I should be there with them.

Last but not least, the financial support provided by the Chinese Scholarship Council (China) is gratefully acknowledged.

Résumé

Aujourd'hui la nécessité d'un développement durable de la société humaine et les problèmes écologiques, environnementaux et économiques associés ont suscité une inquiétude généralisée au sein de la communauté internationale. Par conséquent, une grande attention est accordée à la chimie verte, aux technologies propres et aux processus respectueux de l'environnement. L'économie respectueuse de l'environnement devient le principal moteur de l'innovation technologique, qui pose de nouveaux défis à la chimie, en particulier la chimie de synthèse.

Des réglementations plus strictes ont été introduites pour protéger l'environnement par les gouvernements du monde entier, incitant l'industrie chimique à se concentrer sur l'élimination ou la réduction de la production de déchets à la source. Cela entraînera inévitablement de nouvelles exigences pour la science et la technologie des produits chimiques et leurs processus de production.

L'un des moyens les plus importants d'atteindre ces objectifs est la catalyse, sous ces diverses formes allant de la catalyse chimique à la biocatalyse. Un processus catalytique est un processus qui augmente la vitesse d'une réaction chimique en ajoutant une substance appelée catalyseur, qui peut effectuer une réaction de façon répétée sans être consommée dans le processus.¹ Par conséquent, la catalyse est considérée comme un processus à forte économie d'atomes et est donc considérée comme verte.

La catalyse joue un rôle important dans la société moderne. Un bon exemple est l'évolution du processus de production de la lazabemide (un médicament contre la maladie de Parkinson) développé par F. Hoffmann-La Roche AG. Le processus de synthèse initial comprenait 8 étapes avec un rendement de 8%, le schéma de synthèse a été ramené à une étape en faisant appel à un catalyseur au palladium avec un rendement global de 65%.²

Jusqu'à présent, un grand nombre de types de catalyseurs sont utilisés dans le commerce, notamment des catalyseurs hétérogènes (solides poreux), des catalyseurs homogènes (dissous dans le mélange réactionnel liquide), des catalyseurs biologiques (sous forme d'enzymes).³ Respectueux de l'environnement, des exemples de catalyse combinant à la fois une catalyse hétérogène ou homogène et enzymatique sont apparus récemment. Les processus catalytiques verts impliquent que les processus chimiques soient rendus respectueux de l'environnement en tirant parti des rendements élevés et de la sélectivité possibles pour les produits cibles, avec peu ou pas de produits secondaires indésirables et aussi souvent une efficacité énergétique élevée.⁴

Vu la demande croissante de catalyse respectueuse de l'environnement, la biocatalyse est un élément incontournable. Le catalyseur (une enzyme) lui-même est fabriqué à partir de ressources renouvelables facilement disponibles, est biodégradable et non toxique.⁵ L'enzyme fonctionne dans des conditions douces (dans l'eau, à température ambiante et à pression atmosphérique), et ne génère

que peu de sous-produits.⁶ Ce modèle de développement durable, illustré par un processus catalysé par des enzymes, est exactement ce que recherche ce siècle.

Parmi toutes les enzymes possédant la capacité de fonctionner comme biocatalyseur dans l'industrie, la laccase est une enzyme particulièrement robuste qui a été largement utilisée dans diverses applications. Elle a fait l'objet d'une attention considérable de la part des chercheurs depuis 1883, et sa première description par un scientifique japonais dans la sécrétion laiteuse d'un arbre très commun au Japon appelé *Rhus vernicifera*.⁷ En fait, la laccase est un biocatalyseur utile pour une variété d'organismes en raison de sa grande capacité à oxyder de manière non spécifique de nombreux substrats et à utiliser l'oxygène moléculaire facilement disponible comme accepteur final d'électrons.⁸ Cependant, l'utilisation industrielle des laccases est limitée par divers facteurs. Par exemple, le processus de purification pour la production de laccase nécessite un temps relativement long et un investissement économique substantiel. De plus, la difficulté de séparation du mélange réactionnel après catalyse limite leur recyclabilité, entraînant une augmentation supplémentaire des coûts d'application. Par ailleurs, le potentiel redox des laccases ne leur permet pas de catalyser directement la dégradation de la plupart des substrats non phénoliques.⁹ Enfin, la réaction d'auto-couplage de l'intermédiaire radicalaire produit lors de l'oxydation par la laccase conduit à la formation de dimères ou de polymères,¹⁰ ce qui indique un manque de sélectivité et affecte négativement le potentiel applicatif de cette enzyme.

De nombreux travaux ont déjà été réalisés pour améliorer les performances de la laccase en tant que biocatalyseurs. Diverses techniques de culture ont été développées pour produire efficacement de la laccase à l'échelle industrielle.¹¹ Les rendements accrus et le processus de purification simplifié dans la production de laccase sont maintenant disponibles grâce au développement de systèmes d'expression hétérologues robustes, réduisant ainsi les coûts.¹² L'ingénierie des protéines offre le potentiel d'adapter les besoins spécifiques pour une conception efficace des biocatalyseurs.¹³ Par exemple, les systèmes laccase + médiateur redox (LMS) sont explorés pour aider l'action des laccases sur une gamme étendue de substrats allant des composés phénoliques aux composés non phénoliques.¹⁴ L'immobilisation de laccases sur des variétés de matériaux pour différentes applications permet la séparation et le recyclage, etc.¹⁵ Conférant des propriétés améliorées aux laccases, ces méthodes facilitent grandement l'application généralisée des laccases dans le domaine de la biochimie.

En raison de leur performance élevée pour des transformations chimiques allant de l'oxydation des groupes fonctionnels au couplage hétéromoléculaire pour la production de nouveaux dérivés d'antibiotiques, ou comme étape clé dans la synthèse de molécules complexes,¹⁶ les laccases ont trouvé des applications importantes en synthèse organique. Cependant, comme déjà mentionné, les réactions d'auto-couplage des intermédiaires radicalaires générés par les laccases forment

généralement un mélange de produits allant de dimères aux oligomères supérieurs, mettant en évidence le manque de sélectivité de l'enzyme. En fait, il s'agit d'un schéma dans lequel sans contrôle supplémentaire et/ou environnement physiologique spécial, des produits racémiques seront produits. Cette situation est clairement défavorable, notamment dans le domaine de la synthèse pharmaceutique où seule la forme physiologiquement active d'un produit ou médicament naturel est souhaitée, car les autres formes peuvent être inactives voire toxiques (un exemple malheureusement célèbre est celui de la thalidomide).¹⁷ L'obtention de substances sous forme optiquement pure est très importante pour la synthèse de médicaments pour éviter des procédures de séparation chirale ou l'utilisation d'un catalyseur chiral coûteux. De ce point de vue, la laccase est toujours confrontée au défi d'effectuer des réactions en plusieurs étapes avec une sélectivité élevée afin de réaliser des économies d'énergie et l'élimination des sous-produits indésirables.

Peu de travaux ont été consacrés à l'introduction d'une certaine sélectivité dans les réactions catalysées par la laccase. Le système médié par la laccase-TEMPO est connu pour être capable de catalyser l'oxydation régiosélective des groupes hydroxyles primaires des dérivés de sucres, permettant la fonctionnalisation de polymères.¹⁸ De plus, il a été rapporté qu'un changement de solvants peut avoir une grande influence sur la sélectivité de la réaction catalysée par la laccase (affinité du substrat, sélectivité ee, regio et chimio).¹⁹ Danieli et ses collègues ont décrit pour la première fois une influence significative et inattendue des solvants sur le rapport relatif de deux dimères obtenus lors du couplage oxydant des phénols catalysés par les laccases, qui donne de nouveaux indices pour l'application synthétique des laccases en biocatalyse.²⁰ Par ailleurs, depuis la fin du siècle dernier, une protéine végétale (protéine dirigeante, DIR) est connue pour avoir la capacité de diriger la synthèse stéréosélective de produits optiquement purs à partir de radicaux de monolignols dans une réaction qui sans facteur externe conduit à un mélange de produits racémique.²¹ D'un point de vue mécanistique, il semble que la DIR lie spécifiquement deux radicaux et les maintient en place (dans la cavité d'un β barrel) pour faciliter la formation sélective de liaisons C-C.

L'action des protéines dirigeantes est une source d'inspiration pour le développement de réactions sélectives catalysées par des laccases. En effet, il serait intéressant de pouvoir contrôler la spécificité d'une réaction en introduisant un effecteur (par exemple une autre enzyme ou des molécules non biologiques) dans le système catalytique à base de laccase. Les cyclodextrines par exemple, sont de petites cages organiques qui sont de simples imitations DIR affectant le sort des réactions médiées par la laccase.²² Bien au-delà des molécules, des matériaux amenés près de la surface de l'enzyme, comme cela se produit lors de l'immobilisation de la laccase, pourraient en quelque sorte être assimilés à de tels effecteurs, les matériaux étant ici considérés comme des effecteurs externes. En effet l'immobilisation sur des matériaux au-delà du rôle communément admis dans l'amélioration

des performances enzymatiques telles que la stabilité opérationnelle, la résistance aux températures élevées, etc., pourrait être envisagé pour introduire de la sélectivité dans les processus chimiques catalysés par des laccases.

Le concept d'utilisation de techniques d'immobilisation pour moduler la sélectivité des enzymes se renforce du fait que le processus d'immobilisation influence de manière significative les propriétés des enzymes en: i) réduisant la mobilité des groupes protéiques; ii) provoquant des changements de conformation des protéines, dans certains cas, déformant même le site actif; iii) affectant le contact avec le substrat et l'enzyme en raison d'un obstacle stérique, iv) générant éventuellement différents environnements physicochimiques entourant l'enzyme. Par conséquent, selon la nature du support et le mode d'interaction entre le support et l'enzyme, l'exposition de la même région protéique à différents matériaux ou l'exposition du même matériau à une région différente de la protéine peut entraîner différents changements conformationnels ou distorsions enzymatiques. Les illustrations sur un contrôle par le matériau sont diffusées dans la littérature dédiée à l'immobilisation enzymatique. Il existe cependant quelques exemples comme celui d'un rapport sur l'immobilisation d'une lipase sur différents supports conduisant à une énantiosélectivité différente même dans les mêmes conditions expérimentales selon la nature du support.²³ Nous croyons fermement que la prise en compte de ces différences dans la conception de la modification de surface représente un potentiel d'introduire (et de contrôler) de la sélectivité dans les réactions catalysées par des enzymes.

Parmi toutes les sortes de supports utilisés jusqu'à présent pour l'immobilisation d'enzymes, les particules super paramagnétiques (MNP) sont l'un des matériaux les plus populaires. En effet leurs structures cœur-coquille spéciales, la grande variété des groupements fonctionnels disponibles pour l'immobilisation des protéines en fait un matériau de choix. De plus en raison de leurs propriétés super paramagnétiques, une séparation et un recyclage faciles peuvent être réalisés de manière pratique en utilisant un simple aimant, ce qui augmente considérablement leur intérêt pour le développement de processus catalytique. Jusqu'à présent, le potentiel des MNP pour moduler les propriétés enzymatiques vers la sélectivité n'a pas encore été étudié mais mérite d'être exploré. En combinant l'immobilisation des enzymes d'une manière spécifique et une variation de la nature de la couche de fonctionnalisation, un contrôle de la sélectivité dans les réactions à plusieurs étapes peut être attendu. Ainsi, les besoins énergétiques seront minimisés et les sous-produits indésirables seront éliminés.

En conclusion, la laccase est un catalyseur robuste avec des applications répandues dans les domaines biochimiques. Mais le couplage des radicaux catalysés par la laccase manque de sélectivité et a tendance à former un mélange de produits allant des dimères aux oligomères supérieurs, ce qui n'est pas respectueux de l'environnement car il entraîne la formation de produits indésirables. Par ailleurs, les protéines dirigeantes végétales dirigent le couplage stéréosélectif des phénols offrant un

site pour contrôler le devenir des produits d'oxydation. En nous inspirant d'un site exogène DP contrôlant la réactivité de la laccase, nous proposons de greffer la surface de la laccase avec des matériaux afin d'induire de la sélectivité dans les réactions de couplage non sélectives. Les particules magnétiques semblent avoir un grand potentiel pour stimuler la sélectivité dans les réactions catalysées par la laccase.

L'objectif principal de ce travail de recherche était d'étudier les possibilités de moduler les propriétés catalytiques de la laccase par l'ajout de facteurs externes modifiant le (micro) environnement de la laccase. Ainsi, nous avons brièvement étudié la protéine dirigeante végétale *AtDIR6* en tant que modèle naturel d'effecteur de laccase et conçu un système bio-inspiré consistant en des MNP fonctionnalisés par laccase dans lesquels à la fois la nature chimique et l'orientation de l'enzyme peuvent être modulées au niveau de la nano- surface des particules.

Concernant la partie *AtDIR6*, prolongeant le travail précédemment effectué dans notre laboratoire,²⁴ nous avons confirmé que: i) *AtDIR6* augmente la durée de vie des radicaux issus de l'oxydation de l'alcool coniférylique comme vu pour la première fois par RPE; ii) les tyrosines dans la cavité d'*AtDIR6* sont marquées avec une sonde radicalaire (ABTS); iii) l'unité allylique de l'alcool coniférylique peut être modifiée comme en témoigne la formation sélective de dimères issus de l'oxydation de l'acétate de coniferyl en présence de DP. Nous avons ensuite développé des stratégies: iv) pour identifier les acides aminés dans la cavité d'*AtDIR6* qui sont impliqués dans le contrôle stéréosélectif en utilisant des radicaux d'alcool coniférylique comme sonde, et v) pour explorer la réactivité d'*AtDIR6* en utilisant des analogues synthétiques de l'alcool coniférylique.

En ce qui concerne la partie MNP fonctionnalisée par laccase, nous avons exploré le couplage de laccases à des MNP ayant différentes fonctions chimiques à leur surface: -NH₂, -CHO, -N₃, et pour certaines comparées différentes densités de fonctions chimiques: linéaire vs dendritique (coll. Hongtao Ji et Karine Heuzé, Université Bordeaux). Nous avons utilisé deux types de laccases: a) LAC3 possédant deux lysine situées à l'opposé du site actif de l'enzyme qui après greffage aux MNP expose son site actif au solvant, et b) son variant UniK₁₆₁ possédant une seule lysine localisée à proximité du site actif qui après greffage aux MNPs expose le site actif à la surface du MNP. L'activité des laccases immobilisées a été testée avec différents substrats: ABTS (synthétique), syringaldazine (phénol) et alcool coniférylique (monolignol). Ensemble, ces modulations nous ont permis d'étudier le système en plusieurs dimensions: orientation du biocatalyseur, nature de l'environnement chimique à l'interface, densité des fonctions chimiques, chimio, régio et stéréosélectivité. Nous apportons ici des preuves que l'activité d'une enzyme non sélective peut être modulée par la conception du micro-environnement autour de son site actif.

Ainsi, ce manuscrit est organisé en trois chapitres:

Dans le premier chapitre, une étude bibliographique décrit brièvement la laccase, les MNP et les protéines dirigeantes. Également, la structure, le mécanisme de fonctionnement et l'application de ces trois objets ont également été passés en revue.

Le deuxième chapitre se concentre sur l'étude de *AtDIR6*, l'une des premières protéines dirigeantes caractérisées, dirigeant le couplage des radicaux phénoxyls pour former un lignan optiquement pur : le (-) - pinorésinol. Tout d'abord, *AtDIR6* a été purifié et son activité a été évaluée sur l'oxydation de l'alcool coniférylique. Ensuite, des analogues d'alcool coniférylique ont été synthétisés et ont été utilisés pour explorer la plasticité d'*AtDIR6* vers de nouveaux substrats. De plus, la stabilisation des radicaux analogues de l'alcool coniférylique par *AtDIR6* a été contrôlée par RPE. Enfin, les radicaux alcool coniférylique ont été utilisés comme sonde pour identifier les acides aminés d'*AtDIR6* qui sont impliqués dans le contrôle stéréosélectif.

Le troisième chapitre est consacré à l'immobilisation orientée de deux variants de laccase (LAC3 et UniK161) sur différentes MNP. Trois particules ont été étudiées, des particules fonctionnalisées avec un aldéhyde (à la fois commerciales et autoproduites), des particules fonctionnalisées avec un azide et les particules fonctionnalisées avec une amine, qui sont décrites dans des sous-sections de manière indépendante. Dans chaque sous-section, la caractérisation des particules, l'exploration des conditions d'immobilisation, les problèmes rencontrés lors de ces explorations ainsi que les résultats finaux d'immobilisation sont présentés en détail. De plus, l'activité spécifique de ces deux variants de laccase après immobilisation a été comparée à la fois sur l'oxydation de l'ABTS et sur la biotransformation de l'alcool coniférylique.

Reference

- (1) IUPAC - catalyst (C00876) <http://goldbook.iupac.org/terms/view/C00876> (accessed Jul 8, 2019). <https://doi.org/10.1351/goldbook.C00876>.
- (2) Schmid, R. Homogeneous Catalysis with Metal Complexes in a Pharmaceuticals' and Vitamins' Company: Why, What for, and Where to Go? 4.
- (3) Catalysis - an overview | ScienceDirect Topics <https://www.sciencedirect.com/topics/materials-science/catalysis> (accessed Jul 8, 2019).
- (4) Knözinger, H.; Kochloefl, K. Heterogeneous Catalysis and Solid Catalysts; 2003. https://doi.org/10.1002/14356007.a05_313.
- (5) Sheldon, R. A.; Woodley, J. M. Role of Biocatalysis in Sustainable Chemistry. *Chem. Rev.* **2017**, *118* (2), 801–838.
- (6) Arnold, F. H. Combinatorial and Computational Challenges for Biocatalyst Design. *Nature* **2001**, *409* (6817), 253.
- (7) Yoshida, H. CHEMISTRY OF LACQUER (URUSHI) Chemistry of Lacquer (Urushi). Part I. Communication from the Chemical Society of Tokio. *J. Chem. Soc. Trans.* **1883**, *43*, 472–486.
- (8) Matera, I.; Gullotto, A.; Tilli, S.; Ferraroni, M.; Scozzafava, A.; Briganti, F. Crystal Structure of the Blue Multicopper Oxidase from the White-Rot Fungus *Trametes Troglia* Complexed with p-Toluate. *Inorganica Chim. Acta* **2008**, *361* (14–15), 4129–4137. <https://doi.org/10.1016/j.ica.2008.03.091>.
- (9) yaohua, G.; ping, X.; feng, J.; keren, S. Co-Immobilization of Laccase and ABTS onto Novel Dual-Functionalized Cellulose Beads for Highly Improved Biodegradation of Indole. *J. Hazard. Mater.* **2019**, *365*, 118–124. <https://doi.org/10.1016/j.jhazmat.2018.10.076>.
- (10) Llevot, A.; Grau, E.; Carlotti, S.; Grelier, S.; Cramail, H. Selective Laccase-Catalyzed Dimerization of Phenolic Compounds Derived from Lignin: Towards Original Symmetrical Bio-Based (Bis) Aromatic Monomers. *J. Mol. Catal. B Enzym.* **2016**, *125*, 34–41.
- (11) Brijwani, K.; Rigdon, A.; Vadlani, P. V. Fungal Laccases: Production, Function, and Applications in Food Processing. *Enzyme Res.* **2010**, *2010*.
- (12) Ayala, M.; Pickard, M. A.; Vazquez-Duhalt, R. Fungal Enzymes for Environmental Purposes, a Molecular Biology Challenge. *J. Mol. Microbiol. Biotechnol.* **2008**, *15* (2–3), 172–180. <https://doi.org/10.1159/000121328>.

- (13) Rodgers, C. J.; Blanford, C. F.; Giddens, S. R.; Skamnioti, P.; Armstrong, F. A.; Gurr, S. J. Designer Laccases: A Vogue for High-Potential Fungal Enzymes? *Trends Biotechnol.* **2010**, *28* (2), 63–72. <https://doi.org/10.1016/j.tibtech.2009.11.001>.
- (14) Morozova, O. V.; Shumakovich, G. P.; Shleev, S. V.; Yaropolov, Y. I. Laccase-Mediator Systems and Their Applications: A Review. *Appl. Biochem. Microbiol.* **2007**, *43* (5), 523–535.
- (15) Fernández-Fernández, M.; Sanromán, M. Á.; Moldes, D. Recent Developments and Applications of Immobilized Laccase. *Biotechnol. Adv.* **2013**, *31* (8), 1808–1825. <https://doi.org/10.1016/j.biotechadv.2012.02.013>.
- (16) Kunamneni, A.; Camarero, S.; García-Burgos, C.; Plou, F. J.; Ballesteros, A.; Alcalde, M. Engineering and Applications of Fungal Laccases for Organic Synthesis. *Microb. Cell Factories* **2008**, *7* (1), 32. <https://doi.org/10.1186/1475-2859-7-32>.
- (17) Vargesson, N. Thalidomide-Induced Teratogenesis: History and Mechanisms: Thalidomide-Induced Teratogenesis. *Birth Defects Res. Part C Embryo Today Rev.* **2015**, *105* (2), 140–156. <https://doi.org/10.1002/bdrc.21096>.
- (18) Fabbrini, M.; Galli, C.; Gentili, P.; Macchitella, D. An Oxidation of Alcohols by Oxygen with the Enzyme Laccase and Mediation by TEMPO. *Tetrahedron Lett.* **2001**, *42* (43), 7551–7553. [https://doi.org/10.1016/S0040-4039\(01\)01463-0](https://doi.org/10.1016/S0040-4039(01)01463-0).
- (19) Klibanov, A. M. Improving Enzymes by Using Them in Organic Solvents. *Nature* **2001**, *409* (6817), 241–246. <https://doi.org/10.1038/35051719>.
- (20) Intra, A.; Nicotra, S.; Riva, S.; Danieli, B. Significant and Unexpected Solvent Influence on the Selectivity of Laccase-Catalyzed Coupling of Tetrahydro-2-Naphthol Derivatives. *Adv. Synth. Catal.* **2005**, *347* (7–8), 973–977. <https://doi.org/10.1002/adsc.200505043>.
- (21) Davin, L. B.; Wang, H.-B.; Crowell, A. L.; Bedgar, D. L.; Martin, D. M.; Sarkanen, S.; Lewis, N. G. Stereoselective Bimolecular Phenoxy Radical Coupling by an Auxiliary (Dirigent) Protein Without an Active Center. *Science* **1997**, *275* (5298), 362–367. <https://doi.org/10.1126/science.275.5298.362>.
- (22) Tarrago, L.; Modolo, C.; Yemloul, M.; Robert, V.; Rousselot-Pailley, P.; Tron, T. Controlling the Polymerization of Coniferyl Alcohol with Cyclodextrins. *New J. Chem.* **2018**, *42* (14), 11770–11775.

(23) Mateo, C.; Palomo, J. M.; Fernandez-Lorente, G.; Guisan, J. M.; Fernandez-Lafuente, R. Improvement of Enzyme Activity, Stability and Selectivity via Immobilization Techniques. *Enzyme Microb. Technol.* **2007**, *40* (6), 1451–1463. <https://doi.org/10.1016/j.enzmictec.2007.01.018>.

(24) Modolo, C. L'intrigant couplage radicalaire stéréosélectif médié par la protéine dirigeante AtDIR6, Aix Marseille university, 2017.

Contents

Contents

List of Figures	1
List of Tables.....	1
List of Abbreviations.....	3
General Introduction	15
Chapter I Bibliographical Survey.....	25
1 Laccase.....	27
1.1 Introduction to Laccase	27
1.2 Laccase structure and active site	27
1.3 Catalytic mechanism of laccase	29
1.4 Laccase mediator system (LMS).....	30
1.5 Biochemical applications of laccase	31
2 Dirigent protein	35
2.1 From lignan biosynthesis to dirigent protein.....	35
2.2 Structure and proposed Mechanism of dirigent protein	38
2.2.1 Structure of DIRs	38
2.2.2 Active site of DIRs	40
2.2.3 Proposed mechanism of DIRs	41
2.2.4 Biotechnological application of the DIRs	42
3 Magnetic Nanoparticles (MNPs).....	45
3.1 Immobilization of Laccase for industrial application	45
3.1.1 Immobilization methods.....	45
3.1.2 Materials used for enzyme immobilization	48
3.2 Introduction to magnetic nanoparticles	53
3.2.1 Structure of MNPs.....	53
3.2.2 Magnetic features of MNPs.....	54
3.3 MNPs in laccase immobilization.....	54
4 Scope of this research work	59
Reference.....	60
Chapter II Stereoselective Radical Coupling Mediated by the Dirigent Protein <i>Az</i>DIR6.....	77
1 Introduction	79
2 Production of <i>Az</i> DIR6.....	79

2.1	Purification of <i>At</i> DIR6	79
2.2	<i>At</i> DIR6 activity on Coniferyl Alcohol oxidation	81
2.2.1	Activity measurement principle	81
2.2.2	HPLC chromatogram	82
2.2.3	Effect of <i>At</i> DIR6 on oxidation kinetics of CA and formation of dimers	83
2.2.4	Effects of varying <i>At</i> DIR6 concentration.....	84
2.2.5	Activities of DP1 and DP2 samples	85
3	Exploration of <i>At</i> DIR6 activity with synthetic CA analogues	87
3.1	Introduction	87
3.2	<i>At</i> DIR6 Activity on CA analogues.....	88
3.2.1	Ferulic Acid (FA)	88
3.2.2	Coniferyl Acetate (CAC)	91
3.2.3	Coniferyl Azide (CAZ)	93
3.3	Conclusion and prospect	94
4	Direct evidence of radical stabilization by <i>At</i> DIR6	95
4.1	Introduction	95
4.2	Analysis of EPR signals	96
4.3	Analysis of non-laccase substrate (NOS).....	97
4.4	Conclusion.....	98
5	Attempts to identify amino acids involved in the stereoselective control within the cavity of DIRs	99
5.1	Introduction	99
5.2	Results and discussion.....	100
6	Conclusion.....	101
	Appendix: Materials and Methods Chapter II.....	103
1	General	103
1.1	His-Tag affinity Chromatography	103
1.2	Size Exclusion Chromatography	103
1.3	SDS-PAGE.....	103
1.4	<i>At</i> DIR6 concentration measurement	104
1.5	Laccase	104
1.6	Bioconversion of coniferyl alcohol and analogues by <i>At</i> DIR6.....	104
1.7	HPLC analysis.....	105
1.8	Chiral HPLC.....	105
1.9	EPR X-band.....	105

1.10	ESI-MS analysis.....	105
1.11	NMR spectroscopy.....	106
1.12	MALDI TOF MS	106
2	Production of <i>At</i> DIR6.....	106
3	Dirigent activity assay of the produced <i>At</i> DIR6	106
4	Identification activity of <i>At</i> DIR6 to CA analogues.....	107
6	Studies of radical stabilization by <i>At</i> DIR6.....	109
7	HPLC chromatogram of the NOS samples	110
8	Analysis of the amino acids involving in stereoselective coupling	110
	Reference.....	111
Chapter III Oriented Functionalization Of Magnetic Particles with Laccases.....		113
1	Introduction	115
2	Commercial Aldehyde Particles (C21)	117
2.1	Information of the commercial Aldehyde particles.....	117
2.2	Results and discussion.....	118
2.2.1	Preliminary results on immobilization	118
2.2.2	Study on the dispersion of magnetic particles.....	121
2.2.3	Characterization of the surface functional groups on MNPs	127
2.2.4	Exploration of the experimental conditions	133
2.2.5	Final results of C21 immobilization.....	138
2.3	Conclusions	147
3	Custom-made aldehyde particles (H23) immobilization	149
3.1	Information of the custom-made aldehyde particles	149
3.2	Results and discussion.....	150
3.2.1	Relationship between initial laccase and activity.....	150
3.2.2	Enzyme loading.....	151
3.2.3	Activity and Specific Activity evaluation of free and immobilized laccase towards ABTS	153
3.2.4	Coniferyl alcohol biotransformation with H23 immobilized laccase	154
3.3	Conclusions	156
4	Immobilization on commercial azide particles	157
4.1	Information on azide particles.....	157
4.2	Optimization of immobilization reaction conditions	158
4.2.1	Effect of initial enzyme concentration on activity	158

4.2.2	Effect of particles amount on activity	158
4.2.3	Effect of particle pretreatment method on activity.....	159
4.3	Results and discussion.....	160
4.3.1	Enzyme loading.....	160
4.3.2	Evaluation of Specific Activity for free and immobilized laccase towards ABTS....	162
4.3.3	Coniferyl alcohol biotransformation with laccase immobilized on azide particles ...	165
4.4	Conclusions	167
5	Amino particles immobilization of laccase	167
5.1	Information of amino particles	167
5.2	Results and discussion.....	169
5.2.1	Characterization of the Amino particles (MNP-NH ₂).....	169
5.2.2	Optimization of immobilization reaction conditions	170
5.2.3	Immobilization of laccase onto MNPs	171
5.3	Conclusion.....	176
6	Conclusions	177
Appendix: Materials and Methods chapter III		179
1	General	179
1.1	Laccase	179
1.2	Zetametry measurements.....	179
1.3	FT-IR.....	179
1.4	HPLC test	179
2	Immobilization	180
2.1	Aldehyde particles immobilization	180
2.2	Azide particles immobilization	180
2.3	Amino particles immobilization.....	181
3	Enzyme loading measurement	181
3.1	Enzyme loading measurement by UV-visible spectrophotometry.....	181
3.2	Enzyme loading measurement by Bradford Protein Assay.....	182
3.3	Enzyme loading test by ELISA (Enzyme-Linked ImmunoSorbent Assay).....	182
4	Fluorescence Qualitative Experiment	183
5	Biotransformation of Coniferyl Alcohol	183
Reference.....		184
General Conclusion		187
Appendix		193

List of Figures

- Fig. I-1-1 Structure of copper center/active site of laccases (a) the three types of copper coordination, including interatomic distances among all relevant ligands²⁷ (b) structure of the laccase active sites with arrows marking the flow of substrates, electrons (e⁻) and O₂³³28
- Fig. I-1-2 Three-dimensional representation of a fungal laccase based on the coordinates of the PDB entry 2HRG. Cupredoxin domains are colored from blue (D1) to green (D2) to red (D3). Light-orange spheres depict copper ions, an isolated Cu (II) T1 close to the surface of the enzyme in D3 and a Cu (II) T2-T3 trinuclear cluster embedded in the enzyme at the D1-D3 boundaries.29
- Fig. I-1-3 Schematic representation of laccase-catalyzed redox cycles for substrates oxidation in the (a) direct or (b) in-direct (with present of chemical mediators) way.³⁷29
- Fig. I-1-4 Structure of three typical artificial mediators using in LMS: (a) ABTS (2,2'-Azino-bis (3 ethylbenzothiazoline-6-sulfonic acid)); (b) HBT (1-hydroxybenzotriazole); (c) TEMPO (2,2,6,6 tetramethylpiperidine-1-oxyl) and their corresponding mechanisms proposed: (d) Electron transfer (ET) route of laccase-ABTS system; (e) Radical H-atom transfer (HAT) pathway of laccase-HBT system; (f) Ionic oxidation mechanism of laccase-TEMPO system.30
- Fig. I-1-5 Examples of polymerization of laccase-generated radicals. (1) production of polycatechol from catechol monomers. (2) the coupling of p-hydroquinones and aromatic amines.....31
- Fig. I-2-1 Chemical structure of the three commonly occurring monolignols.....35
- Fig. I-2-2 Lignan core structures35
- Fig. I-2-3 Bimolecular phenoxy radical coupling products from E-coniferyl alcohol. (a) Stereoselective coupling generating (+)-pinoresinol. (b) Dimeric lignans formed via “random” coupling.36
- Fig. I-2-4 Biosynthesis of gossypol by free radical coupling of hemigossypol generated by peroxidase in the presence or absence of a cotton dirigent protein.⁹³37
- Fig. I-2-5 Structure of the DIRs monomer. (a) Monomer of (-)-pinoresinol forming DIR AtDIR6, showing strands 1 to 8.¹⁰² (b) Monomer of (+)-pinoresinol forming DIR PsDRR206. Left, ribbon representation of the eight-stranded β-barrel rainbow-colored from the N terminus (blue) to the C terminus (red), showing the secondary structure

- labeling; right, the PsDRR206 monomer rotated 90° about a vertical axis and colored to show the two component β -sheets in blue (β -sheet 1) and red (β -sheet 2).⁸³ (c) Comparison of *At*DIR6 with PsDRR206. Overlay of monomer of *At*DIR6 (gray) with monomer of DRR206 (cyan; PDB accession code 4REV).¹⁰²39
- Fig. I-2-6 Structure of DIR trimers. (a) PsDRR206 trimer viewed down the 3-fold c-axis of the H32 space group, the a- and b-axes are indicated. (b) same structure as in (a) rotated 90° about the a-axis. One of the extended β 2 strands (blue) traverses the trimer interface into neighboring monomer (green), and this region is highlighted by the black oval. (c) structure of *At*DIR6 trimer at top view. (d) structure of *At*DIR6 trimer at side view. Each monomer is shown in a different color. The location of the active site is highlighted by a black circle in one of the monomers.39
- Fig. I-2-7 Active site with the interior lined residues in (a) PsDRR206 and (b) *At*DIR6. Potential binding mode of DIRs supported by energy minimization of the manually placed ligands in (c) PsDRR206 and (d) *At*DIR6.40
- Fig. I-2-8¹⁰⁴ Schematic representation of the bisQM intermediate cyclization catalyzed by *At*DIR6. The cartoon combines the side view on the active site as shown in Fig. I-2-7 (d) with the key functional residues highlighted (sticks). The mechanism of bisQM cyclization proposed by Gasper et al.¹⁰² via acid catalysis (left) or hydrogen bond formation (right) is schematically shown. Both mechanisms seem to result in a partial or full positive charge on C7 that facilitates the nucleophilic attack during bisQM cyclization42
- Fig. I-3-1 Schematic diagram of laccase immobilization methods: (a) Adsorption of enzymes onto a support by ionic forces. (b) Covalent binding between the nucleophilic groups of the enzyme and the support. (c) Entrapment of enzymes into a porous solid matrix. (d) Encapsulation of enzymes (e) Self-immobilization: model of cross-linked enzyme aggregates (CLEAs).¹⁵46
- Fig. I-3-2 Structure of magnetic particles (Figure from https://www.cd-bioparticles.com/s/Magnetic-Beads-Modification_34.html)53
- Fig. I-3-3 Illustration of superparamagnetic MNP response to applied magnetic fields.¹⁴⁸ ...54
- Fig. I-3-4 Scheme of the chemical strategy for immobilization of laccase to the silica coated amino particles a) the synthesis of the magnetic core, b) the silica coating, c) the surface functionalization with amine groups, d) the activation with glutaraldehyde (GLU) and e) the immobilization of laccase (L).¹⁵⁰55

- Fig. I-3-5 Scheme for conjugating laccase onto the surface of the nanoparticles via two different strategies. (A) Random immobilization via covalent binding. (B) oriented immobilization via interaction between Con A and glycosyl of laccase.....56
- Fig. I-3-6 Metal affinity adsorption of laccase onto PEI modified Fe₃O₄ nanoparticles (Fe₃O₄-NH₂-PEI NPs) chelated with Cu²⁺57
- Fig. I-3-7 Scheme of laccase immobilization onto Fe₃O₄-CS nanoparticles (a) by EDAC and (b) by CC.....57
- Fig. I-3-8 Alkyne-azide click chemistry using in surface modification of MNPs and immobilization of biomolecules. (a) an example of alkyne functionalized MNPs and (b) an example of azide functionalized silica particle. (c) covalently immobilization of alkyne-functionalized MBP onto azide MNPs via the Cu(I)-catalyzed cycloaddition58
- Fig. II-2-1 Elution profile of the His-Trap column. The red line displays the absorbance at 415 nm, and the blue line indicates the absorbance at 280 nm, the green line displays the imidazole concentration gradient.79
- Fig. II-2-2 Elution profile on Size Exclusion Chromatography.....80
- Fig. II-2-3 SDS-PAGE analysis of samples from the purification of *At*DIR6. 5µg of protein loaded per lane. Lane M: molecular weight makers; lane1: IMAC elution peak 1; lane 2: IMAC elution peak 2; lane 3: SEC elution peak 1 (from IMAC elution peak 2); lane4; SEC elution peak 2 (from IMAC elution peak 2).....81
- Fig. II-2-4 Oxidation and coupling of coniferyl alcohol. A: Resonance forms of the coniferyl radical produced upon oxidation. B: chemical structure of the dimers obtained from coniferyl alcohol oxidation.....82
- Fig. II-2-5 HPLC chromatogram of the oxidized Coniferyl Alcohol coupling. The chromatograms reflect the disappearance of the CA and the appearance of the products. In the absence of DP, the main product is DCA while in the present of DP it is PINO. Experimental conditions:1.6mM CA and 1U/L LAC3 with or without 500µM DP in a final volume of 100µL, 0.1M acetate buffer pH 5.0. Thermomixer 1000rpm at 30°C, T=20 hours.83
- Fig. II-2-6 CA consumption and dimers generation over time. Left: absence of *At*DIR6; Right: presence of *At*DIR6. Experimental conditions:1.6mM CA and 1U/L LAC3 with no DP or 100µM DP in a final volume of 1mL, 0.1M acetate buffer pH 5.0. Thermomixer 1000rpm at 30°C, for a maximum 25 hours. Samples were taken for testing over time progress. Y

axis is the ratio of the peak area corresponding to each substance to the peak area of the reference in HPLC chromatogram.	84
Fig. II-2-7 Effect of varying DP concentration on coniferyl alcohol derived coupling products	84
Fig. II-2-8 Comparison of activity between <i>At</i> DIR6 samples. S6DP and S7DP were purified using successively Ni-NTA Agarose and Sephacryl S-200 columns; S8DP and S9DP were purified using successively His Trap TM HP and Superdex® 75 10/300 GL columns. Experimental condition: 1.6mM CA and 1U/L LAC3 with 100µM DP in a final volume of 100µL, 0.1M acetate buffer pH 5.0. Thermomixer 1000rpm at 30°C, T≈20 hours. DP: sample prior SEC; DP1: SEC peak 1; DP2: SEC peak 2.	85
Fig. II-2-9 Analysis of PINO by chiral chromatography. Experimental condition: 1.6mM CA and 1U/L LAC3 with 100µM S6DP or S6DP2 in a final volume of 100µL, 0.1M acetate buffer pH 5.0. Thermomixer 1000rpm at 30°C, T=15 hours.	86
Fig. II-3-1 The three potential substrates of dirigent protein tested by Lewis et.al. From the comparison, the red dotted circle indicates the part that is mandatory for DP activity, the green dotted circle indicates the part studied in this manuscript.....	87
Fig. II-3-2 Coniferyl alcohol analogues	88
Fig. II-3-3 HPLC chromatogram of Ferulic Acid oxidation products ± <i>At</i> DIR6.....	89
Fig. II-3-4 Structure of FA and its proposed dimers	90
Fig. II-3-5 HPLC chromatogram of Coniferyl Acetate oxidation products ± <i>At</i> DIR6..	91
Fig. II-3-6 Structure of CAC and its proposed dimers.....	92
Fig. II-3-7 Mechanism of action envisaged with coniferyl acetate.....	92
Fig. II-3-8 HPLC chromatogram of Coniferyl Azide oxidation products ± <i>At</i> DIR6.....	93
Fig. II-3-9 Structure of CAC and its proposed dimers.....	94
Fig. II-4-1 EPR spectra of substrates (CA, FA and CAC) and <i>At</i> DIR6 under continuous photo-irradiation. Deoxygenated acetate buffered (100 mM pH 5) 1.6 mM substrate solutions in the presence of 100µM <i>At</i> DIR6. Controls: 1.6 mM of CA (blue line); 350 µM <i>At</i> DIR6 (yellow line). Irradiation conditions: white light (200<λ<800 nm) lamp 200 W. Left: the EPR spectra of the individual samples; Right: comparison of all the samples.	96

Fig. II-4-2 View of the <i>At</i> DIR6 active site showing (left): important residues in pocket A in green, pocket B in blue, and Tyr-106 and Phe-175 separating the two pockets in red.(right) Potential binding mode of two CA substrate radicals supported by energy minimization of the manually placed ligands. ¹⁰	97
Fig. II-4-3 Structure of the non-laccase substrate (NOS) molecule.	97
Fig. II-5-1 Comparison of mass spectra of deglycosylated proteins.	100
Fig. II-A-1 Mass Spectrum (MS) in electrospray negative mode of the FA-peak1 sample ...	107
Fig. II-A-2 Mass Spectrum (MS) in electrospray negative mode of the FA-peak1 sample ...	107
Fig. II-A-3 SUPRASIL Standard TE02 cavity aqueous cell (http://www.cortecnet.com)	109
Fig. II-A-4 HPLC chromatogram of the NOS samples.....	110
Fig. III-1-1 3D model illustrating the potential in the orientation of the enzyme upon immobilization. The figure is modified from reference. ¹ Immobilizing LAC3 onto MNPs, the exposition of the T1 site to the solvent is achieved; immobilizing UniK ₁₆₁ , the exposition of the T1 site to the MNP surface is obtained.	115
Fig. III-2-1 Schematic diagram of the Reductive alkylation reaction used in aldehyde particles immobilization.	117
Fig. III-2-2 Schematic diagram of commercial aldehyde particles C21	118
Fig. III-2-3 Activity of (Laccase-MNP) system after immobilization (A) qualitatively observed by the color change upon Syringaldazine (SGZ) oxidation catalyzed by laccase. (B) quantitatively measured by using SGZ as substrate.....	120
Fig. III-2-4 Commercial Aldehyde particles dispersed by different physical methods (1mg/mL in MQ water). (A) Pipetting (B) Vortexing at 1min and 5min respectively (C) Bath sonication at 1min and 10 min respectively.	122
Fig. III-2-5 Commercial Aldehyde particles dispersed by probe sonication for 3 mins (1mg/mL in MQ water)	124
Fig. III-2-6 1mg/mL commercial Aldehyde particles dispersed in MQ water with 0.05% Tween 20. (A) the particles were dispersed by vortexing. (B) the dispersion state after wash three times by MQ water	125
Fig. III-2-7 Effect of pH on the surface charge of commercial particles.	127
Fig. III-2-8 ATR FT-IR spectrum of commercial aldehyde particles after storage	128

Fig. III-2-9 FT-IR spectrum of commercial aldehyde particles measured rapidly upon receipt	129
Fig. III-2-10 Schematic representation of the grafting of the fluorescent dye on MNPs for determination of the surface aldehyde groups.....	129
Fig. III-2-11 Fluorescence spectroscopy measurement of the standard solutions. (A) Fluorescence intensity spectra of standard solutions at different concentrations (B) Relationship between solution concentration and fluorescence intensity. The wavelength of the excitation light was set at 379 nm and wavelength of the emission light was scanned from 400 to 600 nm, slits 1nm, 20°C. Fluorescence intensity of the solution was taken at the maximum emission at 521 nm.....	131
Fig. III-2-12 Calibration curve for quantitative determination of aldehyde groups on the surface of MNPs by fluorescent dye coupling method.....	131
Fig. III-2-13 Fluorescence spectroscopy measurement of the supernatants and washing solutions	132
Fig. III-2-14 Relationship of the particles amount and the final enzyme loading. The total volume of the reaction system is 1mL, and the initial enzyme concentration used is 5µM. Three groups of immobilizations were performed for 2mg and 10mg particles respectively. Enzyme loading was tested by Bradford methods as previously described.....	134
Fig. III-2-15 The special magnetic support used for MNPs manipulations on microplate (A) and the Schematic diagram of the mechanism of ELISA (B) (refer to the reference ⁷ add notes according to the actual situation)	136
Fig. III-2-16 Regions of conformational stability for CALB/fumed silica adsorbates. The dotted vertical line at ~200%SC separates two different regions of conformational stability: region I delimited by a long-dash-dot line where adsorbates exhibit low conformational stability, and region III delimited by a short-dash-dot line where adsorbates have highly stable conformations. The presence of these two regions is likely to be responsible for the observed catalytic activity (r_0) of the lyophilized adsorbates in hexane (inset). The low catalytic activity observed at low %SC can be linked to region I. Even though the structure is well preserved in region III, multi-layer packing is likely responsible for diffusional limitations of catalysis. The maximum in activity between those two regions can be attributed to an optimal arrangement on the surface where the structure is relatively well maintained without excessive clustering (region II, delimited by a dotted line) ⁸	137

- Fig. III-2-17 Relationship between the initial laccase concentration and the immobilized laccase activity for the commercial aldehyde particles. LAC3 was used as model protein. Particles concentration 2mg/mL. Reaction temperature: 30°C. Rotating speed: thermomixer 1000 rpm. The maximum activity point of the grafted LAC3 is reached for an initial enzyme concentration of 500µM. 138
- Fig. III-2-18 Enzyme loading tested by ELISA for the commercial aldehyde particles. Three groups of immobilizations (Group 1, 2 and 3 corresponds to A, B and C) were tested separately under the same conditions: particles concentration: 2mg/mL. Immobilization buffer: 50 mM phosphate contains 0.1M sodium formate, pH 7.4. Initial laccase concentration: 500µM. Total volume: 200µL. Ir catalyst: 10 eq[E]. Reaction temperature: 30°C. Rotating on thermomixer at 1000rpm. 2µg and 1µg particles immobilized with different laccase were triplicated in the microwell respectively. Error bar were less than 11% for the immobilized samples. 139
- Fig. III-2-19 Activity of commercial aldehyde particles immobilized laccase towards ABTS, at pH 5.57, 30°C. 141
- Fig. III-2-20 Oxidation of Coniferyl alcohol and the coupling products 143
- Fig. III-2-21 Control experiments of coniferyl alcohol biotransformation. The control samples contain: 1.6 mM CA only(blank); 1.6 mM CA solutions added with a final concentration of 1 mg/mL bare particles; 1.6 mM CA plus free laccase (LAC3 or UniK₁₆₁, final 1U/L tested by ABTS). Experiments were incubated in 0.1M pH=5,7 acetate buffer, at 30°C in a thermomixer at 1000rpm, for maximum 25 hours, in a final volume of 500µL. The ordinate is the ratio of the area of the peak corresponding to the reactant on the HPLC chromatogram to the area of the peak corresponding to the benzophenone reference. .. 144
- Fig. III-2-22 Oxidation of coniferyl alcohol catalyzed by immobilized laccases. Experiments were incubated in 0.1M pH=5,5 Acetate buffer, at 30°C in a thermomixer at 1000rpm, for maximum 25 hours, in a final volume of 500µL and CA concentration of 1.6 mM. The ordinate is the ratio of the area of the peak corresponding to the reactant on the HPLC chromatogram to the area of the peak corresponding to the reference benzophenone. Three groups of immobilized laccases were tested and the amount of laccase used is as follows: Group 1: 554 ng immobilized enzyme; Group 2: 695 ng immobilized enzyme; Group 3: 250 ng immobilized enzyme in the total reaction system. CA: coniferyl alcohol; DCA: dehydroconiferyl alcohol..... 145
- Fig. III-3-1 Schematic diagram of custom-made aldehyde particles H23 149

- Fig. III-3-2 Relationship between the initial laccase concentration and the immobilized laccase activity for the custom-made aldehyde particles H23. LAC3 was used as model protein in these cases. Particles concentration 2mg/mL. Reaction temperature: 30°C. Rotating speed: thermomixer 1000 rpm. The maximum activity point for the grafted LAC3 appears for an initial enzyme concentration of 100µM. 150
- Fig. III-3-3 Enzyme loading tested by ELISA for the custom-made aldehyde particles. Three independent immobilizations were performed separately under the same conditions: particles concentration: 2mg/mL, immobilization buffer: 50 mM phosphate contains 0.1M sodium formate, pH 7.4. Initial laccase concentration: 100µM. Total system volume: 200µL. Ir catalyst: 10 eq [E]. Reaction temperature: 30°C. Thermomixer rotation set at 1000rpm. 2µg, 1µg and 0.5µg particles immobilized with different laccase were triplicated in the microwell for measurements. The points on the graph are representing the average value of the triplicate tests in the microwell. A and B are the enzyme loading of LAC3 and UniK₁₆₁ respectively. Error bar were less than 12% for the immobilized samples. 151
- Fig. III-3-4 Activity of self-produced aldehyde particles immobilized laccase towards ABTS, at pH 5.5, 30°C 153
- Fig. III-3-5 Oxidation of coniferyl alcohol catalyzed by immobilized laccases. The experiments were performed in 0.1M pH=5,5 Acetate buffer, at 30°C in a thermomixer set at 1000rpm, for maximum 22 hours, in a final volume of 500µL and CA concentration of 1.6mM, 340 ng immobilized enzyme. The ordinate is the ratio of the area of the peak corresponding to the reactant on the HPLC chromatogram to the area of the peak corresponding to the reference benzophenone. 154
- Fig. III-4-1 The inner core and outer shell of commercial azide particles (pictures are from <http://www.turbobeads.com/>) 157
- Fig. III-4-2 Schematic illustration of the immobilization of laccase onto the azide particle surface. A: reductive alkylation; B: Huisgen cycloaddition 157
- Fig. III-4-3 Relationship between the initial laccase concentration and the activity of the immobilized laccase for the commercial azide particles. Particles concentration 10mg/mL. Reaction temperature: room temperature. Rotating speed: thermomixer 1000rpm, final volume 1mL. Laccase activity were tested with ABTS as substrate in 0.1M acetate buffer pH 5.7 at 30°C. The maximum activity point of the grafted laccase appears at the initial enzyme concentration of 1µM. 158

Fig. III-4-4 Relationship between particles amount and the activity of the immobilized laccase. The final volume of the reaction system is 1mL; particles were tested at 1mg/mL and 10mg/mL, and the initial enzyme concentration used is 1 μ M and 10 μ M respectively to keep the ratio of surface functional groups and laccase (the stoichiometric ratio) unchanged. Reaction temperature: room temperature. Rotating speed: thermomixer 1000rpm. Laccase activity was tested with ABTS as substrate in 0.1M acetate buffer pH 5.5 at 30°C. 159

Fig. III-4-5 Effect of particle pretreatment on the immobilized laccase activity. Particles concentration 10mg/mL. The initial enzyme concentration is 10 μ M. Reaction temperature: room temperature. Rotating speed: thermomixer 1000rpm. The final volume of the reaction system is 1mL. Laccase activity were tested with ABTS in 0.1M acetate buffer pH 5.7 at 30°C..... 159

Fig. III-4-6 Enzyme loading tested by ELISA for the commercial azide particles. Three independent immobilizations were performed separately for each enzyme (A, B and C). 10 μ g, 20 μ g and 50 μ g particles immobilized with each laccase were triplicated in the microwell for measurement. The points in the graph are the average value of the triplicated tests in the microwell..... 160

Fig. III-4-7 Activity of laccases immobilized oncommercial azide particles towards ABTS, at pH 5.57, 30°C..... 162

Fig. III-4-8 Ratios of specific activities of free and immobilized laccase for different particles 164

Fig. III-4-9 Schematic diagram of aldehyde particles immobilization (reductive alkylation reaction) and Azide particles immobilization (reductive alkylation reaction plus Click chemistry)..... 164

Fig. III-4-10 Oxidation of coniferyl alcohol catalyzed by laccases immobilized on azide particles. Hybrids were incubated in 0.1M acetate buffer, pH=5,7 at 30°C on thermomixer 1000rpm, for a maximum of 3 hours, in a final volume of 1mL and CA concentration of 1.6mM, 323ng immobilized enzyme. The ordinate is the ratio of the area of the peak corresponding to the reactant on the HPLC chromatogram to the area of the peak corresponding to the reference benzophenone. 165

Fig. III-5-1 Surface modification of the custom-made magnetic particles 168

Fig. III-5-2 Microscopic morphology of amino particles 169

Fig. III-5-3 Effect of pH on the surface charge of amino particles 169

Fig. III-5-4 FT-IR spectrum of amino particles	170
Fig. III-5-5 Effect of initial laccase concentration on activities of immobilized laccase.....	171
Fig. III-5-6 Enzyme leaking in the supernatant after washing	173
Fig. III-5-7 Methods for preventing the leakage of immobilized laccase on MNPs.....	174

List of Tables

Table I-1-1 Several recent reports on laccase applications (without mediators)	32
(Continued) Table I-1-2 Several recent reports on laccase applications (with mediators)	33
Table I-2-1 Identified Dirigent proteins with a stereoselective coupling activity	38
Table I-2-2 Amino acid essential to the respective activity of <i>At</i> DIR6 and PsDRR206 as found in each pocket (reproduced from ref 83,102).....	41
Table I-3-1 Summary of the commonly used chemical reaction for immobilization of laccase	48
Table I-3-2 Materials for immobilization of laccase in some recently reported literatures	49
Table II-4-1 Ratio of (NOS samples/Benzo) in the HPLC chromatogram	98
Table II-A-1 Gradient analysis HPLC 30 min	105
Table III-2-1 Preliminary results of immobilization (1 mg particles, 0.021 μ mol laccase, total volume 1mL).....	119
Table III-2-2 Commercial aldehyde particles grafted with BSA.....	126
Table III-2-3 Surface functional groups calculated by the calibration curve.....	133
Table III-2-4 Enzyme loading calculations for commercial aldehyde particles immobilization	140
Table III-2-5 Specific Activity of free and immobilized laccase for commercial aldehyde particles	143
Table III-2-6 Normalized value of the consumed substrate [(initial CA area/benzo area) – (remaining CA area/benzo area)] of the free and immobilized laccase at the 6th hours. Area represent the peak area on the HPLC chromatogram	146
Table III-3-1 Enzyme loading calculations for self-produced aldehyde particles immobilization	152
Table III-3-2 Specific Activity of free and immobilized laccase for self-produced aldehyde particles (H23).....	154
Table III-3-3 Normalized value of the consumed substrate [(initial CA area/benzo area) – (remaining CA area/benzo area)] of the free and immobilized laccase at the 6th hours. Area represent the peak area on the HPLC chromatogram	155

Table III-4-1 Enzyme loading calculations for commercial azide particles immobilization ..	162
Table III-4-2 Specific Activities of free and immobilized laccases for commercial azide particles	163
Table III-4-3 Normalized value of the consumed substrate [(initial CA area/benzo area) – (remaining CA area/benzo area)] of the free and immobilized laccase at the 6th hours. Area represent the peak area on the HPLC chromatogram	166
Table III-5-1 Influence of buffers on immobilization reaction	170
Table III-5-2 Immobilization of LAC3 on different magnetic particles	172
Table III-5-3 Immobilization of LAC3 on MNPs with reductive agent	174
Table III-5-4 Immobilization of LAC3 on different magnetic particles with terephthalaldehyde as bridge	176

List of Abbreviations

A	ABTS	2,2'-azino-bis (3-ethylbenzothiazoline-6-sulphonic acid)
	AOC	Allene oxide cyclase
	AS	Acetosyringone
	AP	Alkaline phosphatase
B	bis-QM	bis-quinone methide (bis-QM)
	BPA	Bisphenol A
	BET	Brunauer–Emmett–Teller
	BSA	Bovine Serum Albumin
C	CA	Coniferyl Alcohol
	CLEAs	Cross-linked enzyme aggregates
	CS	Chitosan
	CC	Cyanuric Chloride
	CAC	Coniferyl Acetate
	CAZ	Coniferyl Azide
	CAM	Coniferyl Amino
D	DIRs	Dirigent Proteins
	DP	Dirigent Protein
	DCA	Dehydrodiconiferyl alcohol
	DMF	Dimethylformamide
	DMSO	Dimethyl sulfoxide
E	ET	Electron transfer
	EPR	Electron Paramagnetic Resonance
	EDAC	Carbodiimide
	ELISA	Enzyme linked immunosorbent assay
F	FA	Ferulic acid
	FPLC	Fast Protein Liquid Chromatography
G	GLU	Glutaraldehyde
	GUA	Guaiacylglycerol
H	HBT	1-hydroxybenzotriazole
	HB	Hydrogen Bond
	HAT	H-atom transfer
	HPLC	High-performance liquid chromatography
I	IDA	Iminodiacetic Acid
	IMAC	Immobilized Metal Affinity Chromatography

	IEP	Isoelectric point
	IR-ATR	Attenuated total reflection
	ISO	Isoeugenol
	IR-DRIFT	Diffuse reflectance infrared fourier transform spectroscopy
L	LMS	Laccase mediator system
	LC-MS	Liquid chromatography–mass spectrometry
M	MBP	Maltose binding protein
	IMA	Metal Affinity Immobilization
	MOF	Metal organic framework
	MNPs	Magnetic Nanoparticles
	MES	2-(N-morpholino) ethanesulfonic acid
	MALDI-TOF-MS	Matrix Assisted Laser Desorption Ionization-Time of Flight
N	NHE	Normal Hydrogen Electrode
	NHS	N-hydroxysuccinimide
	NMR	Nuclear Magnetic Resonance
	NOS	Non-laccase substrate
P	PDB	Protein Data Bank
	PEI	Polyethylenimine
	PCA	p-coumaric acid
	PINO	Pinoresinols
	PNPP	<i>p</i> -Nitrophenyl Phosphate
R	RT	Retention time
S	SBE	Soybean Meal Extract
	SA	Syringaldehyde
	SDS-PAGE	Sodium dodecyl sulfate polyacrylamide gel electrophoresis
	SEC	Size Exclusion Chromatography
	SGZ	Syringaldazine
	STDEV	Standard deviation
	SA	Specific Activity
T	TC	Tetracycline
	TEMPO	2,2,6,6 tetramethylpiperidine-1-oxyl
	TNC	Trinuclear Cluster
U	UV	Ultraviolet
	VIS	Visible

General Introduction

Nowadays, the need for a sustainable development of human society and the ecological, environmental, economic issues involved in are causing extensive concern in the international community. Therefore, green chemistry, clean technology, and environmentally friendly processes have been highly emphasized. Environmentally friendly economy is becoming a major driver of technological innovation, which poses to chemistry, especially synthetic chemistry new challenges.

More stringent regulations have been introduced to protect the environment by governments around the world, prompting the chemical industry to focus on eliminating or reducing the generation of waste from the source. This will inevitably put forward new requirements to the science and technology of chemicals and their production processes.

One of the most important pathways to achieve the above-mentioned targets is catalysis, including various forms of chemical catalysis and biocatalysis. Catalytic processes is the process of increasing the rate of chemical reactions by adding substances known as catalysts which can act repeatedly without being consumed during the process.¹ Thus, catalysis has been regarded as a process of high atom economies and therefore seen as green.

As it is defined, catalysis accelerates chemical reactions, thus playing an important role in modern society. An excellent example to illustrate that is the evolution of the production processes for lazabemide—an anti-*Parkinson* medicine developed by F. Hoffmann-La Roche AG company. The original synthesis process contains 8-steps with 8% yields, which had been shortened to only one-step by a Pd-catalyzed amidocarbonylation protocol with a yield of 65%.²

Until now, a large number of catalysts and catalyst types are utilized commercially, including heterogeneous catalysts (porous solids), homogeneous catalysts (dissolved in liquid reaction mixture), biological catalysts (as enzymes).³ Environmentally friendly, examples of catalysis combining both heterogeneous or homogeneous and enzymatic catalysis together have appeared recently. Green catalytic processes implies that chemical processes are made environmentally benign by taking advantage of the possible high yields and selectivity for the target products, with little or no unwanted side products and also often high energy efficiency.⁴

Referring to the increasing demand for environmentally friendly catalysis, biocatalysis is a part that cannot be ignored. The catalyst (an enzyme) itself is produced from readily available renewable resources, is biodegradable and essentially nonhazardous and nontoxic;⁵ enzymes do their work under mild conditions (in water, at room temperature and atmospheric pressure), and generate little waste products.⁶ Such sustainable development model displayed by enzyme-catalyzed process is exactly what is pursued in the present century.

Among all the enzymes possessing the ability to work as biocatalysts in the industry, laccase is a particular robust one which has been widely used in a variety of biocatalytic applications, it has received considerable attention from researchers since 1883, its first description by a Japanese scientist in the milky secretion of a very common tree in Japan named *Rhus vernicifera*.⁷ Indeed, owing to their high non-specific-substrate oxidation capacity, and the use of readily available molecular oxygen as final electron acceptor, laccases are useful biocatalysts for diverse biotechnological applications.⁸ However, the utilization of laccase in industry is limited by various factors. For instance, the purification process of laccase production requires relatively long time and large amount of economic investment. In addition, separation difficulties from the reaction mixture after catalysis restrict their recyclability, resulting in a further increased application cost. Also, the redox potential of laccase is relatively low, impairing their capacity to directly catalyze the degradation of most non-phenol substrates.⁹ What's more, the self-coupling reaction of radical intermediates generated by laccases oxidation tends to form a mixture of products from dimers to higher oligomers,¹⁰ underlining to a lack of selectivity, which is detrimental to the efficiency.

Much works have been done to improve the performance of laccase as biocatalysts. Various cultivation techniques that have been developed to efficiently produce laccase at the industrial scale.¹¹ Boosted yields and simplified purification process in laccase production are now available due to the development of robust heterologous expression systems, thus reducing costs.¹² Protein engineering offers the potential to tailor specific needs for efficient biocatalysts design.¹³ Besides, efforts have also been put into looking for the outside effectors to overcome limitations of laccase when working alone. For example, Laccase mediator systems (LMS) are explored to assist the action of laccases with extended substrate range from phenolic compounds to non-phenolic compounds.¹⁴ Immobilization of laccase on varieties of materials for different applications allows separation and recycling, *etc.*¹⁵ By imparting improved properties to laccases, these methods greatly facilitate the widespread application of laccases in biochemical fields.

Due to their exquisite performance towards transformation ranging from the oxidation of functional groups to the heteromolecular coupling for production of new antibiotics derivatives, or as a key steps in the synthesis of complex molecules,¹⁶ laccase have found significant applications in organic synthesis. However, as already mentioned, self-coupling reactions of radical intermediates generated by laccases generally form a mixture of products from dimers to higher oligomers, highlighting the lack of selectivity of the enzyme. In fact, this is a pattern in which radical polymerization universally occurs as a result of adapting the thermodynamical trends: without additional control and/or special physiological environment, racemic products will be produced. This situation is clearly unfavorable in some cases of synthesis area, especially in the field of pharmaceutical synthesis where the physiologically active form of a natural product or drug are

desired, because the other forms can be inactive or even toxic (a sadly famous example of such drugs is Thalidomide, the instructive history and detailed information on which can be found in a review¹⁷). Obtaining directly optically pure substances is very beneficial for the synthesis of pharmaceutical drugs to avoid chiral separation procedures or the use of expensive chiral catalyst. From this point of view, laccase is still facing the challenge of carrying out multistep reactions with high selectivity in order to achieve energy economy and elimination of undesirable by-products.

Few works have been dedicated to the introduction of some selectivity in laccase catalyzed reactions. Laccase-TEMPO mediated system is known to be capable of catalyzing the regioselective oxidation of the primary hydroxyl groups of sugar derivatives, allowing polymer functionalization.¹⁸ Also, it has been reported that by switching from one solvent to another can have a great influence on the selectivity of laccase catalyzed reaction (substrate affinity, ee, regio and chemo selectivity).¹⁹ Danieli and coworkers described for the first time a significant and unexpected solvent influence on the relative ratio of two dimers obtained upon oxidative coupling of phenols catalyzed by laccases, which gives new clues for the synthetic application of laccases in biocatalysis.²⁰ Besides, since the end of last century, a plant protein (dirigent protein, DIR) is known to have the ability to direct the stereoselective biosynthesis of optically pure products from monolignol-derived radicals in a reaction that otherwise would result in a mixture of racemic reaction products as mentioned above.²¹ Mechanistically speaking it seems that DIR binds specifically two radicals and holds them in place (in the cavity of a β barrel) to mediate selective C-C bond formation.

The action of dirigent proteins is inspiring for the development of selective laccases catalyzed reactions. Indeed, it would be of interest to be able to control the specificity of a reaction by introducing an effector (e.g. another enzyme or non-biological molecules) in the laccase based catalytic system. Cyclodextrins for example, are small organic cages that are simple DIR mimics affecting the fate of laccase mediated reactions.²² Far beyond molecules, exogenous materials brought close to the surface of the enzyme, like this happens during immobilization of laccase could be somehow assimilated to such a process, materials being here thought as external effectors. Indeed, beyond the commonly accepted role in the improvement of enzyme performance such as operational stability, resistance to high temperatures, *etc.*, why not considering the possibility of support materials introducing selectivity into the laccase catalytic process?

The concept of utilizing immobilization techniques to modulate selectivity of enzymes is getting strength on the fact that the process significantly influences enzymes properties as: i) it reduces the mobility of protein groups; ii) it causes protein conformation changes, in some cases even distort the active site; iii) it affects substrate and enzyme contact due to steric hindrance, iv) it possibly generates different physicochemical environments surrounding the enzyme. Therefore, depending on the nature of the support and the mode of the interaction between support and enzyme, exposing the

same protein region to different materials or exposing the same material to different region of the protein different conformational changes or enzyme distortion may be expected to occur. Illustrations on a control by the material are diffuse in the literature dedicated to enzyme immobilization. For example, from a report on the immobilization of a lipase on different supports leading to different enantioselectivity even in the same experimental conditions depending on the nature of support.²³ We strongly believe that taking these differences into account in the design of surface modification represents a potential to introduce (and control) further selectivity in enzyme catalyzed reactions.

Among all kinds of supports used so far for enzyme immobilization, superparamagnetic particles are one of the most popular materials. Due to their special core-shell structures, a variety of binding methods are available for the immobilization of proteins in different orientation. Besides, as a result of their superparamagnetic properties, an easy separation and recycling can be realized conveniently by using a simple magnet, a fact that greatly increase their interest in processes. So far, the potential of MNPs surface to modulate the enzyme properties towards selectivity has not yet been studied but is worth exploring. Combining the immobilization of enzymes in a specific manner and a variation of the nature of the functionalization layer, a control of selectivity in multistep reactions can be expected. Thus, the energy requirement will be minimized and undesirable by-products will be eliminated.

In conclusion, laccase is a robust catalyst with widespread applications in the biochemical fields. But laccase catalyzed radicals coupling lacks selectivity and tends to form a mixture of products from dimers to higher oligomers, which is not environmentally friendly as it carries undesired products formation. However, plant dirigent proteins direct the stereoselective coupling of phenols offering a site to control the fate of oxidation products. Taking inspiration from a DP exogenous site controlling laccase reactivity, we propose to graft laccase surface with materials as a way to induce selectivity in non-selective coupling reactions. Magnetic particles appear to have a great potential to drive selectivity in laccase catalyzed reactions.

Thus, this manuscript is organized into three chapters.

In the first chapter, a bibliography survey described the brief introduction of laccase, MNPs and dirigent proteins. Meanwhile, the structure, mechanism of function and application of these three objects were also reviewed.

The second chapter is focused on the study of *AtDIR6*, one of the first characterized dirigent protein, directing the coupling of phenoxy radicals to form an optically pure lignan: the (-)-pinoresinol. In this chapter, a continued research of *AtDIR6* on the mechanism of its function was investigated. First, *AtDIR6* was purified and its activity was assessed during coniferyl alcohol oxidation. Then analogues of coniferyl alcohol were synthesized and were used to explore the

plasticity of *AtDIR6* towards new substrates. Moreover, the stabilization of coniferyl alcohol analogues radicals by *AtDIR6* was monitored by EPR. Finally, coniferyl alcohol radicals was used as a probe to identify amino acids within the cavity of *AtDIR6* which are involved in the stereoselective control.

The third chapter is dedicated to the orientational immobilization of two variants of laccase (LAC3 and UniK161, representing different immobilization directions) onto different MNPs. Three particles were investigated, including Aldehyde particles (both commercial and self-produced one), Azide particles and Amino particles, which were described in subsections independently. In each subsection, the characterization of particles, exploration of the immobilization conditions, issues encountered during the exploration, as well as the final immobilization results were shown in details. In addition, the specific activity of these two variants of laccase after immobilization has been compared both towards ABTS oxidation and coniferyl alcohol biotransformation.

Reference

- (1) IUPAC - catalyst (C00876) <http://goldbook.iupac.org/terms/view/C00876> (accessed Jul 8, 2019). <https://doi.org/10.1351/goldbook.C00876>.
- (2) Schmid, R. Homogeneous Catalysis with Metal Complexes in a Pharmaceuticals' and Vitamins' Company: Why, What for, and Where to Go? 4.
- (3) Catalysis - an overview | ScienceDirect Topics <https://www.sciencedirect.com/topics/materials-science/catalysis> (accessed Jul 8, 2019).
- (4) Knözinger, H.; Kochloefl, K. Heterogeneous Catalysis and Solid Catalysts; 2003. https://doi.org/10.1002/14356007.a05_313.
- (5) Sheldon, R. A.; Woodley, J. M. Role of Biocatalysis in Sustainable Chemistry. *Chem. Rev.* **2017**, *118* (2), 801–838.
- (6) Arnold, F. H. Combinatorial and Computational Challenges for Biocatalyst Design. *Nature* **2001**, *409* (6817), 253.
- (7) Yoshida, H. CHEMISTRY OF LACQUER (URUSHI) Chemistry of Lacquer (Urushi). Part I. Communication from the Chemical Society of Tokio. *J. Chem. Soc. Trans.* **1883**, *43*, 472–486.
- (8) Matera, I.; Gullotto, A.; Tilli, S.; Ferraroni, M.; Scozzafava, A.; Briganti, F. Crystal Structure of the Blue Multicopper Oxidase from the White-Rot Fungus *Trametes Troglitii* Complexed with p-Toluate. *Inorganica Chim. Acta* **2008**, *361* (14–15), 4129–4137. <https://doi.org/10.1016/j.ica.2008.03.091>.
- (9) yaohua, G.; ping, X.; feng, J.; keren, S. Co-Immobilization of Laccase and ABTS onto Novel Dual-Functionalized Cellulose Beads for Highly Improved Biodegradation of Indole. *J. Hazard. Mater.* **2019**, *365*, 118–124. <https://doi.org/10.1016/j.jhazmat.2018.10.076>.
- (10) Llevot, A.; Grau, E.; Carlotti, S.; Grelier, S.; Cramail, H. Selective Laccase-Catalyzed Dimerization of Phenolic Compounds Derived from Lignin: Towards Original Symmetrical Bio-Based (Bis) Aromatic Monomers. *J. Mol. Catal. B Enzym.* **2016**, *125*, 34–41.
- (11) Brijwani, K.; Rigdon, A.; Vadlani, P. V. Fungal Laccases: Production, Function, and Applications in Food Processing. *Enzyme Res.* **2010**, *2010*.
- (12) Ayala, M.; Pickard, M. A.; Vazquez-Duhalt, R. Fungal Enzymes for Environmental Purposes, a Molecular Biology Challenge. *J. Mol. Microbiol. Biotechnol.* **2008**, *15* (2–3), 172–180. <https://doi.org/10.1159/000121328>.

- (13) Rodgers, C. J.; Blanford, C. F.; Giddens, S. R.; Skamnioti, P.; Armstrong, F. A.; Gurr, S. J. Designer Laccases: A Vogue for High-Potential Fungal Enzymes? *Trends Biotechnol.* **2010**, *28* (2), 63–72. <https://doi.org/10.1016/j.tibtech.2009.11.001>.
- (14) Morozova, O. V.; Shumakovich, G. P.; Shleev, S. V.; Yaropolov, Y. I. Laccase-Mediator Systems and Their Applications: A Review. *Appl. Biochem. Microbiol.* **2007**, *43* (5), 523–535.
- (15) Fernández-Fernández, M.; Sanromán, M. Á.; Moldes, D. Recent Developments and Applications of Immobilized Laccase. *Biotechnol. Adv.* **2013**, *31* (8), 1808–1825. <https://doi.org/10.1016/j.biotechadv.2012.02.013>.
- (16) Kunamneni, A.; Camarero, S.; García-Burgos, C.; Plou, F. J.; Ballesteros, A.; Alcalde, M. Engineering and Applications of Fungal Laccases for Organic Synthesis. *Microb. Cell Factories* **2008**, *7* (1), 32. <https://doi.org/10.1186/1475-2859-7-32>.
- (17) Vargesson, N. Thalidomide-Induced Teratogenesis: History and Mechanisms: Thalidomide-Induced Teratogenesis. *Birth Defects Res. Part C Embryo Today Rev.* **2015**, *105* (2), 140–156. <https://doi.org/10.1002/bdrc.21096>.
- (18) Fabbrini, M.; Galli, C.; Gentili, P.; Macchitella, D. An Oxidation of Alcohols by Oxygen with the Enzyme Laccase and Mediation by TEMPO. *Tetrahedron Lett.* **2001**, *42* (43), 7551–7553. [https://doi.org/10.1016/S0040-4039\(01\)01463-0](https://doi.org/10.1016/S0040-4039(01)01463-0).
- (19) Klibanov, A. M. Improving Enzymes by Using Them in Organic Solvents. *Nature* **2001**, *409* (6817), 241–246. <https://doi.org/10.1038/35051719>.
- (20) Intra, A.; Nicotra, S.; Riva, S.; Danieli, B. Significant and Unexpected Solvent Influence on the Selectivity of Laccase-Catalyzed Coupling of Tetrahydro-2-Naphthol Derivatives. *Adv. Synth. Catal.* **2005**, *347* (7–8), 973–977. <https://doi.org/10.1002/adsc.200505043>.
- (21) Davin, L. B.; Wang, H.-B.; Crowell, A. L.; Bedgar, D. L.; Martin, D. M.; Sarkanen, S.; Lewis, N. G. Stereoselective Bimolecular Phenoxy Radical Coupling by an Auxiliary (Dirigent) Protein Without an Active Center. *Science* **1997**, *275* (5298), 362–367. <https://doi.org/10.1126/science.275.5298.362>.
- (22) Tarrago, L.; Modolo, C.; Yemloul, M.; Robert, V.; Rousselot-Pailley, P.; Tron, T. Controlling the Polymerization of Coniferyl Alcohol with Cyclodextrins. *New J. Chem.* **2018**, *42* (14), 11770–11775.

(23) Mateo, C.; Palomo, J. M.; Fernandez-Lorente, G.; Guisan, J. M.; Fernandez-Lafuente, R. Improvement of Enzyme Activity, Stability and Selectivity via Immobilization Techniques. *Enzyme Microb. Technol.* **2007**, *40* (6), 1451–1463. <https://doi.org/10.1016/j.enzmictec.2007.01.018>.

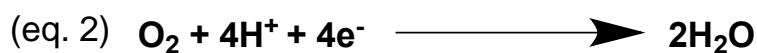
Chapter I

Bibliographical Survey

1 Laccase

1.1 Introduction to Laccase

Laccases (EC 1.10.3.2, p-diphenol: dioxygen oxidoreductase) belong to a group of polyphenol oxidases containing copper ions in their catalytic center and for that reason usually called multicopper oxidases (MCOs).¹ Due to the presence of the copper ions in their catalytic center, laccases have a distinctive ability to catalyze the oxidation of a wide range of aromatic and non-aromatic compounds including substituted phenols, some inorganic ions, and variety of non-phenolic compounds (eq. 1),² concomitantly with the reduction of molecular oxygen to water (eq. 2).³



Even though laccases were first found in plants, they were also discovered in insects, fungi as well as in bacteria, displaying various functions depending on their organism source, physiological and pathological conditions.⁴ Plant laccase are identified to be related to wound responses and lignin polymerization, while fungal laccases bring about the opposite process, participating in lignin degradation, morphogenesis, pathogenesis, and stress defense. Bacterial laccases participate in pigmentation, morphogenesis, toxin oxidation and protection against oxidizing agents and UV light; laccases from insects are mainly associated with cuticle sclerotization.⁵

Laccases are widely used in various industrial and biotechnological fields, such as bio bleaching in textile industry and lignin degradation in paper industry, they are eco-friendly enzymes also work in bioremediation process, organic synthesis¹² and in the cathodic compartment of biofuel cells.⁷

1.2 Laccase structure and active site

Laccase contains four copper ions located in two active centers, a schematic representation of which is shown in **Fig. I-1-1** (a) and (b). These ions are classified in three groups based on their coordination and spectroscopy properties. A large amount of literature is available providing detailed descriptions on the three types of copper.^{3,4,8-11} Briefly, they are described as follows:

Type 1 copper ion: present in a mononuclear site (oxidation center), the paramagnetic type 1 copper shows an intense electronic absorption band at the wavelength near 600 nm ($\epsilon = 5000 \text{ M}^{-1} \cdot \text{cm}^{-1}$) which is responsible for the deep blue color of the enzyme in the oxidized state, and also exhibits a weak parallel superfine splitting in the EPR spectrum. The T1 copper site is coordinated to two histidine and one cysteine. In some cases, one methionine is found as additional axial ligand.

Type 2 copper ion: present in a trinuclear cluster forming the dioxygen reduction center, the T2 copper ion is not visible in the electron absorption spectra and displays ultrafine splitting in EPR spectra typical for copper ions in tetragonal complexes. The Type 2 copper has two histidine and water as ligands.

Type 3 copper pair: The Type-3 copper is a binuclear site coordinated to three histidines and a bridging hydroxyl ligand (bis- μ -hydroxo). This site can be identified by the presence of a shoulder at 330 nm in the UV region of the spectrum. As the result of the anti-ferromagnetic coupling of the copper pair there is no EPR signal.

The T1 copper site is the primary electron acceptor in a laccase catalyzed reaction, where four single-electron oxidations of a reducing substrate occur. The type 2 and type 3 copper ions form together a trinuclear cluster (TNC), where the reduction of molecular oxygen and release of water takes place.

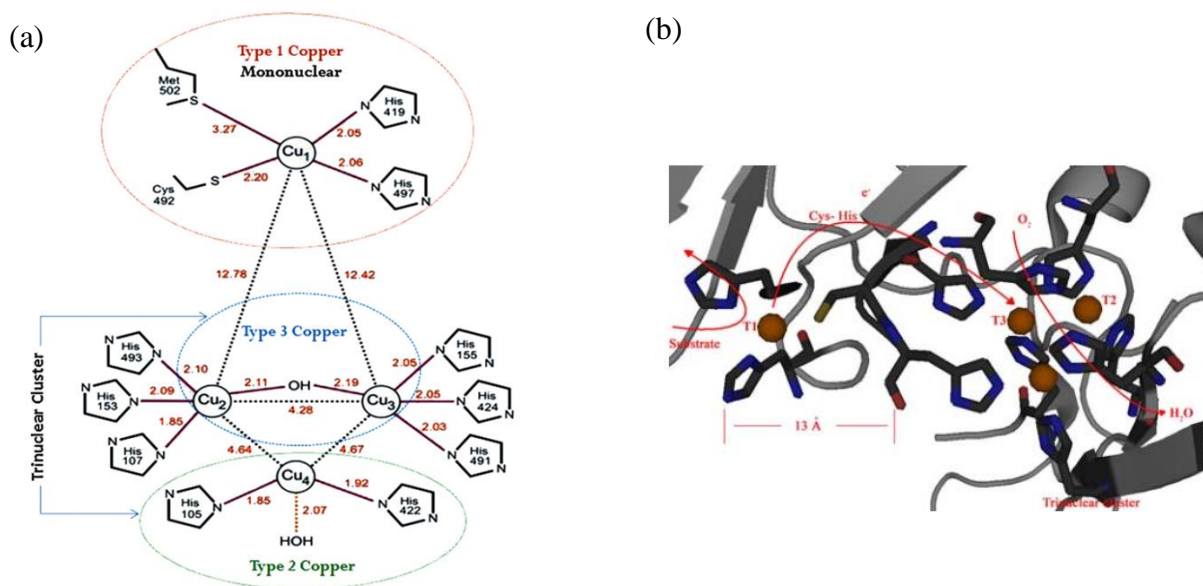


Fig. I-1-1 Structure of copper center/active site of laccases (a) the three types of copper coordination, including interatomic distances among all relevant ligands ⁴ (b) structure of the laccase active sites with arrows marking the flow of substrates, electrons (e^-) and O_2 ¹⁰

Laccases have pronounced structural homology despite their different sources. The overall structure of laccase consist of three consecutively connected cupredoxin-like domains designated as D1 (N-terminal), D2, and D3 twisted in a tight globule,¹² as exemplified by a fungal laccase in **Fig. I-1-2**.¹³ Usually, the structure is stabilized by one or two disulfide bridges between D1 and D2. The TNC is placed between D1 and D3, while the type 1 copper ion is found in D3 (C-terminal). Domain 2 does not participate directly in the formation of the active sites; it most likely contributes to the stability of the protein assembly as a functional unit.¹¹



Fig. I-1-2 Three-dimensional representation of a fungal laccase based on the coordinates of the PDB entry 2HRG. Cupredoxine domains are colored from blue (D1) to green (D2) to red (D3). Light-orange spheres depict copper ions, an isolated Cu (II) T1 close to the surface of the enzyme in D3 and a Cu (II) T2-T3 trinuclear cluster embedded in the enzyme at the D1-D3 boundaries.

1.3 Catalytic mechanism of laccase

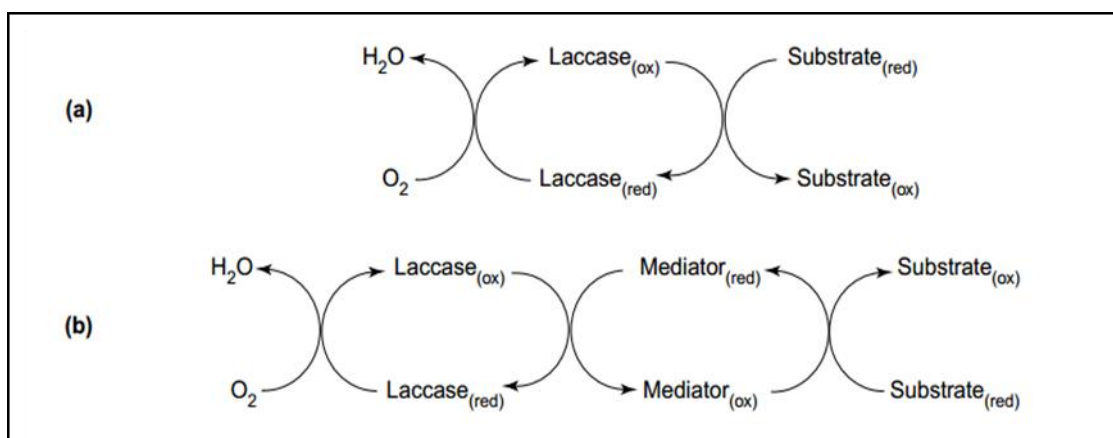


Fig. I-1-3 Schematic representation of laccase-catalyzed redox cycles for substrates oxidation in the (a) direct or (b) in-direct (with present of chemical mediators) way.¹⁴

As mentioned above, due to the copper ions present in their active sites and their specific structure, laccase is able to drive electrons from a reducing substrate through the type 1 copper site to the TNC where molecular oxygen is reduced. Reactions catalyzed by laccase can be divided into two types: direct oxidation (**Fig. I-1-3 (a)**) and indirect (mediated) oxidation (**Fig. I-1-3 (b)**).

Direct oxidation, i.e. the oxidation of substrate to the corresponding radical as a result of direct interaction, happens only in compounds the ionization potential of which does not exceed the redox potential of the T1 copper ion.¹⁵ The mediated oxidation is a two-step process: first the enzyme catalyzes the oxidation of a molecule acting as a redox mediator, then the oxidized mediator oxidizes the substrate.^{16,17}

1.4 Laccase mediator system (LMS)

As described above, the redox potential difference between T1 copper ion and substrate plays a crucial role in laccase catalytic efficiencies.¹⁸ Laccase is able to directly oxidize structure unit of phenol, because phenolic substrates have a potential of 0.5~0.9V vs. NHE (Normal Hydrogen Electrode), which is well matched with the redox potential at which laccase operates (0.5~0.8V vs. NHE depending on the fungal source).¹⁹ But substrates like aliphatic alcohols and ether groups in native lignin with a high redox potential (above 1.2V vs. NHE) cannot be directly oxidized by laccases.²⁰ Additionally, the chemical structure of the substrate is also an important factor influencing its oxidation by laccase.²¹ Bulky compounds are unable to access the active site of due to steric hindrance²² and therefore are not directly oxidized by laccase. Thus, a redox mediator that can act as an intermediate substrate is required.

A mediator is a small molecule acting as “electron shuttle”²³ between the laccase and the substrate; it is continuously oxidized by the laccase and subsequently reduced by the substrate during the catalytic process.²² The combination of laccase and a redox mediator constitutes the so-called “laccase-mediator system” or LMS.^{24, 25}

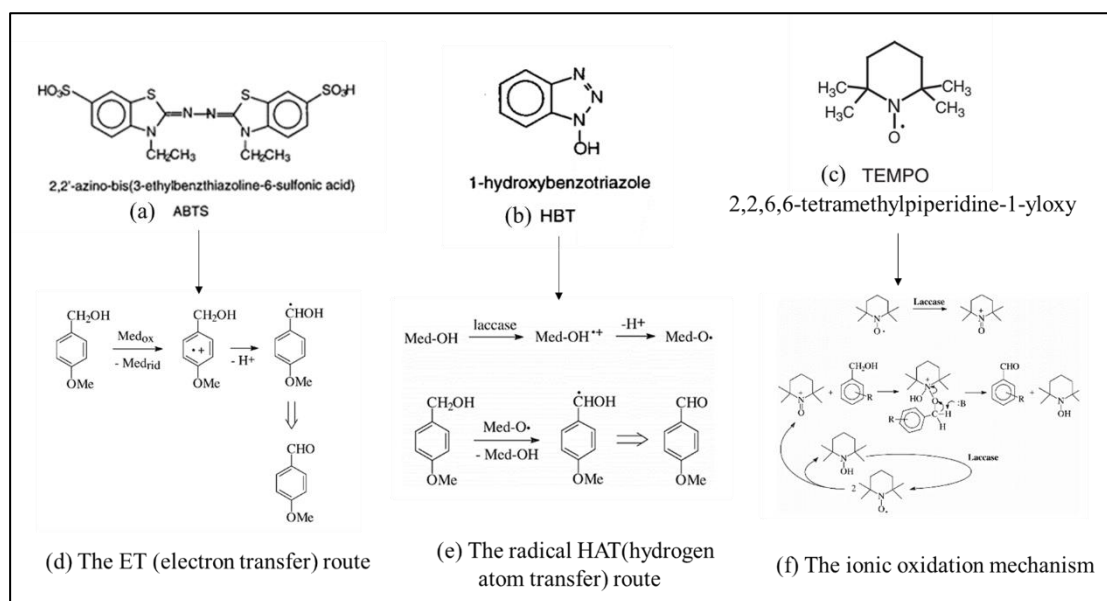


Fig. I-1-4 Structure of three typical artificial mediators using in LMS: (a) ABTS (2,2'-Azino-bis (3 ethylbenzothiazoline-6-sulfonic acid)); (b) HBT (1-hydroxybenzotriazole); (c) TEMPO (2,2,6,6 tetramethylpiperidine-1-oxyl) and their corresponding mechanisms proposed: (d) Electron transfer (ET) route of laccase-ABTS system; (e) Radical H-atom transfer (HAT) pathway of laccase-HBT system; (f) Ionic oxidation mechanism of laccase-TEMPO system.

2,2'-Azino-bis (3-ethylbenzothiazoline-6-sulfonic acid) (ABTS), 1-hydroxybenzotriazole (HBT), and 2,2,6,6-tetramethylpiperidine-1-oxyl (TEMPO) are three typical artificial mediators using in laccase mediator system for oxidation of non-phenolic lignin compounds, each of them

possess distinct reaction mechanism depending on their chemical structure (see **Fig. I-1-4** for their formulas and proposed mechanisms).^{26, 27}

Although Synthetic mediators like ABTS and HBT are widely used for laccase in numerous applications, such as dye decolorization, lignin degradation and biotransformation of pharmaceuticals (see (Continued) **Table I-1-2** for some of recent reports on LMS applications), the applications of artificial mediators in industrial processes are still restricted by their high costs and safety concerns regarding, for example, explosiveness and toxicity.²⁸ Therefore, natural mediators as more economically feasible and environmentally friendly mediators to overcome this hurdles are coming up.²⁹ The most common examples of natural mediators include lignin derived phenol compounds, such as acetosyringone, syringaldehyde and vanillin.³⁷

1.5 Biochemical applications of laccase

In nature, laccases play a key role in the formation or degradation of lignin. Moreover, assisted by LMS, the range of laccase applications has been extended to other fields like bio bleaching for dyes decolorization, modification of pulp, treatment of wastewater, and more recently, degradation of pharmaceuticals.

Besides, using laccases in organic synthesis has drawn considerable attentions recently, since laccase or LMS have broad substrate range and demonstrate many advantages over conventional chemical catalysts for example relatively inexpensive, highly selective, and are active in aqueous solvents and under mild conditions.³⁰ Indeed, laccases enable to abstract hydrogen from phenolic hydroxyl groups using molecular oxygen as electron acceptor, which forms phenoxy radicals; these radicals undergo self-coupling reactions to form different C-O and C-C dimers before oligomerization and polymerization reactions. Based on this mechanism, laccase was exploited for the mild polymerization of natural compound derivatives, for example, to produce polycatechol from catechol monomers (**Fig. I-1-5 (1)**).³¹

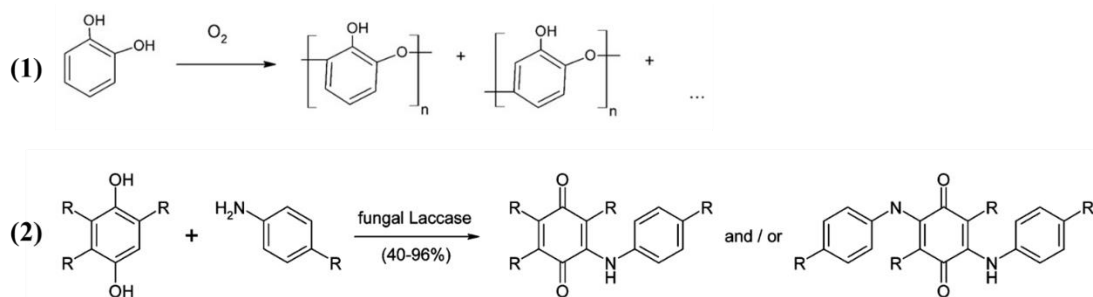


Fig. I-1-5 Examples of polymerization of laccase-generated radicals. (1) production of polycatechol from catechol monomers. (2) the coupling of p-hydroquinones and aromatic amines.

Another example of polymerization related to laccase-generated radicals includes laccase-catalyzed cross-coupling reaction, where the reactive intermediates are trapped and do not form the usual family of derivatives, for example: the coupling of p-hydroquinones and aromatic amines (**Fig. I-1-5 (2)**).^{32,33}

Laccase catalyzed peptide synthesis are also reported, one example is that laccases were used for the selective removal of phenylhydrazide-protecting groups in a mild process that causes neither oxidative modification nor destruction of methionine or tryptophan side chains.³⁴ Furthermore, Laccase is also used to oxidatively transform organic compounds to produce pharmaceutical importance products such as penicillin X derivatives.³²

In brief, because of their variety biochemical properties, high stability, broad substrate range, and widespread applications, laccases are very impressive and valuable biocatalysts in biotechnology. More applications of laccase, including application of LMS, reported in the recent years are summarized in **Table I-1-1**.

Although laccases are good biocatalysts for a wide range of applications, their main drawback is a lack of selectivity and the generation of radical species that evolve independently of the enzyme. If suitable methods to direct regio- and chemoselective polymerizations were to be found, functional and useful polymers which normally are difficult to synthesize by classical methodologies could be yielded. From this point of view, laccase-catalyzed chemical synthesis would have great potentials. In the next subsection, dirigent protein as a natural effector to bring stereoselectivity to laccase catalyzed coupling of monolignols will be introduced.

Table I-1-1 Several recent reports on laccase applications (without mediators)

Source of laccase	Application
<i>Pleurotus ostreatus</i>	Synthesis of gold nanoparticles ³⁵
<i>Moniliophthora roreri</i>	Micropollutant degradation ³⁶
<i>Myrothecium verrucaria</i>	Dye Decolorization ³⁷
<i>Trametes villosa</i>	Synthesis of 2,3-ethylenedithio-1,4-quinones ³⁰
<i>Saccharomyces cerevisiae</i>	Synthesis of C–N heteropolymeric dye ³⁸
Suberase®	Synthesis of coumestan derivatives ³⁹
<i>Yarrowia lipolytica</i>	Decolorization of environmental pollutant dyes ⁴⁰
<i>Trichoderma harzianum</i>	Decolorize fungal pigments on aging paper and parchment ⁴¹
<i>Trametes versicolor</i>	Synthesis of arylsulfonyl triazolinediones ⁴²
<i>Trametes versicolor</i>	Biofuel Cells ⁴³

(Continued) **Table I-1-2** Several recent reports on laccase applications (with mediators)

Mediators	Source of laccase	Application
Syringaldehyde (SA), acetosyringone (AS) and p-coumaric acid (PCA)	<i>Pycnoporus cinnabarinus</i>	Biobleaching of flax pulp ⁴⁴
VLA, violuric acid	<i>Trametes villosa</i>	Degradation of lignin in wood pulp of paper industry ⁴⁵
Vanillin	<i>Trametes</i> species	Crosslinking of milk proteins ⁴⁶
1-hydroxybenzotriazole (HBT) syringaldehyde (SA)	<i>Peroneutypa scoparia</i>	Degradation of leather dyes ⁴⁷
2,2,6,6-tetramethylpiperidine 1-oxyl (TEMPO)	<i>Galerina</i> sp.	Azo dye decolorization ⁴⁸
p-coumaric acid, syringaldehyde, acetosyringone	<i>Trametes versicolor</i>	Biocatalytic degradation of carbamazepine ⁴⁹
HBT, ABTS, syringaldehyde, acetosyringone, p-coumaric acid, methyl syringate (Novozymes®)	<i>Trametes villosa</i> etc.	Biodeinking of flexographic inks ⁵⁰
ABTS	<i>Trametes versicolor</i>	Biotransformation of carbamazepine ⁵¹
Acetosyringone, methyl syringate	<i>Streptomyces ipomoeae</i>	Decolorization and detoxification of textile dyes ⁵²
acetosyringone	<i>T. trogii</i>	Decolourization and detoxification of textile industry wastewater ⁵³
soybean meal extract (SBE)	<i>Trametes versicolor</i>	Degradation of antibiotics metabolites (sulfadimethoxine) ⁵⁴
HBT	<i>Trametes versicolor</i>	Degradation of the herbicide isoproturon ⁵⁵
Syringaldehyde	<i>Pycnoporus sanguineus</i>	Pharmaceuticals degradation ⁵⁶
HBT	<i>Trametes versicolor</i>	degradation of antiepileptic drug (Carbamazepine) ⁵⁷
HBT	<i>Ganoderma lucidum</i>	transformation of antimicrobial agent (TCS) ⁵⁸
1-hydroxybenzotriazole (HBT), syringaldehyde (SA),	<i>Trametes versicolor</i>	Rare organic contaminant degradation ^{59,60}

2 Dirigent protein

Although the oxidative coupling of phenols only produces racemic products *in vitro*, the coupling reaction takes place in a deterministic way in nature. In *vivo*, regio- and stereoselective phenol coupling can be observed both in plant secondary metabolism and in bacteria, lichen, and fungi.⁶¹ It seems that these organisms clearly control the coupling reaction; how they do it, what can we learn from them is therefore stimulating and worth exploring. The discovery of dirigent protein (DP) is the first step toward the understanding on how nature control the coupling of phenols in plants. Here in this section, the currently available information about DP will be described, including their discovery, the resolution of DP 3D structures, and hypotheses on their mechanism of action.

2.1 From lignan biosynthesis to dirigent protein

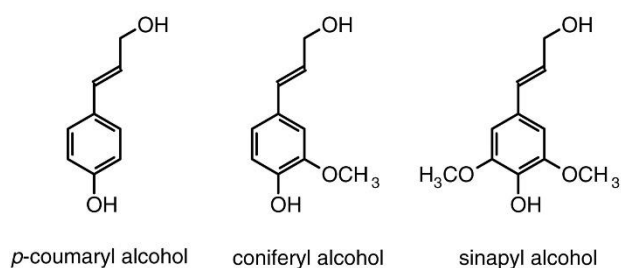


Fig. I-2-1 Chemical structure of the three commonly occurring monolignols

Lignans are natural products that occur widely in the plant kingdom. They are generated via monolignol (**Fig. I-2-1**) coupling in terrestrial vascular plants, typically forming dimers and/or higher oligomers.⁶² The recognized physiological role of lignan in *planta* involves plant defense, particularly in leaf, (heart)-wood, knot, and seed coat tissues by acting as phytoestrogens and antioxidants. The term lignan is structurally identified as a class of dimeric phenylpropanoid (C_6C_3) metabolites linked by an interunit linkage 8-8' bond (**Fig. I-2-2**).⁶³ Other types of coupling (e.g. 8-5') are designed as neo-lignan.

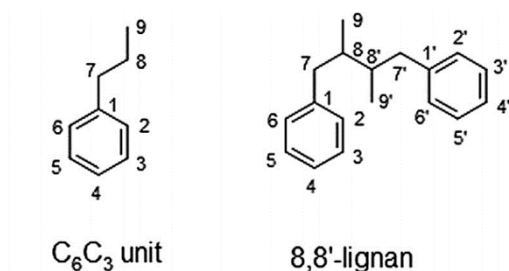


Fig. I-2-2 Lignan core structures

The lignan pinoresinol, a central precursor of many 8-8' linked plant lignans, is obtained by stereoselective coupling of two entities derived from E-coniferyl alcohol.⁶⁴ The dimerization of E-coniferyl alcohol to form lignans generally involves two steps. In the first step, a single-electron oxidation of E-coniferyl alcohol catalyzed by an oxidase/oxidant (such as peroxidases, laccase or ammonium peroxydisulfate) occurs, forming the corresponding phenoxy radical species. In the second step, radicals dimerize to yield *in vivo* optically pure pinoresinol under strict regio- and stereospecific control (Fig. I-2-3 (a)) whereas *in vitro* the oxidative coupling of E-coniferyl alcohol by peroxidases or laccases lacking regio- and stereoselectivity, results in a mixture of (+/-) 8,8', (+/-) 8,5', and 8-O-4' linkages (Fig. I-2-3 (b)).⁶⁵

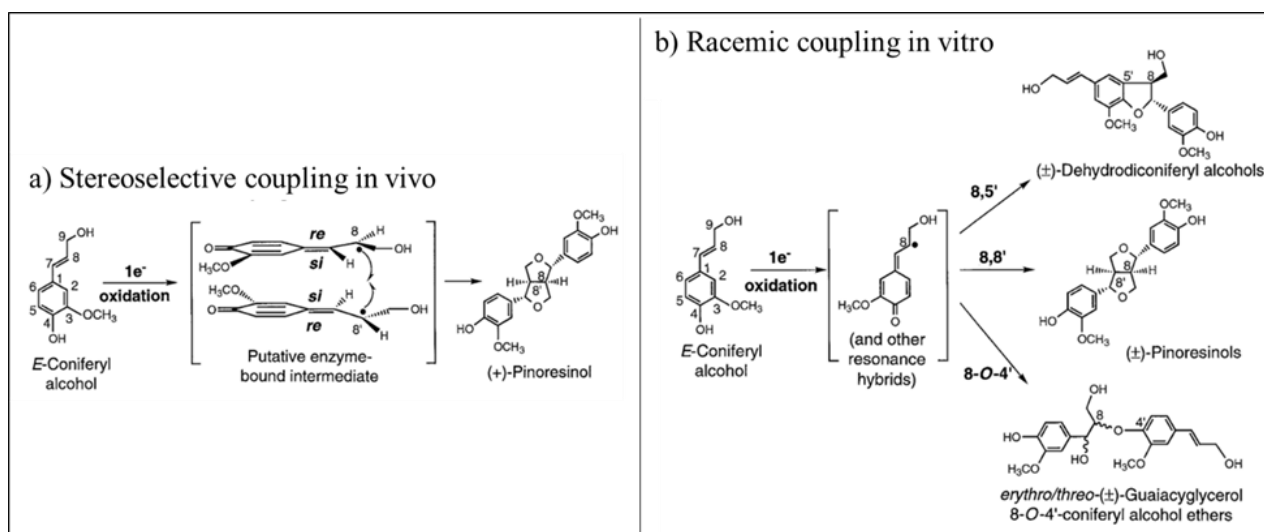


Fig. I-2-3 Bimolecular phenoxy radical coupling products from E-coniferyl alcohol. (a) Stereoselective coupling generating (+)-pinoresinol. (b) Dimeric lignans formed via “random” coupling.

The aforementioned ability of vascular plants to control the regio- and stereoselectivity in products like 8,8'-coupled (+)-pinoresinol has been shown to involve a dedicated protein working as a template. This ability has been first recognized by Lewis *et al.* in the crude cell wall extracts of *Forsythia intermedia*.⁶⁶ The protein they purified has no detectable catalytic activity but is mandatory to orient the coniferyl alcohol-derived free radicals for a stereoselective coupling, and therefore has been designated as dirigent protein (Latin: dirigere, to align or guide).⁶⁵ Dirigent proteins or DIRs form a new class of proteins, originally annotated as wound healing proteins, able to direct selective radical coupling reactions.

In addition to the *Forsythia* dirigent protein (*FiDIRs*), (+)-pinoresinol-forming dirigent proteins (*DIRs*) have been also found in other plants. For example: *TpDIR5* and *TpDIR8* have been identified in *Thuja plicata*,⁶⁷ *ScDIR1* in *Schisandra chinensis*.⁶⁸

Additionally, lignans derived from (–)-pinoresinol isolated from a variety of plants like (–)-secoisolariciresinol from *Wikstroemia sikokiana*⁶⁹ and (–)-lariciresinol from *Arabidopsis thaliana*,⁷⁰ indirectly indicate the existence of an enantio-complementary DIR. (–)-pinoresinol forming DIR such as AtDIR6 and AtDIR5 have been characterized from *Arabidopsis thaliana*. They have a high sequence similarity with the known (+)-pinoresinol-forming DIRs⁷¹ and are able to generate (–)-pinoresinol both *in vivo* and *in vitro*.⁷²

E-coniferyl alcohol is not the only substrate for which the coupling is guided by a dirigent protein. A (+)-gossypol-forming dirigent protein that mediates a peroxidase catalyzed reaction in steering the stereoselective coupling of a terpenoid pathway substrate, hemigossypol, to (+)-gossypol has been also identified (Fig. I-2-4).

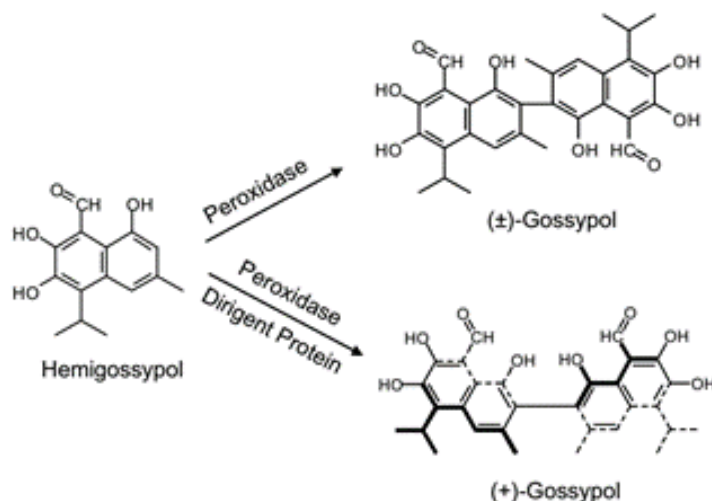


Fig. I-2-4 Biosynthesis of gossypol by free radical coupling of hemigossypol generated by peroxidase in the presence or absence of a cotton dirigent protein.⁷³

At present, numerous DIRs having the ability to guide stereoselective coupling of radicals have been identified. Most of them direct the polymerization of monolignols into the (+)-pinoresinol or (–)-pinoresinol. Some of the functionally identified dirigent protein are summarized in **Table I-2-1**.

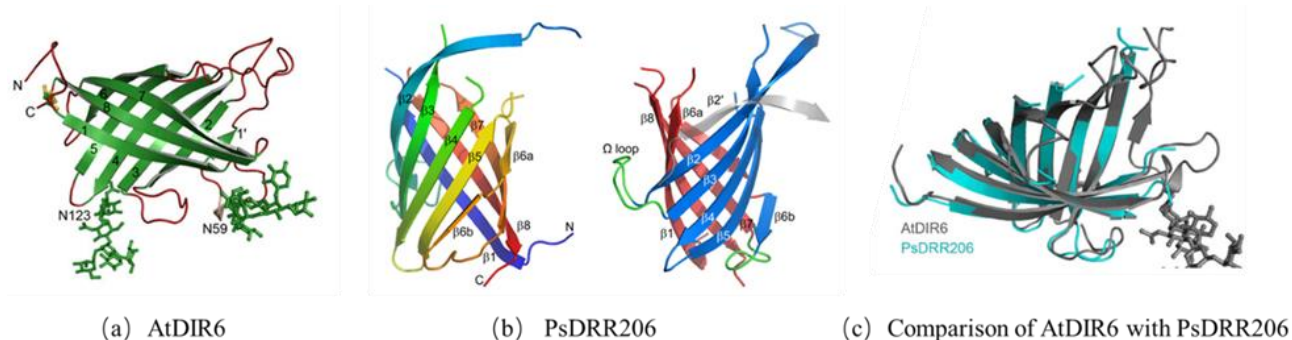
Table I-2-1 Identified Dirigent proteins with a stereoselective coupling activity

Plant	Dirigent protein	Enantioselective product	Reference
<i>Forsythia intermedia</i>	<i>FiDIR1</i>	(+)-pinoresinol	65
<i>Thuja plicata</i>	<i>TpDIR5, TpDIR8</i>	(+)-pinoresinol	67
<i>Arabidopsis thaliana</i>	<i>AtDIR6</i>	(-)-pinoresinol	71
	<i>AtDIR5</i>	(-)-pinoresinol	68
<i>Schisandra chinensis</i>	<i>ScDIR1</i>	(+)-pinoresinol	68
<i>Linum usitatissimum</i>	<i>LuDIR1-4</i>	(+)-pinoresinol	74
	<i>LuDIR5 and 6</i>	(-)-pinoresinol	74
<i>Pisum sativum</i>	<i>PsDRR206</i>	(+)-pinoresinol	75
<i>Pyrus bretschneideri</i>	<i>PbDIR4</i>	(+)-pinoresinol	76
<i>Triticum aestivum</i>	<i>TaDIR13</i>	(+)-pinoresinol	77
<i>Gossypium barbadense</i>	<i>GbDIR1 and 2</i>	(+)-gossypol	78
<i>Gossypium hirsutum</i>	<i>GhDIR3</i>	(+)-gossypol	79
	<i>GhDIR4</i>	(+)-gossypol	80

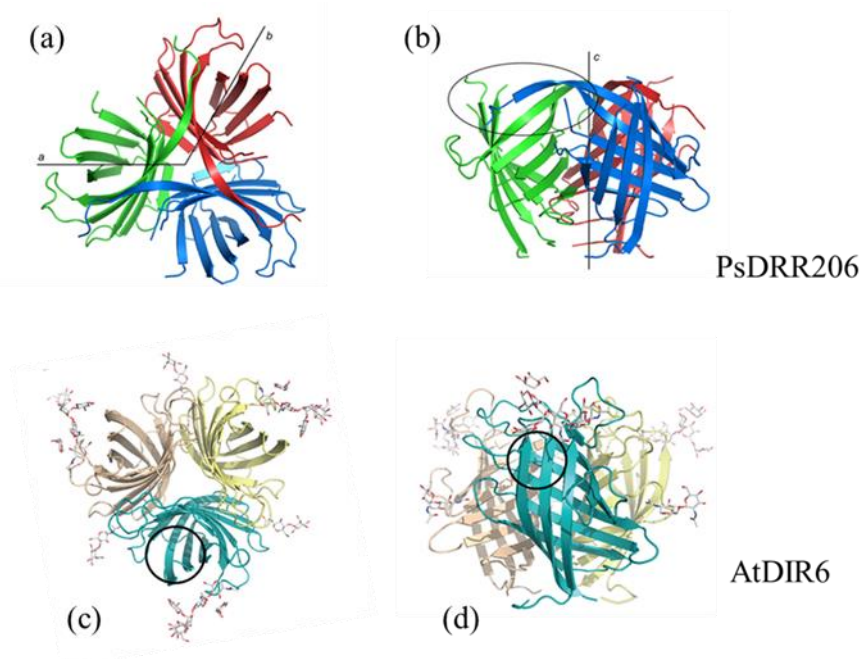
2.2 Structure and proposed Mechanism of dirigent protein

2.2.1 Structure of DIRs

The first structural model of DIRs was proposed for *AtDIR6*, using the structural and functional similarities with allene oxide cyclase (AOC) and lipocalins.⁸¹ The homology-based *AtDIR6* model reveals the DIR monomer as an eight-stranded antiparallel β -barrel (the strands were labelled $\beta 1$ to $\beta 8$, **Fig. I-2-5 (a)**), with a hydrophilic protein surface facing the solvent and a hydrophobic cavity. This eight-stranded antiparallel β -barrels structure has been later confirmed by the resolution of the structure of *AtDIR6*⁸² and that of the enantiocomplementary (+)-pinoresinol-forming DIRs *PsDRR206*.⁶² As depicted in cartoon of the structure of *PsDRR206* (**Fig. I-2-5 (b)**), the β -barrel can be viewed as two highly curved anti-parallel sheets formed by strands $\beta 2$, $\beta 3$, $\beta 4$, and $\beta 5$ (β -sheet 1) and by strands $\beta 6$, $\beta 7$, $\beta 8$, and $\beta 1$ (β -sheet 2), respectively. The superimposition of the barrels the *At* and *Ps* monomers reveals a similar arrangement of the β -sheets indicating the same barrel diameter in both proteins (**Fig. I-2-5 (c)**). In crystals, both *PsDRR206* and *AtDIR6* form tightly packed homotrimers (**Fig. I-2-6**).^{62, 82}

Fig. I-2-5 Structure of the DIRs monomer. (a) Monomer of (-)-pinoreosinol forming DIR *AtDIR6*, showing strands

1 to 8.⁸² (b) Monomer of (+)-pinoreosinol forming DIR *PsDRR206*. Left, ribbon representation of the eight-stranded β -barrel rainbow-colored from the N terminus (blue) to the C terminus (red), showing the secondary structure labeling; right, the *PsDRR206* monomer rotated 90° about a vertical axis and colored to show the two component β -sheets in blue (β -sheet 1) and red (β -sheet 2).⁶² (c) Comparison of *AtDIR6* with *PsDRR206*. Overlay of monomer of *AtDIR6* (gray) with monomer of *DRR206* (cyan; PDB accession code 4REV).⁸²

Fig. I-2-6 Structure of DIR trimers. (a) *PsDRR206* trimer viewed down the 3-fold *c*-axis of the H32 space group,

the *a*- and *b*-axes are indicated. (b) same structure as in (a) rotated 90° about the *a*-axis. One of the extended β 2 strands (blue) traverses the trimer interface into neighboring monomer (green), and this region is highlighted by the black oval. (c) structure of *AtDIR6* trimer at top view. (d) structure of *AtDIR6* trimer at side view. Each monomer is shown in a different color. The location of the active site is highlighted by a black circle in one of the monomers.

PsDRR206 and *AtDIR6* are representative of enantiocomplementary pinosresinol-forming DIRs. Globally, they share similar structures as shown in **Fig. I-2-5** and **Fig. I-2-6**, but several differences can be highlighted: i) in *AtDIR6*, all the loops at the open end of the barrel are well resolved. In *PsDRR206*, on the other hand, the loops surrounding the cavity are more flexible and therefore not well resolved. ii) the strands leading to these loops are bent inward in *AtDIR6*, which in contrast, point more toward the solvent in *PsDRR206*. As a result, the cavity of *PsDRR206* appears flatter and more open (**Fig. I-2-5** (c)). iii) in *PsDRR206*, the loop connecting the first two strands traverses the interface into the neighboring monomers (**Fig. I-2-6** (a) (b)) thus adding a sixth strand to β -sheet 1, but no such domain connection is seen in *AtDIR6*.

2.2.2 Active site of DIRs

The putative active site in the DIRs would consist of two pockets, pocket A and B, divided by conserved residues, each pocket lined with a set of hydrophilic and potentially functional residues (**Fig. I-2-7** (a) and (c)).^{62,82} Some of these residues are conserved between (+)- and (–)-pinosresinol forming DIRs, indicating a significant responsibility to the DIR activity.

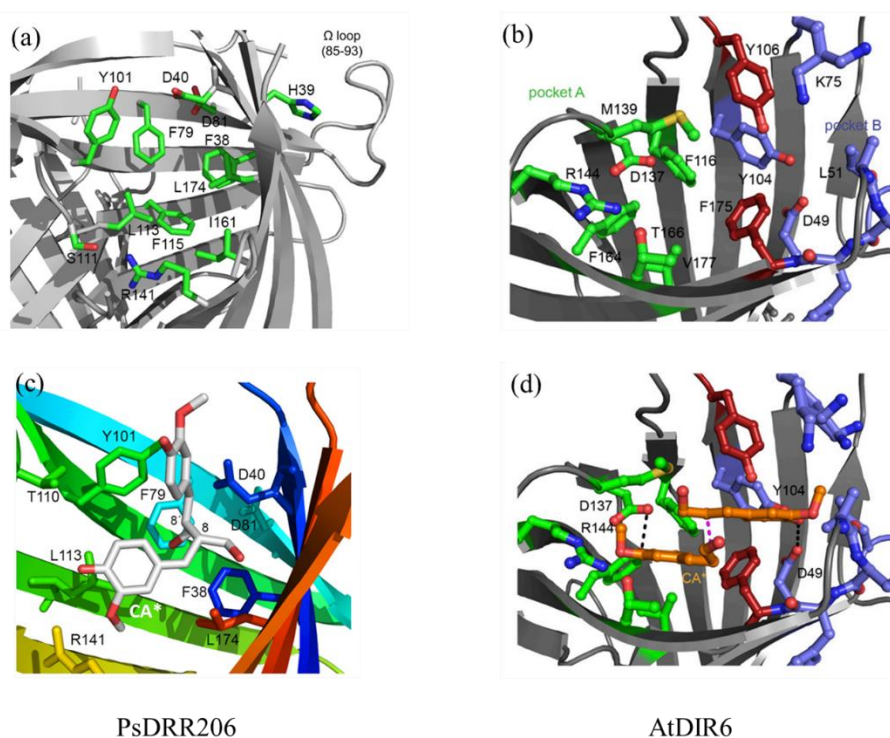


Fig. I-2-7 Active site with the interior lined residues in (a) *PsDRR206* and (b) *AtDIR6*. Potential binding mode of DIRs supported by energy minimization of the manually placed ligands in (c) *PsDRR206* and (d) *AtDIR6*.

Site-directed mutagenesis has been used to study the interior of each pocket and the results have highlighted some amino acid residues essential to the specific activity of each of the enantiocomplementary DIRs (**Table I-2-2**).

Table I-2-2 Amino acid essential to the respective activity of *AtDIR6* and *PsDRR206* as found in each pocket (reproduced from ref ^{62,82})

	<i>AtDIR6</i>	<i>PsDRR206</i>
Pockets A	D137, R144, T166	D134, R141
Pockets B	D49, K75, K78	H39, T84, S91
The boundary between A and B	Y104, Y106	E169, R173

2.2.3 Proposed mechanism of DIRs

Based on the 3D structure of DIRs it has been deduced that the inner hydrophobic surface of DIRs cavities forms a binding site for coniferyl alcohol radicals. The product formation is directed by the binding and positioning of the substrate and by steric restrictions imposed by the protein environment to the enzyme-bound substrate.⁸¹ The DIRs promoted regio and stereoselective coupling of laccase catalyzed coniferyl alcohol radicals can be divided into the following steps:

I Laccase catalyze coniferyl alcohol oxidation into radicals

Free-radical species from E-coniferyl alcohol, rather than the E-coniferyl alcohol itself, is supposed to be the true substrates that bind to the dirigent protein prior to coupling.⁶⁵ *In vitro*, the radicals can be produced by single-electron oxidation of E-coniferyl alcohol catalyzed by laccase, or other oxidase/oxidant such as peroxidases, laccase or ammonium peroxydisulfate.

II Dirigent protein accommodate CA radicals in an orientation that favors 8-8' coupling

Due to the overall organization of the trimer structures and the size of the monomer cavity of DIRs, it has been proposed that each subunit of the DIRs homotrimer can capture and bind two phenoxy radicals in its cavity. The accommodation of the two CA[•] inside the cavity places the propionyl side chains in a precisely positioned orientation to enable 8–8' coupling: in *PsDRR206*, the binding pocket binds two CA[•] in an orientation which allows the *si-si* coupling to form the R,R-configured bis-quinone methide (bisQM) as precursor of (+)-pinoresinol (**Fig. I-2-7 (c)**); in the homologue *AtDIR6*, pockets A and B accommodate both radicals in an orientation that enable coupling through the *re-re* faces yielding the S,S-bisQM intermediate as the precursor of (–)-pinoresinol (**Fig. I-2-7 (d)**). In addition, the trimeric DIRs structure guarantees each active site is kept isolated from each other, thus avoiding the interaction of two substrates bounded at two different active sites.

III Cyclization of the bis-QM reaction intermediate via hydrogen bond (HB) formation or acid catalysis

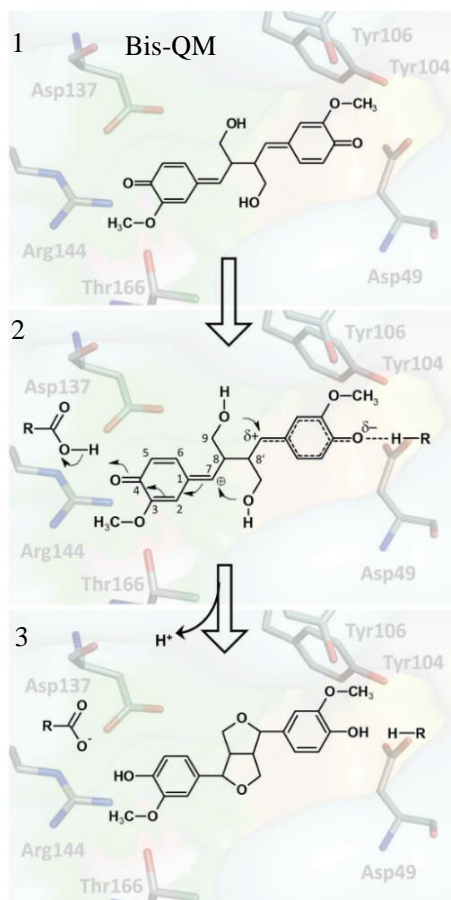


Fig. I-2-8⁸⁴ Schematic representation of the bisQM intermediate cyclization catalyzed by *At*DIR6. The cartoon combines the side view on the active site as shown in **Fig. I-2-7 (d)** with the key functional residues highlighted (sticks). The mechanism of bisQM cyclization proposed by Gasper et al.⁸² via acid catalysis (left) or hydrogen bond formation (right) is schematically shown. Both mechanisms seem to result in a partial or full positive charge on C7 that facilitates the nucleophilic attack during bisQM cyclization

2.2.4 Biotechnological application of the DIRs

Although the function mechanism of DIRs has not been fully understood, DIRs has shown great potential acting as tools for stereospecific radical coupling in organic synthesis.

From an economic and ecological point of view, the use of phenoxy radical coupling agents in organic synthesis is often hindered because of its limited specificity and sometimes the need for high concentrations of toxic oxidants.⁷² The use of DIRs in combination with a suitable oxidizing agent (such as laccase) provides an attractive solution to these problems. For instance, the most widely identified substrate for DIRs is coniferyl alcohol. DIRs direct the coupling of coniferyl alcohol radicals to generate optical purity (+)-pinoresinol or (-)-pinoresinol depending on the DIRs used. (+)-Pinoresinol, a biologically active lignan which has antifungal, anti-inflammatory, antioxidation,

The oriented radical-radical coupling leads to the formation of a bis-quinone methide (bis-QM) intermediate (**Fig. I-2-8 1**) that is electron deficient at C7 and, thus, susceptible to a nucleophilic attack.⁸³ During the formation of pinoresinol, the terminal OH groups of the propionyl side chains can act as nucleophile. 1,4-Addition to the *p*-quinone methides allows the cyclization of the furan rings and re-aromatization of the cyclohexadienones. (**Fig. I-2-8 2**)^{82,84}

DIRs not only provides the cavity structure for the proper orientation of the radicals, but is also probably directly involved in the cyclization of the bis-QM intermediate. The latter could be triggered by donation of a proton to the hexadienone ring carbonyl of the bis-QM via either acid catalysis or hydrogen bond formation. Strictly conserved amino acid residues inside the cavity of (-)-DIRs, such as D49, D137 and R144, are supposed to be available as potential HB donors.

and hypoglycemic activities for many dietary plants, was recently reported to exhibit significant inhibition of human hepatocellular carcinoma proliferation and revealed a pro-apoptotic effect of HepG2 cells *in vitro*.⁸⁵ Currently, (+)-pinoresinol is mainly isolated from seeds, fruits, and vegetables with low efficiency, but, with DIRs, the chemical and enzymatic approaches for the synthesis of (+)-pinoresinol will become available. Therefore, the development of DIRs can provide a biotechnological solution for the regio and stereospecific control of phenoxy radical coupling reactions, thereby providing a highly efficient green synthetic route to obtain a large number of pharmaceutically interesting compounds.

Nevertheless, challenges still exist. First, the discovery of new DIRs with activity on different substrates is limited. Although various DIRs have been described for the formation of pinoresinol or gossypol, there is still no evidence for DIRs involving in other radical coupling processes. In addition, the limited availability restricted the utilization of DIRs in organic synthesis, as the general way to obtain DIRs is extraction from nature source (plant species). Therefore, it is meaningful to understand the mechanism of action of DIRs, which not only provides valuable information for the development of DIRs having new substrate, but also provide important references for the engineering of artificial DIRs, in specific, for the preparation of non-biological molecules with similar characteristics, structures, and function with DIRs. The research results on DIRs would be very important especially in industrial or health biotechnology.

3 Magnetic Nanoparticles (MNPs)

3.1 Immobilization of Laccase for industrial application

As mentioned in the previous subsection, the natural plant protein-DIRs as an external effector, have effects on the enantioselective polymerization of laccase-catalyzed lignin monomer, which improves the performance of laccase catalyzed reaction systems in a great degree. However, issues associated to the use of laccase as biocatalysts at industrial scales still exist. Two main issues concern the activity of laccase that can be damaged by the system environment during the long-term operation and the costly and complex separation procedures leading to a low reusability. So far, one of the most effective solutions to improve enzymes stability and reusability is to use them in their immobilized forms.⁴⁹

Plenty of researches have focused on the immobilization of laccase onto diverse materials by various methods for applications such as degradation of aromatic pollutants. These aromatic pollutants mainly come from textiles production, explosives, pulp, paper and dye industries or agrochemicals, pharmaceuticals. Improved operational stability and tolerance to high temperature or pH has been achieved by immobilizing laccase on to solid materials. Amongst materials, immobilization of enzymes onto superparamagnetic particles is enormously facilitating the separation and reusability of the catalysts. Therefore, eco-friendly enzymatic catalysis can be combined with a convenient recycling and reuse process through immobilization, making enzymes even more favorable alternatives in industrial applications.

3.1.1 Immobilization methods

Immobilization of enzymes is defined as the coupling of enzymes to an insoluble support matrix (carrier) so that the resulting material holds enzymes in a proper geometry allowing both to retain their activity and an easy and cheap recovery from the reaction mixture.⁸⁶ Depending on the nature of the solid materials and the purposes of application, the mode of association of enzymes and supports can vary. Like any other enzyme, laccases can be immobilized by physical adsorption, covalent binding, encapsulation and entrapment and as cross-linked enzyme aggregates (CLEAs). See **Fig. I-3-1** for the schematic diagram of laccase immobilization methods.⁸⁷

Adsorption

Physical adsorption is a simple and straightforward way for immobilization of laccases.⁸⁸ The interactions between the carrier and the enzyme in physical adsorption include van der Waals forces, ionic interactions and hydrogen bonding,⁸⁹ which are rather weak so it typically does not change the native structure of the enzyme thus generally allowing the enzyme to retain its activity.⁹⁰ But weak interactions leave the possibility of enzyme leaching.⁵⁹ Therefore, certain conditions must be considered in order to realize successful adsorption: i) the support should have high surface area and chemical stability to overcome the limited adsorption capacity;⁸⁸ ii) the presence of specific active groups on the carrier should enable the generation of the enzyme-carrier interactions and assure the enzyme-carrier affinity. For the latter case, introducing intermediate agents (carrier modifiers) has proved to be an effective way.⁸⁹

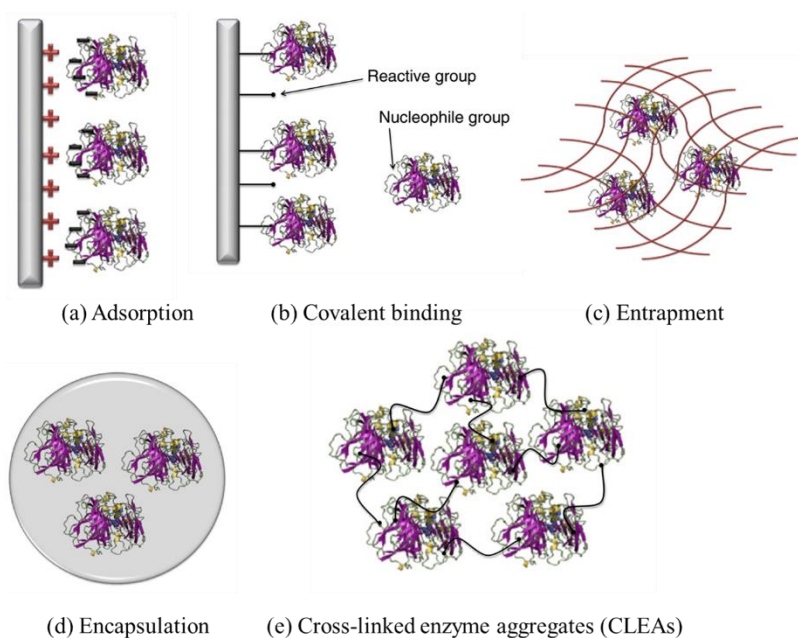


Fig. I-3-1 Schematic diagram of laccase immobilization methods: (a) Adsorption of enzymes onto a support by ionic forces. (b) Covalent binding between the nucleophilic groups of the enzyme and the support. (c) Entrapment of enzymes into a porous solid matrix. (d) Encapsulation of enzymes (e) Self-immobilization: model of cross-linked enzyme aggregates (CLEAs).⁸⁷

Entrapment

Entrapment refers to a process of physical retention of enzymes in a porous solid matrix. The enzyme is first suspended in a monomer solution then trapped through the subsequent polymerization of the monomer.⁸⁷ Suitable supports such as gelatin, sodium alginate, starch, chitosan, polyvinyl alcohol, nylon membrane, cellulose acetate, *etc.*, are used to trap the enzyme molecules or enzymatic preparations within a matrix.⁹¹ Because of the formation of a polymer network,⁹² enzymes are protected by preventing direct contact with the environment, thereby minimizing the effects of gas bubbles, mechanical stress and hydrophobic solvents.⁹³ The process of entrapment is mild and

induces relatively little damage to the enzyme native structure,⁹⁴ but limited by mass transfer limitations and low enzyme loading.⁹⁵

Encapsulation

Encapsulation is similar to entrapment but with slight difference. Entrapment is a process based on the positioning of the enzyme within the lattice of the polymer matrix or membrane, while encapsulation involves entrapment of the enzyme in a semipermeable membrane (e.g., nitrocellulose membrane and nylon-based membrane). So it fully embed the enzyme molecules within the supports and prevent contact with the external interface.⁹⁶ When the enzyme is encapsulated in the core of the supporter materials its structure will potentially remain unaltered⁹⁵ helping in the retention of the activity. But the special location of the enzyme makes the transfer of the reaction mixture more difficult.⁹²

An alternative method for encapsulation is microencapsulation, in which encapsulated laccases are surrounded by semipermeable membranes, such as polymers (e.g., polyethyleneimine) or inorganic materials (e.g., SiO₂),⁹⁷ the core of the capsules provides an aqueous environment for enzymatic activity, and the capsule (wall) serves as a container for the substrates to diffuse.⁹⁸

Covalent binding

The method of covalent bonding refers to the formation of a covalent bond between the protein and reactive groups on the support surface.⁹⁹ Covalent binding contains two situations: direct grafting onto the solid supports or the use of a bifunctional reagent to work as bridge that connect the enzyme at one side and link the matrix on other side. The resulting heterogeneous biocatalyst can be much more stable than those prepared by adsorption or entrapment, with a minimal protein leaching and a better storage ability/shelf-life. Thus, covalent immobilization of enzymes is usually preferred for long-lasting, real-scale and continuous applications,¹⁰⁰ where the protein value is high, minimal protein leaching from the support is required or rational control of the biocatalyst properties is desired.⁹³

For most enzymes, the reactive group chosen is an amino group (N-terminus, Lysine side chain), because these groups are often present on the protein surface and have high reactivity.⁹⁵ Other functional groups such as hydroxyl groups (serine, threonine and tyrosine), thiol (cysteine) and carboxylate groups (aspartic acid and glutamic acid) are also used for covalent bonding. **Table I-3-1** summarized the commonly used surface functional groups both at the protein and at the solid supports surface as well as the corresponding chemical reactions between them based on an article of Marco Frasconi *et al.*¹⁰¹

Table I-3-1 Summary of the commonly used chemical reaction for immobilization of laccase

Functional groups at the support side	Functional groups at the protein side	Reaction
Maleimide groups	Thiols (cysteine residue) Amino (Lysine residue)	Michael addition of thiol or amino groups to the maleimide double bond
Amino groups	Carboxyl (Aspartic acid, Glutamic acid or the C-terminals)	In situ formation of NHS ester on protein carboxyl sites via carbodiimide chemistry, followed by amide bond formation
Aldehyde groups	Amino (Lysine residue)	Reductive amination
N-hydroxysuccinimide (NHS) Ester	Amino (Lysine residue)	Amide bond formation
Epoxide	Thiol (Cysteine residue) Amino (Lysine residue)	Nucleophilic ring-opening of epoxide by amino or thiol groups

Although covalent binding has become the most interesting method of laccase immobilization for industrial applications, the efficiency of immobilized laccase by covalent bond is restricted by the possible conformational change and limited mass transfer. Also, this method needs modifications of functional groups at the surface of the carrier, which often means complications and extra expenses.

Cross-linked enzyme aggregates (CLEAs)

The general procedure of CLEAs consists in an enzyme precipitation step and a subsequent cross-linking with a bifunctional agent.¹⁰² This approach offers clear advantages, for instance, easiness of the preparation, a highly concentrated enzyme activity in the solid catalyst, high stability and low cost production due to the exclusion of additional carriers.¹⁰³

3.1.2 Materials used for enzyme immobilization

The characteristics of an ideal support for enzyme immobilization include low cost production; ability to stabilize a significant amount of enzyme per weight unit; low hydrophobicity; inertness after immobilization; microbial resistance; pH, thermal and mechanical resistance.

Since the first immobilization experiment in 1916,¹⁰⁴ numerous materials have been applied to immobilize enzymes, such as agarose, silica, TiO₂, organic gel, chitosan, kaolinite, multiwalled carbon nanotubes and graphene oxide. Materials commonly used in literatures to immobilize laccase are summarized in **Table I-3-2**.

Table I-3-2 Materials for immobilization of laccase in some recently reported literatures

Materials	Advantages	Biding methods	Application	Effect	Reference
Biochars					
Micro-biochar	Cost-effectiveness, Strong physicochemical resistance; waste valorization, porous structure and moderate surface area	Adsorption, electrostatic interactions Covalent binding	Bioremediation of micro-pollutants such as carbamazepine and diclofenac	Higher pH, temperature and storage stability compared to free laccase. 70% of initial activity maintained after 3 cycles excellent removal of diclofenac.	88,100,105-107
Agarose					
Monoaminoethyl-N-aminoethyl agarose gel	Easy immobilization, eco-friendly, low-cost	Ionic adsorption	Degradation of plastics, epoxy resins and textile dyes decolorization	More efficient in the degradation of bisphenol A, >90% of original laccase activity retained after 15 cycles.	108
Alginate beads Ca alginate beads		Entrapment + crosslinking laccase enzymes	Biodegradation of textile dyes Bisphenol A (BPA)	efficient BPA removal in 10 successive batches with a removal percentage > 70% at the end of the last batch	109,110
Bentonite					
Bentonite-derived mesoporous materials	Eco-friendly, inexpensive, and accessible, highly improved cation exchange capacity and surface area after etching	Physical adsorption contact	Removal of tetracycline	Increased operating temperature Promising potential for practical continuous applications.	111
Titania (TiO₂)					
Functionalized TiO ₂ nanoparticles	Low price, good stability, and biocompatibility; Coordination ability with amine and carboxyl groups	Covalent bonding	Micro-pollutant in wastewater	Performances comparable to that of the purified commercial enzymes.	112

(Continued) **Table I-3-2** Materials for immobilization of laccase in some recently reported literatures

Materials	Advantages	Biding methods	Application	Effect	Reference
Carbon-based nanomaterials					
Graphene oxide nanosheets	Incredible physical and mechanical properties, large surface area, extremely high electrical conductivity, high adsorption capacity, superior enzyme loading capacity, unique tubular geometrical structure	Covalent immobilization	Biodegradation of azo dyes	Operational stability and good reusability	113
		Physical adsorption and covalent bonding	Treatment of effluents	Increased stability of the enzyme against severe changes of pH and temperature, retention of operational activity	114
Functionalized graphene oxide (fGO)	unique tubular geometrical structure	Multipoint covalent	Decolorization of industrial dye	Enhanced thermal stability, higher activity than the free enzyme, increased operational stability	115
Multi-walled carbon nanotubes (MWNTs)		Non-covalent bonding (including van der Waals, π - π stacking, electrostatic, hydrophobic interactions)		Long-term storage stability and reusability a decrease in the thermal stability of laccase was observed after immobilization.	116
Hollow mesoporous carbon nanospheres (HMCs)	Large hollow volume and inner surface, superior conductivity, biocompatibility and corrosion resistance	Physical adsorption or covalent bonding.	Antibiotic contaminants removal	Excellent thermo-stability, pH stability, storage stability and reusability	117
Chitosan					
Chitosan beads	Cheap, eco-friendly and efficient, easy chemical modification, high adsorption capacity, inert, biocompatible and hydrophilic material	Covalent bonds (Glutaraldehyde-crosslinked)	Removal of sulfur dyes from water	Rather high catalytic ability even at low concentrations.	118
Chitosan microspheres		Crosslinking (GLU as a crosslinking agent)	Decolorize textile dyes	Improved thermal and storage stability, increased affinity toward substrate	119
Chitosan beads		Entrapment	Degrade synthetic dyes	Enhanced pH adaptability and resistance to thermal denaturation	120,121

Table I-3-2 (Continued) Materials for immobilization of laccase in some recently reported literatures

Materials	Advantages	Biding methods	Application	Effect	Reference
Magnetic nanoparticles (MNPs)					
Amino-functionalized MNPs		Cross-linked aggregates	enzyme Degradation of antibiotics (tetracycline)	Improve mechanical properties of CLEAs, easy separation and recycling, significantly reduced antimicrobial activity of TC (tetracycline)	122
		Metal affinity adsorption (PEI modified Fe ₃ O ₄ nanoparticles (Fe ₃ O ₄ -NH ₂ -PEI MNPs) chelated with Cu ²⁺)		Higher specific activity than free enzymes, increased stability against severe changes of pH and temperature	123
Silica					
Porous silica beads	Stable structural, low cost, environmentally friendly, resistant to organic solvents and microbial attacks	Covalent binding	Elimination and detoxification of sulfathiazole and sulfamethoxazole	Improvement of thermal and operational stabilities	124
epoxy-functionalized silica particles		Covalent binding (nucleophilic attack of amino groups of laccases to epoxy groups of the support)	Biodegradation of phenolic compounds	Improved stability, good enzyme loading and reusability, broader temperature profiles and organic solvent tolerance than the free laccase	125
Metal-organic frameworks (MOFs)					
Micro-mesoporous Zr-metal organic framework (Zr-MOF)	Good Brunauer-Emmett-Teller (BET) surface areas and excellent dispersity, can be synthetically modified to introduce a desired functionality	Physical adsorption	Biotechnological applications	Broader pH and temperature profiles, better stability and repeatability	126

3.2 Introduction to magnetic nanoparticles

Among all the material used for laccase immobilization, magnetic nanoparticles (MNPs) are the most eye-catching ones. Their specificities are mainly linked to their core shell structure and their unique superparamagnetic performance, which allow MNPs immobilized enzymes to be manipulated easily under control of external magnetic fields, so that the catalysts can be separated and recovered without time consuming, expensive or complicated process.

3.2.1 Structure of MNPs

The MNPs used for enzyme immobilization generally have a core-shell structure (**Fig. I-3-2**). This special structure benefits the enzyme immobilization, the functional shell is available for enzymes binding, and the magnetic core makes the catalysts move easily under control of a simple external magnetic field.

The core of MNPs are usually made of magnetic elements such as magnetite (Fe_3O_4), maghemite ($\gamma\text{-Fe}_2\text{O}_3$), cobalt ferrite (Fe_2CoO_4) and chromium dioxide (CrO_2).¹²⁷ In the field of biotechnology, the most commonly used core materials are Fe_3O_4 or $\gamma\text{-Fe}_2\text{O}_3$, because the iron oxide is non-toxic and stable compared to pure metals or cobalt and nickel oxides. $\gamma\text{-Fe}_2\text{O}_3$ is an oxidation product of Fe_3O_4 , with only slightly reduced magnetic properties (about 10%) compared with Fe_3O_4 , and unchanged crystal structure and surface properties.

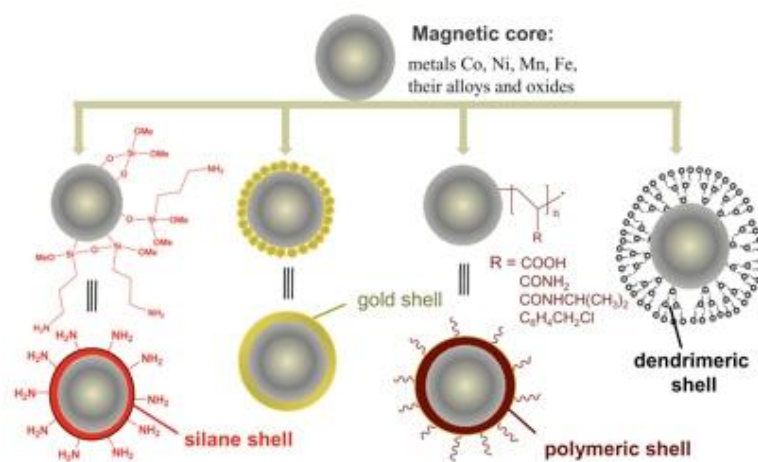


Fig. I-3-2 Structure of magnetic particles (Figure from https://www.cd-bioparticles.com/s/Magnetic-Beads-Modification_34.html)

The shell is made through coating the core by polymer or inorganic layers such as silica or carbon. The shell itself is often functionalized with various functional groups for binding target molecules depending on the desired application. Nowadays, different kinds of commercial MNPs are available for use. Most of the commercial MNPs are modified with amino or carboxylic acid groups. Some other functional groups like aldehyde, epoxy, NHS ester, *etc.* are also found, providing

multiple possibilities for choice. Usually, the manufacturer gives a detailed selection guide and manipulation protocol for their particles, which makes them convenient to use.

3.2.2 Magnetic features of MNPs

The easy manipulation of magnetic particles under the control of magnetic fields is linked to their superparamagnetic characters. The term “superparamagnetism” refers to an analogy between the behavior of the small magnetic moment of a single paramagnetic atom and that of the much larger magnetic moment of a nanosized magnetic particle which arises from the coupling of many atomic spins.¹²⁸ Phenomenally speaking, on application of an external magnetic field, MNPs become magnetized and can work as a small magnets, but on removal of the magnetic field, they no longer exhibit any residual magnetic interaction.¹²⁹

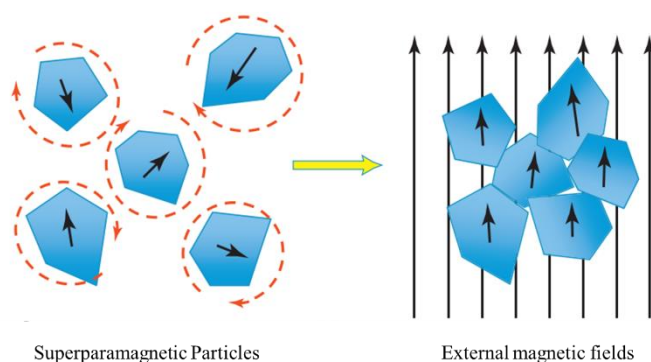


Fig. I-3-3 Illustration of superparamagnetic MNP response to applied magnetic fields.¹³⁰

Superparamagnetism is a size-dependent property. It generally appears when the size of the particles is small enough so that MNPs can be regarded as a single magnetic domain and exhibits random spinning of magnetic moments upon thermal fluxes. The average magnetization of these moments reaches zero by its random orientation in the absence of the applied magnetic field. In contrast, on application of a magnetic field, these nanoparticles re-orientate by crystals rotating to align with the direction of the external magnetic field, thus being magnetized up to their saturation magnetization (**Fig. I-3-3**).¹³⁰ The critical size required to achieve superparamagnetism varies between core materials, but is typically <30 nm for iron oxide crystals.¹³¹ Considering this threshold, MNPs with a core larger than 30 nm typically consist of clusters of multiple smaller iron-oxide domains rather than a single large crystal.¹³⁰

3.3 MNPs in laccase immobilization

In theory, all the methods mentioned in section 3.1.1 can be used to immobilize laccase onto the surface of magnetic particles. The selection of the method depends on the purpose of the immobilization. However, for laccases immobilized on magnetic particles, the methods reported in literature mainly focus on a few of them. Several representative examples are summarized below.

These methods, all as expected, were reported to improve the operational stability, thermal and pH resistance as well as storability of laccase, whereas in the meantime undoubtedly impart simple and quick separation and recovery properties to laccase. But, their influence on laccase activity is different, as it will be discussed for each of the methods.

Methods 1: Covalent bond with glutaraldehyde as bifunctional linker

The conventional immobilization methods are based on covalent bond formation with a bifunctional linker. Often, as showed in **Fig. I-3-4**, the surface of the particles is coated with amorphous silica then subsequently modified with $-NH_2$ groups by using (3-aminopropyl) trimethoxysilane. Glutaraldehyde is widely used as a bifunctional linker. The functionalization of the protein surface is random if more than one amino group is available for grafting.

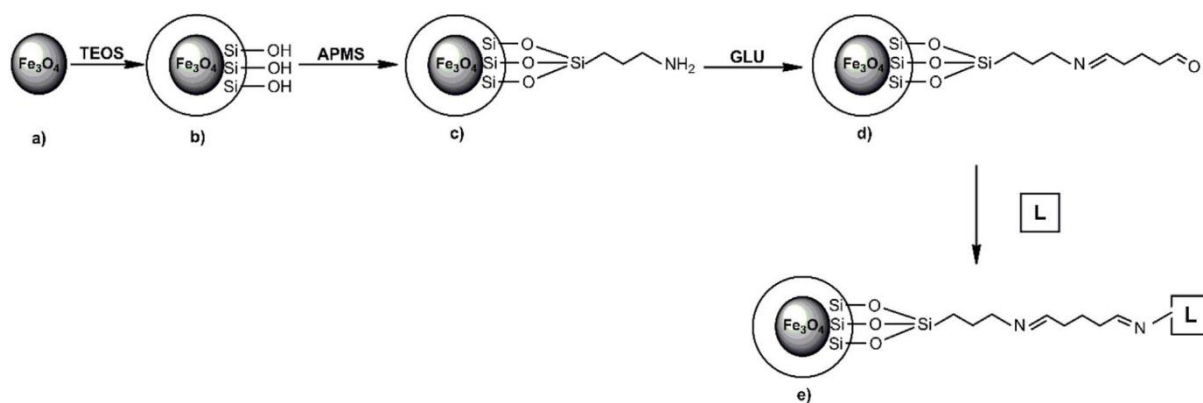


Fig. I-3-4 Scheme of the chemical strategy for immobilization of laccase to the silica coated amino particles a) the synthesis of the magnetic core, b) the silica coating, c) the surface functionalization with amine groups, d) the activation with glutaraldehyde (GLU) and e) the immobilization of laccase (L).¹³²

It has been reported that after laccase immobilization by this method, the operational and thermal stability of laccase increased but the activity (the total activity of the immobilized laccase divided by the total activity of the equal amount of free laccase) and substrate affinity decreased.¹³² Several published works contain the same results using similar methods.^{133–135} Mass transfer limitations or conformational changes of the protein during covalent binding are considered responsible for the decreased activity and lowered affinity of immobilized enzymes.¹³⁶ Here, the covalent bond formation may hinder the activity of laccase not only because of mass transfer limitations or conformational changes induced during the process but also because the random cross-linking between proteins and supports may involve amino acid residues of the active center. An orientated immobilization strategy based on a single specific interaction could overcome this issue.

Methods 2: Bioaffinity-based strategy

In the method reported (Fig. I-3-5)¹³⁷, the lectin concanavalin A (Con A) is used to interact with the glycosyls decorating the surface of a (fungal)laccase via lectin–sugar interactions to immobilize the enzyme at the surface of silica coated particles. The author of this study reported only a 6.2 % loss in the activity of the MNPs-Con A-L (Fig. I-3-5 route B) as compared to the activity of the free laccase, which is lower (17.6% decline) than the covalent immobilization studied in parallel (Fig. I-3-5 route A). A plausible explanation given by the authors is that the affinity adsorption mediated by Con A minimize conformational changes in laccase during immobilization. Also, the glycosyl groups of laccases (from *E. taxodii*) could be far from the active center preventing any steric hindrance.

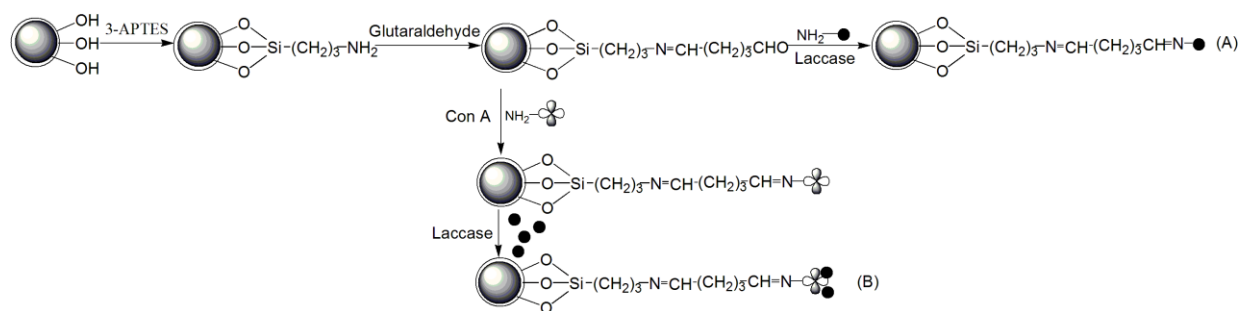


Fig. I-3-5 Scheme for conjugating laccase onto the surface of the nanoparticles via two different strategies. (A) Random immobilization via covalent binding. (B) oriented immobilization via interaction between Con A and glycosyl of laccase.

Besides, MNPs-Con A-L exhibit a higher affinity for the synthetic substrate ABTS than either the free laccase or MNPs-L. This phenomenon has been also observed in the immobilization of inulinase on Con A-attached super microporous cryogel and explained by a non-specific affinity of inulin for the cryogel support.¹³⁸

Methods 3: Metal affinity adsorption

Another affinity adsorption method related to enzyme immobilization is metal chelate affinity, which are derived from metal affinity (IMA) separation. The principle of IMA is based on the interaction between chelated metal ions (Co²⁺, Zn²⁺, Ni²⁺ or Cu²⁺) and the thiol group of cysteine, the indoyl group of tryptophan or the imidazole group of histidine of proteins.¹³⁹ A typical route to illustrate this method is shown at Fig. I-3-6.¹⁴⁰ Amine-functionalized Fe₃O₄ nanoparticles are first functionalized with polyethylenimine (PEI) using glutaraldehyde (GA) as a linker, then the resultant modified Fe₃O₄-PEI MNPs are derivatized with iminodiacetic acid (IDA)-Cu²⁺ groups allowing an adsorption of laccase via surface available ligands (Fig. I-3-6).

Following this strategy, it has been reported that laccase immobilization resulted in an increase of activity post immobilization, which is contrasting with results reported when using the previous two methods.^{141–144} The reason for this discrepancy has been explained as follows: on one side, PEI

is a flexible spacer-arm and, to some extent, it can move laccase molecules away from the surface of MNPs which is beneficial to reduce steric hindrance and thus minimize the dispersion limitation; it also prevent particle agglomeration by electrostatic repulsive force and steric hindrance, thus increasing enzymatic catalytic efficiency. On the other hand, Cu^{2+} can stimulate the activity of laccase.¹²³ Moreover, the coordination bonds formed between transition metal ions and laccase are strong; this is not only minimizing conformational changes of laccase, but could also overcome leakages.

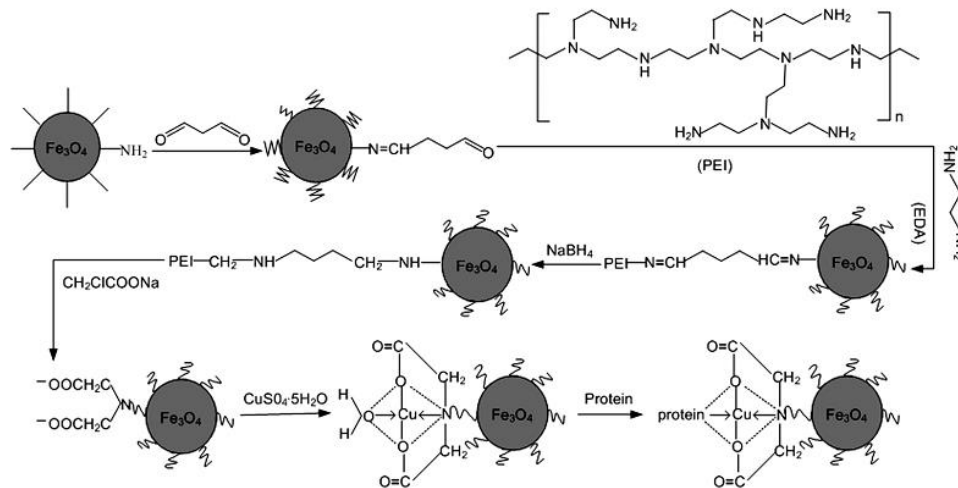


Fig. I-3-6 Metal affinity adsorption of laccase onto PEI modified Fe_3O_4 nanoparticles ($\text{Fe}_3\text{O}_4\text{-NH}_2\text{-PEI}$ NPs) chelated with Cu^{2+}

Methods 4: Covalent bond on activated hydroxyl groups of chitosan coated MNPs

Laccase has been recently immobilized onto chitosan (CS) coated MNPs via covalent binding by activating the hydroxyl groups of the particles with carbodiimide (EDAC) or cyanuric chloride (CC) (**Fig. I-3-7**).¹⁴⁵

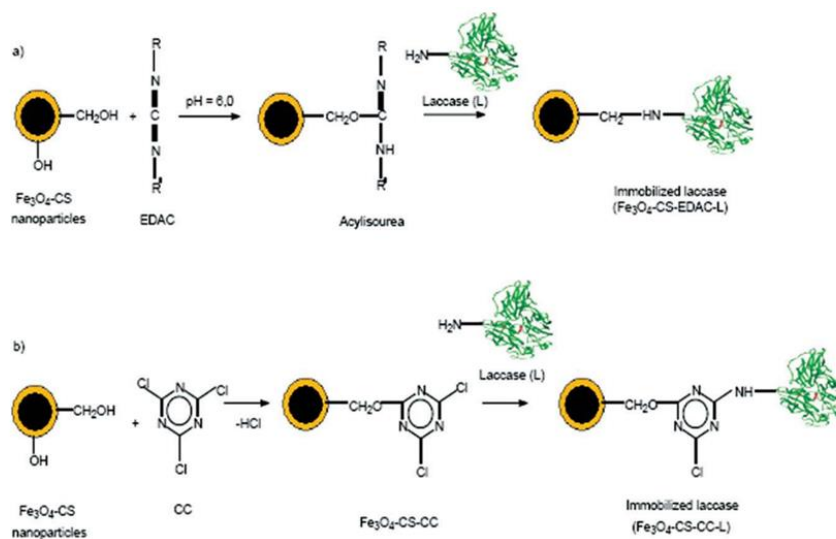


Fig. I-3-7 Scheme of laccase immobilization onto $\text{Fe}_3\text{O}_4\text{-CS}$ nanoparticles (a) by EDAC and (b) by CC.

In this case, a significant substrate affinity decrease has been observed for the immobilized enzyme as reflected by an increase in K_m values. These variations have been attributed to conformational changes, steric hindrance, and partitioning effects of protein.¹⁴⁵ It has been also reported that, with the same kind of immobilization methods, the specific activity of the immobilized laccase decreased dramatically compared with the free laccase.¹⁴⁶ In fact, the decrease of activity of the immobilized form is a common phenomenon. Immobilization imposes restriction of mobility of the enzyme, which can in turn affect mobility of the substrates. This phenomenon, referred as mass transfer effects, could lead to a reduced reaction rate, in other words to a reduced efficiency as compared to the free enzyme.¹⁴⁷

Methods 5: Potential method by click chemistry

The alkyne–azide click chemistry has been recently developed for the synthesis and surface modification of MNPs (see **Fig. I-3-8** (a)¹⁴⁸ for an example of alkyne functionalized MNPs and (b)¹⁴⁹ for an example of azide functionalized silica particle). The main advantage of this reaction is its specificity and the absence of byproducts.¹⁵⁰ However, in practice, azide functionalized particles are not as common as their amine ($-\text{NH}_2$), carboxyl (COOH), aldehyde (CHO) counterparts and especially for the application of laccase immobilization no report has been found so far. Their potential is however testified by several other representative MNPs-biomolecules constructs such as that with the Maltose binding protein (MBP) shown in **Fig. I-3-8** (c),¹⁵¹ biotin and estradiol *etc.*¹⁵² The remarkable properties of the Cu(I)-catalyzed cycloaddition makes it potentially an alternative method for laccase immobilization.

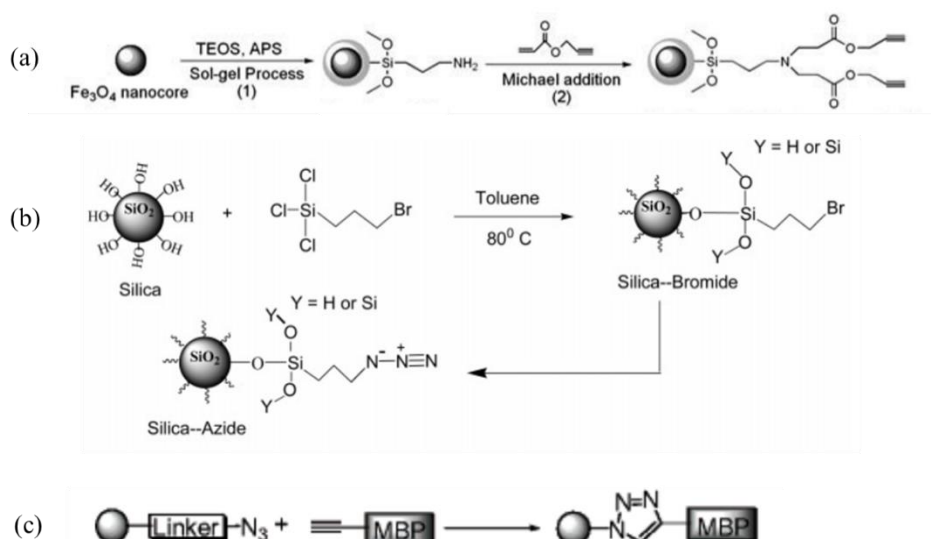


Fig. I-3-8 Alkyne–azide click chemistry using in surface modification of MNPs and immobilization of biomolecules. (a) an example of alkyne functionalized MNPs and (b) an example of azide functionalized silica particle. (c) covalently immobilization of alkyne-functionalized MBP onto azide MNPs via the Cu(I)-catalyzed cycloaddition

4 Scope of this research work

The main objective of this research work was to study possibilities to modulate laccase catalytic properties through the addition of external factors modifying the (micro)-environment of laccase. Thus, we briefly studied the plant dirigent protein *AtDIR6* as a natural model of laccase effector and designed a bio-inspired system consisting in laccase functionalized MNPs in which both the chemical nature and the orientation of the enzyme can be modulated at the of the nano-particle surface.

On the *AtDIR6* part, prolonging the work previously done in our lab,¹⁵³ we confirmed that: i) *AtDIR6* increases the life time of coniferyl alcohol radicals as seen for the first time by EPR; ii) tyrosines in the cavity of *AtDIR6* are labeled with a radical probe (ABTS); iii) the propenyl unit of the coniferyl alcohol can be modified as evidenced by the formation of DP-dependent formation of selective products of coniferyl acetate. We then developed strategies: iv) to identify amino acids within the cavity of *AtDIR6* that are involved in the stereoselective control using coniferyl alcohol radicals as a probe, and v) to explore the reactivity of *AtDIR6* using synthetic analogues of coniferyl alcohol.

On the laccase-functionalized MNPs part, we explored the coupling of laccases to MNPs harboring different chemical function at their surface: -NH₂, -CHO, -N₃, and for some compared different densities of chemical functions: linear vs dendritic (coll. with Hongtao Ji and Karine Heuzé, Univ. Bordeaux). We used two kinds of laccases: a) LAC3 harboring two lysine residues so located that grafting the enzyme to MNPs expose its active site to the solvent, and b) its variant UniK₁₆₁ harboring a single lysine residue so located that grafting the enzyme to MNPs expose its active site to the MNP surface. The activity of the immobilized laccases was tested with different substrates: ABTS (synthetic), syringaldazine (phenol) and coniferyl alcohol (monolignol). All together, these modulations allowed us to study the system in multiple dimensions: orientation of the biocatalyst, nature of the chemical environment at the interface, density of chemical functions, chemo- regio- and stereo-selectivity. We bring here evidences that the activity a non-selective enzyme can be modulated by design of the micro-environment of its active site.

Reference

- (1) Baldrian, P. Fungal Laccases – Occurrence and Properties. *FEMS Microbiol. Rev.* **2006**, *30* (2), 215–242. <https://doi.org/10.1111/j.1574-4976.2005.00010.x>.
- (2) Mehra, R. A Structural-Chemical Explanation of Fungal Laccase Activity. *Sci. Rep.* **2018**, *16*.
- (3) Santhanam, N.; Vivanco, J. M.; Decker, S. R.; Reardon, K. F. Expression of Industrially Relevant Laccases: Prokaryotic Style. *Trends Biotechnol.* **2011**, *29* (10), 480–489. <https://doi.org/10.1016/j.tibtech.2011.04.005>.
- (4) Dwivedi, U. N.; Singh, P.; Pandey, V. P.; Kumar, A. Structure–Function Relationship among Bacterial, Fungal and Plant Laccases. *J. Mol. Catal. B Enzym.* **2011**, *68* (2), 117–128. <https://doi.org/10.1016/j.molcatb.2010.11.002>.
- (5) Mate, D. M.; Alcalde, M. Laccase: A Multi-Purpose Biocatalyst at the Forefront of Biotechnology. *Microb. Biotechnol.* **2017**, *10* (6), 1457–1467. <https://doi.org/10.1111/1751-7915.12422>.
- (6) Madhavi, V.; Lele, S. S. Laccase: Properties and Applications. *BioResources* **2009**, *4* (4), 1694–1717.
- (7) Solomon, E. I.; Szilagyi, R. K.; DeBeer George, S.; Basumallick, L. Electronic Structures of Metal Sites in Proteins and Models: Contributions to Function in Blue Copper Proteins. *Chem. Rev.* **2004**, *104* (2), 419–458.
- (8) Liu, Y.; Yan, M.; Geng, Y.; Huang, J. Laccase Immobilization on Poly(p-Phenylenediamine)/Fe₃O₄ Nanocomposite for Reactive Blue 19 Dye Removal. *Appl. Sci.* **2016**, *6* (8), 232. <https://doi.org/10.3390/app6080232>.
- (9) Claus, H. Laccases: Structure, Reactions, Distribution. *Micron* **2004**, *35* (1–2), 93–96. <https://doi.org/10.1016/j.micron.2003.10.029>.
- (10) Giardina, P.; Faraco, V.; Pezzella, C.; Piscitelli, A.; Vanhulle, S.; Sannia, G. Laccases: A Never-Ending Story. *Cell. Mol. Life Sci.* **2009**, *67* (3), 369–385. <https://doi.org/10.1007/s00018-009-0169-1>.
- (11) Mot, A. C.; Silaghi-Dumitrescu, R. Laccases: Complex Architectures for One-Electron Oxidations. *Biochem. Mosc.* **2012**, *77* (12), 1395–1407. <https://doi.org/10.1134/S0006297912120085>.

- (12) Morozova, O. V.; Shumakovich, G. P.; Gorbacheva, M. A.; Shleev, S. V.; Yaropolov, A. I. “Blue” Laccases. *Biochem. Mosc.* **2007**, *72* (10), 1136–1150.
- (13) Lazarides, T.; Sazanovich, I. V.; Simaan, A. J.; Kafentzi, M. C.; Delor, M.; Mekmouche, Y.; Faure, B.; Réglie, M.; Weinstein, J. A.; Coutsolelos, A. G.; et al. Visible Light-Driven O₂ Reduction by a Porphyrin–Laccase System. *J. Am. Chem. Soc.* **2013**, *135* (8), 3095–3103. <https://doi.org/10.1021/ja309969s>.
- (14) Riva, S. Laccases: Blue Enzymes for Green Chemistry. *Trends Biotechnol.* **2006**, *24* (5), 219–226. <https://doi.org/10.1016/j.tibtech.2006.03.006>.
- (15) Morozova, O. V.; Shumakovich, G. P.; Shleev, S. V.; Yaropolov, Y. I. Laccase-Mediator Systems and Their Applications: A Review. *Appl. Biochem. Microbiol.* **2007**, *43* (5), 523–535.
- (16) Matera, I.; Gullotto, A.; Tilli, S.; Ferraroni, M.; Scozzafava, A.; Briganti, F. Crystal Structure of the Blue Multicopper Oxidase from the White-Rot Fungus *Trametes Troglia* Complexed with *p*-Toluate. *Inorganica Chim. Acta* **2008**, *361* (14–15), 4129–4137. <https://doi.org/10.1016/j.ica.2008.03.091>.
- (17) Agrawal, K.; Chaturvedi, V.; Verma, P. Fungal Laccase Discovered but yet Undiscovered. *Bioresour. Bioprocess.* **2018**, *5* (1), 4. <https://doi.org/10.1186/s40643-018-0190-z>.
- (18) Garzillo, A. M. V.; Colao, M. C.; Caruso, C.; Caporale, C.; Celletti, D.; Buonocore, V. Laccase from the White-Rot Fungus *Trametes Troglia*. *Appl. Microbiol. Biotechnol.* **1998**, *49* (5), 545–551. <https://doi.org/10.1007/s002530051211>.
- (19) d’Acunzo, F.; Galli, C.; Gentili, P.; Sergi, F. Mechanistic and Steric Issues in the Oxidation of Phenolic and Non-Phenolic Compounds by Laccase or Laccase-Mediator Systems. The Case of Bifunctional Substrates. *New J. Chem.* **2006**, *30* (4), 583. <https://doi.org/10.1039/b516719a>.
- (20) Munk, L.; Punt, A. M.; Kabel, M. A.; Meyer, A. S. Laccase Catalyzed Grafting of –N–OH Type Mediators to Lignin via Radical–Radical Coupling. *RSC Adv.* **2017**, *7* (6), 3358–3368. <https://doi.org/10.1039/C6RA26106J>.
- (21) Ashe, B.; Nguyen, L. N.; Hai, F. I.; Lee, D.-J.; Merwe, J. P. van de; Leusch, F. D. L.; Price, W. E.; Nghiem, L. D. Impacts of Redox-Mediator Type on Trace Organic Contaminants Degradation by Laccase: Degradation Efficiency, Laccase Stability and Effluent Toxicity. *Int. Biodeterior. Biodegrad.* **2016**, *113*, 169–176. <https://doi.org/10.1016/j.ibiod.2016.04.027>.
- (22) Christopher, L. P.; Yao, B.; Ji, Y. Lignin Biodegradation with Laccase-Mediator Systems. *Front. Energy Res.* **2014**, *2*. <https://doi.org/10.3389/fenrg.2014.00012>.

- (23) Kunamneni, A.; Ballesteros, A.; Plou, F. J.; Alcalde, M. Fungal Laccase—a Versatile Enzyme for Biotechnological Applications. *Commun. Curr. Res. Educ. Top. Trends Appl. Microbiol.* **2007**, *1*, 233–245.
- (24) Bourbonnais, R.; Paice, M. G. Oxidation of Non-Phenolic Substrates: An Expanded Role for Laccase in Lignin Biodegradation. *FEBS Lett.* **1990**, *267* (1), 99–102. [https://doi.org/10.1016/0014-5793\(90\)80298-W](https://doi.org/10.1016/0014-5793(90)80298-W).
- (25) Rivera-Hoyos, C. M.; Morales-Álvarez, E. D.; Poutou-Piñales, R. A.; Pedroza-Rodríguez, A. M.; Rodríguez-Vázquez, R.; Delgado-Boada, J. M. Fungal Laccases. *Fungal Biol. Rev.* **2013**, *27* (3–4), 67–82. <https://doi.org/10.1016/j.fbr.2013.07.001>.
- (26) Moilanen, U.; Kellock, M.; Várnai, A.; Andberg, M.; Viikari, L. Mechanisms of Laccase-Mediator Treatments Improving the Enzymatic Hydrolysis of Pre-Treated Spruce. *Biotechnol. Biofuels* **2014**, *7* (1), 177. <https://doi.org/10.1186/s13068-014-0177-8>.
- (27) Fabbrini, M.; Galli, C.; Gentili, P. Comparing the Catalytic Efficiency of Some Mediators of Laccase. *J. Mol. Catal. B Enzym.* **2002**, *16* (5–6), 231–240. [https://doi.org/10.1016/S1381-1177\(01\)00067-4](https://doi.org/10.1016/S1381-1177(01)00067-4).
- (28) Camarero, S.; Cañas, A. I.; Nousiainen, P.; Record, E.; Lomascolo, A.; Martínez, M. J.; Martínez, Á. T. *p*-Hydroxycinnamic Acids as Natural Mediators for Laccase Oxidation of Recalcitrant Compounds. *Environ. Sci. Technol.* **2008**, *42* (17), 6703–6709. <https://doi.org/10.1021/es8008979>.
- (29) Cañas, A. I.; Camarero, S. Laccases and Their Natural Mediators: Biotechnological Tools for Sustainable Eco-Friendly Processes. *Biotechnol. Adv.* **2010**, *28* (6), 694–705. <https://doi.org/10.1016/j.biotechadv.2010.05.002>.
- (30) Cannatelli, M. D.; Ragauskas, A. J. Laccase-Catalyzed Synthesis of 2,3-Ethylenedithio-1,4-Quinones. *J. Mol. Catal. B Enzym.* **2015**, *119*, 85–89. <https://doi.org/10.1016/j.molcatb.2015.05.016>.
- (31) Aktas, N. Reaction Conditions for Laccase Catalyzed Polymerization of Catechol. *Bioresour. Technol.* **2003**, *87* (3), 209–214. [https://doi.org/10.1016/S0960-8524\(02\)00254-7](https://doi.org/10.1016/S0960-8524(02)00254-7).
- (32) Niedermeyer, T. H.; Mikolasch, A.; Lalk, M. Nuclear Amination Catalyzed by Fungal Laccases: Reaction Products of *p*-Hydroquinones and Primary Aromatic Amines. *J. Org. Chem.* **2005**, *70* (6), 2002–2008.
- (33) Manda, K.; Hammer, E.; Mikolasch, A.; Niedermeyer, T.; Dec, J.; Jones, A. D.; Benesi, A. J.; Schauer, F.; Bollag, J.-M. Laccase-Induced Cross-Coupling of 4-Aminobenzoic Acid with

Para-Dihydroxylated Compounds 2, 5-Dihydroxy-N-(2-Hydroxyethyl)-Benzamide and 2, 5-Dihydroxybenzoic Acid Methyl Ester. *J. Mol. Catal. B Enzym.* **2005**, *35* (4–6), 86–92.

(34) Semenov, A. N.; Lomonsova, I. V.; Berezin, V. I.; Titov, M. I. Peroxidase and Laccase as Catalysts for Removal of the Phenylhydrazide Protecting Group under Mild Conditions. *Biotechnol. Bioeng.* **1993**, *42* (10), 1137–1141.

(35) El-Batal, A. I.; ElKenawy, N. M.; Yassin, A. S.; Amin, M. A. Laccase Production by *Pleurotus Ostreatus* and Its Application in Synthesis of Gold Nanoparticles. *Biotechnol. Rep.* **2015**, *5*, 31–39.

(36) Bronikowski, A.; Hagedoorn, P.-L.; Koschorreck, K.; Urlacher, V. B. Expression of a New Laccase from *Moniliophthora Roreri* at High Levels in *Pichia Pastoris* and Its Potential Application in Micropollutant Degradation. *AMB Express* **2017**, *7* (1), 73.

(37) Sun, J.; Guo, N.; Niu, L.-L.; Wang, Q.-F.; Zang, Y.-P.; Zu, Y.-G.; Fu, Y.-J. Production of Laccase by a New *Myrothecium Verrucaria* MD-R-16 Isolated from Pigeon Pea [*Cajanus Cajan* (L.) Millsp.] and Its Application on Dye Decolorization. *Molecules* **2017**, *22* (4), 673.

(38) Vicente, A. I.; Viña-Gonzalez, J.; Santos-Moriano, P.; Marquez-Alvarez, C.; Ballesteros, A. O.; Alcalde, M. Evolved Alkaline Fungal Laccase Secreted by *Saccharomyces Cerevisiae* as Useful Tool for the Synthesis of C–N Heteropolymeric Dye. *J. Mol. Catal. B Enzym.* **2016**, *134*, 323–330. <https://doi.org/10.1016/j.molcatb.2016.10.004>.

(39) Qwebani-Ogunleye, T.; Kolesnikova, N. I.; Steenkamp, P.; de Koning, C. B.; Brady, D.; Wellington, K. W. A One-Pot Laccase-Catalysed Synthesis of Coumestan Derivatives and Their Anticancer Activity. *Bioorg. Med. Chem.* **2017**, *25* (3), 1172–1182. <https://doi.org/10.1016/j.bmc.2016.12.025>.

(40) Darvishi, F.; Moradi, M.; Jolival, C.; Madzak, C. Laccase Production from Sucrose by Recombinant *Yarrowia Lipolytica* and Its Application to Decolorization of Environmental Pollutant Dyes. *Ecotoxicol. Environ. Saf.* **2018**, *165*, 278–283.

(41) Abd El Monssef, R. A.; Hassan, E. A.; Ramadan, E. M. Production of Laccase Enzyme for Their Potential Application to Decolorize Fungal Pigments on Aging Paper and Parchment. *Ann. Agric. Sci.* **2016**, *61* (1), 145–154. <https://doi.org/10.1016/j.aos.2015.11.007>.

(42) Rahimi, A.; Habibi, D.; Rostami, A.; Ali Zolfigol, M.; Mallakpour, S. Laccase-Catalyzed, Aerobic Oxidative Coupling of 4-Substituted Urazoles with Sodium Arylsulfonates: Green and Mild Procedure for the Synthesis of Arylsulfonyl Triazolinediones. *Tetrahedron Lett.* **2018**, *59* (4), 383–387. <https://doi.org/10.1016/j.tetlet.2017.12.048>.

- (43) Ji, C.; Hou, J.; Wang, K.; Ng, Y. H.; Chen, V. Single-Enzyme Biofuel Cells. *Angew. Chem. Int. Ed.* **2017**, *56* (33), 9762–9766. <https://doi.org/10.1002/anie.201703980>.
- (44) Fillat, A.; Colom, J. F.; Vidal, T. A New Approach to the Biobleaching of Flax Pulp with Laccase Using Natural Mediators. *Bioresour. Technol.* **2010**, *101* (11), 4104–4110. <https://doi.org/10.1016/j.biortech.2010.01.057>.
- (45) Baiocco, P.; Barreca, A. M.; Fabbrini, M.; Galli, C.; Gentili, P. Promoting Laccase Activity towards Non-Phenolic Substrates: A Mechanistic Investigation with Some Laccase–Mediator Systems. *Org Biomol Chem* **2003**, *1* (1), 191–197. <https://doi.org/10.1039/B208951C>.
- (46) Mookoonlall, A.; Sykora, L.; Pfannstiel, J.; Nöbel, S.; Weiss, J.; Hinrichs, J. A Feasibility Study on the Application of a Laccase-Mediator System in Stirred Yoghurt at the Pilot Scale. *Food Hydrocoll.* **2016**, *60*, 119–127. <https://doi.org/10.1016/j.foodhyd.2016.03.027>.
- (47) Pandi, A.; Marichetti Kuppaswami, G.; Numbi Ramudu, K.; Palanivel, S. A Sustainable Approach for Degradation of Leather Dyes by a New Fungal Laccase. *J. Clean. Prod.* **2019**, *211*, 590–597. <https://doi.org/10.1016/j.jclepro.2018.11.048>.
- (48) Mendoza, L.; Jonstrup, M.; Hatti-Kaul, R.; Mattiasson, B. Azo Dye Decolorization by a Laccase/Mediator System in a Membrane Reactor: Enzyme and Mediator Reusability. *Enzyme Microb. Technol.* **2011**, *49* (5), 478–484. <https://doi.org/10.1016/j.enzmictec.2011.08.006>.
- (49) Ji, C.; Hou, J.; Wang, K.; Zhang, Y.; Chen, V. Biocatalytic Degradation of Carbamazepine with Immobilized Laccase-Mediator Membrane Hybrid Reactor. *J. Membr. Sci.* **2016**, *502*, 11–20. <https://doi.org/10.1016/j.memsci.2015.12.043>.
- (50) Fillat, U.; Prieto, A.; Camarero, S.; Martínez, Á. T.; Martínez, M. J. Biodeinking of Flexographic Inks by Fungal Laccases Using Synthetic and Natural Mediators. *Biochem. Eng. J.* **2012**, *67*, 97–103. <https://doi.org/10.1016/j.bej.2012.05.010>.
- (51) Naghdi, M.; Taheran, M.; Brar, S. K.; Kermanshahi-pour, A.; Verma, M.; Surampalli, R. Y. Biotransformation of Carbamazepine by Laccase-Mediator System: Kinetics, by-Products and Toxicity Assessment. *Process Biochem.* **2018**, *67*, 147–154. <https://doi.org/10.1016/j.procbio.2018.02.009>.
- (52) Blánquez, A.; Rodríguez, J.; Brissos, V.; Mendes, S.; Martins, L. O.; Ball, A. S.; Arias, M. E.; Hernández, M. Decolorization and Detoxification of Textile Dyes Using a Versatile *Streptomyces* Laccase-Natural Mediator System. *Saudi J. Biol. Sci.* **2019**, *26* (5), 913–920. <https://doi.org/10.1016/j.sjbs.2018.05.020>.

- (53) Khlifi, R.; Belbahri, L.; Woodward, S.; Ellouz, M.; Dhouib, A.; Sayadi, S.; Mechichi, T. Decolourization and Detoxification of Textile Industry Wastewater by the Laccase-Mediator System. *J. Hazard. Mater.* **2010**, *175* (1–3), 802–808. <https://doi.org/10.1016/j.jhazmat.2009.10.079>.
- (54) Liang, S.; Luo, Q.; Huang, Q. Degradation of Sulfadimethoxine Catalyzed by Laccase with Soybean Meal Extract as Natural Mediator: Mechanism and Reaction Pathway. *Chemosphere* **2017**, *181*, 320–327. <https://doi.org/10.1016/j.chemosphere.2017.04.100>.
- (55) Zeng, S.; Qin, X.; Xia, L. Degradation of the Herbicide Isoproturon by Laccase-Mediator Systems. *Biochem. Eng. J.* **2017**, *119*, 92–100. <https://doi.org/10.1016/j.bej.2016.12.016>.
- (56) Parra Guardado, A. L.; Belleville, M.-P.; Rostro Alanis, M. de J.; Parra Saldivar, R.; Sanchez-Marcano, J. Effect of Redox Mediators in Pharmaceuticals Degradation by Laccase: A Comparative Study. *Process Biochem.* **2019**, *78*, 123–131. <https://doi.org/10.1016/j.procbio.2018.12.032>.
- (57) Hata, T.; Shintate, H.; Kawai, S.; Okamura, H.; Nishida, T. Elimination of Carbamazepine by Repeated Treatment with Laccase in the Presence of 1-Hydroxybenzotriazole. *J. Hazard. Mater.* **2010**, *181* (1–3), 1175–1178. <https://doi.org/10.1016/j.jhazmat.2010.05.103>.
- (58) Murugesan, K.; Chang, Y.-Y.; Kim, Y.-M.; Jeon, J.-R.; Kim, E.-J.; Chang, Y.-S. Enhanced Transformation of Triclosan by Laccase in the Presence of Redox Mediators. *Water Res.* **2010**, *44* (1), 298–308. <https://doi.org/10.1016/j.watres.2009.09.058>.
- (59) Nguyen, L. N.; Hai, F. I.; Kang, J.; Leusch, F. D. L.; Roddick, F.; Magram, S. F.; Price, W. E.; Nghiem, L. D. Enhancement of Trace Organic Contaminant Degradation by Crude Enzyme Extract from *Trametes Versicolor* Culture: Effect of Mediator Type and Concentration. *J. Taiwan Inst. Chem. Eng.* **2014**, *45* (4), 1855–1862. <https://doi.org/10.1016/j.jtice.2014.03.021>.
- (60) Nguyen, L. N.; van de Merwe, J. P.; Hai, F. I.; Leusch, F. D. L.; Kang, J.; Price, W. E.; Roddick, F.; Magram, S. F.; Nghiem, L. D. Laccase–Syringaldehyde-Mediated Degradation of Trace Organic Contaminants in an Enzymatic Membrane Reactor: Removal Efficiency and Effluent Toxicity. *Bioresour. Technol.* **2016**, *200*, 477–484. <https://doi.org/10.1016/j.biortech.2015.10.054>.
- (61) Bringmann, G.; Günther, C.; Ochse, M.; Schupp, O.; Tasler, S. Biaryls in Nature: A Multi-Faceted Class of Stereochemically, Biosynthetically, and Pharmacologically Intriguing Secondary Metabolites. In *Fortschritte der Chemie organischer Naturstoffe / Progress in the Chemistry of Organic Natural Products*; Herz, W., Falk, H., Kirby, G. W., Moore, R. E., Eds.; Springer Vienna: Vienna, 2001; Vol. 82, pp 1–249. https://doi.org/10.1007/978-3-7091-6227-9_1.

- (62) Kim, K.-W.; Smith, C. A.; Daily, M. D.; Cort, J. R.; Davin, L. B.; Lewis, N. G. Trimeric Structure of (+)-Pinoresinol-Forming Dirigent Protein at 1.95 Å Resolution with Three Isolated Active Sites. *J. Biol. Chem.* **2015**, *290* (3), 1308–1318. <https://doi.org/10.1074/jbc.M114.611780>.
- (63) Moss, G. P. (IUPAC Recommendations 2000). *Pure Appl. Chem.* **2000**, *31*.
- (64) Halls, S. C.; Lewis, N. G. Secondary and Quaternary Structures of the (+)-Pinoresinol-Forming Dirigent Protein †. *Biochemistry* **2002**, *41* (30), 9455–9461. <https://doi.org/10.1021/bi0259709>.
- (65) Davin, L. B.; Wang, H.-B.; Crowell, A. L.; Bedgar, D. L.; Martin, D. M.; Sarkanen, S.; Lewis, N. G. Stereoselective Bimolecular Phenoxy Radical Coupling by an Auxiliary (Dirigent) Protein Without an Active Center. *Science* **1997**, *275* (5298), 362–367. <https://doi.org/10.1126/science.275.5298.362>.
- (66) Davin, L. B.; Bedgar, D. L.; Katayama, T.; Lewis, N. G. On the Stereoselective Synthesis of (+)-Pinoresinol in *Forsythia Suspensa* from Its Achiral Precursor, Coniferyl Alcohol. *Phytochemistry* **1992**, *31* (11), 3869–3874. [https://doi.org/10.1016/S0031-9422\(00\)97544-7](https://doi.org/10.1016/S0031-9422(00)97544-7).
- (67) Kim, M. K.; Jeon, J.-H.; Fujita, M.; Davin, L. B.; Lewis, N. G. The Western Red Cedar (*Thuja Plicata*) 8-8' DIRIGENT Family Displays Diverse Expression Patterns and Conserved Monolignol Coupling Specificity. *Plant Mol. Biol.* **2002**, *49* (2), 199–214.
- (68) Kim, K.-W.; Moinuddin, S. G. A.; Atwell, K. M.; Costa, M. A.; Davin, L. B.; Lewis, N. G. Opposite Stereoselectivities of Dirigent Proteins in *Arabidopsis* and *Schizandra* Species. *J. Biol. Chem.* **2012**, *287* (41), 33957–33972. <https://doi.org/10.1074/jbc.M112.387423>.
- (69) Okunishi, T.; Umezawa, T.; Shimada, M. Enantiomeric Compositions and Biosynthesis Of Wikstroemia Sikokiana Lignans. *J. Wood Sci.* **2000**, *46* (3), 234–242. <https://doi.org/10.1007/BF00776455>.
- (70) Nakatsubo, T.; Mizutani, M.; Suzuki, S.; Hattori, T.; Umezawa, T. Characterization of *Arabidopsis Thaliana* Pinoresinol Reductase, a New Type of Enzyme Involved in Lignan Biosynthesis. *J. Biol. Chem.* **2008**, *283* (23), 15550–15557. <https://doi.org/10.1074/jbc.M801131200>.
- (71) Pickel, B.; Constantin, M.-A.; Pfannstiel, J.; Conrad, J.; Beifuss, U.; Schaller, A. An Enantiocomplementary Dirigent Protein for the Enantioselective Laccase-Catalyzed Oxidative Coupling of Phenols. *Angew. Chem. Int. Ed.* **2010**, *49* (1), 202–204. <https://doi.org/10.1002/anie.200904622>.

(72) Pickel, B.; Schaller, A. Dirigent Proteins: Molecular Characteristics and Potential Biotechnological Applications. *Appl. Microbiol. Biotechnol.* **2013**, *97* (19), 8427–8438. <https://doi.org/10.1007/s00253-013-5167-4>.

(73) Jinggao, L.; Stipanovic, R. D.; Bell, A. A.; Puckhaber, L. S.; Magill, C. W. Stereoselective Coupling of Hemigossypol to Form (+)-Gossypol in Moco Cotton Is Mediated by a Dirigent Protein. *Phytochemistry* **2008**, *69* (18), 3038–3042. <https://doi.org/10.1016/j.phytochem.2008.06.007>.

(74) Dalisay, D. S.; Kim, K. W.; Lee, C.; Yang, H.; Rübél, O.; Bowen, B. P.; Davin, L. B.; Lewis, N. G. Dirigent Protein-Mediated Lignan and Cyanogenic Glucoside Formation in Flax Seed: Integrated Omics and MALDI Mass Spectrometry Imaging. *J. Nat. Prod.* **2015**, *78* (6), 1231–1242. <https://doi.org/10.1021/acs.jnatprod.5b00023>.

(75) Seneviratne, H. K.; Dalisay, D. S.; Kim, K.-W.; Moinuddin, S. G. A.; Yang, H.; Hartshorn, C. M.; Davin, L. B.; Lewis, N. G. Non-Host Disease Resistance Response in Pea (*Pisum Sativum*) Pods: Biochemical Function of DRR206 and Phytoalexin Pathway Localization. *Phytochemistry* **2015**, *113*, 140–148. <https://doi.org/10.1016/j.phytochem.2014.10.013>.

(76) Cheng, X.; Su, X.; Muhammad, A.; Li, M.; Zhang, J.; Sun, Y.; Li, G.; Jin, Q.; Cai, Y.; Lin, Y. Molecular Characterization, Evolution, and Expression Profiling of the Dirigent (DIR) Family Genes in Chinese White Pear (*Pyrus bretschneideri*). *Front. Genet.* **2018**, *9*, 136. <https://doi.org/10.3389/fgene.2018.00136>.

(77) Ma, Q.-H.; Liu, Y.-C. TaDIR13, a Dirigent Protein from Wheat, Promotes Lignan Biosynthesis and Enhances Pathogen Resistance. *Plant Mol. Biol. Report.* **2015**, *33* (1), 143–152. <https://doi.org/10.1007/s11105-014-0737-x>.

(78) Zhu, L.; Zhang, X.; Tu, L.; Zeng, F.; Nie, Y.; Guo, X. ISOLATION AND CHARACTERIZATION OF TWO NOVEL DIRIGENT-LIKE GENES HIGHLY INDUCED IN COTTON (*GOSSYPIUM BARBADENSE* AND *G. HIRSUTUM*) AFTER INFECTION BY *VERTICILLIUM DAHLIAE*. *J. Plant Pathol.* **2007**, *6*.

(79) Effenberger, I.; Harport, M.; Pfannstiel, J.; Klaiber, I.; Schaller, A. Expression in *Pichia Pastoris* and Characterization of Two Novel Dirigent Proteins for Atropselective Formation of Gossypol. *Appl. Microbiol. Biotechnol.* **2017**, *101* (5), 2021–2032. <https://doi.org/10.1007/s00253-016-7997-3>.

(80) Effenberger, I.; Zhang, B.; Li, L.; Wang, Q.; Liu, Y.; Klaiber, I.; Pfannstiel, J.; Wang, Q.; Schaller, A. Dirigent Proteins from Cotton (*Gossypium* Sp.) for the Atropselective Synthesis of

Gossypol. *Angew. Chem. Int. Ed.* **2015**, *54* (49), 14660–14663. <https://doi.org/10.1002/anie.201507543>.

(81) Pickel, B.; Pfannstiel, J.; Steudle, A.; Lehmann, A.; Gerken, U.; Pleiss, J.; Schaller, A. A Model of Dirigent Proteins Derived from Structural and Functional Similarities with Allene Oxide Cyclase and Lipocalins. *FEBS J.* **2012**, *279* (11), 1980–1993. <https://doi.org/10.1111/j.1742-4658.2012.08580.x>.

(82) Gasper, R.; Effenberger, I.; Kolesinski, P.; Terlecka, B.; Hofmann, E.; Schaller, A. Dirigent Protein Mode of Action Revealed by the Crystal Structure of *AtDIR6*. *Plant Physiol.* **2016**, *172* (4), 2165–2175. <https://doi.org/10.1104/pp.16.01281>.

(83) Ralph, J.; Schatz, P. F.; Lu, F.; Kim, H.; Akiyama, T.; Nelsen, S. F. Quinone Methides in Lignification. In *Quinone Methides*; Rokita, S. E., Ed.; John Wiley & Sons, Inc.: Hoboken, NJ, USA, 2009; pp 385–420. <https://doi.org/10.1002/9780470452882.ch12>.

(84) Paniagua, C.; Bilkova, A.; Jackson, P.; Dabravolski, S.; Riber, W.; Didi, V.; Houser, J.; Gigli-Bisceglia, N.; Wimmerova, M.; Budínská, E.; et al. Dirigent Proteins in Plants: Modulating Cell Wall Metabolism during Abiotic and Biotic Stress Exposure. *J. Exp. Bot.* **2017**, *68* (13), 3287–3301. <https://doi.org/10.1093/jxb/erx141>.

(85) Zhang, Y.; Haobin, Z.; Yichao, D.; Qi, L.; Dongyan, S.; Junling, S.; Qingsheng, H. Antitumor Activity of Pinoresinol in Vitro: Inducing Apoptosis and Inhibiting HepG2 Invasion. *J. Funct. Foods* **2018**, *45*, 206–214. <https://doi.org/10.1016/j.jff.2018.04.009>.

(86) Asgher, M.; Shahid, M.; Kamal, S.; Iqbal, H. M. N. Recent Trends and Valorization of Immobilization Strategies and Ligninolytic Enzymes by Industrial Biotechnology. *J. Mol. Catal. B Enzym.* **2014**, *101*, 56–66. <https://doi.org/10.1016/j.molcatb.2013.12.016>.

(87) Fernández-Fernández, M.; Sanromán, M. Á.; Moldes, D. Recent Developments and Applications of Immobilized Laccase. *Biotechnol. Adv.* **2013**, *31* (8), 1808–1825. <https://doi.org/10.1016/j.biotechadv.2012.02.013>.

(88) Naghdi, M.; Taheran, M.; Brar, S. K.; Kermanshahi-pour, A.; Verma, M.; Surampalli, R. Y. Immobilized Laccase on Oxygen Functionalized Nanobiochars through Mineral Acids Treatment for Removal of Carbamazepine. *Sci. Total Environ.* **2017**, *584–585*, 393–401. <https://doi.org/10.1016/j.scitotenv.2017.01.021>.

(89) Jesionowski, T.; Zdarta, J.; Krajewska, B. Enzyme Immobilization by Adsorption: A Review. *Adsorption* **2014**, *20* (5–6), 801–821. <https://doi.org/10.1007/s10450-014-9623-y>.

- (90) Hernandez, K.; Fernandez-Lafuente, R. Control of Protein Immobilization: Coupling Immobilization and Site-Directed Mutagenesis to Improve Biocatalyst or Biosensor Performance. *Enzyme Microb. Technol.* **2011**, *48* (2), 107–122.
- (91) Durán, N.; Rosa, M. A.; D'Annibale, A.; Gianfreda, L. Applications of Laccases and Tyrosinases (Phenoloxidases) Immobilized on Different Supports: A Review. *Enzyme Microb. Technol.* **2002**, *31* (7), 907–931.
- (92) Sheldon, R. A. Enzyme Immobilization: The Quest for Optimum Performance. *Adv. Synth. Catal.* **2007**, *349* (8–9), 1289–1307. <https://doi.org/10.1002/adsc.200700082>.
- (93) Lalonde, J.; Margolin, A. Immobilization of Enzymes. In *Enzyme Catalysis in Organic Synthesis*; Drauz, K., Waldmann, H., Eds.; Wiley-VCH Verlag GmbH: Weinheim, Germany, 2002; pp 163–184. <https://doi.org/10.1002/9783527618262.ch6>.
- (94) Basak, B.; Bhunia, B.; Dey, A. Studies on the Potential Use of Sugarcane Bagasse as Carrier Matrix for Immobilization of *Candida Tropicalis* PHB5 for Phenol Biodegradation. *Int. Biodeterior. Biodegrad.* **2014**, *93*, 107–117. <https://doi.org/10.1016/j.ibiod.2014.05.012>.
- (95) Brady, D.; Jordaan, J. Advances in Enzyme Immobilisation. *Biotechnol. Lett.* **2009**, *31* (11), 1639.
- (96) Mateo, C.; Palomo, J. M.; Fernandez-Lorente, G.; Guisan, J. M.; Fernandez-Lafuente, R. Improvement of Enzyme Activity, Stability and Selectivity via Immobilization Techniques. *Enzyme Microb. Technol.* **2007**, *40* (6), 1451–1463. <https://doi.org/10.1016/j.enzmictec.2007.01.018>.
- (97) Rochefort, D.; Kouisni, L.; Gendron, K. Physical Immobilization of Laccase on an Electrode by Means of Poly (Ethyleneimine) Microcapsules. *J. Electroanal. Chem.* **2008**, *617* (1), 53–63.
- (98) Rochefort, D.; Kouisni, L.; Gendron, K. Physical Immobilization of Laccase on an Electrode by Means of Poly(Ethyleneimine) Microcapsules. *J. Electroanal. Chem.* **2008**, *617* (1), 53–63. <https://doi.org/10.1016/j.jelechem.2008.01.027>.
- (99) Arroyo, D. M. Inmovilización de enzimas. Fundamentos, métodos y aplicaciones. **1998**, 17.
- (100) Lonappan, L.; Liu, Y.; Rouissi, T.; Pourcel, F.; Brar, S. K.; Verma, M.; Surampalli, R. Y. Covalent Immobilization of Laccase on Citric Acid Functionalized Micro-Biochars Derived from Different Feedstock and Removal of Diclofenac. *Chem. Eng. J.* **2018**, *351*, 985–994. <https://doi.org/10.1016/j.cej.2018.06.157>.

- (101) Frasconi, M.; Mazzei, F.; Ferri, T. Protein Immobilization at Gold–Thiol Surfaces and Potential for Biosensing. *Anal. Bioanal. Chem.* **2010**, 398 (4), 1545–1564. <https://doi.org/10.1007/s00216-010-3708-6>.
- (102) Sheldon, R. A. Characteristic Features and Biotechnological Applications of Cross-Linked Enzyme Aggregates (CLEAs). *Appl. Microbiol. Biotechnol.* **2011**, 92 (3), 467–477.
- (103) Linqiu, C.; van Langen, L.; Sheldon, R. A. Immobilised Enzymes: Carrier-Bound or Carrier-Free? *Curr. Opin. Biotechnol.* **2003**, 14 (4), 387–394.
- (104) Nelson, J. M.; Griffin, E. G. ADSORPTION OF INVERTASE. *J. Am. Chem. Soc.* **1916**, 38 (5), 1109–1115. <https://doi.org/10.1021/ja02262a018>.
- (105) Shackley, S.; Carter, S.; Knowles, T.; Middelink, E.; Haeefe, S.; Sohi, S.; Cross, A.; Haszeldine, S. Sustainable Gasification–Biochar Systems? A Case-Study of Rice-Husk Gasification in Cambodia, Part I: Context, Chemical Properties, Environmental and Health and Safety Issues. *Energy Policy* **2012**, 42, 49–58. <https://doi.org/10.1016/j.enpol.2011.11.026>.
- (106) Lonappan, L.; Liu, Y.; Rouissi, T.; Brar, S. K.; Verma, M.; Surampalli, R. Y. Adsorptive Immobilization of Agro-Industrially Produced Crude Laccase on Various Micro-Biochars and Degradation of Diclofenac. *Sci. Total Environ.* **2018**, 640–641, 1251–1258. <https://doi.org/10.1016/j.scitotenv.2018.06.005>.
- (107) Chintala, R.; Schumacher, T. E.; Kumar, S.; Malo, D. D.; Rice, J. A.; Bleakley, B.; Chilom, G.; Clay, D. E.; Julson, J. L.; Papiernik, S. K.; et al. Molecular Characterization of Biochars and Their Influence on Microbiological Properties of Soil. *J. Hazard. Mater.* **2014**, 279, 244–256. <https://doi.org/10.1016/j.jhazmat.2014.06.074>.
- (108) Brugnari, T.; Pereira, M. G.; Bubna, G. A.; de Freitas, E. N.; Contato, A. G.; Corrêa, R. C. G.; Castoldi, R.; de Souza, C. G. M.; Polizeli, M. de L. T. de M.; Bracht, A.; et al. A Highly Reusable MANAE-Agarose-Immobilized Pleurotus Ostreatus Laccase for Degradation of Bisphenol A. *Sci. Total Environ.* **2018**, 634, 1346–1351. <https://doi.org/10.1016/j.scitotenv.2018.04.051>.
- (109) Lassouane, F.; Aït-Amar, H.; Amrani, S.; Rodriguez-Couto, S. A Promising Laccase Immobilization Approach for Bisphenol A Removal from Aqueous Solutions. *Bioresour. Technol.* **2019**, 271, 360–367. <https://doi.org/10.1016/j.biortech.2018.09.129>.
- (110) Daâssi, D.; Rodríguez-Couto, S.; Nasri, M.; Mechichi, T. Biodegradation of Textile Dyes by Immobilized Laccase from *Coriolopsis Gallica* into Ca-Alginate Beads. *Int. Biodeterior. Biodegrad.* **2014**, 90, 71–78. <https://doi.org/10.1016/j.ibiod.2014.02.006>.

- (111) Wen, X.; Zeng, Z.; Du, C.; Huang, D.; Zeng, G.; Xiao, R.; Lai, C.; Xu, P.; Zhang, C.; Wan, J.; et al. Immobilized Laccase on Bentonite-Derived Mesoporous Materials for Removal of Tetracycline. *Chemosphere* **2019**, *222*, 865–871. <https://doi.org/10.1016/j.chemosphere.2019.02.020>.
- (112) Ji, C.; Nguyen, L. N.; Hou, J.; Hai, F. I.; Chen, V. Direct Immobilization of Laccase on Titania Nanoparticles from Crude Enzyme Extracts of *P. Ostreatus* Culture for Micro-Pollutant Degradation. *Sep. Purif. Technol.* **2017**, *178*, 215–223. <https://doi.org/10.1016/j.seppur.2017.01.043>.
- (113) Kashefi, S.; Borghei, S. M.; Mahmoodi, N. M. Covalently Immobilized Laccase onto Graphene Oxide Nanosheets: Preparation, Characterization, and Biodegradation of Azo Dyes in Colored Wastewater. *J. Mol. Liq.* **2019**, *276*, 153–162. <https://doi.org/10.1016/j.molliq.2018.11.156>.
- (114) Skoronski, E.; Souza, D. H.; Ely, C.; Broilo, F.; Fernandes, M.; Junior, A. F.; Ghislandi, M. G. Immobilization of Laccase from *Aspergillus Oryzae* on Graphene Nanosheets. *Int. J. Biol. Macromol.* **2017**, *99*, 121–127.
- (115) Patila, M.; Kouloumpis, A.; Gournis, D.; Rudolf, P.; Stamatis, H. Laccase-Functionalized Graphene Oxide Assemblies as Efficient Nanobiocatalysts for Oxidation Reactions. *Sensors* **2016**, *16* (3), 287. <https://doi.org/10.3390/s16030287>.
- (116) Tavares, A. P. M.; Silva, C. G.; Dražić, G.; Silva, A. M. T.; Loureiro, J. M.; Faria, J. L. Laccase Immobilization over Multi-Walled Carbon Nanotubes: Kinetic, Thermodynamic and Stability Studies. *J. Colloid Interface Sci.* **2015**, *454*, 52–60. <https://doi.org/10.1016/j.jcis.2015.04.054>.
- (117) Shao, B.; Liu, Z.; Zeng, G.; Liu, Y.; Yang, X.; Zhou, C.; Chen, M.; Liu, Y.; Jiang, Y.; Yan, M. Immobilization of Laccase on Hollow Mesoporous Carbon Nanospheres: Noteworthy Immobilization, Excellent Stability and Efficacious for Antibiotic Contaminants Removal. *J. Hazard. Mater.* **2019**, *362*, 318–326. <https://doi.org/10.1016/j.jhazmat.2018.08.069>.
- (118) Nguyen, T. A.; Fu, C.-C.; Juang, R.-S. Effective Removal of Sulfur Dyes from Water by Biosorption and Subsequent Immobilized Laccase Degradation on Crosslinked Chitosan Beads. *Chem. Eng. J.* **2016**, *304*, 313–324. <https://doi.org/10.1016/j.cej.2016.06.102>.
- (119) Asgher, M.; Noreen, S.; Bilal, M. Enhancing Catalytic Functionality of *Trametes Versicolor* IBL-04 Laccase by Immobilization on Chitosan Microspheres. *Chem. Eng. Res. Des.* **2017**, *119*, 1–11. <https://doi.org/10.1016/j.cherd.2016.12.011>.

- (120) Zheng, F.; Cui, B.-K.; Wu, X.-J.; Meng, G.; Liu, H.-X.; Si, J. Immobilization of Laccase onto Chitosan Beads to Enhance Its Capability to Degrade Synthetic Dyes. *Int. Biodeterior. Biodegrad.* **2016**, *110*, 69–78. <https://doi.org/10.1016/j.ibiod.2016.03.004>.
- (121) Jaiswal, N.; Pandey, V. P.; Dwivedi, U. N. Immobilization of Papaya Laccase in Chitosan Led to Improved Multipronged Stability and Dye Discoloration. *Int. J. Biol. Macromol.* **2016**, *86*, 288–295. <https://doi.org/10.1016/j.ijbiomac.2016.01.079>.
- (122) Yang, J.; Lin, Y.; Yang, X.; Ng, T. B.; Ye, X.; Lin, J. Degradation of Tetracycline by Immobilized Laccase and the Proposed Transformation Pathway. *J. Hazard. Mater.* **2017**, *322*, 525–531. <https://doi.org/10.1016/j.jhazmat.2016.10.019>.
- (123) Xia, T.-T.; Liu, C.-Z.; Hu, J.-H.; Guo, C. Improved Performance of Immobilized Laccase on Amine-Functioned Magnetic Fe₃O₄ Nanoparticles Modified with Polyethylenimine. *Chem. Eng. J.* **2016**, *295*, 201–206.
- (124) Rahmani, K.; Faramarzi, M. A.; Mahvi, A. H.; Gholami, M.; Esrafil, A.; Forootanfar, H.; Farzadkia, M. Elimination and Detoxification of Sulfathiazole and Sulfamethoxazole Assisted by Laccase Immobilized on Porous Silica Beads. *Int. Biodeterior. Biodegrad.* **2015**, *97*, 107–114. <https://doi.org/10.1016/j.ibiod.2014.10.018>.
- (125) Mohammadi, M.; As'habi, M. A.; Salehi, P.; Yousefi, M.; Nazari, M.; Brask, J. Immobilization of Laccase on Epoxy-Functionalized Silica and Its Application in Biodegradation of Phenolic Compounds. *Int. J. Biol. Macromol.* **2018**, *109*, 443–447. <https://doi.org/10.1016/j.ijbiomac.2017.12.102>.
- (126) Pang, S.; Wu, Y.; Zhang, X.; Li, B.; Ouyang, J.; Ding, M. Immobilization of Laccase via Adsorption onto Bimodal Mesoporous Zr-MOF. *Process Biochem.* **2016**, *51* (2), 229–239. <https://doi.org/10.1016/j.procbio.2015.11.033>.
- (127) Cousin, F.; Cabuil, V.; Levitz, P. Magnetic Colloidal Particles as Probes for the Determination of the Structure of Laponite Suspensions. *Langmuir* **2002**, *18* (5), 1466–1473. <https://doi.org/10.1021/la010947u>.
- (128) Schütt, W.; Grüttner, C.; Häfeli, U.; Zborowski, M.; Teller, J.; Putzar, H.; Schümichen, C. Applications of Magnetic Targeting in Diagnosis and Therapy—Possibilities and Limitations: A Mini-Review. *Hybridoma* **1997**, *16* (1), 109–117.
- (129) Wahajuddin; Arora. Superparamagnetic Iron Oxide Nanoparticles: Magnetic Nanoplatforms as Drug Carriers. *Int. J. Nanomedicine* **2012**, 3445. <https://doi.org/10.2147/IJN.S30320>.

(130) Cole, A. J.; Yang, V. C.; David, A. E. Cancer Theranostics: The Rise of Targeted Magnetic Nanoparticles. *Trends Biotechnol.* **2011**, *29* (7), 323–332. <https://doi.org/10.1016/j.tibtech.2011.03.001>.

(131) Singamaneni, S.; Bliznyuk, V. N.; Binek, C.; Tsymbal, E. Y. Magnetic Nanoparticles: Recent Advances in Synthesis, Self-Assembly and Applications. *J. Mater. Chem.* **2011**, *21* (42), 16819. <https://doi.org/10.1039/c1jm11845e>.

(132) Fortes, C. C. S.; Daniel-da-Silva, A. L.; Xavier, A. M. R. B.; Tavares, A. P. M. Optimization of Enzyme Immobilization on Functionalized Magnetic Nanoparticles for Laccase Biocatalytic Reactions. *Chem. Eng. Process. Process Intensif.* **2017**, *117*, 1–8. <https://doi.org/10.1016/j.cep.2017.03.009>.

(133) Patel, S. K. S.; Kalia, V. C.; Choi, J.-H.; Haw, J.-R.; Kim, I.-W.; Lee, J. K. Immobilization of Laccase on SiO₂ Nanocarriers Improves Its Stability and Reusability. *J. Microbiol. Biotechnol.* **2014**, *24* (5), 639–647. <https://doi.org/10.4014/jmb.1401.01025>.

(134) Wang, H.; Zhang, W.; Zhao, J.; Xu, L.; Zhou, C.; Chang, L.; Wang, L. Rapid Decolorization of Phenolic Azo Dyes by Immobilized Laccase with Fe₃O₄/SiO₂ Nanoparticles as Support. *Ind. Eng. Chem. Res.* **2013**, *52* (12), 4401–4407. <https://doi.org/10.1021/ie302627c>.

(135) Rouhani, S.; Rostami, A.; Salimi, A. Preparation and Characterization of Laccases Immobilized on Magnetic Nanoparticles and Their Application as a Recyclable Nanobiocatalyst for the Aerobic Oxidation of Alcohols in the Presence of TEMPO. *RSC Adv.* **2016**, *6* (32), 26709–26718. <https://doi.org/10.1039/C6RA00103C>.

(136) Xiaobing, Z.; Qi, W.; Yanjun, J.; Jing, G. Biomimetic Synthesis of Magnetic Composite Particles for Laccase Immobilization. *Ind. Eng. Chem. Res.* **2012**, *51* (30), 10140–10146. <https://doi.org/10.1021/ie3000908>.

(137) Shi, L.; Ma, F.; Han, Y.; Zhang, X.; Yu, H. Removal of Sulfonamide Antibiotics by Oriented Immobilized Laccase on Fe₃O₄ Nanoparticles with Natural Mediators. *J. Hazard. Mater.* **2014**, *279*, 203–211. <https://doi.org/10.1016/j.jhazmat.2014.06.070>.

(138) Altunbaş, C.; Uygun, M.; Uygun, D. A.; Akgöl, S.; Denizli, A. Immobilization of Inulinase on Concanavalin A-Attached Super Macroporous Cryogel for Production of High-Fructose Syrup. *Appl. Biochem. Biotechnol.* **2013**, *170* (8), 1909–1921.

(139) Arnold, F. H. Metal-Affinity Separations: A New Dimension in Protein Processing. *Nat. Biotechnol.* **1991**, *9* (2), 151–156. <https://doi.org/10.1038/nbt0291-151>.

- (140) Xia, T.; Guan, Y.; Yang, M.; Xiong, W.; Wang, N.; Zhao, S.; Guo, C. Synthesis of Polyethylenimine Modified Fe₃O₄ Nanoparticles with Immobilized Cu²⁺ for Highly Efficient Proteins Adsorption. *Colloids Surf. Physicochem. Eng. Asp.* **2014**, *443*, 552–559. <https://doi.org/10.1016/j.colsurfa.2013.12.026>.
- (141) Wang, K.-F.; Liu, C.; Sui, K.; Guo, C.; Liu, C.-Z. Efficient Catalytic Oxidation of 5-Hydroxymethylfurfural to 2,5-Furandicarboxylic Acid by Magnetic Laccase Catalyst. *ChemBioChem* **2018**, *19* (7), 654–659. <https://doi.org/10.1002/cbic.201800008>.
- (142) Wang, Y.; Chen, X.; Liu, J.; He, F.; Wang, R. Immobilization of Laccase by Cu²⁺ Chelate Affinity Interaction on Surface-Modified Magnetic Silica Particles and Its Use for the Removal of 2,4-Dichlorophenol. *Environ. Sci. Pollut. Res.* **2013**, *20* (9), 6222–6231. <https://doi.org/10.1007/s11356-013-1661-6>.
- (143) Türkmen, D.; Yavuz, H.; Denizli, A. Synthesis of Tentacle Type Magnetic Beads as Immobilized Metal Chelate Affinity Support for Cytochrome c Adsorption. *Int. J. Biol. Macromol.* **2006**, *38* (2), 126–133. <https://doi.org/10.1016/j.ijbiomac.2006.01.018>.
- (144) Feng, W.; Chen, G.; Liang-rong, Y.; Chun-Zhao, L. Magnetic Mesoporous Silica Nanoparticles: Fabrication and Their Laccase Immobilization Performance. *Bioresour. Technol.* **2010**, *101* (23), 8931–8935. <https://doi.org/10.1016/j.biortech.2010.06.115>.
- (145) Kalkan, N. A.; Aksoy, S.; Aksoy, E. A.; Hasirci, N. Preparation of Chitosan-Coated Magnetite Nanoparticles and Application for Immobilization of Laccase. *J. Appl. Polym. Sci.* **2012**, *123* (2), 707–716.
- (146) Jořenek, M.; Zajoncová, L. Immobilization of Laccase on Magnetic Carriers and Its Use in Decolorization of Dyes. *Chem. Biochem. Eng. Q.* **2015**, *29* (3), 457–466.
- (147) Tischer, W.; Wedekind, F. Immobilized Enzymes: Methods and Applications. In *Biocatalysis—from discovery to application*; Springer, 1999; pp 95–126.
- (148) Min, L.; Li Qun, X.; Liang, W.; Y. P., W.; Li, J.; Neoh, K.-G.; Kang, E.-T. Clickable Poly (Ester Amine) Dendrimer-Grafted Fe₃O₄ Nanoparticles Prepared via Successive Michael Addition and Alkyne–Azide Click Chemistry. *Polym. Chem.* **2011**, *2* (6), 1312–1321.
- (149) Ranjan, R.; Brittain, W. J. Combination of Living Radical Polymerization and Click Chemistry for Surface Modification. *Macromolecules* **2007**, *40* (17), 6217–6223. <https://doi.org/10.1021/ma0705873>.

(150) White, M. A.; Johnson, J. A.; Koberstein, J. T.; Turro, N. J. Toward the Syntheses of Universal Ligands for Metal Oxide Surfaces: Controlling Surface Functionality through Click Chemistry. *J. Am. Chem. Soc.* **2006**, *128* (35), 11356–11357. <https://doi.org/10.1021/ja064041s>.

(151) Lin, P.-C.; Ueng, S.-H.; Yu, S.-C.; Jan, M.-D.; Adak, A. K.; Yu, C.-C.; Lin, C.-C. Surface Modification of Magnetic Nanoparticle via Cu(I)-Catalyzed Alkyne-Azide [2 + 3] Cycloaddition. *Org. Lett.* **2007**, *9* (11), 2131–2134. <https://doi.org/10.1021/ol070588f>.

(152) Sun, E. Y.; Josephson, L.; Weissleder, R. “Clickable” Nanoparticles for Targeted Imaging. *Mol. Imaging* **2006**, *5* (2), 7290.2006.00013. <https://doi.org/10.2310/7290.2006.00013>.

(153) Modolo, C. L'intrigant couplage radicalaire stéréosélectif médié par la protéine dirigeante *AtDIR6*, Aix Marseille university, 2017.

Chapter II

*Stereoselective Radical Coupling
Mediated by
the Dirigent Protein AtDIR6*

1 Introduction

Looking for factors changing the fate of laccase catalyzed reactions, studies on dirigent proteins have recently started at our lab.^{1,2} AtDIR6, one of the first characterized proteins, is directing the coupling of laccase produced phenoxy radicals to form an optically pure lignan: the (-)-pinoresinol. Achievements made with AtDIR6 prompted us to prospects for its use for the controlled formation of new enatiopure products.

Beyond the results of our previous research on AtDIR6, new experiments and results are collected in this chapter. First, AtDIR6 was purified and its activity was assessed during coniferyl alcohol oxidation. Then analogues of coniferyl alcohol were synthesized and were used to explore the plasticity of AtDIR6 towards new substrates. Next, the stabilization of coniferyl alcohol analogues radicals by AtDIR6 was monitored by EPR. Last, we tried to use coniferyl alcohol radicals as a probe to identify amino acids within the cavity of AtDIR6 that are involved in the stereoselective control.

2 Production of AtDIR6

To study the mechanism of dirigent protein, obtaining pure AtDIR6 is the first necessary step. The production of the recombinant protein (C-terminally His tagged) in *Pichia Pastoris* is well established in our lab. AtDIR6 was purified from culture supernatants of *Pichia Pastoris*.

2.1 Purification of AtDIR6

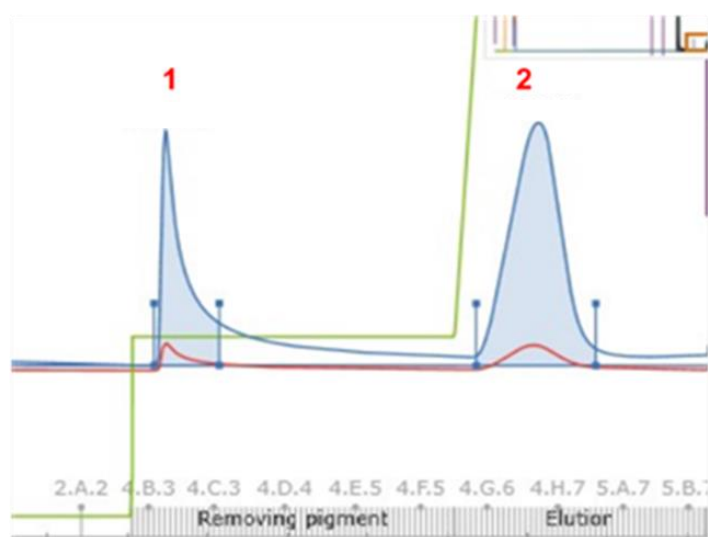


Fig. II-2-1 Elution profile of the His-Trap column. The red line displays the absorbance at 415 nm, and the blue line indicates the absorbance at 280 nm, the green line displays the imidazole concentration gradient.

AtDIR6 was first purified directly from culture supernatants by Immobilized Metal Affinity Chromatography (IMAC). Part of the chromatogram (elution profile) is seen in **Fig. II-2-1**. Two peaks corresponding to the elution of separated protein materials were observed: the first one (marked as 1) contains an unknown contaminant protein (see the SDS-PAGE gel in **Fig. II-2-3**) washed out at low imidazole concentration (23 mM); the second one (numbered as 2) contains the dirigent protein *AtDIR6* which was eluted at about 180 mM imidazole. Fractions corresponding to the *AtDIR6* peak were pooled and concentrated, then stored in 0.1 M pH=5 acetate buffer at 4°C prior further use.

AtDIR6 purified from affinity Chromatography still displayed a significant absorbance at 415nm (as shown in the Chromatogram in **Fig. II-2-1**) reminiscent of a pigment making the protein solution slightly yellow. Since the effect of this yellow substance on the protein was not known, a further purification step by Size Exclusion Chromatography (SEC) was applied to try to remove the color.

Elution profile from the SEC Chromatogram is shown **Fig. II-2-2**. Two protein peak, potentially corresponding to different oligomerization states of *AtDIR6*, were separated. The material absorbing at 415nm co-eluted with the major protein peak (smaller elution volume) whereas it was found absent from a peak of proteins eluting at higher volume of buffer. The two different “states” of the *AtDIR6* protein after SEC were called DP1 and DP2 respectively.

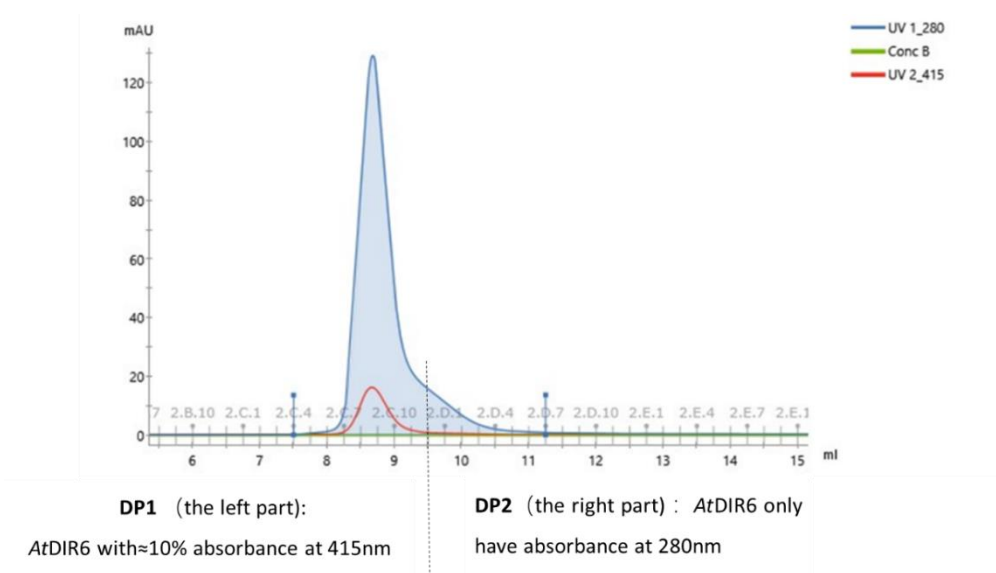


Fig. II-2-2 Elution profile on Size Exclusion Chromatography

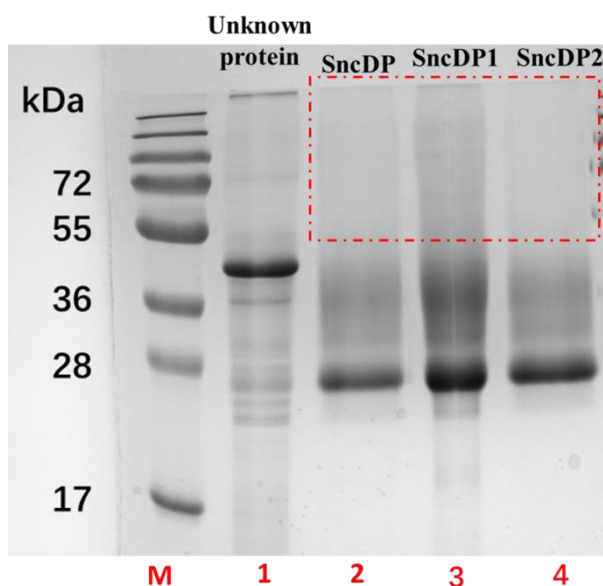


Fig. II-2-3 SDS-PAGE analysis of samples from the purification of *AtDIR6*. 5 μ g of protein loaded per lane. Lane M: molecular weight makers; lane1: IMAC elution peak 1; lane 2: IMAC elution peak 2; lane 3: SEC elution peak 1 (from IMAC elution peak 2); lane4; SEC elution peak 2 (from IMAC elution peak 2).

Protein fractions collected from the purification steps were analyzed on SDS-PAGE (**Fig. II-2-3**). A main band at ~40kDa was observed in the unknown protein fraction. In lanes 2, 3 and 4 a band around 25kDa is distinctly visible as well as smears between 35 and 40 kDa. These features are consistent with that of DP as for example described in the article of Kazenwadel *et al.*,³ in which they have conducted MALDI-TOF-MS analysis and determined the molecular mass of glycosylated *AtDIR6* derived from *P. pastoris* as 24.6 kDa. Smears are attributed to post translational modification of the recombinant protein in the *P. pastoris* expression system. High molecular weight material present in DP1 sample and absent in DP and DP2 ones may be the main responsible of the absorbing material in the collected fraction (**Fig. II-2-3** red dotted square).

2.2 *AtDIR6* activity on Coniferyl Alcohol oxidation

2.2.1 Activity measurement principle

The recombinant *AtDIR6* was employed in laccase-catalyzed bioconversion of coniferyl alcohol to monitor its control on the activity. Coniferyl alcohol belongs to the monolignols family which are building blocks in the biosynthesis of natural product such as lignans and neo-lignans.⁴

The dimerization of coniferyl alcohol generally involves two steps. In the first step: a single-electron oxidation of coniferyl alcohol occurs catalyzed by an oxidase/oxidant (such as peroxidases, laccase or ammonium peroxydisulfate), forming the corresponding phenoxy radical species (**Fig. II-**

2-4 A). In a second step, radicals dimerize to yield a mixture of (\pm)-dehydrodiconiferyl alcohols, (\pm)-pinoresinols, and (\pm)-guaiacylglycerol 8-O-4'-coniferyl alcohol ethers (Fig. II-2-4 B) prior further polymerization. In presence of DIRs optically pure pinoresinol is obtained as major product under a strict regio- and stereospecific control.⁵ Based on this mechanism, the dirigent activity of a DP can be monitored by the quantification of the products formed during the DP-mediated coupling of oxidized CA.

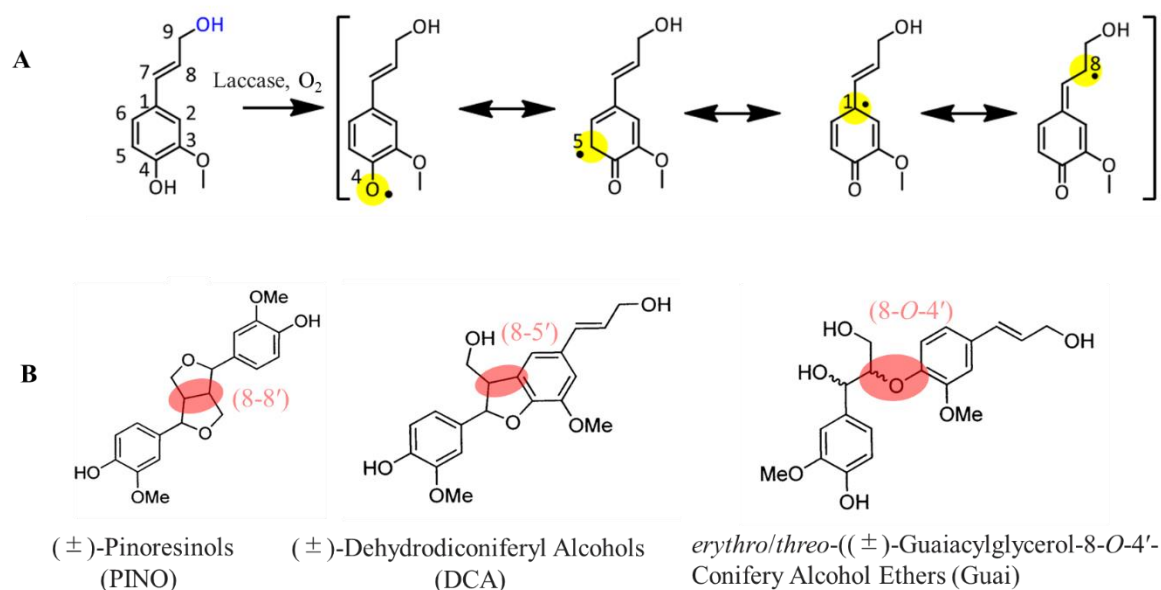


Fig. II-2-4 Oxidation and coupling of coniferyl alcohol. A: Resonance forms of the coniferyl radical produced upon oxidation. B: chemical structure of the dimers obtained from coniferyl alcohol oxidation.

2.2.2 HPLC chromatogram

HPLC analyses were carried out following the detailed procedure described in Appendix: Materials and Methods Chapter II. One typical chromatogram containing basic information about products obtained during CA oxidation in the presence or in the absence of DP is shown in Fig. II-2-5. The retention time for each compound are listed as follows: RT(CA)= 10.23 min; RT (GUA) = 13.67 min; RT (DCA)= 16.99 min; RT (PINO) = 18.57 min; RT (Benzo, reference) = 25.29 min.

A simple inspection of chromatograms of samples incubated with or without DP reveals changes in the composition of products mix. In the absence of AtDIR6, the main product is DCA>PINO>GUA, while in the presence of AtDIR6 (500 μ M) the relative content of products

changes: radicals dimerization in the presence of DP forms more PINO and less of the other two dimers.

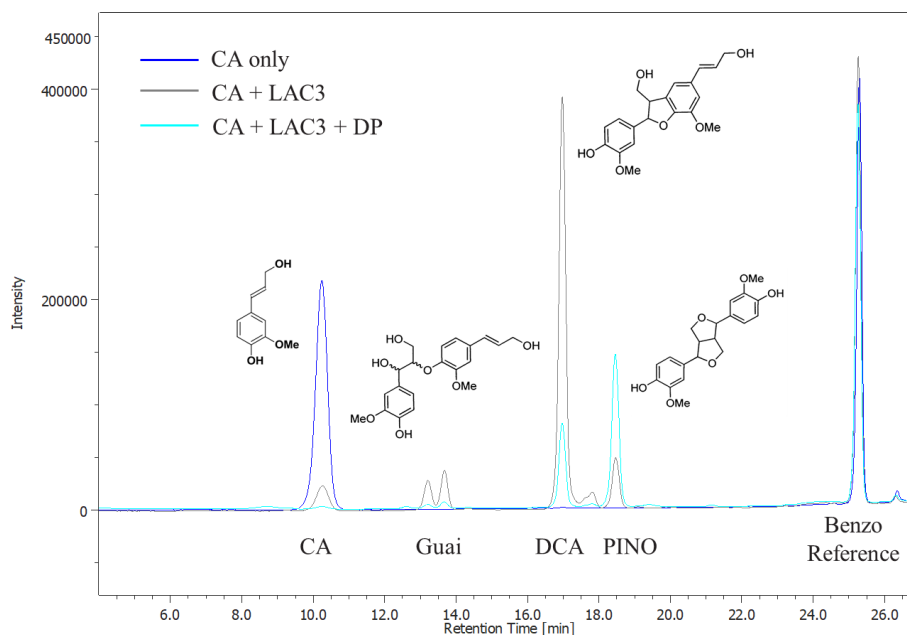


Fig. II-2-5 HPLC chromatogram of the oxidized Coniferyl Alcohol coupling. The chromatograms reflect the disappearance of the CA and the appearance of the products. In the absence of DP, the main product is DCA while in the presence of DP it is PINO. Experimental conditions: 1.6mM CA and 1U/L LAC3 with or without 500 μ M DP in a final volume of 100 μ L, 0.1M acetate buffer pH 5.0. Thermomixer 1000rpm at 30 $^{\circ}$ C, T=20 hours.

2.2.3 Effect of AtDIR6 on oxidation kinetics of CA and formation of dimers

CA oxidation kinetics were separately followed in the presence or absence of AtDIR6. To minimize over polymerization of the neo formed dimers (i.e. they laccase substrate as well), the reaction time was set to 25 hours with a controlled amount of laccase (1U/L). The relative contents of CA and dimers are represented by the ratio of *the peak area of each substance* to *the peak area of the reference Benzo* from the HPLC chromatogram.

In the absence of DP, CA oxidation catalyzed by laccase formed DCA as a major (**Fig. II-2-6**). In the presence of AtDIR6, the GUA formation is diminished, the rate of DCA formation decreases while that of PINO increases (**Fig. II-2-6** right part).

Base on our previous experience with *AtDIR6*, the ratio DCA/PINO is positively correlated with the enantiomeric excess (ee) of PINO, so this ratio is considered as a criterion for determining DP activity.¹ In the following discussion, we will focus on this ratio. The smaller the ratio is, the greater the dirigent effect of *AtDIR6* on the reaction is.

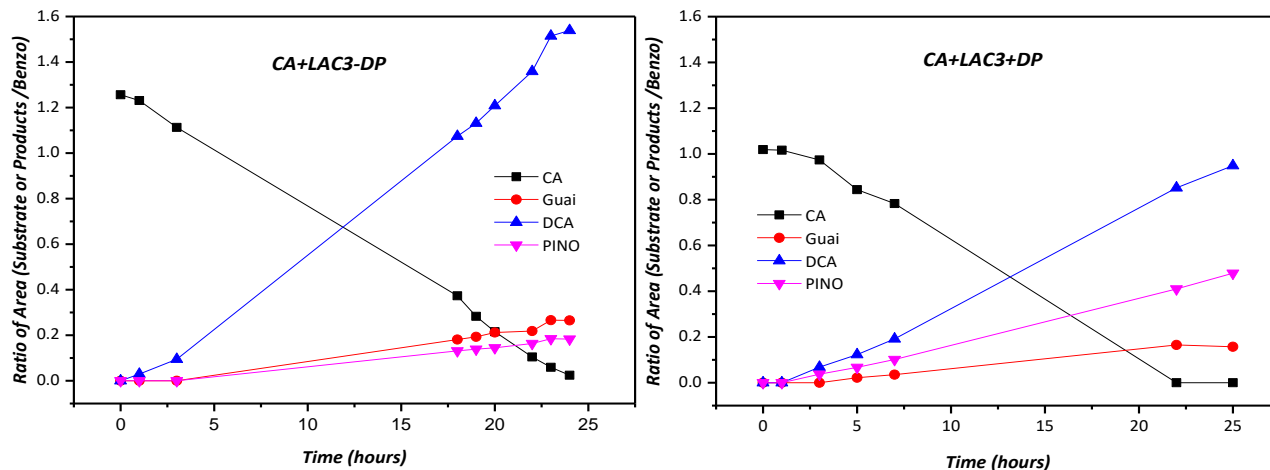


Fig. II-2-6 CA consumption and dimers generation over time. **Left:** absence of *AtDIR6*; **Right:** presence of *AtDIR6*. Experimental conditions: 1.6mM CA and 1U/L LAC3 with no DP or 100 μ M DP in a final volume of 1mL, 0.1M acetate buffer pH 5.0. Thermomixer 1000rpm at 30 $^{\circ}$ C, for a maximum 25 hours. Samples were taken for testing over time progress. Y axis is the ratio of the peak area corresponding to each substance to the peak area of the reference in HPLC chromatogram.

2.2.4 Effects of varying *AtDIR6* concentration

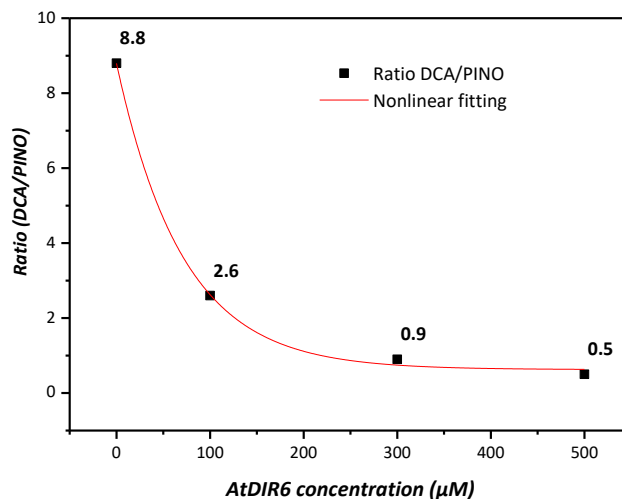


Fig. II-2-7 Effect of varying DP concentration on coniferyl alcohol derived coupling products

AtDIR6 concentration was varied to further characterize the produced recombinant protein. From **Fig. II-2-7** it can be seen that higher concentration of *AtDIR6* caused greater impact. When the DP concentration reached 300 μ M, the ratio of DCA and PINO was 0.9, which is much smaller than

the ratio (8.8) in the absence of AtDIR6. And it is almost three times the ratio at concentration 100 μ M (2.7), this corresponds to the triple relationship between DP concentrations.

However, the difference between the ratio at 300 μ M and 500 μ M (ratio= 0.5, in which PINO has exceeded DCA as the main product) is not significant, indicating that when the DP concentration is increased to a certain value, the extra addition of the DP had limited effect on the dimerization. This trend is consistent with the results reported in the literature ⁵ and the previous studies in our laboratory.

2.2.5 Activities of DP1 and DP2 samples

As mentioned above (Chapter II section 2.1), after SEC purification two samples of DP with different purities (DP1 and DP2) were obtained. In these DP fractions there is a substance bearing an absorbance at 415 nm, accounting for about 10% of the intensity of the 280nm absorbance (see the chromatogram Fig. II-2-1; not mentioned in the literature ³). Whether the existence of this substance has an effect on the activity of AtDIR6 or not was investigated on several batches of purification.

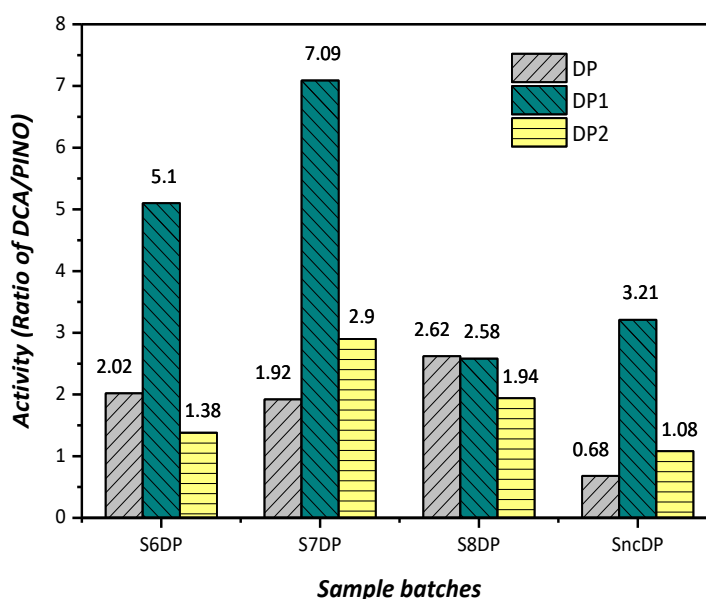


Fig. II-2-8 Comparison of activity between AtDIR6 samples. S6DP and S7DP were purified using successively Ni-NTA Agarose and Sephacryl S-200 columns; S8DP and SncDP were purified using successively His Trap™ HP and Superdex® 75 10/300 GL columns. Experimental condition: 1.6mM CA and 1U/L LAC3 with 100 μ M DP in a final volume of 100 μ L, 0.1M acetate buffer pH 5.0. Thermomixer 1000rpm at 30°C, T \approx 20 hours. DP: sample prior SEC; DP1: SEC peak 1; DP2: SEC peak 2.

From Fig. II-2-8 it can be seen that after SEC purification, the sample of protein devoid of yellow pigment (DP2) is the most active (low DCA/PINO ratio) in the tested batches. However, the difference in activity of the DP sample prior SEC and DP2 is small. So, although the SEC does

separate contaminants or less active proteins from the active AtDIR6, the relationship to the yellow pigment is not that clear.

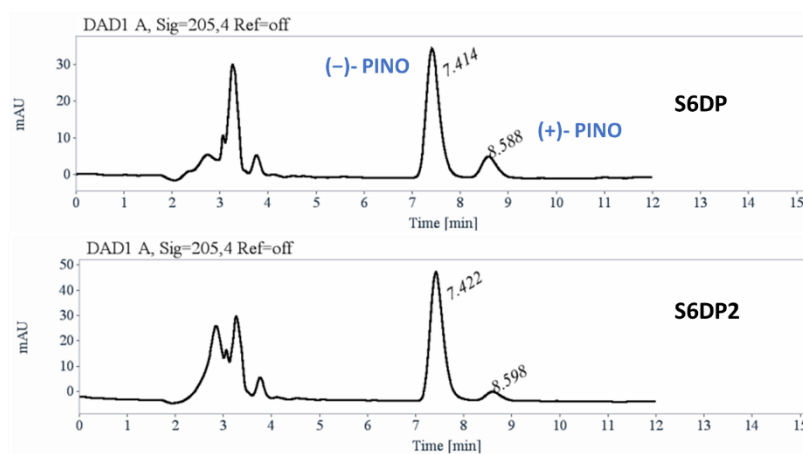


Fig. II-2-9 Analysis of PINO by chiral chromatography. Experimental condition: 1.6mM CA and 1U/L LAC3 with 100 μ M S6DP or S6DP2 in a final volume of 100 μ L, 0.1M acetate buffer pH 5.0. Thermomixer 1000rpm at 30 $^{\circ}$ C, T=15 hours.

For further verification, the enantiomeric excess (ee) of PINO obtained from DP or DP2 was analyzed using S6DP or S6DP2 as samples (**Fig. II-2-9**). PINO was separated and collected from HPLC and analyzed by chiral chromatography on a Chiralpak AZ-H column. The retention time is about 7.4 min for (–)-pinoresinol and about 8.6 min for (+)-pinoresinol. Enantiomeric excesses (ee) of PINO derived from S6DP and S6DP2 were 84% and 92% respectively. Obviously, the most purified fraction (DP2) has a higher “activity”, but the difference between the two is not huge, which is in agreement with the results determined by the ADC/PINO ratio.

In summary, the AtDIR6 we produced (both DP and DP2 fractions) has the desired dirigent activity and can be used in CA bioconversion investigations. From the above observations, since the difference in activity between DP and DP2 preparations is not large, considering the low yield of the SEC purification (less than 2mg/L) and the large amount of protein consumption in analysis, we decided to use routinely DP preparations right after IMAC (i.e. with no SEC step), DP2 being used only if necessary.

Since the absorbance at 415 nm in the samples interfere with the determination of DP concentration by UV-Vis spectrophotometry at 280 nm (overestimation of the actual concentration) Bradford protein assay instead of spectrophotometry was used, unless specified for DP2.

3 Exploration of AtDIR6 activity with synthetic CA analogues

3.1 Introduction

When Lewis *et.al.* first discovered that dirigent protein could guide the coupling of phenoxy radical dimerization, they reported in the meantime that the process was substrate specific.^{4,6} From the three monolignols, *p*-coumaryl alcohol, coniferyl alcohol, sinapyl alcohol (**Fig. II-3-1**) they have tested as potential DP substrates, only coniferyl alcohol undergoes stereoselective coupling in the presence of the dirigent protein. This indicates that 2-methoxy-phenol and the absence of substituent in the symmetric position (red dotted circle in **Fig. II-3-1**) are essential for the recognition of the molecule by DP. However, whether the allylic hydroxyl group of the molecule (green dotted circle in **Fig. II-3-1**) can be modified or not has not yet been investigated so far.

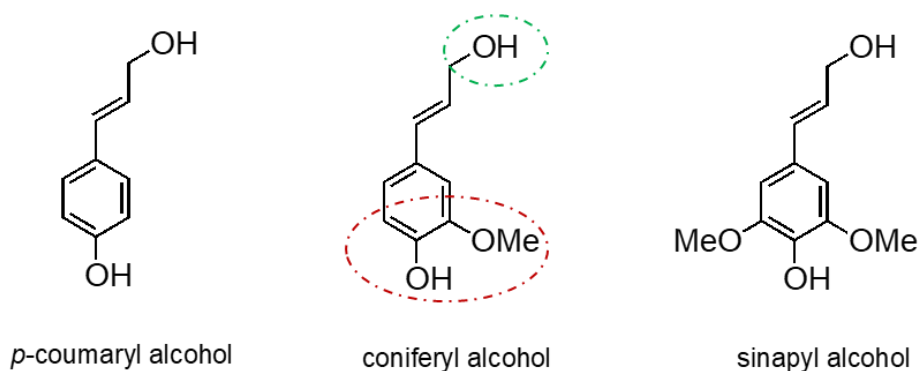


Fig. II-3-1 The three potential substrates of dirigent protein tested by Lewis *et.al.* From the comparison, the red dotted circle indicates the part that is mandatory for DP activity, the green dotted circle indicates the part studied in this manuscript.

Therefore, CA analogues (**Fig. II-3-2**), including Ferulic Acid (FA); Coniferyl Acetate (CAC); Coniferyl Azide (CAZ); Coniferyl Amino (CAM) and Isoeugenol (ISO) were considered. Except for Ferulic Acid and Isoeugenol, which are commercial reagents, the other three analogues used in this study were all synthesized by Nino MODESTO (master 2) during his internship in our laboratory. These analogues, which differ from coniferyl alcohol only by the substituent on the allylic chain, once tested as potential substrates of DP, represent potential probes for a deeper insight into the enantioselective coupling mechanism regarding both the substrate recognition and its binding to the protein active site. Moreover, they also provide possibilities to synthesize new optically pure compounds.

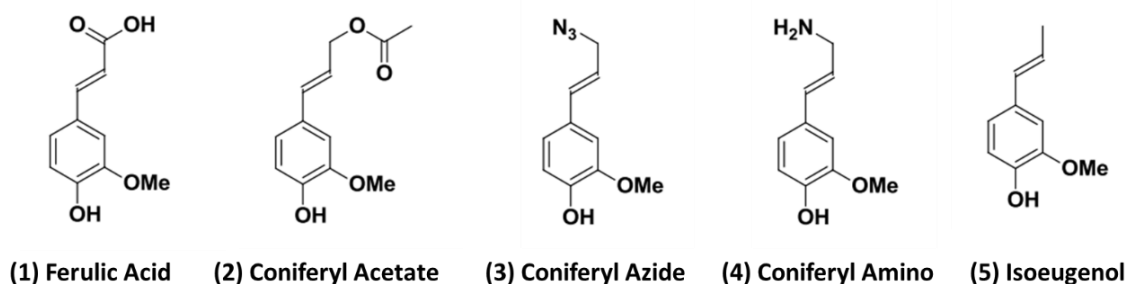


Fig. II-3-2 Coniferyl alcohol analogues

3.2 AtDIR6 Activity on CA analogues

It has been proposed that the real substrate of DP is the CA radical instead of CA itself.⁴ Thus, it was necessary first to set conditions of CA oxidation by laccase. The general experimental conditions established in the lab on CA ensures that the oxidation reaction is maintained at a low speed (ca. 20 hours for complete reaction) to avoid over polymerization. Due to the chemical differences of substrates, adjustment was made when necessary prior DP was introduced to the reaction system. The oxidation of substrate analogues by laccase in the absence or present of DP was monitored by HPLC following the method described in the Appendix. Results are shown below.

3.2.1 Ferulic Acid (FA)

From Fig. II-3-3 (up) it can be seen that, FA oxidation by laccase leads to at least to six different products as detected on the chromatogram. The retention time (RT) for each products are listed as follows: RT (FA)= 12.97 min; RT (Peak 1) = 16.84 min; RT (Peak 2)= 17.94 min; RT (Peak 3) = 18.70 min; RT (Peak 4) = 20.49 min; RT (Peak 5)= 23.36 min; RT (Peak 6) = 23.92 min; RT (Benzo, reference) = 25.29 min. The separated products were collected and analyzed by ESI-MS and NMR.

AtDIR6 was then added to the reaction system to check whether it has a dirigent activity on this new substrate. The chromatogram is shown in Fig. II-3-3 (down). Compared to the results in Fig. II-3-3 (up), peaks 4 and 5 almost disappeared and a slight change in the relative contents of Peak 1 and 3 was observable.

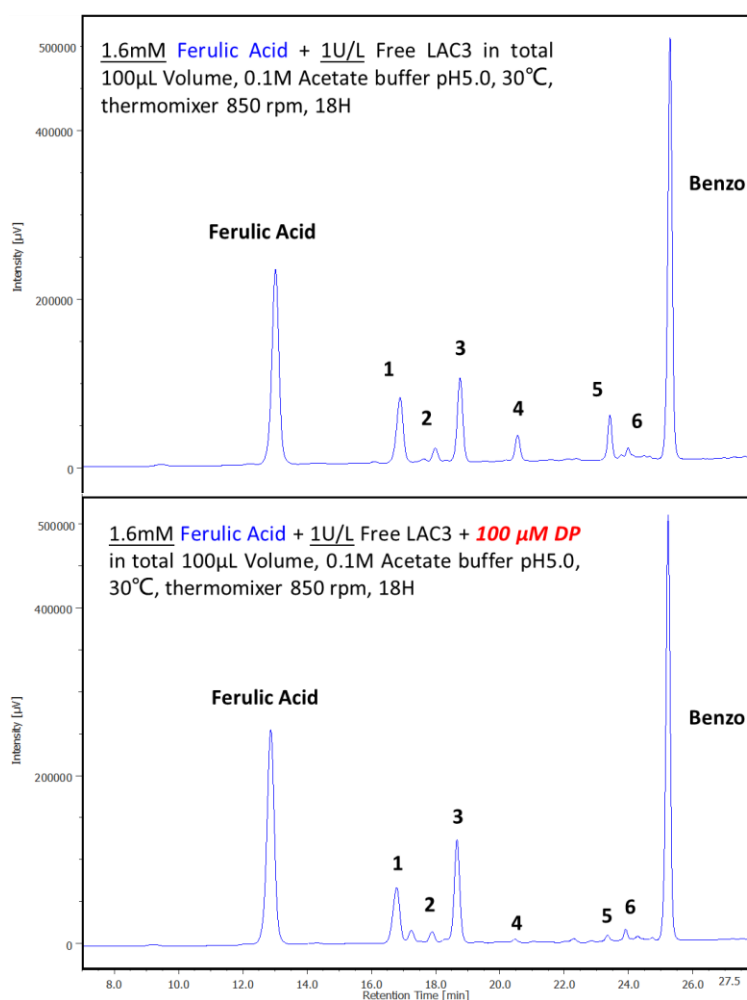


Fig. II-3-3 HPLC chromatogram of *Ferulic Acid* oxidation products \pm *AtDIR6*.

The ratio of the area (FA-Peak 3/FA-Peak 1) varies from 1.0 without *AtDIR6* to 1.5 with *AtDIR6*. It can be provisionally deduced that the addition of the DP, is potentially favoring the generation of the product corresponding to Peak3 at the expense of the other products. This behavior is very similar to that of *AtDIR6* in the presence of CA suggesting that the DP could have the ability to direct the coupling of FA radicals in an oriented manner.

Analysis of the results of mass spectrometry electrospray ionization in positive mode did not allow to find the diagnostic ions of the expected compounds for the FA-peaks 2, 4 and 6. A possible explanation for this absence is the low content (below the limit of detection) of material present in these samples. LC-MS analysis of the oxidation products peaks 1, 3 and 5 in negative mode showed dominant signals at m/z 385.1, suggesting that these oxidation products could be dimers of ferulic acid (exact mass [M] 386.1); when the mass spectrometer was set to run in positive mode $[M+H]^+$ ion signals were observed at m/z 387.1, thus confirming that the molecules are indeed dimers.

However, the main difficulty encountered comes from the similarity between the products forms. Indeed, the dimers forms all have the same molecular mass and the same formula. Mass spectrometry experiments and the NMR analysis were therefore relatively difficult to exploit since they only very rarely allowed to identify precisely (until now) the different products formed during oxidation.

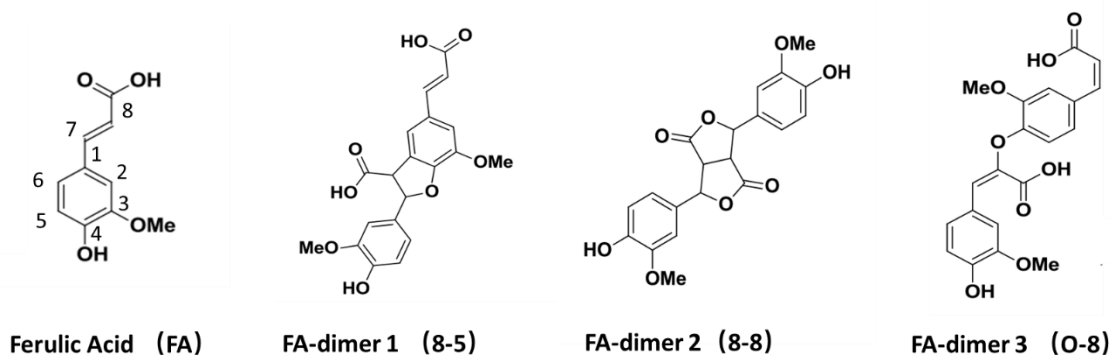


Fig. II-3-4 Structure of FA and its proposed dimers

Though the complete identification of the products being still in progress, the main dimers of FA can be speculated (**Fig. II-3-4**) by analogy with products obtained with CA. On the other hand, laccase-catalyzed dimerization of ferulic acid has been studied by several researcher. Oluyemisi E. Adedokun *et. al.* have elucidated the structures of two isolated dimers (8–5 and 8–8) formed during laccase-catalyzed oxidation of FA in organic media.⁷ FA dimers covalently bound through 8-5 linkage and 8-8 linkage could be considered as analogues of DCA and PINO obtained during CA oxidation. According to the assumption of Federica Carunchio *et. al.* six coupling modes are possible (8–8, 8–5, 8–O, 5–5, 5–O and O–O) from three intermediate radicals, although the O–O coupling is not likely in view of the instability of diaryl peroxides.⁸ The six peaks observed in the HPLC chromatogram above could therefore correspond to these six proposed coupling dimers, a speculation awaiting for the full identification of each of the compounds.

Indeed, through the results of NMR analysis although not very certain, combined with the contents of the literature, we can generally predict that: peak1 (FA-Peak 1) is probably a dimer of two ferulic acid monomers covalently bound through 8-5 linkage (**Fig. II-3-4**, dimer 1) while the result for peak 3 (FA-Peak 3) possible suggest dimerization through 8-8 linkage (**Fig. II-3-4**, dimer 2) and Peak 5 (FA-Peak 5) were speculated as dimerized through O-8 (**Fig. II-3-4**, dimer 3), which corresponds to the products of DCA, PINO and Guai from CA oxidation respectively.

3.2.2 Coniferyl Acetate (CAC)

HPLC separation of the products of Coniferyl Acetate (RT=19.57) oxidized by laccase is shown in **Fig. II-3-5** Three main products: CAC-Peak 1 (RT=8.34), CAC-Peak 2 (RT=10.61) and CAC-Peak 3 (RT=17.25) are observable on the chromatogram.

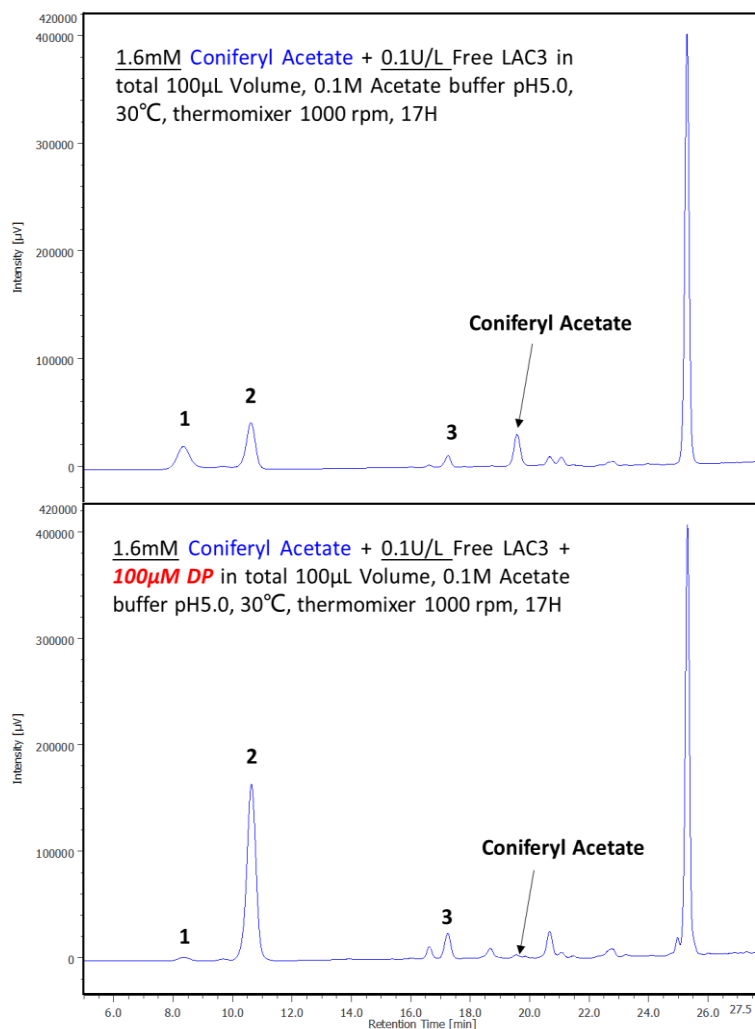


Fig. II-3-5 HPLC chromatogram of *Coniferyl Acetate* oxidation products \pm *AtDIR6*..

Laccase mediated oxidation of CAC in the presence of DP was carried out under the same conditions. A significant difference is observable between the relative contents of the main products (Peak 1 and Peak 2) in the presence and absence of *AtDIR6* (**Fig. II-3-5** down). The ratio of the normalized area CAC-Peak 2/CAC-Peak 1 moved from 1.5 in the absence of *AtDIR6* to 45.5 in the presence of *AtDIR6*. Obviously, the product under Peak 2 is becoming the major product when *AtDIR6* is present. Therefore, it seems that as demonstrated for CA and postulated for FA, *AtDIR6* has the ability to direct the regioselective coupling of Coniferyl Acetate radicals. Note that the evolution of minor peaks (growth) is coincident to the almost complete disappearance of the CAC peak and therefore are considered as over oxidation products.

The experiment (without AtDIR6) was scaled up in a 1 L flask to produce a large quantity of products for identification. Three products were separated on a silica column and were collected for NMR analysis. (Work of Nino MODESTO), but the same issues are encountered with FA. Mass spectrometry experiments and the NMR analysis (1D experiments only) were not enough to identify the products since all the dimers hold the same molecular mass and the same formula.

But we can still roughly speculate from the results of NMR analysis that: CAC-Peak 1 is probably a dimer of two coniferyl acetate monomers covalently bound through O-8 linkage (**Fig. II-3-6 dimer 1**) while the result for CAC-Peak 2 can be speculated as a dimerization through 8-5 linkage (**Fig. II-3-6 dimer 2**) and CAC-Peak 3 were dimerized through 5-O linkage.

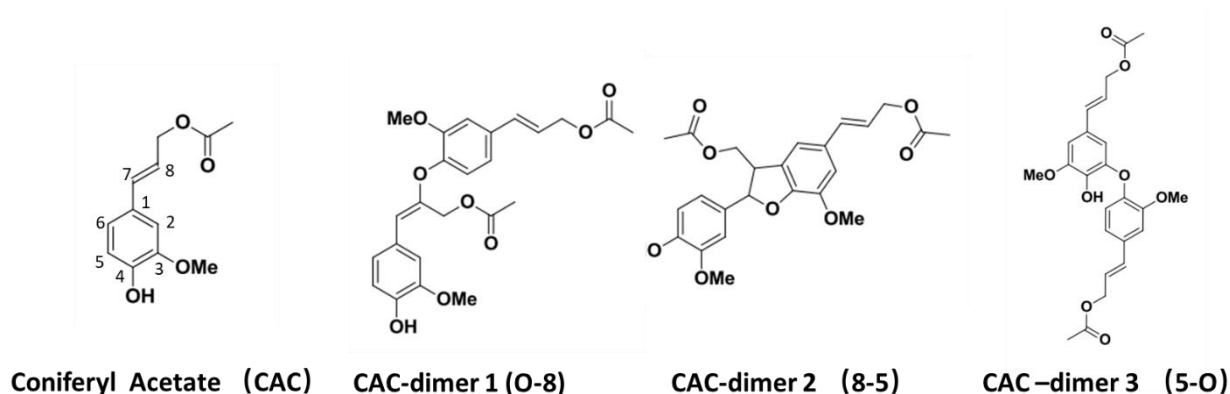


Fig. II-3-6 Structure of CAC and its proposed dimers

Here, we did not observe the analog of PINO (dimerization through 8-8 linkage) because the alcohol function of the aliphatic chain is protected by an acetate function, which should have the consequence of blocking the intramolecular cyclization reaction after the formation of the first carbon-carbon bond in the coupling mechanism (**Fig. II-3-7**).¹

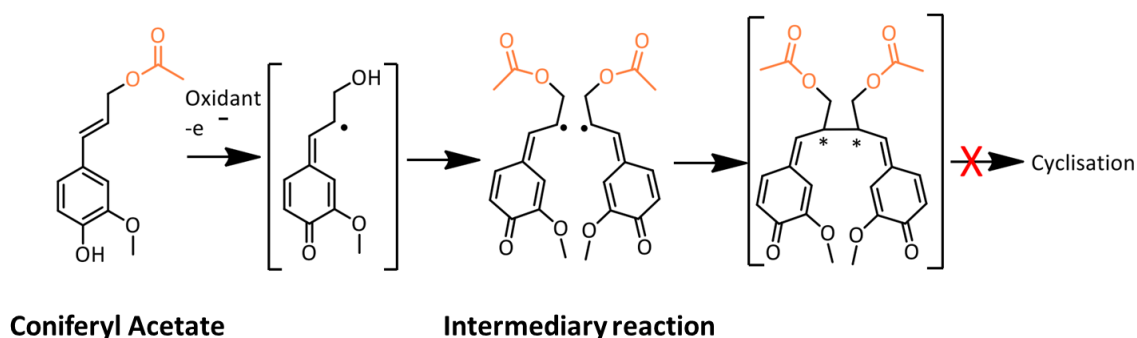


Fig. II-3-7 Mechanism of action envisaged with coniferyl acetate.

3.2.3 Coniferyl Azide (CAZ)

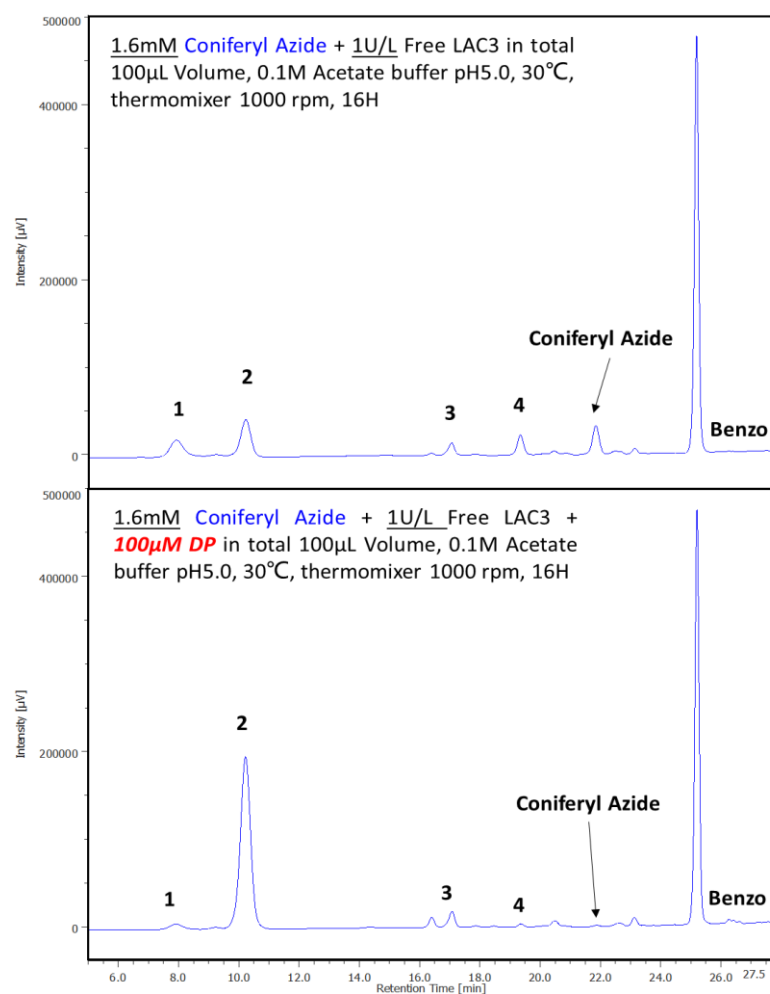


Fig. II-3-8 HPLC chromatogram of *Coniferyl Azide* oxidation products \pm *AtDIR6*

The oxidation profile of Coniferyl Azide in the presence or absence of *AtDIR6* is presented (**Fig. II-3-8**). Four main products of oxidation of CAZ (RT=21.87): CAZ-Peak 1 (RT=7.94), CAZ -Peak 2 (RT=10.25), CAZ-Peak 3 (RT=17.08) and CAZ-Peak 4 (RT=19.37) are observable on the chromatogram. As previously seen for the oxidation of CAC there is a remarkable difference in the relative contents of the main products (Peak 1 and Peak 2) obtained in the absence (**Fig. II-3-8** top) or presence (**Fig. II-3-8** bottom) of *AtDIR6*. Indeed, this ratio moves from 1.7 to 29.6. This indicates that like for CAC, *AtDIR6* is strongly influencing the selectivity of the coupling of Coniferyl Azide radicals.

The experiment (without *AtDIR6*) was scaled up in a 1 L flask to produce a large quantity of products for products identification like the previous substrate. Only Two products were separated on a silica column and were collected for NMR analysis. Similar issues are encountered with FA and CAC. Mass spectrometry experiments and the NMR analysis obtained until now were not enough to identify the products since all the dimers hold the same molecular mass and the same formula.

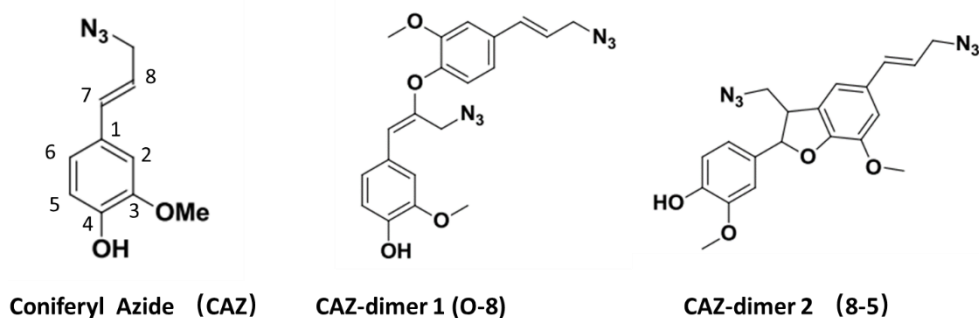


Fig. II-3-9 Structure of CAZ and its proposed dimers

But we can still roughly speculate from the results of NMR analysis that Coniferyl Azide shared a similar dimerization way to Coniferyl acetate. CAZ-Peak 1 probably is a dimer of two coniferyl acetate monomers covalently bound through O-8 linkage (**Fig. II-3-9** dimer 1) while the result for CAC-Peak 2 can be speculated as a dimerization through 8-5 linkage (**Fig. II-3-9** dimer 2).

These results underline the importance of the hydrogen bonds that could be established between the terminal function of the allylic chain and the protein within the active sites, in particular for example with the aspartic acids present. The fact that a selectivity is observed when there is no H-link donor on the allylic chain is more complex to explain but it may be thought that this time it is the alcohol of the phenol which becomes the donor of connection H.

3.3 Conclusion and prospect

In this subsection, CA analogues including Ferulic Acid (FA); Coniferyl Acetate; Coniferyl Azide were studied. All the three substrates seem to be taken in charge by AtDIR6, indicating that AtDIR6 may not be limited to CA as substrate. However, until now, products of each substrate have not been fully identified, limiting insights into the mechanism of DP. In order to look into the action of AtDIR6 with these analogues, further and continue analysis is required to determine which of these products would be the counterparts of the CA products. In addition, the main reaction products would have to be isolated for ee measurement after product structure confirmation.

4 Direct evidence of radical stabilization by AtDIR6

4.1 Introduction

CA radical, rather than CA, has been proposed to be the real substrate of dirigent proteins.^{4,5} According to the authors, this assumption is based on two observations: i) equilibrium binding assays have revealed that coniferyl alcohol is only weakly bound to the DP *Fi*DIR1, with a K_D of 370 ± 65 μ M, which tends to discount CA as being the true substrate. ii) examination of DP-mediated (+)-pinoresinol production as a function of estimated CA[•] concentration has led to the conclusion that *Fi*DIR1 has a strong binding constant for CA[•] ($K_d = 10$ nM).

So far, a direct interaction of DP and CA[•] has been proposed but never directly evidenced. Recently, our lab obtained a substantial evidence of such an interaction. In a previous work, the influence of *At*DIR6 on the evolution of the elusive coniferyl alcohol radical has been studied by Electron Paramagnetic Resonance spectroscopy (EPR). EPR is clearly the technique of choice for the direct observation of a radical. A signal of CA[•] obtained from UV irradiation (310nm) of the coniferyl alcohol has been observed by low-temperature EPR in the mid-seventies.⁹ From this study, it comes that the unpaired electron is delocalized over the entire molecule and that the half-life of the radical is approximately 10 s at 223K. Therefore, one can easily predict that the life time of CA[•] is not long enough to allow its observation at room temperature. This unless it can be stabilized enough by an external factor such as *At*DIR6. UV light irradiation of CA coupled to room temperature EPR were used to decipher whether or not *At*DIR6 is able to stabilize CA[•]. From this study, the evidence that *At*DIR6 stabilizes coniferyl alcohol radicals prior to direct their coupling towards the formation of (-)-pinoresinol has been clearly shown.¹

In the last section (Chapter II section 3), the influence of *At*DIR6 on the radical coupling of CA analogues (FA, CAC and CAZ) was evidenced. Whether *At*DIR6 has the ability to stabilize radicals of these analogues or not needed to be investigated, with an expectation of getting further evidences on the mechanism of DP-mediated coupling.

In this section, radicals of ferulic acid (FA) and coniferyl acetate (CA) were generated by photo-irradiation in the presence of *At*DIR6 and compared to the reference experiment performed with CA. The photogeneration system was chosen to avoid the presence of any unpaired electron in the reaction medium.

4.2 Analysis of EPR signals

EPR spectra recorded under continuous white light irradiation (xenon lamp 200W, $200 < \lambda < 800$ nm) are shown in **Fig. II-4-1**. Control experiments were performed first. No signal was observed for the irradiation of CA into the cavity of the EPR spectrometer (**Fig. II-4-1** blue line). This is because the half-life of the radical is too short to allow its observation at room temperature ($t_{1/2} \approx 10$ s at 223K)⁹. No signal as well was observed for the irradiation of AtDIR6 alone under the same irradiation conditions (**Fig. II-4-1** yellow line). In other words, the protein does not appear to be photoactivatable in these conditions.

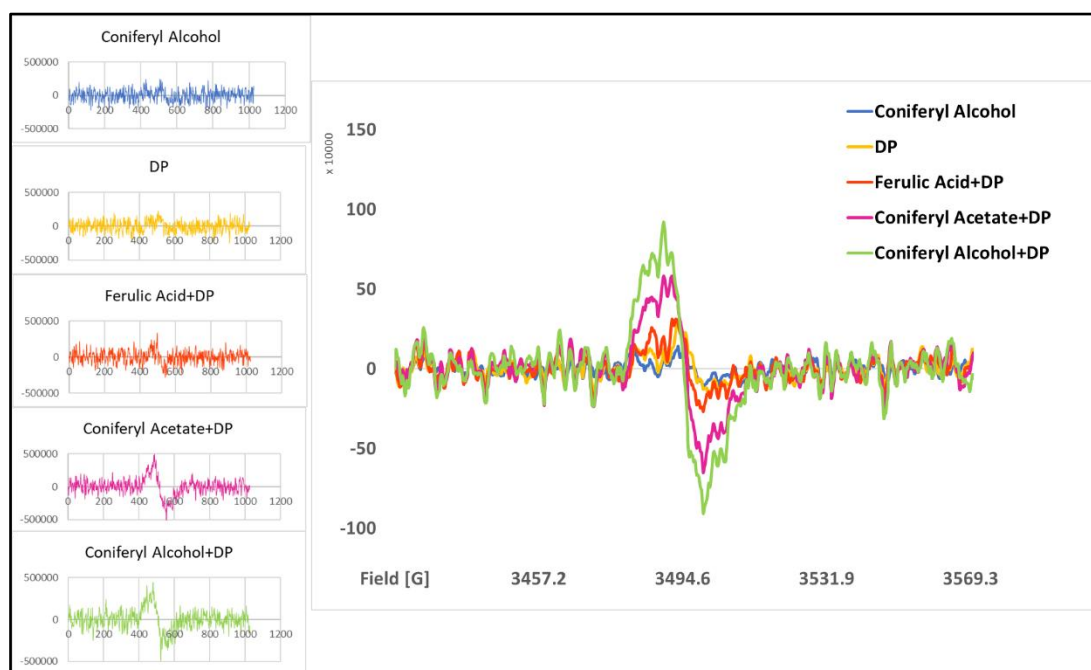


Fig. II-4-1 EPR spectra of substrates (CA, FA and CAC) and AtDIR6 under continuous photo-irradiation. Deoxygenated acetate buffered (100 mM pH 5) 1.6 mM substrate solutions in the presence of 100 μ M AtDIR6. Controls: 1.6 mM of CA (blue line); 350 μ M AtDIR6 (yellow line). Irradiation conditions: white light ($200 < \lambda < 800$ nm) lamp 200 W. Left: the EPR spectra of the individual samples; Right: comparison of all the samples.

When CA and AtDIR6 were mixed and photo irradiated together, a typical signal arising from an organic radical was observed (**Fig. II-4-1** green line). This situation contrasts sharply with the control experiment carried out in the absence of AtDIR6, in which no signal of the radical from the CA is observed (**Fig. II-4-1** blue line). Furthermore, similar signals were observed for samples of CAC (**Fig. II-4-1** pink line) and FA (**Fig. II-4-1** red line), though the signal intensity of these two samples were relatively weaker compared to CA. Such a weaker intensity is perhaps due to a weaker interaction of the radical and the amino acids within the protein pocket (**Fig. II-4-2**).

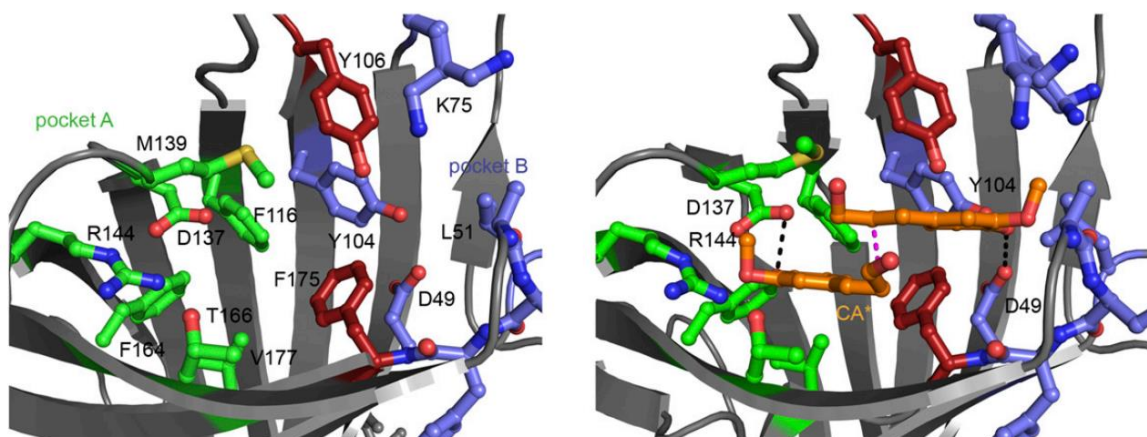


Fig. II-4-2 View of the *AtDIR6* active site showing (left): important residues in pocket A in green, pocket B in blue, and Tyr-106 and Phe-175 separating the two pockets in red.(right) Potential binding mode of two CA substrate radicals supported by energy minimization of the manually placed ligands.¹⁰

From these observations it is reasonable to think that *AtDIR6* serves as matrix for the radicals of CA and its analogues, and by this way stabilize them. The life time of those radicals is too short to be observed in solution and without any external factor. An *AtDIR6* stabilizing the radicals of CA analogues is consistent with what was observed from the biocatalyst experiments.

4.3 Analysis of non-laccase substrate (NOS)

In order to verify that DP is not active in the absence of free radicals, a molecule that is not a laccase substrate (**Fig. II-4-3**) was investigated by HPLC following the same methodology than for CA and its analogues. The molecule is the (4- 3-methoxyphenyl)-2-propen-1-ol in which a methoxy replaces the -OH group in position 4 on the phenyl ring of CA.

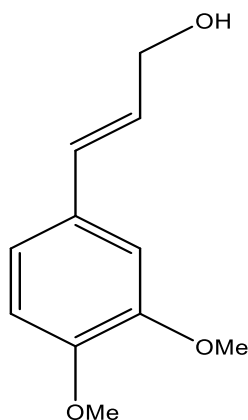


Fig. II-4-3 Structure of the non-laccase substrate (NOS) molecule.

Chromatograms can be seen in the Appendix section. Except a deviation of the sample/reference ratio equally observed after 16h incubation time for each of the sample (from ≈ 1.1 to ≈ 2.5 (**Table II-4-1**)), no changes were found to occur for all the samples (NOS alone, NOS+LAC3, NOS+DP, NOS+LAC3+DP) confirming our expectation that DP can act only on radicals.

Table II-4-1 Ratio of (NOS samples/Benzo) in the HPLC chromatogram

	T=0			T=16H		
	NOS	Benzo	Ratio (NOS/Benzo)	NOS	Benzo	Ratio (NOS/Benzo)
NOS	1413694	1381186	1.02	1906056	743440	2.56
NOS+LAC3	982957	876286	1.12	3579258	1327837	2.70
NOS+S7DP	998253	883657	1.13	4004013	1510782	2.65
NOS+LAC3+S7DP	1082114	958643	1.13	2988037	1088105	2.75

4.4 Conclusion

EPR was used to observe the radicals of CA and analogues generated by photo-irradiation. Results allowed us to confirm experimentally that AtDIR6 stabilizes the radical of CA and analogues whereas free radicals in solution are too fleeting to be observed. Moreover, using a non-laccase substrate, no difference was observed between the four samples (NOS alone, NOS+LAC3, NOS+DP, NOS+LAC3+DP) indicated that DP would lack activity without free radicals.

5 Attempts to identify amino acids involved in the stereoselective control within the cavity of DIRs

5.1 Introduction

To understand the stereo coupling mechanism controlled precisely by *AtDIR6*, one of the strategies used in our lab has been to study the inactivation of *AtDIR6* by the covalent grafting of a radical probe to the surface of the protein. The idea of inactivation is based on published data of a low-molecular-weight (26kDa) glycoprotein structurally related to dirigent protein.^{11,12} In particular, this protein has been studied for its ability to trap organic radicals. The demonstration of trapping was obtained using the radical cation of ABTS which forms a covalent adduct with an intense purple color onto the protein. The authors proposed a mechanism via an electron relay in which the thiolate function of a cysteine reduces the radical ABTS^{•+}; the thyl radical formed would then oxidize a tyrosine that would react in turn with the radical ABTS^{•+} to form a stable purple adduct. Thus, the reaction of *AtDIR6* and ABTS^{•+} should allow the labeling of tyrosines which are accessible.

From our previous work,¹ such an ABTS^{•+} radical labeling method revealed that four tyrosines (Y63, Y75, Y77, Y155 or Y158) are always labeled, and that the *AtDIR6*-ABTS sample retained approximately 40% of the initial activity of *AtDIR6*. These results are generally consistent with what has been published concerning the role of the Ys in the mechanism of DP action, that is orienting the propylenic side chain during the coupling to form an 8-8 'bond.¹⁰

Since ABTS is not a substrate of *AtDIR6*, how is the real radical substrate (e.g. CA[•]) reacting with *AtDIR6*, whether or not it can also form adducts like ABTS radical still need to be figured out. To answer the questions, MALDI TOF (Matrix Assisted Laser Desorption Ionization-Time of Flight) experiment was performed to analyze the state of *AtDIR6* after reaction with CA and laccase.

5.2 Results and discussion

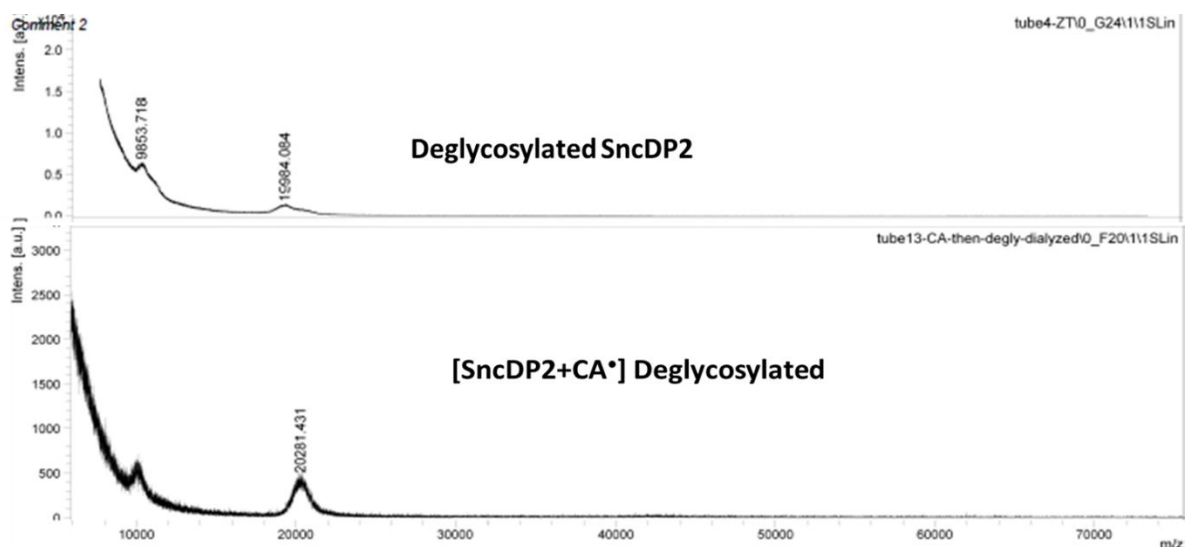


Fig. II-5-1 Comparison of mass spectra of deglycosylated proteins.

A sample of *AtDIR6* of the highest purity (SncDP2) was used to avoid any interference of impurities. After reaction with CA^{*}, the potentially labeled protein ([*AtDIR6*-CA^{*}]) was deglycosylated by chemical means using the GlycoProfile™ IV Chemical Deglycosylation Kit of Sigma Aldrich following the manufacturer protocol, allowing the total elimination of all N and O glycans while preserving the primary structure of the protein.

A mass difference of approximately 300 Da distinguish the deglycosylated [*AtDIR6*-CA^{*}] from the deglycosylated *AtDIR6* protein itself. In first analysis, this which could approximately correspond to two CA (C₁₀H₁₂O₃, 180g/mol) radicals (**Fig. II-5-1**). This preliminary result indicates that as ABTS^{*} did, CA radicals could potentially also form *AtDIR6*-CA^{*} adducts on the protein. Mass experiments are in progress to confirm this preliminary result and identify *AtDIR6*-CA^{*} adducts. Progress in this direction would help to understand the role of amino acids in the selective coupling of CA radicals.

6 Conclusion

In this chapter, AtDIR6 was isolated and purified from the culture broth of *Pichia Pastoris* by IMAC purification first. The produced AtDIR6 was employed in laccase-catalyzed bioconversion of coniferyl alcohol and proved to have significant influences on the dimerization of CA radicals, as displayed by the changed ratio of DCA/PINO. Further SEC purification of the AtDIR6 resulted in a purer protein fraction DP2 in limited yields but with better performance.

Used in bioconversion experiments (laccase mediated) of ferulic acid, coniferyl acetate, coniferyl azide, the produced AtDIR6 is active on CA analogues. Indeed, all three molecules seem to interact with AtDIR6, as revealed by the analysis of the bioconversion products. Therefore, we have here the first evidence that molecules influenced by AtDIR6 are not limited to CA. Confirmation of the structure of the obtained products is under progress in order to get information about the mechanism of action of AtDIR6 with these analogues. In future studies, performing the determination of the *ee* for the main product will help to ascertain the enantioselective character of the AtDIR6 mediated radical coupling of CA analogs.

Using EPR, we provided the first direct observation of the radicals of CA and analogues generated by photo-irradiation. Although the intensity of the EPR signal derived from each substrate is different, the results allow us to confirm experimentally that AtDIR6 stabilizes the radical of CA and analogues whereas these radicals are too fleeting free in solution to be observed. Meanwhile, we confirmed that AtDIR6 is not converting non-oxidizable substrates indicating that the is lacking activity in the absence of free radicals.

At last, MALDI TOF mass spectrometry experiment was performed to analyze the state of AtDIR6 after reaction with CA and laccase. The protein was proved to form AtDIR6-CA[•] adducts. Revealing the nature of this adduct (under investigation) will help in understanding the enantioselective radical coupling mechanism of dirigent proteins.

Appendix: Materials and Methods Chapter II

1 General

1.1 His-Tag affinity Chromatography

The clear culture broth was applied to the ÄKTA FPLC (Fast Protein Liquid Chromatography, GE Healthcare, Japan) system for His-Tag purification. A **His Trap™ HP** 5ml column (GE Healthcare, UK) charged with Ni²⁺ was equilibrated with 10 column volumes of 50mM sodium phosphates buffer pH 7.4 containing 150mM NaCl (buffer A); samples of 800mL were loaded onto the column at a flow rate of 5 mL·min⁻¹. Afterwards, the column was washed with 30 column volumes of buffer A. Followed by is washing with 95.4% buffer A plus 4.8% buffer B (50mM sodium phosphates buffer pH 7.4 containing 150mM NaCl and 500mM imidazole) for removing pigment. Both the previous two steps are performed at flow rate of 5 mL·min⁻¹. *AtDIR6* was eluted from the column with a gradient step (from 4.6% buffer B to 100% buffer B) using 20 column volumes at a flow rate of 5 mL·min⁻¹. Protein-containing fractions were detected by absorption measurements at 280 nm automatically.

1.2 Size Exclusion Chromatography

The above desalted and concentrated *AtDIR6* was further purified by Size Exclusion Chromatography on a **Superdex® 75 10/300 GL** column (GE Healthcare, UK) at an ÄKTA FPLC system (GE Healthcare, Japan). The column (25 mL column volume (CV)) was equilibrated with 2 CV buffer A (50mM sodium phosphates buffer pH 7.4 containing 150mM NaCl) at a flow rate of 1.0 mL·min⁻¹. No more than 250µL *AtDIR6* samples were applied to the column from a 500µL loop at flow rate of 0.5 mL·min⁻¹. Then the samples were eluted from the column with 1.5 CV of buffer A at flow rate of 0.5 mL·min⁻¹. Protein-containing fractions were detected by absorption measurements at 280 nm automatically.

1.3 SDS-PAGE

In the sodium dodecyl sulfate polyacrylamide gel electrophoresis (SDS–PAGE) experiments, a stacking gel of 4% acrylamide and a running gel of 12% acrylamide were used. Samples of *AtDIR6* proteins were mixed with 4× LDS sample buffer (contains lithium dodecyl sulfate (LDS) at pH 8.4, (life technologies, CA) in a 1 to 4 ratio. The solution mixtures were heated at 95 °C for 5 min. A Prestained Protein Ladder Plus #06P-0211 (EUROMEDEX, France) were used as molecular weight markers. Electrophoretic migration was carried out at room temperature with a constant voltage 180 Volts. Subsequent staining was performed with a Coomassie based staining solution InstantBlue Stain (Expedeon, UK).

1.4 AtDIR6 concentration measurement

The concentration of the purified AtDIR6 was determined using Bio-Rad Bradford Protein Assays (Bio-Rad Laboratories, USA) according to manufacturer's instructions¹³ in 1mL spectrophotometer SEMI-MICRO cuvette (Biosigma S.r.l., Italy). The absorbance at 595nm was measured using Agilent Cary 60 UV-Vis Spectrophotometer (Agilent Technologies, USA). Each sample was measured in triplicates from individual dilutions. BSA (Bovine serum albumin) was used to establish a standard curve.

1.5 Laccase

Laccase used in this study (CA or CA analogues oxidation) is LAC3 from *Trametes* sp C30, which is produced in *Aspergillus niger* and purified in our lab.¹⁴

1.5.1 Concentration determination

Laccase concentration was estimated by UV-visible spectroscopy (Cary 60, Agilent Technologies, USA) using an $\epsilon_{610\text{ nm}} = 5600\text{ M}^{-1}\cdot\text{cm}^{-1}$ for the T1 copper site.

1.5.2 Activity measurement

Laccase activity was assayed using 2,2'-azino-bis (3-ethylbenzthiazoline-6-sulphonic acid) (ABTS) as substrate. Oxidation of ABTS was detected by following the absorbance at 420 nm ($\epsilon_{420\text{ nm}} = 36000\text{ M}^{-1}\cdot\text{cm}^{-1}$) during 2 min with a spectrophotometer (Cary 60, Agilent Technologies, USA). The reaction mixture (1 mL) contained 10 μL of appropriately diluted enzyme sample, 890 μL of acetate buffer (100 mM pH 5.7) and 100 μL of 50mM ABTS in Milli Q[®] Water at 30°C. The ABTS was added to initiate the reaction. One unit (U) of laccase was defined as one micromole of substrate oxidized per minute in these described conditions.

1.6 Bioconversion of coniferyl alcohol and analogues by AtDIR6

The standard reaction condition consisted of 1.6 mM coniferyl alcohol (or CA analogues), 1U/L LAC3, 100 μM AtDIR6 (in further experimental setups, concentration of AtDIR6 was varied in a range from 100 μM to 500 μM) in 100 mM Acetate buffer at pH 5. The final volume is 100 μL for single measurement at ~20 hours (for kinetics is 1mL). All the materials were added into a 2mL centrifuge tube (with holes in the cover to receive oxygen r from the atmosphere). The reaction was incubated on thermomixer (Eppendorf, Germany) at 30 °C and 850~1000 rpm.

1.7 HPLC analysis

HPLC analysis was carried out by JASCO LC-4000 series HPLC (JASCO, Japan) on a reversed phase Nucleosil 100-5 C18 column (Macherey-Nagel, Germany). The mobile phase was composed of a mixture of water - acetic acid 3% (solvent A) and acetonitrile (solvent B) with the following gradient (Table II-A-1). The absorbance at 280nm was monitored.

Table II-A-1 Gradient analysis HPLC 30 min

Time(mins)	A%	B%
0	90	10
5	90	10
25	50	50
27	50	50
28	90	10
30	90	10

1.8 Chiral HPLC

The pinosresinol of the bioconversion products was collected from HPLC analytics and lyophilized to determine the enantiomeric excess (ee) by Chiral HPLC. The ee determination was performed by the chiral chromatography platform, Chirosciences, on Chiralpak AZ-H using a mixture Heptane/Ethanol (volume ratio 1:1) at flow rate of 1mL/min as mobile phase or on Chiralpak IC using the same mobile phase.

1.9 EPR X-band

EPR spectra were obtained using a BRUKER ELEXSYS 500 X-band CW-EPR spectrometer. A flat quartz EPR cell containing a deoxygenated solution of substrates (CA, FA, Coniferyl Acetate; 1.6mM) in acetate buffer (100 mM pH 5.5) in the presence or absence of 100 μ M AtDIR6 was maintained under continuous irradiation in the EPR cavity. Irradiation conditions: white light (200 $200 < \lambda < 800$) lamp 200 W, modulation 20%.

1.10 ESI-MS analysis

The tests were performed by Service d'analyse de la fédération de chimie. The analyzes were performed with a SYNAPT G2 HDMS (Waters) mass spectrometer equipped with a pneumatically assisted atmospheric pressure ionization (API) source. The sample was ionized in positive electrospray mode under the following conditions: electrospray voltage: 2.8 kV; orifice voltage: 20 V; Nebulization gas flow (nitrogen): 100 L / h. The sample was also ionized in negative electrospray mode under the following conditions: electrospray voltage: - 2.27 kV; orifice voltage: - 20 V; Nebulization gas flow (nitrogen): 100 L/h. Mass spectra (MS) were obtained with a flight time

analyzer (TOF). The exact mass measurement was done in triplicate with an external calibration. In high resolution MS / MS experiments, argon was used as the collision gas.

1.11 NMR spectroscopy

The ^1H NMR spectra were recorded on a BRUKER Avance III nanobay - 300MHz equipped with a BBFO + probe as well as on a BRUKER Avance III nanobay - 400MHz equipped with a BBFO + probe. The treatment was done with the MestReNova software. The chemical displacements are reported in part per million (ppm) relative to the residual peak of the solvent.

1.12 MALDI TOF MS

MALDI TOF experiments were performed by Maya Belghazi UMR S7286. The samples were dialysed against H_2O (30 min on a membrane) then deposited on target with sinapic acid as matrix.

2 Production of AtDIR6

AtDIR6 was expressed in *Pichia Pastoris* and purified from the concentrated culture broth. Since a polyhistidine-tag (6-His) was added to the protein, so the His-tagged AtDIR6 could be purified based on His-Tag Affinity Purification.

Before purification, the culture broth was adjusted pH with 5N NaOH to pH 7.4 and equilibrated for several hours (1-3h), then the equilibrated culture broth was filtered with Nalgene™ Rapid-Flow™ 0.2 μm PES filter (ThermoFisher Scientific, France) to remove the precipitate.

Then the filtered supernatant was purified by His-Tag affinity Chromatography and SEC (Size Exclusion Chromatography) as the method described in general method 1.1 and 1.2.

The targeted proteins (absorbed at 280 nm) after purification were collected, concentrated and desalted with a nominal molecular mass limit of 10 kDa VIVASPIN 20 (Sartorius Stedim Biotech, Germany) by centrifuging 5~6 times at 3500rpm 4°C to a 0.1M Acetate buffer pH 5.0.

3 Dirigent activity assay of the produced AtDIR6

The oxidative coupling of coniferyl alcohol catalyzed by laccase with presence of AtDIR6 were performed following the method 1.6 to determine the dirigent activity of the produced AtDIR6. CA oxidation samples were taken out at about 20 hours and analyzed by HPLC analytics (HPLC; see above 1.7) after adding 50 % (v/v) 2 mM benzophenone (Benzo). The Benzo was dissolved in acetonitrile and was used as an internal reference, the solvent acetonitrile was used to quench the reaction.

4 Identification activity of AtDIR6 to CA analogues

CA analogues were first undergone the biotransformation as described in (above 1.6), then the sample were taken out at analyzed by HPLC analytics (HPLC; see above 1.7) under similar conditions with CA (see above section 3).

5 Analysis of CA analogues oxidation products

MS (ESI, m/z):

FA sample were collected form HPLC analytics and lyophilized for MS/MS analysis. The sample is dissolved in 300 μ l of methanol and then diluted 1/10 in a solution of methanol at 3 mM ammonium acetate. The solution is introduced into the infusion ionization source at a flow rate of 10 μ l min. Mass Spectrum of FA-peak1 is showed in Fig. II-A-1 and Fig. II-A-2. FA-Peak 3 and FA-Peak 5 are not listed due to the similarity with FA-peak1.

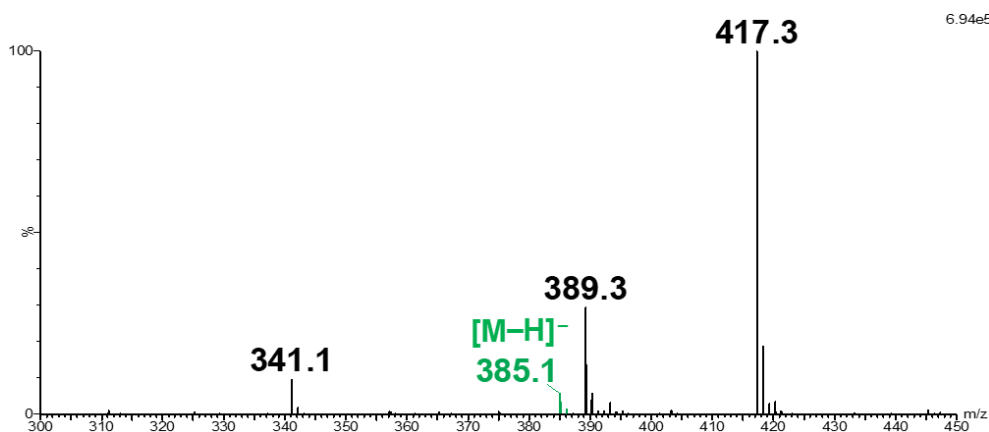


Fig. II-A-1 Mass Spectrum (MS) in electrospray negative mode of the FA-peak1 sample

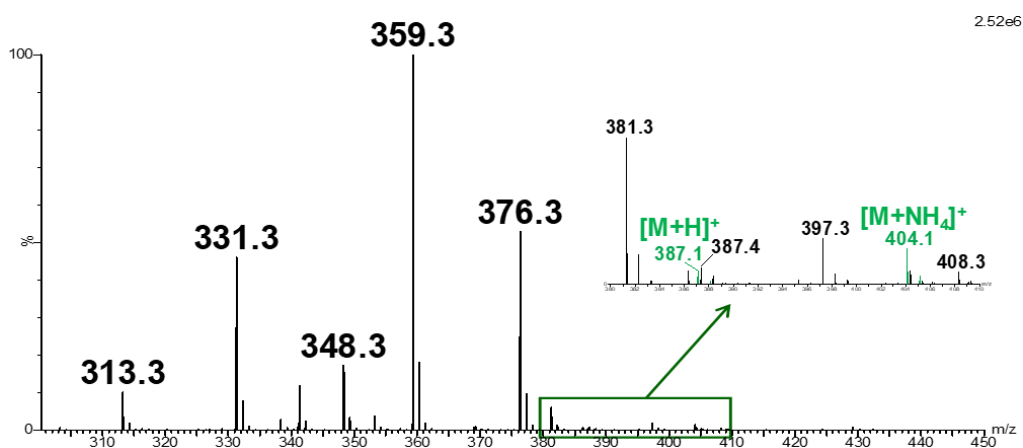


Fig. II-A-2 Mass Spectrum (MS) in electrospray negative mode of the FA-peak1 sample

FA Peak 1:

¹H NMR (MeOD): δ =7.56 ppm (s, 1H, COOH), δ =7.38 ppm (s, 1H, COOH), δ =7.17 ppm (d, 1H, Halcene), δ =6.80 ppm (m, 5H, Ar-H), δ =5.71 ppm (d, 1H, CH), δ =3.99 ppm (s, 1H, CH), δ =3.89 ppm (s, 3H, OMe), δ =3.87 ppm (d, 1H, Halcene), δ =3.8 ppm (s, 3H, OMe)

¹³C NMR (MeOD): δ =180.71, 178.76, 175.23, 150.4, 149.21, 147.94, 140.15, 133.5, 127.45, 126.83, 123.14, 119.33, 116.39, 114.57, 110.28, 84.44, 58.13, 56.69, 56.39, 23.23 ppm. m/z=386

FA Peak 3:

¹H NMR (MeOD): δ =8.55 ppm (s, 1H, CH), δ =7.48 ppm (dd, 1H, CH), δ =7.04 ppm (m, 6H, Ar-H), δ =6.37 ppm (q, 1H, CH), δ =5.86 ppm (dd, 1H, CH), δ =3.90 ppm (s, 3H, OMe), δ =3.83 ppm (s, 3H, OMe),

¹³C NMR (MeOD): δ =177.83, 175.39, 156.53, 149.17, 140.10, 138.37, 135.55, 133.84, 131.35, 124.9, 119.30, 119.12, 116.36, 114.37, 110.36, 84.87, 58.33, 56.40, 29.94, 18.36 ppm. m/z=386.10

FA Peak 5:

¹H NMR (MeOD): (water suppression experiment) : δ =7.56 ppm (s, 1H, COOH), δ =7.38 ppm (s, 1H, COOH), δ =7.16 ppm (dd, 2H, Halcene), δ =6.83 ppm (m, 6H, Ar-H), δ =5.69 ppm (s, 1H, Halcene), δ =5.48 ppm (s, 1H, OH), δ =3.90 ppm (s, 3H, OMe), δ =3.81 ppm (s, 3H, OMe). m/z = 386.10

CAC Peak 1:

¹H NMR (CDCl₃): δ =6.88 ppm (m, 6H, Ar-H), δ =6.20 ppm (m, 1H, Halcene), δ =5.68 ppm (d, 1H, Halcene), δ =5.63 ppm (s, 1H, OH), δ =4.69 ppm (s, 1H, Halcene), δ =6.38 ppm (s, 6H, OMe), δ =3.71 ppm (d, 2H, CH₂), δ =2.04 ppm (s, 6H, CH₃), δ =1.25 ppm (s, 2H, CH₂).

CAC Peak 2:

¹H NMR (CDCl₃): δ =6.87 ppm (m, 5H, Ar-H), δ =6.04 ppm (m, 2H, Halcene), δ =5.67 ppm (s, 1H, OH), δ =5.34 ppm (dt, 2H, CH₂), δ =5.19 ppm (dt, 1H, CH), δ =5.13 ppm (d, 1H, CH), δ =3.89 ppm (s, 6H, OMe), δ =2.05 ppm (m, 2H, CH₂), δ =1.43 ppm (s, 6H, CH₃).

CAC Peak 3:

¹H NMR (CDCl₃): δ =6.87 ppm (m, 5H, Ar-H), δ =6.51 ppm (d, 2H, Halcene), δ =6.25 ppm (dt, 2H, Halcene), δ =5.63 ppm (s, 1H, OH), δ =4.29 ppm (d, 4H, CH₂), δ =3.91 ppm (s, 6H, OMe), δ =1.54 ppm (s, 3H, CH₃), δ =1.26 ppm (s, 3H, CH₃).

CAZ Peak 1:

$^1\text{H NMR}$ (CDCl_3): $\delta=6.86$ ppm (m, 6H, Ar-H), $\delta=6.52$ ppm (d, 1H, Halcene), $\delta=6.21$ ppm (m, 1H, Halcene), $\delta=5.74$ ppm (s, 1H, OH), $\delta=4.28$ ppm (s, 1H, Halcene), $\delta=3.88$ ppm (s, 6H, OMe), $\delta=1.51$ ppm (d, 2H, CH_2), $\delta=1.49$ ppm (s, 2H, CH_2).

CAZ Peak 2:

$^1\text{H NMR}$ (CDCl_3): $\delta=6.88$ ppm (m, 5H, Ar-H), $\delta=6.33$ ppm (m, 1H, Halcene), $\delta=5.64$ ppm (s, 1H, OH), $\delta=6.03$ ppm (m, 1H, Halcene), $\delta=5.81$ ppm (m, 1H, CH), $\delta=5.64$ ppm (s, 1H, OH), $\delta=5.23$ ppm (dd, 1H, CH), $\delta=3.91$ ppm (s, 3H, OMe), $\delta=3.89$ ppm (s, 3H, OMe), $\delta=3.56$ ppm (d, 2H, CH_2), $\delta=1.55$ ppm (d, 2H, CH_2).

6 Studies of radical stabilization by AtDIR6

360 μL of 278 μM AtDIR6 solution and 80 μL of 20 mM substrate solution (except Coniferyl Acetate which is 200 μL of 8 mM substrate solution due to the solubility), along with 560 μL (or 440 μL for Coniferyl Acetate) 0.1 M Acetate buffer pH=5 were prepared in 2 mL centrifuge tubes separately, then mixed and added to a specific EPR tube (see the picture Fig. II-A-3) after degassing 2 hours (keep the caps open) in glove box, sealed the tube well under inert atmosphere and remove out of the glove box for EPR test (see above 1.9).

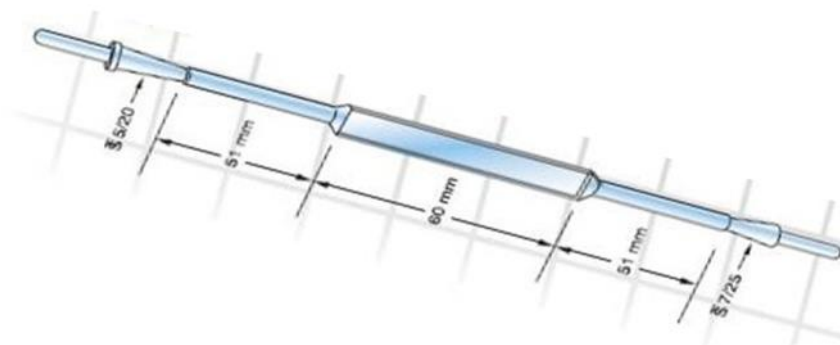


Fig. II-A-3 SUPRASIL Standard TE02 cavity aqueous cell (<http://www.cortecnet.com>)

7 HPLC chromatogram of the NOS samples

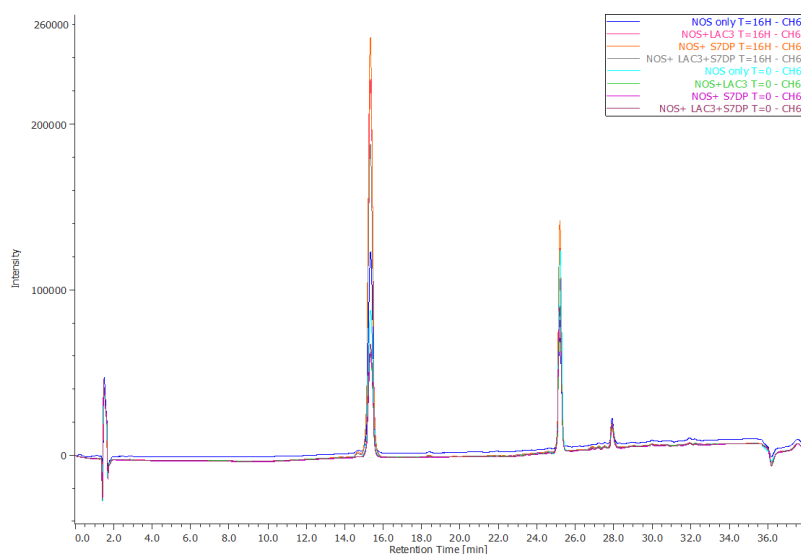


Fig. II-A-4 HPLC chromatogram of the NOS samples

8 Analysis of the amino acids involving in stereoselective coupling

The sample was collected after bioconversion of coniferyl alcohol by 1.5 U/L grafted LAC3 and AtDIR6 under the standard bioconversion of reaction condition in the final volume of 500 μ L. The reaction was inhibited by magnetically separated the LAC3 (magnetic separation and discard the particles). The supernatant left was separated using PD MiniTrap G-25 columns of Sigma Aldrich following by the manufacture's protocol¹⁵ to eliminate other substances and obtain the [AtDIR6-CA \cdot] hybrids. The separated AtDIR6 has been deglycosylated with the GlycoProfile™ IV Chemical Deglycosylation Kit of Sigma Aldrich following by the manufacture's protocol¹⁶ before MALDI TOF Analysis.

Reference

- (1) Modolo, C. L'intrigant couplage radicalaire stéréosélectif médié par la protéine dirigeante AtDIR6, thèse de doctorat Aix Marseille university, 2017.
- (2) Tarrago, L.; Modolo, C.; Yemloul, M.; Robert, V.; Rousselot-Pailley, P.; Tron, T. Controlling the Polymerization of Coniferyl Alcohol with Cyclodextrins. *New J. Chem.* **2018**, *42* (14), 11770–11775.
- (3) Kazenwadel, C.; Klebensberger, J.; Richter, S.; Pfannstiel, J.; Gerken, U.; Pickel, B.; Schaller, A.; Hauer, B. Optimized Expression of the Dirigent Protein AtDIR6 in *Pichia Pastoris* and Impact of Glycosylation on Protein Structure and Function. *Appl. Microbiol. Biotechnol.* **2013**, *97* (16), 7215–7227.
- (4) Davin, L. B.; Wang, H.-B.; Crowell, A. L.; Bedgar, D. L.; Martin, D. M.; Sarkanen, S.; Lewis, N. G. Stereoselective Bimolecular Phenoxy Radical Coupling by an Auxiliary (Dirigent) Protein Without an Active Center. *Science* **1997**, *275* (5298), 362–367. <https://doi.org/10.1126/science.275.5298.362>.
- (5) Halls, S. C.; Davin, L. B.; Kramer, D. M.; Lewis, N. G. Kinetic Study of Coniferyl Alcohol Radical Binding to the (+)-Pinoresinol Forming Dirigent Protein †. *Biochemistry* **2004**, *43* (9), 2587–2595. <https://doi.org/10.1021/bi035959o>.
- (6) Davin, L. B.; Bedgar, D. L.; Katayama, T.; Lewis, N. G. On the Stereoselective Synthesis of (+)-Pinoresinol in *Forsythia Suspensa* from Its Achiral Precursor, Coniferyl Alcohol. *Phytochemistry* **1992**, *31* (11), 3869–3874. [https://doi.org/10.1016/S0031-9422\(00\)97544-7](https://doi.org/10.1016/S0031-9422(00)97544-7).
- (7) Adalakun, O. E.; Kudanga, T.; Parker, A.; Green, I. R.; le Roes-Hill, M.; Burton, S. G. Laccase-Catalyzed Dimerization of Ferulic Acid Amplifies Antioxidant Activity. *J. Mol. Catal. B Enzym.* **2012**, *74* (1–2), 29–35. <https://doi.org/10.1016/j.molcatb.2011.08.010>.
- (8) Carunchio, F. Oxidation of Ferulic Acid by Laccase: Identification of the Products and Inhibitory Effects of Some Dipeptides. *Talanta* **2001**, *55* (1), 189–200. [https://doi.org/10.1016/S0039-9140\(01\)00417-9](https://doi.org/10.1016/S0039-9140(01)00417-9).
- (9) Smith, G. J.; Miller, I. J. Free Radicals of Coniferyl Alcohol and Isoeugenol. *Aust. J. Chem.* **1975**, *28* (1), 193–196.
- (10) Gasper, R.; Effenberger, I.; Kolesinski, P.; Terlecka, B.; Hofmann, E.; Schaller, A. Dirigent Protein Mode of Action Revealed by the Crystal Structure of AtDIR6. *Plant Physiol.* **2016**, *172* (4), 2165–2175. <https://doi.org/10.1104/pp.16.01281>.

(11) Åkerström, B.; Maghzal, G. J.; Winterbourn, C. C.; Kettle, A. J. The Lipocalin α_1 -Microglobulin Has Radical Scavenging Activity. *J. Biol. Chem.* **2007**, 282 (43), 31493–31503. <https://doi.org/10.1074/jbc.M702624200>.

(12) Pickel, B.; Pfannstiel, J.; Steudle, A.; Lehmann, A.; Gerken, U.; Pleiss, J.; Schaller, A. A Model of Dirigent Proteins Derived from Structural and Functional Similarities with Allene Oxide Cyclase and Lipocalins: Characterization of Dirigent Protein AtDIR6. *FEBS J.* **2012**, 279 (11), 1980–1993. <https://doi.org/10.1111/j.1742-4658.2012.08580.x>.

(13) Bio-Rad Protein Assay | Life Science Research | Bio-Rad <https://www.bio-rad.com/en-gf/product/bio-rad-protein-assay?ID=d4d4169a-12e8-4819-8b3e-ccab019c6e13> (accessed Sep 25, 2019).

(14) Simeng, Z.; Rousselot-Pailley, P.; Lu, R.; Charmasson, Y.; Dezord, E. C.; Robert, V.; Tron, T.; Mekmouche, Y. Production and Manipulation of Blue Copper Oxidases for Technological Applications. *Methods Enzymol.* **2018**, 613, 17–61.

(15) PD Minitrap™ G-25 GE28918007
<https://www.sigmaaldrich.com/catalog/product/sigma/ge28918007> (accessed Oct 7, 2019).

(16) GlycoProfile™ IV Chemical Deglycosylation Kit PP0510
<https://www.sigmaaldrich.com/catalog/product/sigma/pp0510> (accessed Oct 7, 2019).

Chapter III

Oriented Functionalization Of Magnetic Particles with Laccases

1 Introduction

In the previous chapter, dirigent proteins were discussed as a natural effector introducing stereoselectivity to the laccase catalyzed reactions. This chapter will cover our use of magnetic nanoparticles as an artificial effector of the enzyme activity.

Magnetic Particles (MNPs) are a commonly used materials for enzyme immobilization. As delineated in the introducing chapter a major focus of research on enzyme immobilization on MNPs is directed towards improving the stability and reusability of the biocatalysts. To the best of our knowledge, the effects of the oriented immobilization of the enzyme or the effect of the physicochemical microenvironments on the activity of enzymes are so far largely underestimated or even ignored. So, the main purpose of the investigations described in this chapter was to study whether the oriented immobilization of the enzyme and consequently the proximity of the functional groups present at the surface of MNPs with the surface accessible active site of laccase could have a direct influence on its activity and beyond on its selectivity.

To achieve the oriented immobilization of the enzyme laccase, we choose to work with variants of laccase (**Fig. III-1-1**) bearing a discrete number of surface accessible lysines as fonctionnalizable residues. The natural enzyme LAC3 from the fungus *Trametes* sp. C30 possesses only two lysines (reactive free NH₂ groups) out of its 501 residues: K40 and K71 are surface located diametrically opposed to the T1copper site with respect to the TNC. Site directed mutagenesis has been used in the laboratory to create a set of LAC3 variants with a unique surface accessible lysine residue, amongst which UniK₁₆₁ (K₄₀->M, K₇₁->H, R₁₆₁->K), the side-chain of which is located nearby the T1 copper site.¹ Unik161 with a single K nearby the T1 site LAC3 with two natural K opposite of the T1 site.

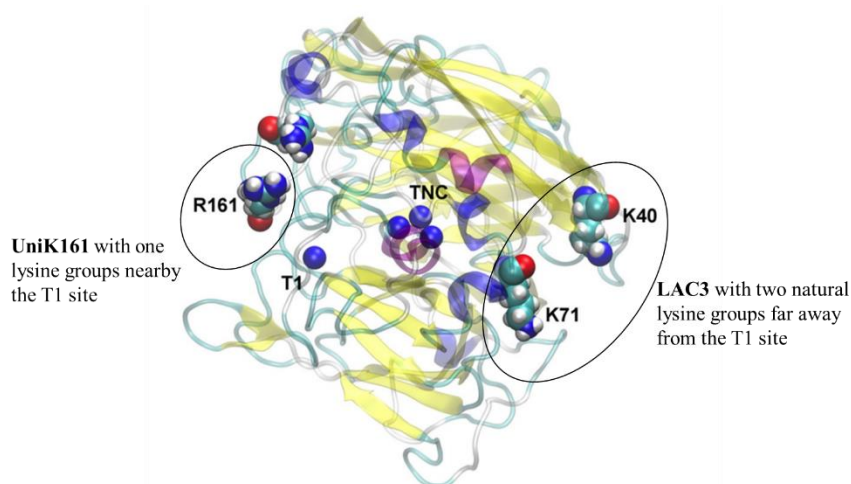


Fig. III-1-1 3D model illustrating the potential in the orientation of the enzyme upon immobilization. The figure is modified from reference. ¹ Immobilizing LAC3 onto MNPs, the exposition of the T1 site to the solvent is achieved; immobilizing UniK₁₆₁, the exposition of the T1 site to the MNP surface is obtained.

On the other hand, commercially available or self-produced MNPs bearing different surface functional groups (*i.e.* aldehyde, azido, amino and maleimide) were used to covalently immobilize the two variants of laccase. Varying the chemical functional groups at the surface of the particles provides not only different possibilities of immobilization reactions but also different physicochemical environments around laccase's T1 active site, the influence of which towards laccase activity was investigated.

This chapter contains a description of the immobilization strategies developed for LAC3 and UniK₁₆₁ onto different MNPs, the characterization of the grafted MNPs and the quantification of the specific activities of the two differentially oriented laccase-MNPs towards ABTS and coniferyl alcohol oxidation.

2 Commercial Aldehyde Particles (C21)

2.1 Information of the commercial Aldehyde particles

Aldehyde particles can be considered as ideal immobilization materials under the circumstances of this study. Indeed, a method convenient for the reductive alkylation of proteins under mild conditions² has been recently adapted to laccase variants in our laboratory.^{1,3} In this reaction, surface located lysine residues of laccase provide amino groups and the surface of magnetic particles aldehyde groups. Enzymes can be grafted on the MNP surface via a reductive alkylation promoted by an iridium catalyst in mild conditions (at room temperature and neutral pH) with formiate (HCOO^-) as hydride donor. This subsection will focus on the determination of the experimental conditions based both on the experience from our lab and based on the distributor's protocol.² A schematic diagram of the reaction is shown in **Fig. III-2-1**.

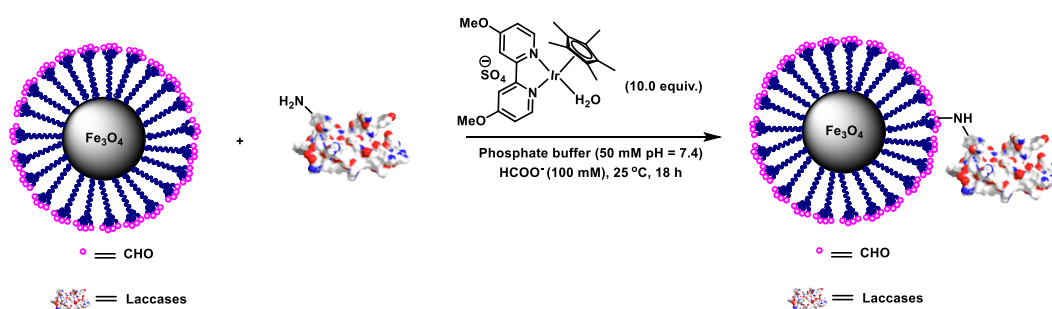


Fig. III-2-1 Schematic diagram of the Reductive alkylation reaction used in aldehyde particles immobilization.

The commercial Aldehyde particles (**Bioclone BcMag™ Aldehyde-activated Magnetic Beads**) were purchased from Bioclone company. The average size of the particle is about 1 μm. The outer layer of the particles is coated with silica. Long-arm linkers (21-C atom) serve as spacer between the silica shell and the terminal aldehyde groups to reduce steric hindrance (see the scheme of the particles in **Fig. III-2-2**). Based on the manufacturer's datasheet a high density of aldehyde functional groups (~210 μmole/g of beads) are grafted on the surface of the superparamagnetic beads, making them suitable to covalently conjugate primary amine-containing ligands or proteins.⁴

The following subsection will describe the oriented immobilization of laccase on the commercial aldehyde particles (simply described as C21). Preliminary immobilization results, pretreatment (dispersion) and characterization of the particles, exploration of the immobilization conditions, issues encountered during the exploration, as well as the final results will be all described in details.

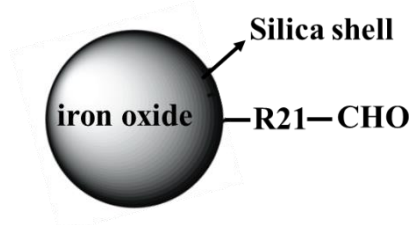


Fig. III-2-2 Schematic diagram of commercial aldehyde particles C21

2.2 Results and discussion

2.2.1 Preliminary results on immobilization

In a first instance, 1 mg of particles (which should correspond to 0.21 μmol surface aldehyde groups based on instructions from the manufacturer) was used in a total volume of 1 ml, and the initial ratio of laccase and aldehyde groups was set to 1:10 (0.021 μmol laccase). Concentration of laccase is determined spectroscopically (UV/vis) and is based on the evaluation of the CuII T1 absorbance at 610 nm ($\epsilon=5600 \text{ L}\cdot\text{mol}^{-1}\cdot\text{cm}^{-1}$). Amount of enzyme immobilized on the magnetic particles (enzyme loading) corresponds to the difference between the initial amount of enzyme engaged in the reaction and the amount of enzyme remaining in the supernatant after reaction (**enzyme loading = (enzyme added)- (enzyme left in the supernatant after reaction)**).

One point that must be mentioned is that: since laccase is reduced in the reaction system by the iridium/hydride catalyst, it is not accurate to measure absorbance at 610nm directly after reaction. Separation of the enzyme from other reactants by desalting column (Sephadex G-25 in PD-10 Desalting Columns) and concentration are necessary steps (i.e. allowing a re-oxidation of the enzyme) before testing the concentration.

Table III-2-1 Preliminary results of immobilization (1 mg particles, 0.021 μmol laccase, total volume 1mL)

	LAC3		UniK ₁₆₁	
	Before reaction	After reaction	Before reaction	After reaction
Sample Volume (μL)	21	550	24	670
Concentration (10^{-6}M)	1000	19	898	27
Amount (10^{-6}mol)	0.020	0.0105	0.022	0.018
Enzyme loading (10^{-6}mol/mg particles)	0.0105		0.0034	
Activity (U/mL for free laccase; U/10 mg particles for grafted laccase)	4027	2.79	2489	1.30
STDEV of Activity	328 (8%)	0.52 (18%)	185 (7%)	0.25 (19%)
Specific Activity (U/mg free or grafted laccase)	50	0.33	35	0.48
Ratio of Specific Activity (LAC3:UniK₁₆₁)	Before Reaction		1.43	
	After Reaction		0.69	

A first set of quantification results is shown in **Table III-2-1**. It can be seen from the table that: after immobilization, (1) the grafting ratio (ratio of initial laccase amount on amount of laccase grafted onto the particles) is 50% for LAC3 and 15% for UniK₁₆₁; (2) the specific activity is apparently decreased about 125 and 70 times compared to the free laccase for LAC3 and UniK₁₆₁ respectively; (3) the ratio of specific activity (LAC3:UniK₁₆₁) changed from about 1.43 to 0.69, it means that after immobilization, UniK₁₆₁ show relatively better activity to LAC3, which is the opposite situation of what happened before immobilization.

The enzyme loading evaluated in this initial experiment is particularly low. This evaluation is probably not reliable because, as mentioned above, the strong reducing environment of the coupling reaction imposing a number of post treatments (such as gel filtration, concentration, and pipetting to measure the final small volume) there is a cumulation of experimental errors that cannot be neglected on a low enzyme loading. Contrary to UV-Vis measurement of the T1 copper center, Bradford test is not affected by the redox state of the enzyme thus avoiding the need of introducing operational steps leading to errors. So, evaluation of enzyme loading was repeated in the same reaction conditions, except that Bradford protein assay was applied to determine enzyme concentration.

Unfortunately, it was not possible to evaluate differences between supernatants before and after reaction from the results of repeated experiments using Bradford as the enzyme loading detection method (data not shown). Even though the initial laccase concentration was increased 10 times to 0.21 $\mu\text{mol/mL}$ (1:1 ratio of initial laccase and aldehyde groups), with an expectation that the enzyme loading would be enlarged, differences between supernatants before and after reaction still did not appeared. Moreover, dilutions required for attaining linearity could cause cumulated errors.

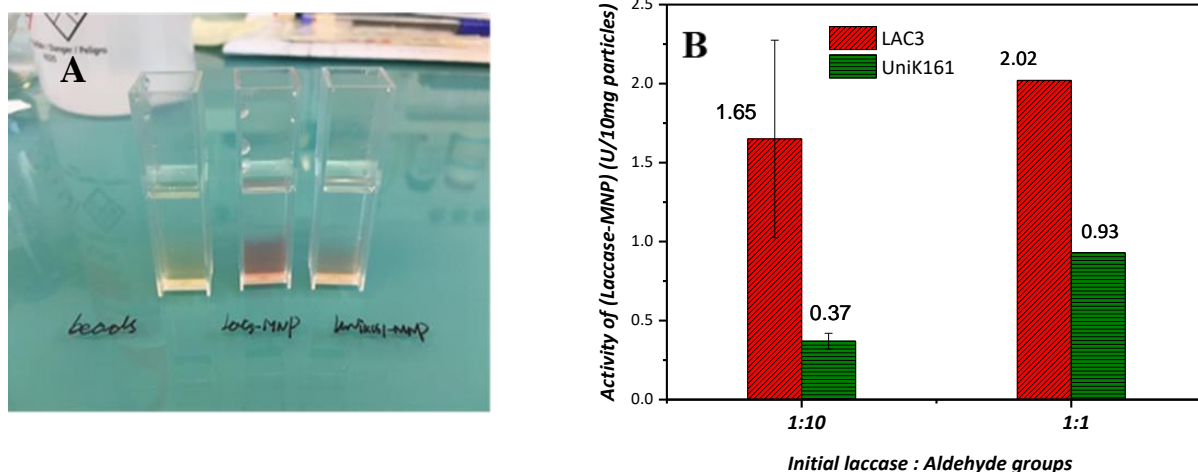


Fig. III-2-3 Activity of (Laccase-MNP) system after immobilization (A) qualitatively observed by the color change upon Syringaldazine (SGZ) oxidation catalyzed by laccase. (B) quantitatively measured by using SGZ as substrate.

After immobilization, particles grafted either with LAC3 or UNIK₁₆₁ showed activity first qualitatively as observed by a color change (Fig. III-2-3 A) then quantitatively as measured following the kinetics of syringaldazine (SGZ) oxidation by laccase (Fig. III-2-3 B). Catalytically active hybrids of magnetic particles (MNP)/enzymes means that there is laccase grafted onto the surface of the particles and that even if we were not able to evaluate a difference in protein concentration in supernatants before and after reaction (i.e. enzyme loading). It is probably because that the amount of immobilized enzyme is too low to be correctly evaluated by the techniques used (UV/VIS, Bradford).

Using the same amount of particle for each hybrid, the examination of activity values (not the specific activities, SA) in Fig. III-2-3 B seems to indicate: (1) the activity of the (laccase-MNP) systems appears to be affected by the grafting process; (2) in hybrids, activity increases modestly with the increase of the initial enzyme concentration for both LAC3 and UniK₁₆₁ suggesting that the particles are may be saturated; (2) LAC3 always displays a higher activity than UniK₁₆₁ (NB: in homogeneous conditions the specific activity of both enzymes is similar) suggesting an effect of the orientation as suspected. However, all these comparisons being based only on activity rather than specific activity of the (laccase-MNP) hybrid since the enzyme loading is unknown, they may represent at the most a tendency.

From this first study on aldehyde particles grafting, we can further state that, although for different reasons, evaluation of the protein concentration based either on Bradford and UV-Vis spectroscopy measurements is not accurate and therefore do not allow to compare specific activities of LAC3 and UniK₁₆₁. As SA is mandatory for normalization more efforts have to be put into the accurate measurement of enzyme loading. Solutions and next plan include adjusting the reaction

parameters in order to potentially increase the amount of immobilized enzyme (enzyme loading) and/or to turn to more sensitive enzyme measurement methods (e.g. immunologic detection).

2.2.2 Study on the dispersion of magnetic particles

As mentioned above, one way to make the evaluation of the enzyme loading more accurate is to try to increase the amount of grafted enzymes. Going that direction, the way particles were handled before reaction and their dispersion state during the reaction were considered. Particles have a tendency to aggregate in the suspension medium (water or buffer) that is depending on particle size, surface charge, temperature, the nature and concentration of ions and magnetic forces. Aggregation will decrease the reaction (grafting) efficiency by decreasing the specific surface area. As any hindrance to the surface functional groups should be avoided as much as possible, here, several methods were used to prevent and/or reverse the aggregation before grafting.

2.2.2.1 Physical methods to prevent aggregation

The outer layer of the commercial aldehyde particles used in this section is silica and is therefore hydrophilic (at least more than polymeric particles) thus reducing the likelihood for hydrophobic interactions as a potential cause for aggregation. Moreover, the mean size of these particles (1 μ m) although making their surface specific area lower than real nano-scale particles is decreasing the likelihood of aggregation due to a relatively low specific surface energy. So, in theory, physical means of dispersion e.g., sonication, vortexing or pipetting should be sufficient to prevent and/or reverse the aggregation of this kind of particles in the medium.

Aggregation conditions were observed under an optical microscope. Before the observation, 1mg of the aldehyde particles (commercial beads) were transferred to a centrifuge tubes and dispersed in 1mL MQ water by different means. The pictures of magnetic particles after processing by pipetting, vortexing and bath sonication are shown in **Fig. III-2-4 A B C** respectively. These pictures are typical from no less than 3 fields.

Pipetting

Generally, the shear forces created by rapid pipetting of a suspension of magnetic particles through a fine pipet tip are often enough to reduce or eliminate aggregation caused by hydrophobic interactions. From **Fig. III-2-4 A** it can be seen that although a small amount of single dispersed particles can be observed, large pieces of particle aggregations are still ubiquitous in the suspension after distributing the particles with extended pipetting for 1~2 mins. This is indicating that pipetting, even if intensely operated, is not strong enough for a good dispersion of the commercial aldehyde particles. Alternatively, this observation may indicate that the dispersed particles re-agglomerated in the medium rapidly.

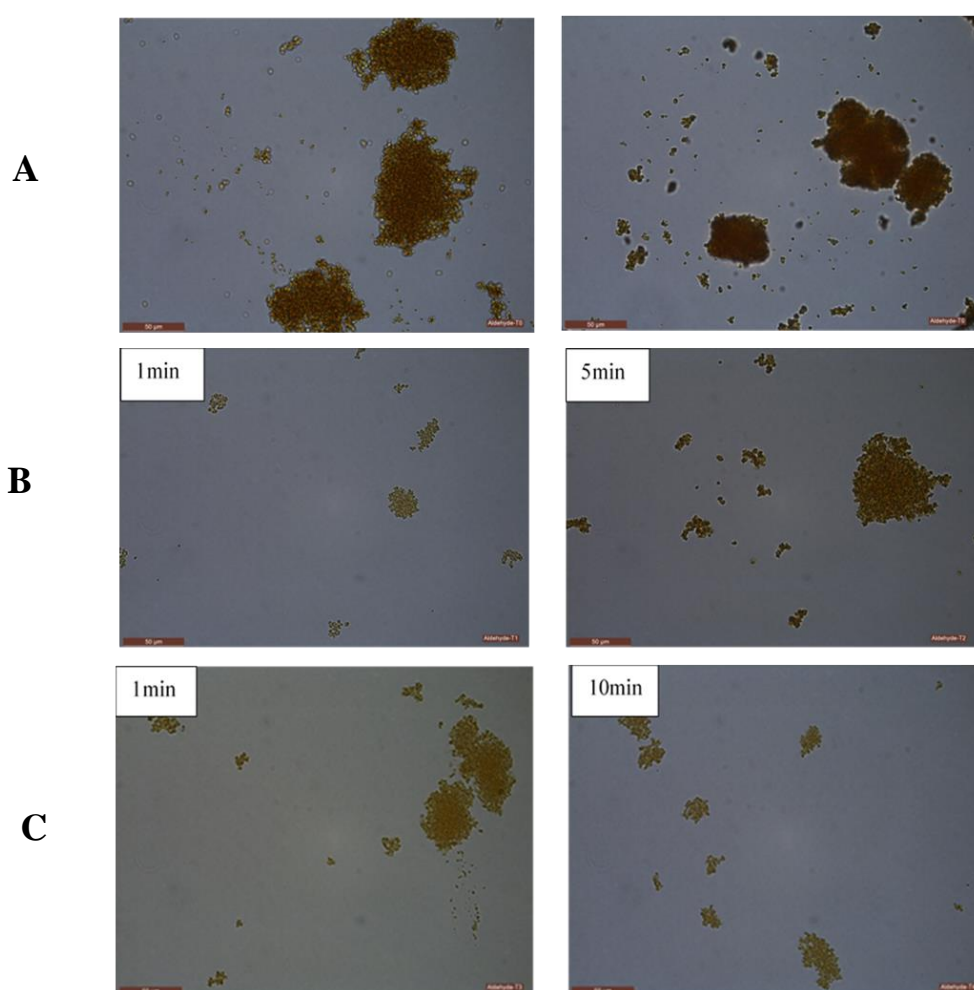


Fig. III-2-4 Commercial Aldehyde particles dispersed by different physical methods (1mg/mL in MQ water). (A) *Pipetting* (B) *Vortexing* at 1min and 5min respectively (C) *Bath sonication* at 1min and 10 min respectively.

Vortexing

Vortexing is the method recommended by the manufacturer to suspend their particles. As found in the instructions, vortexing the suspension 3-5 mins is normally enough for the dispersion. **Fig. III-2-4 B** displays the picture of commercial aldehyde particles after vortexing. It can be seen that: (1) although aggregation of particles is still present, the size of the aggregates is relatively smaller compared to that observed after pipetting. This means that the degree of aggregation is reduced when vortexing is used to separate particles; (2) when the vortexing time was prolonged from 1min to 5min, no obvious improvement was observed in particle aggregation. On the contrary, a small quantity of larger agglomerates started to appear when vortexing for longer time (5min). A possible explanation for this reverse effect is that both dispersion and re-aggregation occurring simultaneously in the suspension during vortexing the effect of prolonged time on particle re-aggregation is greater than on particles dispersion. Therefore, it is not advisable to vortex longer times for dispersion.

Bath sonication

Sonication dispersion method was then investigated. This method allows the ultrasonic energy to reach all over the particles effectively, increasing the likelihood of breaking the aggregates. **Fig. III-2-4 C** gives the picture of commercial aldehyde particles after a sonication treatment (bath type sonicator). The pictures clearly show that in these conditions: (1) ultrasonic energy does not allow to break large aggregates of particles (no single particle was observed); (2) larger particle aggregates were apparently broken into smaller ones after prolonging the sonication time from 1min to 10min, but single particles were still rarely found.

Prolonging the process time until 30 mins was also performed (pictures not shown). Observation under the microscope revealed that extending the time of the bath sonication did not improve the dispersion state over that observed after 10mins. A possible explanation for that observation is that an extended exposure, even in a mild ultrasonic bath, can heat the particles to an undesirable level; increased temperature usually causes an increase in the kinetics of collisions of the particles in the suspension thereby increasing their likelihood of encountering with each other.

Probe sonication

Energy of bath sonication was proven to be not enough to break particles aggregates and increasing the treating time will increase the risk of heating particles, so a more powerful sonicator: a probe sonicator was used as an alternative method. As probe sonicator will provide high ultrasonic energy in a small volume, so in theory, a short pulse will be sufficient for the separation of particles.



Fig. III-2-5 Commercial Aldehyde particles dispersed by *probe sonication* for 3 mins (1mg/mL in MQ water)

Commercial aldehyde particles were treated with probe sonication for 30 seconds at 75W and then dispersed beads were observed under microscope. Observation of several fields revealed that aggregation was still largely present in the medium with a size of aggregates very much like the one obtained previously with bath sonication. In fact, very few (if any) single particles were observed. Extending the sonication time to 3 minutes did not improve the dispersion (aggregates are still visible, **Fig. III-2-5**). Therefore, probe sonication performed in these conditions is not bringing obvious improvements on the aggregation as compared to other ways. In addition, note that some manufacturer is not recommending to treat their particles with probe sonication because an unclean probe tip can contaminate the microsphere suspension and an old tip can shed metal, even if it is clean. Also, once protein is immobilized onto the particles, probe sonication can be deleterious and ruin protein structure and activity when resuspending particles into the medium.

So, from the above results, it can be concluded that among all dispersion methods used here vortexing is apparently the most suitable one for dispersing the commercial aldehyde particles. However, getting rid of large aggregates is hard and any physical methods alone does not seem to be enough to obtain a well dispersed suspension. Therefore, combining a chemical method (such as adding a surfactant) to the physical methods should be considered.

2.2.2.2 Influence of Surfactant on the aggregation

The surfactant investigated is the non-ionic surfactant Tween 20. 0.05% (v/v) Tween 20 was added into MQ water as the suspension medium. 1mg particles was dispersed in 1mL of the suspension medium by vortexing 1~3min, then observed under an optical microscope. It can be seen from **Fig. III-2-6 A** that when Tween was added to the suspending medium, aggregates were dispersed by vortexing and a large number of single particles appeared in the field of the microscope.

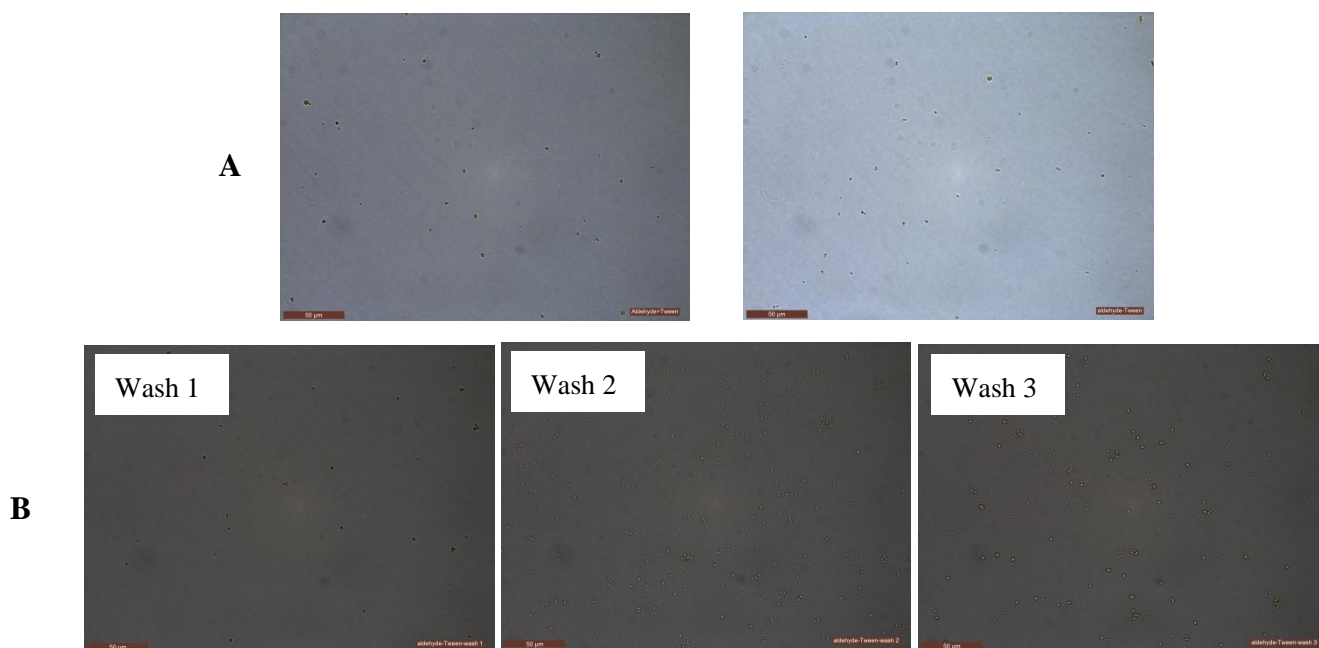


Fig. III-2-6 1mg/mL commercial Aldehyde particles dispersed in MQ water with 0.05% Tween 20. (A) the particles were dispersed by vortexing. (B) the dispersion state after wash three times by MQ water

Since the immobilization process requires particles to be resuspended repeatedly during washing steps (for the elimination of excess of reactants), so the aggregation state after resuspension was investigated further. Vortexed particles suspended in Tween 20 solutions were initially separated on a magnet; then the supernatant was discarded and the particles resuspended in MQ water by vortexing. The process was repeated 3 times and each time the resuspended state was observed under a microscope. As it can be seen **Fig. III-2-6 B**, after 3 washing/capture/resuspension steps, particles are still kept in a well-dispersed state in the medium.

In summary, it can be concluded that addition of 0.05% Tween 20 to the suspension medium is an effective way to obtain a homogeneous dispersion of commercial aldehyde particles.

2.2.2.3 Immobilization experiments with dispersed particles

Immobilization of BSA

Particles dispersed as described above were first used to graft BSA (Bovine Serum Albumin) as a model protein (much cheaper than LAC3) in order to verify the effect of dispersion on enzyme loading. Beyond the fact that it is easier to produce concentrated solutions (10 equivalent of the aldehyde groups) using the commercial BSA than using the lab-produced laccase, BSA contains 59 lysine residues, 30 to 35 of them being solvent exposed (and therefore capable of reaction), providing a situation highly favorable for the grafting and the subsequent determination of the enzyme loading.

Starting BSA concentrations were set to 2.1 $\mu\text{mol/mL}$ and 0.021 $\mu\text{mol/mL}$ respectively, particles 1 mg (0.21 μmol aldehyde groups based on the instruction of the manufacture)/ml; reaction conditions identical to those described previously. Protein contents before and after reaction were tested using the Bradford method (see details in the appendix). Results are listed in **Table III-2-2**. For each experiment, absorbance values of the solutions before and after reaction can be regarded as unchanged. This indicates that there is no or extremely few BSA proteins grafted onto the particles in these conditions, therefore disqualifying that protein as reference for testing protein loading. Because unlike BSA the grafting of an enzyme can be probed based on its activity, immobilization of laccase onto surfactant-dispersed particles was eventually tested.

Table III-2-2 Commercial aldehyde particles grafted with BSA

Starting concentration of BSA ($\mu\text{mol/mL}$)	Ratio of initial protein and aldehyde groups	Absorbance at 595 nm before and after reaction	
2.1	10:1	1.03	(sample was diluted 100 times)
		1.02	
0.021	1:10	0.91	
		0.94	

Immobilization of LAC3

The starting amount of LAC3 was set to 0.021 μmol for 1 mg of particles (0.21 μmol aldehyde) in a final volume of 1 mL. Activities of the reacted particles after four wash with 0.1 M acetate buffer pH=5.7 were tested. Approximately 0.1 U/1 mg particles were quantified which is twice as less than the first grafting results obtained (0.2 U/1 mg particles) in the absence of Tween 20.

From the dispersion study of the particles and the results of the first grafting experiments, the following conclusion can be drawn: (1) from the various physical dispersion methods studied in this section vortexing is apparently the best one. However, vortexing alone does not allow to get rid of aggregates and get single dispersed particles; (2) combining vortex and surfactant (Tween 20) to the dispersion medium makes it possible to obtain stable and well-dispersed particles. The dispersed state of the particles can also be maintained during the separation and redispersion process. However, the use of well dispersed particles for the immobilization of the model protein BSA and the target enzyme LAC3 did not contribute to increase protein loadings to the expected detectable level (measured by the Bradford method). At least in this case there is apparently no obvious link in between a better dispersion and a better immobilization. This may be due at least in part to a certain non-accessibility of functional groups at the surface of the particles. Therefore, it is necessary to verify the amount of accessible functional groups or, in other words, to determine the active state of the surface functional groups.

2.2.3 Characterization of the surface functional groups on MNPs

2.2.3.1 Zeta potential measurement for the surface charge state of MNPs

Measuring zeta potential is a way to evaluate the physical stability of nanosuspensions. The zeta potential represents the electric charge (mV) that a particle acquires through the ions surrounding it when in solution. It is well documented that large positive or negative values for zeta potential of nanocrystals indicate good physical stability of nanosuspensions due to electrostatic repulsion of individual particles. Generally, particles with a zeta potential value outside a -30 mV to $+30$ mV interval is considered to have sufficient repulsive force to remain dispersed.⁵

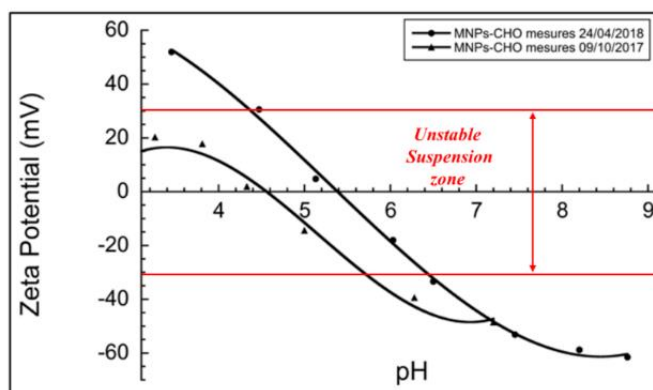


Fig. III-2-7 Effect of pH on the surface charge of commercial particles.

The effect of pH on the surface charges was studied by measuring zeta potentials of MNPs suspensions in pure water varying the pH from 3 to 9. The test was performed twice at different dates and results are shown in Fig. III-2-7. It can be seen that the pH of immobilization used in this study (pH 7.4) is theoretically compatible with the maintenance of the particles in a dispersed state. Indeed, the zeta potential of the particles at pH 7.4 is below -30 mV so it is out of the unstable suspension zone. However, although the isoelectric point (IEP) of the C21 particles was found at pH 4.5 on October 2017 was, the IEP of the same particles tested after a six-month storage period at 4°C (until April 2018) was found at pH 5.4. This shift of almost one pH unit for the IEP reveals that the particles are not stable over the time during storage. Since the laccase IEP is around pH 4, laccase will be electronegative under the conditions of the immobilization reaction (pH 7.4). With the current example, particles are also negatively charged as their IEP is found below pH 7.4. Thus, the possibility of electrostatic adsorption is minimum due to electrostatic repulsion. However, would the IEP of the particle move to above pH 7, the particles would be positively charged under the conditions of the immobilization reaction and electrostatic attraction between laccase (electronegative) and particles (electropositive) would increase and lead to an undesired non-directional immobilization.

Therefore, since the instability of the surface state of the particles has an effect on the immobilization reaction storage conditions of the particles should be carefully monitored.

2.2.3.2 Qualitative characterization

The qualitative characterization of the particle surface groups was performed on IR-ATR spectroscopy. Typical results are illustrated in **Fig. III-2-8**. In the case of commercial aldehyde particles, the presence of ν Fe-O vibration bands as well as ν Si-O-Si vibration bands corresponding to the core of the MNPs can be observed. Also, ν CH₂ vibration bands of alkyl chain (long arm) are detected. The characteristic intense vibration band ν C=O is also present but with an unusual low intensity. This means either that the sample doesn't contain that much aldehyde groups or it is not stable over a long period of time in the packaging proposed by the manufacturer (i.e. dried).

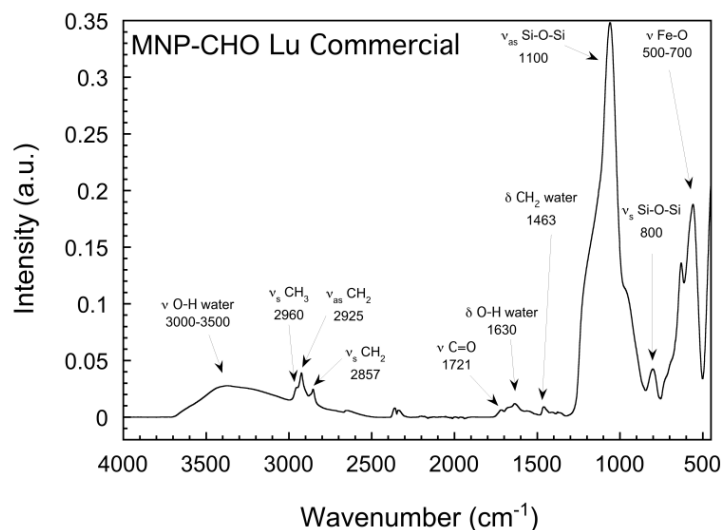


Fig. III-2-8 ATR FT-IR spectrum of commercial aldehyde particles after storage

To verify the quality of the product, a new batch of aldehyde particles was purchased and tested upon receipt by IR-DRIFT spectroscopy. The spectrum shown in **Fig. III-2-9** is similar to the spectrum of the previous sample presented in . The vibration band ν C=O is present but its intensity is still low as already observed. Since the sample was stored carefully at 4°C as instructed by the manufacturer and measured as soon as received, it can be provisionally concluded that the commercial aldehyde particles do not contain much aldehyde groups at their surface.

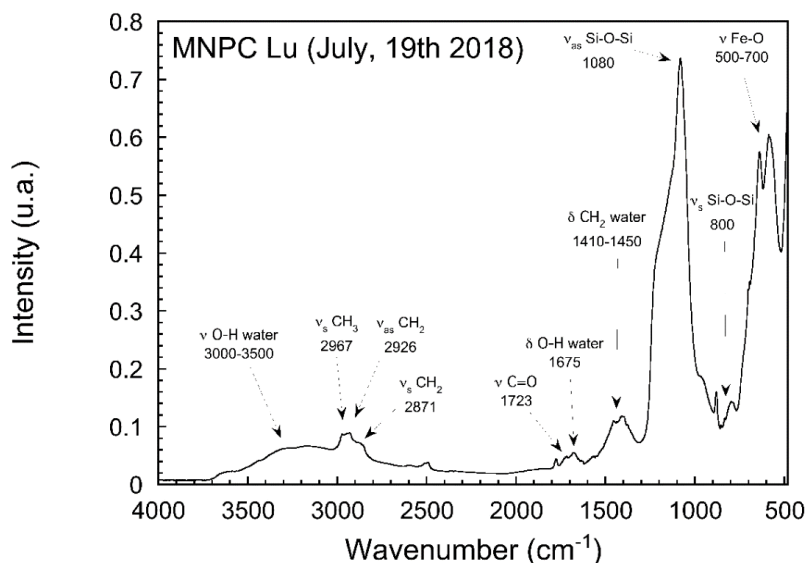


Fig. III-2-9 FT-IR spectrum of commercial aldehyde particles measured rapidly upon receipt

Because the ratio of enzymes over the amount of functional groups is a very important parameter in the immobilization process, quantitative determination of the amount of aldehyde groups on the surface of the particles is essential.

2.2.3.3 Quantitative characterization of the aldehyde reactive group

The principle of quantitative measurement of functional groups on MNPs surface is based on dye coupling reaction reported by Bing Yan *et.al.*⁶ The method relies on the coupling of a fluorescent dye to the functional groups of resin-bound materials. Then, the quantification of the dye remaining in solution allows the quantification of the functional groups of the resin. The dye-coupling principle was reported to be an effective methodology to quantify reaction yields directly on solid phase due to the excellent sensitivity of fluorescence spectroscopy and the ample availability of fluorescent dyes.⁶

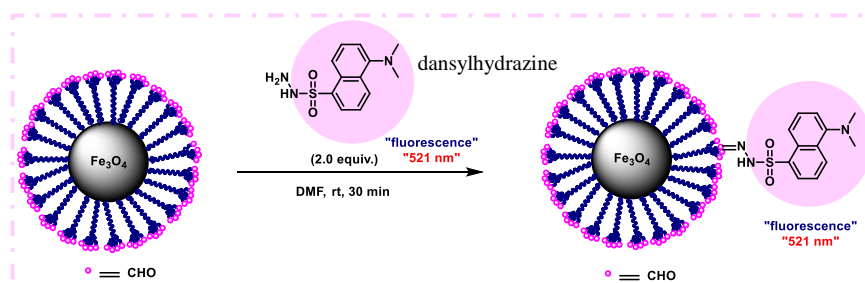


Fig. III-2-10 Schematic representation of the grafting of the fluorescent dye on MNPs for determination of the surface aldehyde groups

Dansylhydrazine was used as the fluorescent dye and was covalently bound to the surface of the particles through its reaction with aldehyde groups (**Fig. III-2-10**). During the reaction process, the surface aldehyde groups are consumed. Since the reaction is stoichiometric, the amount of the surface effective aldehyde groups is equal to the amount of dansylhydrazine coupled on MNPs, which can be calculated by measuring the difference in fluorescence intensity between the supernatant before and after reaction.

A series of standard samples were prepared in DMF and the fluorescence intensity was measured with spectrofluorometer in order to draw a calibration curve and then be able to calculate the concentration of the fluorescent substance in the supernatant. Excitation was set at 379 nm and emission was scanned from 400 to 600 nm; maximum fluorescence intensity was recorded at 521 nm. Raw data are presented in **Fig. III-2-11** and the relationship between the concentration of the dansylhydrazine solution and their fluorescence intensity is shown in **Fig. III-2-11 B**. It can be seen that in a very low concentration range, the fluorescence intensity is linearly related to the concentration of the fluorescent molecule, while at the higher concentration solutions, the fluorescence intensity no longer maintains the linear relationship with the concentration, maybe due to fluorescence quenching and self-absorption. So the calibration curve (**Fig. III-2-12**) was made by just taking the data in the linear part of **Fig. III-2-11 B**. Therefore, special attention was paid when measuring the fluorescence intensity of the supernatant in the reaction system i.e. diluting samples if there were out of the range of the calibration curve.

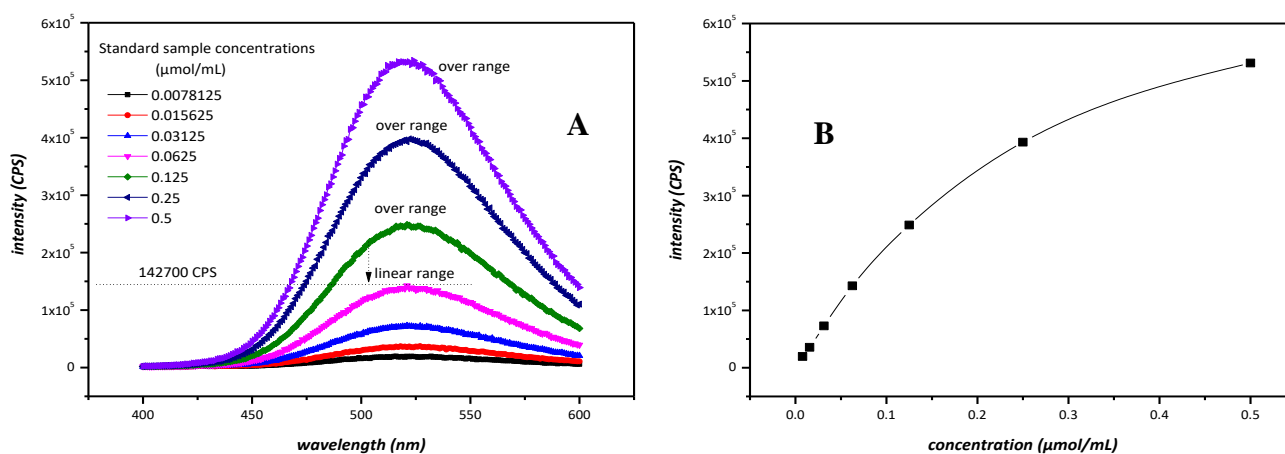


Fig. III-2-11 Fluorescence spectroscopy measurement of the standard solutions. (A) Fluorescence intensity spectra of standard solutions at different concentrations (B) Relationship between solution concentration and fluorescence intensity. The wavelength of the excitation light was set at 379 nm and wavelength of the emission light was scanned from 400 to 600 nm, slits 1nm, 20°C. Fluorescence intensity of the solution was taken at the maximum emission at 521 nm.

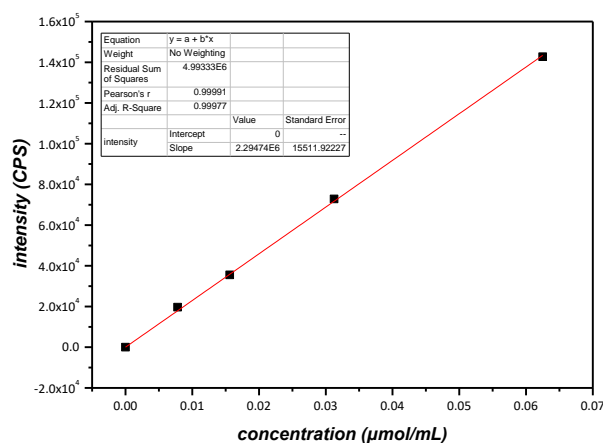


Fig. III-2-12 Calibration curve for quantitative determination of aldehyde groups on the surface of MNPs by fluorescent dye coupling method.

After linear fitting which goes through the (0,0) point, the equation of the curve is determined to be: y (intensity) = $2294740x$ (x concentration: $\mu\text{mol/mL}$). The application scope of this calibration curve is 0~0.0625 $\mu\text{mol/mL}$. It means that the fluorescence intensity of the tested samples should be no more than 142700 CPS.

The dye coupling reaction for aldehyde quantitative measurement was performed at room temperature in a total reaction volume of 1ml. 1mg commercial aldehyde particles was used for coupling with 0.105 μmol initial dansylhydrazine (approximately 1:2 molar ratio relative to the functional group on MNPs). The reaction was incubated at room temperature for 30mins using DMF as solvent. After reaction, beads were magnetically separated and washed by the reaction medium several times. The supernatants and the washing solutions were collected and diluted appropriately

for fluorescence spectroscopy measurement using the same parameters as for standard solutions. Results are shown in **Fig. III-2-13** and the corresponding calculations are given in **Table III-2-3**.

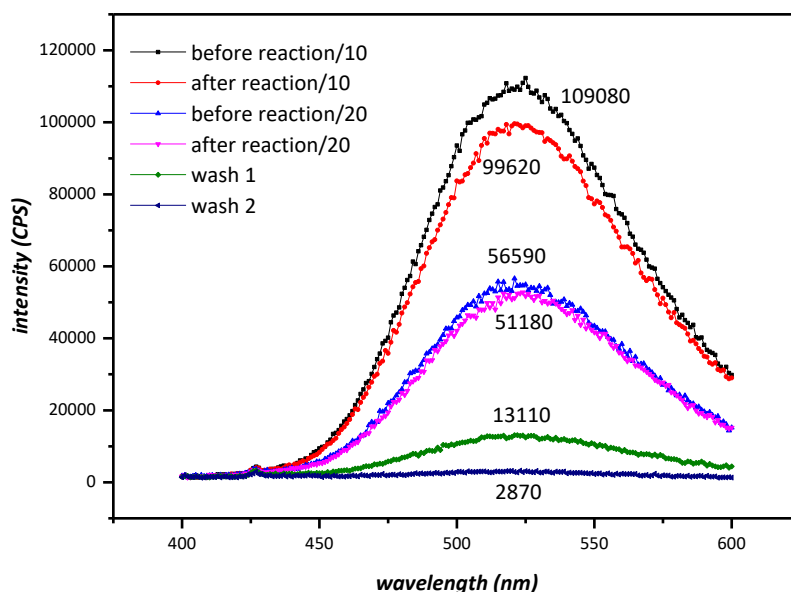


Fig. III-2-13 Fluorescence spectroscopy measurement of the supernatants and washing solutions

As expected, fluorescence intensity in the supernatant diminished after reaction, meaning that part of the dansylhydrazine was effectively coupled with the MNPs. Non specific fluorescence (non-covalently bound dyes) was removed by washing the particles. A density of about 40 μmol of aldehyde/g particles was calculated from supernatants diluted 10 and 20 times respectively (**Table III-2-3**). Considering the inevitable experimental error, these two values can be mutually verified. 34-40 μmol of aldehyde/g particles is much smaller than the 210 $\mu\text{mol}/\text{g}$ value provided by the supplier. The low content of the surface functional groups is consistent with the results of the FT-IR analysis.

It is worth mentioning that, before using DMF as the reaction medium, the storage buffer (20 mM acetate buffer, pH=5.7) was also tested since the immobilization of laccase on MNPs has to be performed in mild conditions (aqueous solution, a certain pH, *etc.*). Although a calibration curve was obtained for standard samples the intensity of fluorescence of the supernatant before and after reaction did not change (data not shown). Dansylhydrazine coupling did not occur in DMSO as well.

Table III-2-3 Surface functional groups calculated by the calibration curve

Samples	Fluorescence intensity (CPS)	Concentration of dilutions ($\mu\text{mol/mL}$)	Concentration of solutions ($\mu\text{mol/mL}$)	Difference value ($\mu\text{mol/mg}$)	Aldehyde contents ($\mu\text{mol/g}$)
Blank contrast diluted 10×	109080	0.047	0.470		
Supernatant diluted 10×	99620	0.043	0.430	0.040	40
Wash 1	13110	-	0.005		
Wash 2	2870	-	0.001		
Blank contrast diluted 20×	56590	0.025	0.490		
Supernatant diluted 20×	51180	0.022	0.450	0.040	40
Wash 1	13110	-	0.006		
Wash 2	2870	-	0.001		

To conclude, the measured contents of the surface functional groups on the commercial aldehyde particles is lower (> 5 times) than the value given by the manufacturer. Moreover, particles are not apparently stable during storage. This may explain the difficulties encountered to evaluate the enzyme loading by conventional methods (UV-VIS, Bradford) as well as to improve reaction yields even though well-dispersed particle suspensions were obtained. Taking this into account the immobilization conditions was adjusted according to the effective contents of surface groups.

2.2.4 Exploration of the experimental conditions

2.2.4.1 Effect of particle amount on enzyme loading

For the purpose of bringing the enzyme load to a detectable level, increased amounts of particles (i.e. representing an increase in total aldehyde groups) were used. The final volume of the reaction system was kept to 1 mL and the initial enzyme concentration used was 5 μM . Three sets of immobilizations were performed for 2 mg and 10 mg particles respectively. Enzyme loading was tested by Bradford methods as previously described. The relationship between particle amounts and enzyme loading is shown in **Fig. III-2-14**. It can be seen that increasing the amount of particles does not increase the enzyme loading but rather diminish it. If the Bradford method is reliable, this phenomenon may result from an increased aggregation linked to a higher frequency of particle collisions in highly concentrated particle suspensions therefore decreasing the availability of functional groups.

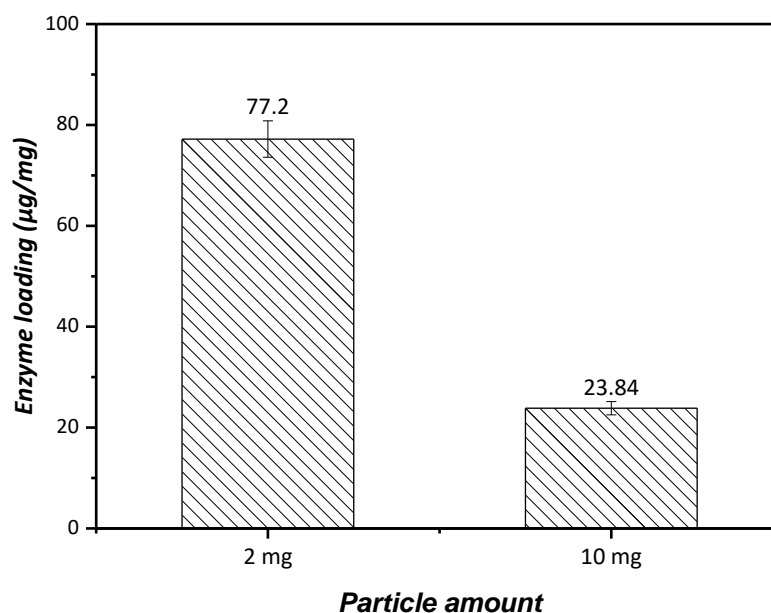


Fig. III-2-14 Relationship of the particles amount and the final enzyme loading. The total volume of the reaction system is 1mL, and the initial enzyme concentration used is 5µM. Three groups of immobilizations were performed for 2mg and 10mg particles respectively. Enzyme loading was tested by Bradford methods as previously described.

2.2.4.2 From Bradford to ELISA for Enzyme loading measurement

It is difficult to increase the enzyme loading in the current situations, limited by the apparent low content of surface functional groups and the nature of the reaction medium (in order not to damage the activity of laccase it is necessary to employ an aqueous solution or a solution containing only a very small amount of organic solvent in the reaction medium). When we quantified aldehyde groups on the surface of C21, it was obvious that the organic solvent DMF is more favorable for the reductive alkylation reaction than the storage buffer this being amplified also by the mass transfer caused by the solid phase. The reaction between the two phases is less probable to proceed completely as compared with reaction in a homogenous solution.

Bradford and UV-Vis are the mostly used methods for enzyme concentration measurement as reported in the literature. These methods are indirect since they are based on measuring the amount of protein in solution before and after incubation with MNPs. However, these methods have some shortcomings. First, the estimation could be inaccurate, because several errors may be introduced since the methodology contains a measurement of two concentrations (concentrations of a solution before and after reaction). Also, in some cases, in order to avoid exceeding the upper limit of detection, the sample needs to be diluted before test. When the dilution factor is large, it is also possible to amplify the experimental error when multiplying it back. In addition, when the immobilized amount is particularly small, the amount of immobilized protein is calculated as a small difference between two large values. It will raise uncertainty because in some cases, the difference is below detection.

Under the cases of this study, where the influence of orientations on immobilized enzymes need to be compared based on the specific activity, an accurate measurement of the enzyme grafted is needed. Because the enzyme loading is a very important factor for computation of the specific activity, any inaccurate measurement will give unveracious results.

So, the challenge is converted into finding ways to detect the enzyme loading at a minute quantity level. The method should be sensitive and accurate. Here, enzyme linked immunosorbent assay (ELISA) was developed to achieve this goal.

ELISA is commonly used in medical research laboratories and for commercial applications, including the detection of disease markers and allergens in diagnostic and food industries. It is a powerful method for detecting and quantifying a specific protein in a complex mixture. The mechanism of a typical ELISA can be described as follows based on a guide book of Thermo SCIENTIFIC (ELISA technical guide and protocols).⁷

1). **Coating/Capture:** to detect an antigen in a complex protein mixture, the antigen should be first immobilized to the wells of a microplate either by direct adsorption or via an antibody adsorption.

2). **Plate Blocking:** the plate is blocked by addition of irrelevant protein or other molecule to cover all unsaturated surface-binding sites of the microplate wells.

3). **Probing/Detection:** incubation with antigen-specific antibodies that affinity-bind to the antigens. The detection antibody may be directly labeled with a signal-generating enzyme or fluorophore or it may be secondarily probed with an enzyme- or fluor-labeled secondary antibody (or avidin-biotin chemistry).

4). **Signal Measurement:** detection of the signal generated via the direct or secondary tag on the specific antibody. For enzymatic detection, the appropriate enzyme substrate is added. The signal observed is proportional to the amount of antigen in the sample. Washing between steps ensures that only specific (high-affinity) binding events are maintained to cause signal at the final step.

In this study, the free and immobilized laccase can be regarded as antigens. The free enzyme used for standard solutions was attached to the microplate by adsorption. The immobilized enzyme was placed in the microwells as well with the MNPs as carriers. The convenient manipulation of MNPs directly on the microplate was achieved by using a special magnetic supporter (**Fig. III-2-15 A**). After coating the microplate with free laccase or laccase-MNPs, BSA was used as a blocking protein to cover all the unsaturated binding sites in the microwell. Thereafter, a biotinylated anti-lac3 detection antibody was added to the microwell to bind the antigen (laccase); the complex was then recognized by an alkaline phosphatase enzyme (AP) conjugated streptavidin. The alkaline phosphatase enzyme catalyzes the transformation of the substrate *p*-Nitrophenyl Phosphate (PNPP)

to form a yellow water-soluble reaction product absorbing light at 405 nm therefore allowing the detection of the complex formation.

The entire process is depicted in the **Fig. III-2-15 B**. The colorimetric titration of product formation is typically in the range of low- to mid-picogram levels of antigen per well, so ELISA has a higher sensitivity compared to conventional methods. Also, the accuracy is higher since it involves the direct detection of immobilized laccase on the particles. Therefore, ELISA has great potentials for the enzyme loading measurement, since a small amount of enzyme can be detected and the experimental error can be reduced.

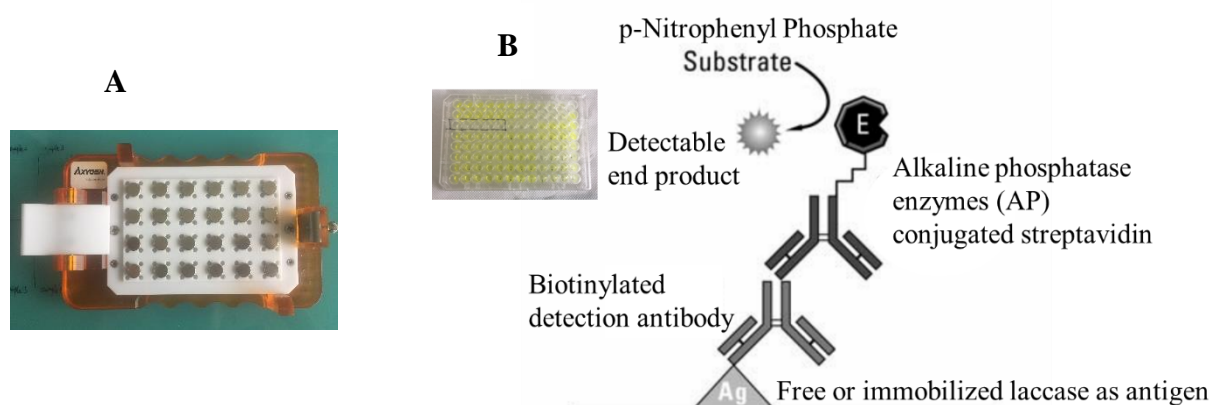


Fig. III-2-15 The special magnetic support used for MNPs manipulations on microplate (A) and the Schematic diagram of the mechanism of ELISA (B) (refer to the reference⁷ add notes according to the actual situation)

2.2.4.3 Effect of initial laccase concentration onto immobilized laccase activity

It is reported that the initial enzyme concentration has an important influence on the activity of the immobilized laccase. As the initial laccase concentration increases, the activity of the immobilized laccase increases first and then keep stable or slightly decreases. The reason is because when excessive enzymes concentration is present in the solution, enzyme conformation and diffusional limitations will occur due to the protein-protein interaction leading to multilayers or clusters of enzyme molecules formation at the surface of the support.⁸

Crutz *et al.* studied the immobilization of a lyophilized enzyme CALB (*Candida antarctica* lipase) adsorbed on fumed silica and put forward the following points. The catalytic activity of the immobilized CALB can be correlated into three regimes of surface loading (**Fig. III-2-16**). Region I: the enzyme conformation-controlled regime, the low surface coverage leads the enzyme molecules to maximize their contact with the surface. This event causes a variation in the native conformation and reduction of the catalytic activity. At intermediate surface coverage Region II: the presence of enzyme-enzyme interactions prevents excessive enzyme surface interactions and preserves active enzyme conformation. At high surface coverage region III, where the enzyme molecules are densely

packed in multi-layers on the surface, mass-transfer limitations are responsible for the reduction of the specific activity of the immobilized enzyme.

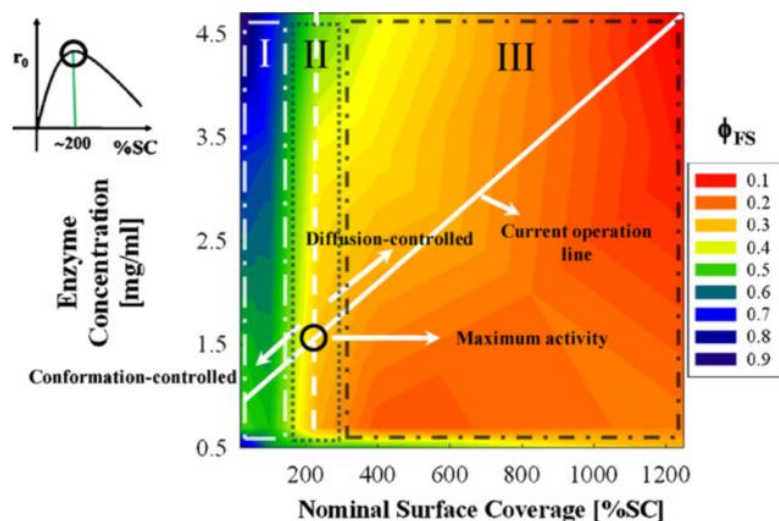


Fig. III-2-16 Regions of conformational stability for CALB/fumed silica adsorbates. The dotted vertical line at $\sim 200\%SC$ separates two different regions of conformational stability: region I delimited by a long-dash-dot line where adsorbates exhibit low conformational stability, and region III delimited by a short-dash-dot line where adsorbates have highly stable conformations. The presence of these two regions is likely to be responsible for the observed catalytic activity (r_0) of the lyophilized adsorbates in hexane (inset). The low catalytic activity observed at low %SC can be linked to region I. Even though the structure is well preserved in region III, multi-layer packing is likely responsible for diffusional limitations of catalysis. The maximum in activity between those two regions can be attributed to an optimal arrangement on the surface where the structure is relatively well maintained without excessive clustering (region II, delimited by a dotted line) ⁸

Therefore, to compare the effect of the oriented immobilization on the laccase activity, the maximum activity point should be found at first. One of the reasons is that: activity measurement at the maximum activity point is relatively accurate due to the high values (lower values will introduce higher experimental errors). Also, the conclusion related to the influence of the orientation will be more accurate, because of the influence of other factors such as the multilayer enzyme cluster that can be avoided at a maximum extent. Therefore, in this section, the relationship between the initial laccase concentration and the immobilized laccase activity will be first studied.

LAC3 was used as the model protein in these studies and the results are shown in the **Fig. III-2-17**. It can be seen from the figure that the relationship between the activity of the enzyme after immobilization and the initial enzyme concentration follow the above theory. That is, in the low concentration range, the activity of the enzyme after immobilization increases as the initial concentration increases, which is due to the increased number of immobilized enzymes. After, when the initial enzyme concentration exceeds a certain value, laccase activity keeps stable or slightly decrease because of the saturation of the MNP or by diffusional limitations caused by multilayer

formation. The maximum activity point of the grafted LAC3 is reached for 500 μ M initial concentration for the commercial aldehyde beads.

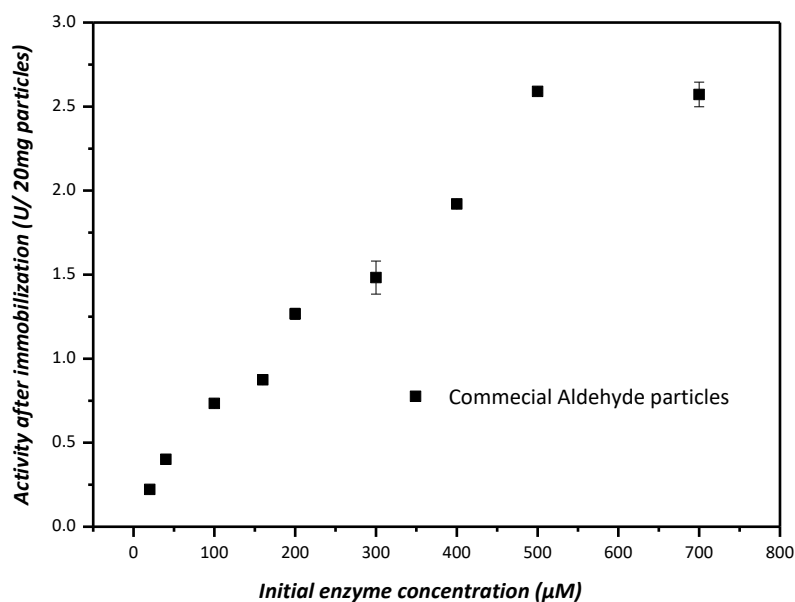


Fig. III-2-17 Relationship between the initial laccase concentration and the immobilized laccase activity for the commercial aldehyde particles. LAC3 was used as model protein. Particles concentration 2mg/mL. Reaction temperature: 30°C. Rotating speed: thermomixer 1000 rpm. The maximum activity point of the grafted LAC3 is reached for an initial enzyme concentration of 500 μ M.

2.2.5 Final results of C21 immobilization

After the major parameter was determined, three successive immobilizations were performed separately. The total concentration of particles and initial enzymes were 2 mg/mL and 500 μ M respectively. The final reaction volume was 200 μ L. The particles were washed 3 times by MQ water before immobilization. The enzymes were buffer changed for the coupling buffer in advance. The reaction mixture was incubated overnight (18~20 hours) in a thermomixer at 1000 rpm and 30°C. After incubation, the particles were washed 5-10 times with a storage buffer to remove unbound and non-covalently adsorbed laccase, then the immobilized particles were stored in the storage buffer for testing. The results of the final immobilizations are discussed in detail below.

2.2.5.1 Enzyme loading

Enzyme loading was tested by ELISA the principle of which is described above (refer to the Experimental Methods section of the appendix in this manuscript for the detailed protocols). The freshly produced UniK₁₆₁ (batch 2018.04) at a concentration of 6.4 mg/mL was diluted and used as standard enzyme for the calibration curve. Both the standard samples and the particle samples immobilized with different laccase were triplicated in the microwell respectively. For each

measurement, the corresponding number of bare particles was used as a blank control and different amounts (2 μ g and 1 μ g) of particles were used for verification.

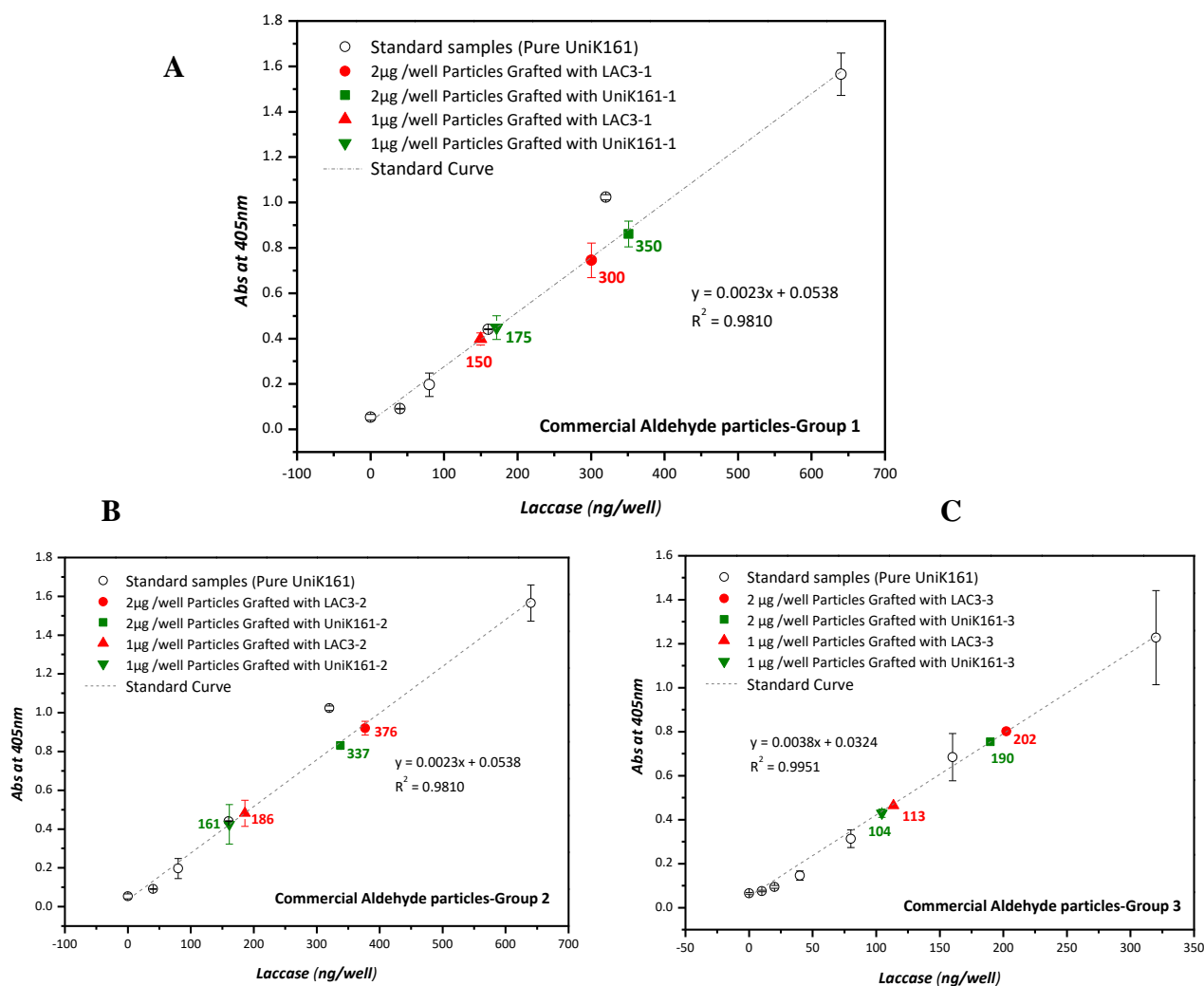


Fig. III-2-18 Enzyme loading tested by ELISA for the commercial aldehyde particles. Three groups of immobilizations (Group 1, 2 and 3 corresponds to A, B and C) were tested separately under the same conditions: particles concentration: 2mg/mL. Immobilization buffer: 50 mM phosphate contains 0.1M sodium formate, pH 7.4. Initial laccase concentration: 500 μ M. Total volume: 200 μ L. Ir catalyst: 10 eq[E]. Reaction temperature: 30 $^{\circ}$ C. Rotating on thermomixer at 1000rpm. 2 μ g and 1 μ g particles immobilized with different laccase were triplicated in the microwell respectively. Error bar were less than 11% for the immobilized samples.

The relationship between the absorbance of the end products at 405nm and the laccase concentration in each microwell is shown in **Fig. III-2-18**. It can be seen that the calibration curves have good linearity and the absorbance of the samples are all located at the middle of the curve, so the results were considered as reliable. It is also indicated that the amounts of particles used in this test is suitable. Higher or lower number of particles would cause deviations of the results from the central region, which may introduce errors. Also it is worth mentioning that the bare particles have only a small absorbance (\sim 0.065 AU), which is almost equivalent to the absorbance value of the

standard sample at concentration 0, suggesting that the particles themselves do not interfere with the measurement process.

According to the calculations, for the first group of immobilizations, the quantities of LAC3 and UniK161 immobilized on 2 μ g particles were 300 and 350 ng respectively, with a standard deviation of 10.2% for LAC3 and 6.6% for UniK161. The reliability of the results and the repeatability of the method were verified by using 1 μ g of particles for the enzyme loading test. It can be seen from the figure that as the number of particles added to each microwells decreased, the measured amounts for both laccases decreased proportionally to 150 and 175 ng respectively, with a standard deviation of 6.7% for LAC3 and 11.6% for UniK₁₆₁. This trend was similar for the second and third immobilizations. The fact that the amount of enzyme immobilized in the third group of MNPs was slightly smaller than that of the first two groups may be caused by the heterogeneous nature of the magnetic nanoparticles. These reproducible results indicate that the measure of the enzyme loading by ELISA is reliable.

The enzyme loading of each immobilization was calculated as the average value of the measurements with different amounts of particles. The calculated enzyme loading is displayed in **Table III-2-4**. It can be seen that for LAC3, the enzyme loadings of the three groups of immobilizations are 150, 187, 107 μ g laccase per mg particles respectively, and for UniK₁₆₁, the enzyme loadings are 175, 165, 100 μ g laccase per mg particles respectively. The difference in enzyme loading between the two laccases as well as among the three groups of immobilizations are small. Deviations may result from the heterogeneous nature of the support materials.

Table III-2-4 Enzyme loading calculations for commercial aldehyde particles immobilization

Samples	Particles used (μ g/well)	Enzyme loaded (ng/well)	Enzyme Loading (μ g/mg)	Average enzyme Loading (μ g/mg)	STEDV
C21 immobilized LAC3-1	2	300	150	150	0.00
	1	150	150		
C21 immobilized UniK161-1	2	350	175	175	0.00
	1	175	175		
C21 immobilized LAC3-2	2	376	188	187	1.41
	1	186	186		
C21 immobilized UniK161-2	2	337	169	165	5.30
	1	161	161		
C21 immobilized LAC3-3	2	202	101	107	8.49
	1	113	113		
C21 immobilized UniK161-3	2	190	95	100	6.36
	1	104	104		

2.2.5.2 Activity and Specific Activity of free and immobilized laccase towards ABTS

Activity of the free and immobilized laccase were determined against ABTS substrate at 30°C in a medium of 0.1 M of Acetate buffer pH 5.5. Formation of the green ABTS radicals cation ($\text{ABTS}^{\bullet+}$) were detected by following the absorbance at 420 nm ($\epsilon=36000 \text{ mol}^{-1}\cdot\text{cm}^{-1}$, calculation factor 27.8) for 2 min using a spectrophotometer (Carry 60, Varian). For the measurement of the free laccase activity, 10 μL of the appropriately diluted enzyme samples was added into 890 μL of 0.1 M of Acetate buffer pH 5.5 at 30°C, and the enzymatic reactions was started by adding 100 μL ABTS solutions (50 mM) into the reaction mixture (1mL in the visible cuvette). For the determination of the immobilized laccase activity, the reaction contains 10 μL of the immobilized laccase containing MNPs (20 μg of particles for 2 mg/ml concentration), 890 μL of 0.1 M Acetate buffer pH 5.5 (heated to 30°C by water bath), and 100 μL ABTS solutions (50 mM). The amount of laccase oxidizing one micromole of substrate per minute was defined as one unit (U). All the experiments were carried out as triplicates and all the results are obtained as average of triplicate experiments.

The activity of laccase after immobilization is shown in **Fig. III-2-19**. For all the three groups of experiments, the immobilized LAC3 demonstrated a higher activity than the immobilized UniK₁₆₁. This difference can be caused either by the effect of the orientation or by the variation of the amount of laccase immobilized per mg particles.

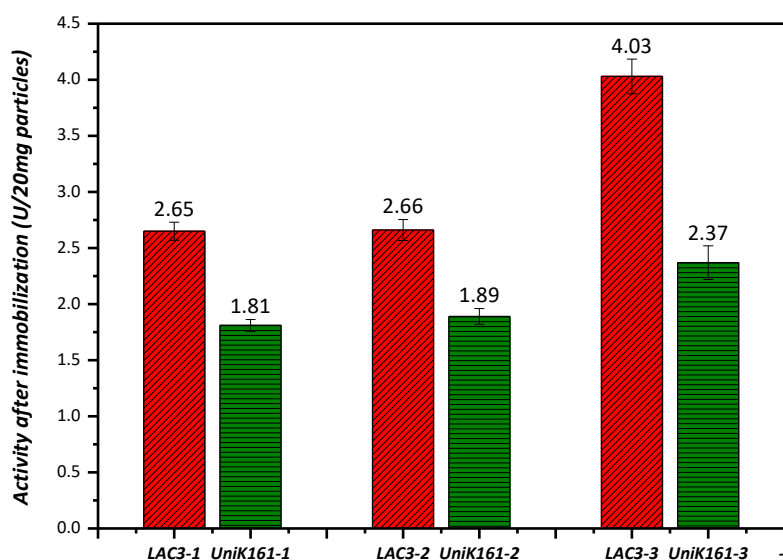


Fig. III-2-19 Activity of commercial aldehyde particles immobilized laccase towards ABTS, at pH 5.57, 30°C.

So, in order to investigate the effect of orientation, the Specific Activity (SA, activity normalized to U per mg enzymes) of the free and immobilized laccase were calculated based on the enzyme loading measured in section 2.2.5.1. The calculation formula is shown below:

$$\text{Specific Activity} = \frac{\text{Activity (U/20mg particles)} \times 1000}{\text{Enzyme loading (\mu g/mg particles)} \times 20}$$

The calculated results are shown in **Table III-2-5**. After immobilization, SA of laccase decreased dramatically compared with the free enzymes, more than 200 times decrease at the maximum extent (C21 immobilized UniK₁₆₁-2). This can be explained by the mass transfer limitations (reduced accessibility of the substrate to the catalytic active center) or the deleterious conformational changes of the protein (loss of the enzyme dynamic properties and/or alteration of the conformational integrity of the enzyme) during covalent binding. Immobilization causes the enzyme molecule to interface with a molecular environment that can be very different from what it has in its native state, which could have an effect on the catalytic activity.

To determine the effect of immobilization directions on the laccase activity, the ratio of the SA of LAC3 and UniK₁₆₁ was calculated as a criterion. It can be seen that before immobilization, the ratio is 0.82 since UniK₁₆₁ has a slightly higher specific activity (111 U/mg) than LAC3 (91 U/mg). After immobilization, a reversed LAC3/UniK₁₆₁ ratio was observed for all the three groups of immobilizations corresponding to a LAC3 with an apparent higher catalytic efficiency than UniK₁₆₁ (**Table III-2-5**). Since mass-transfer limitations caused by an over loading of enzyme or an inaccurate enzyme loading are excluded such an evolution of the LAC3/UniK₁₆₁ ratio can be attributed to the oriented immobilization of the enzyme at the particle surface.

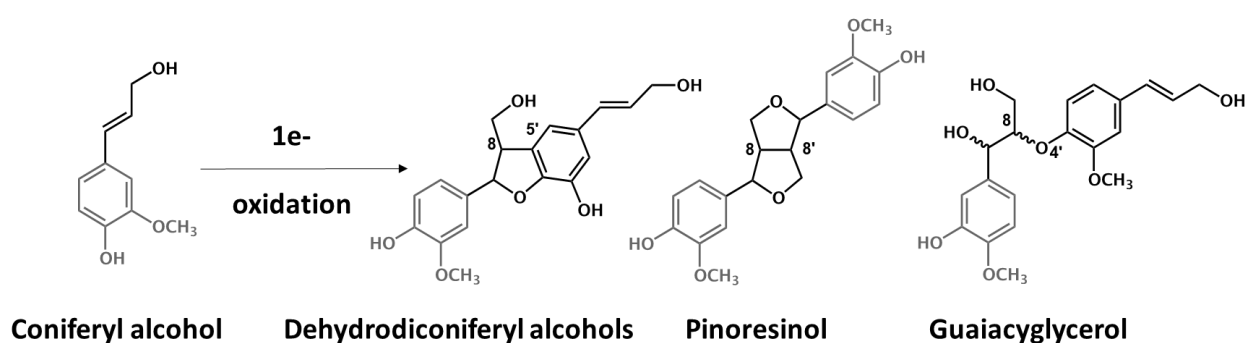
It can be considered that the oriented immobilization modifies the SA ratio of LAC3 and UniK₁₆₁ from 0.8 to 1.5 (the average ratio of the three immobilizations), confirming the influence of the oriented immobilization on the activity of laccase. In UniK₁₆₁, the particles are grafted in such a way that the T1 is located close to the particles surface. Thus, a substrate reaching the active site could be constrained by the particles surface, therefore limiting the activity of the laccase.

Table III-2-5 Specific Activity of free and immobilized laccase for commercial aldehyde particles

Commercial Aldehyde Particles (C21)	Enzyme Loading ($\mu\text{g}/\text{mg}$)	Activity after Graft (ABTS; U/20mg grafted particles)	Specific Activity (ABTS; U/mg laccase)	Ratio of SA: (LAC3/UniK161)
Free LAC3	--	--	91	0.82
Free UniK161	--	--	111	
LAC3-1	150	2.65	0.883	1.70
UniK161-1	175	1.82	0.520	
LAC3-2	187	2.66	0.711	1.23
UniK161-2	165	1.89	0.576	
LAC3-3	107	4.04	1.888	1.58
UniK161-3	99	2.37	1.197	
Average ratio of SA after immobilization (LAC3/UniK₁₆₁):				1.50

2.2.5.3 Coniferyl alcohol biotransformation with immobilized laccase

We showed that the directional immobilization of laccase on MNPs has an influence on the activity of laccase with ABTS as substrate. However, will this effect be observed in the reaction of the laccase with other substrates? This is an issue worth to verify. From Chapter II we know that the laccase LAC3 (as well as UNIK₁₆₁) oxidizes coniferyl alcohol (CA) into coniferyl alcohol radicals (CA \cdot), then these radicals undergo random coupling to form a mixture of products. Here, this well-studied molecule was examined as substrate for oriented immobilized laccase. When studying laccase activity with ABTS as substrate, only changes in ABTS radicals were monitored, while during the oxidation of CA by laccase, what was traced for activity measurement are not radicals but the coupling products (**Fig. III-2-20**).

**Fig. III-2-20** Oxidation of Coniferyl alcohol and the coupling products

Oxidation of coniferyl alcohol catalyzed by free and immobilized laccase was carried out in a 2 ml centrifuge tubes. All experiments were performed in 0.1 M acetate buffer, pH 5.5. The final concentration of CA is 1.6mM, the amount of laccase used depends on the specific experiment (generally 1U/L as measured with ABTS). Thermomixer was used for the incubation at a temperature of 30 °C and 1000 rpm. Samples were taken out at given time points and the reaction was stopped

by addition (ratio 1:1) of an acetonitrile solution of benzophenone to serve as internal reference for HPLC. CA oxidation products were separated and tested by reverse-phase HPLC on a RP-18 column. For immobilized laccase samples, particles were discarded by magnetic separation prior injection on the HPLC column for analysis.

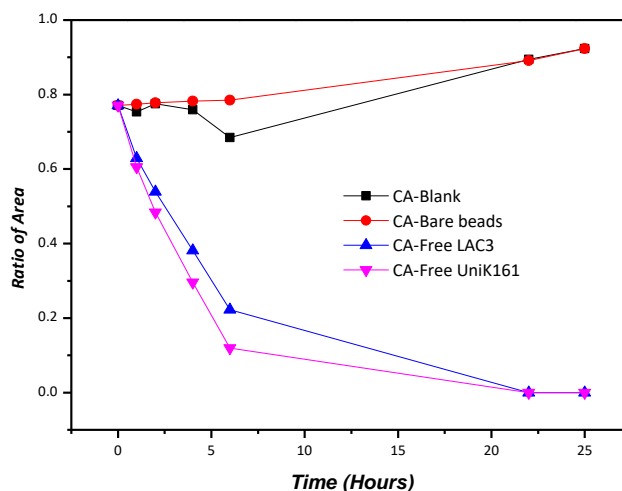


Fig. III-2-21 Control experiments of coniferyl alcohol biotransformation. The control samples contain: 1.6 mM CA only(blank); 1.6 mM CA solutions added with a final concentration of 1 mg/mL bare particles; 1.6 mM CA plus free laccase (LAC3 or UniK₁₆₁, final 1U/L tested by ABTS). Experiments were incubated in 0.1M pH=5,7 acetate buffer, at 30°C in a thermomixer at 1000rpm, for maximum 25 hours, in a final volume of 500μL. The ordinate is the ratio of the area of the peak corresponding to the reactant on the HPLC chromatogram to the area of the peak corresponding to the benzophenone reference.

Control experiments were performed first (**Fig. III-2-21**). The first control sample contained only CA (1.6 mM in 0.1M acetate buffer pH 5.5). It can be seen that the CA level barely changed within 25 hours of incubation. The second control sample is the CA substrate solutions (1.6 mM) supplemented with a final concentration of 1 mg/mL of bare particles. Almost no change is observable as compared to the results of CA only, indicating that the bare particles have no effect on the oxidation of CA. In the third control, 1.6 mM CA was reacted with free laccase (LAC3 or UniK₁₆₁, at 1U/L final tested by ABTS). CA consumption appears slightly faster when catalyzed by UniK₁₆₁ than catalyzed by the same amount (and also the same ABTS activity, since the ratio of the SA of the two laccases is near 1) of LAC3. This difference, not seen for ABTS, might be due to the mutation R₁₆₁->K found in UniK₁₆₁. Indeed, it seems that position 161 is located in an area that may interact with phenolic substrates and not with ABTS.⁹

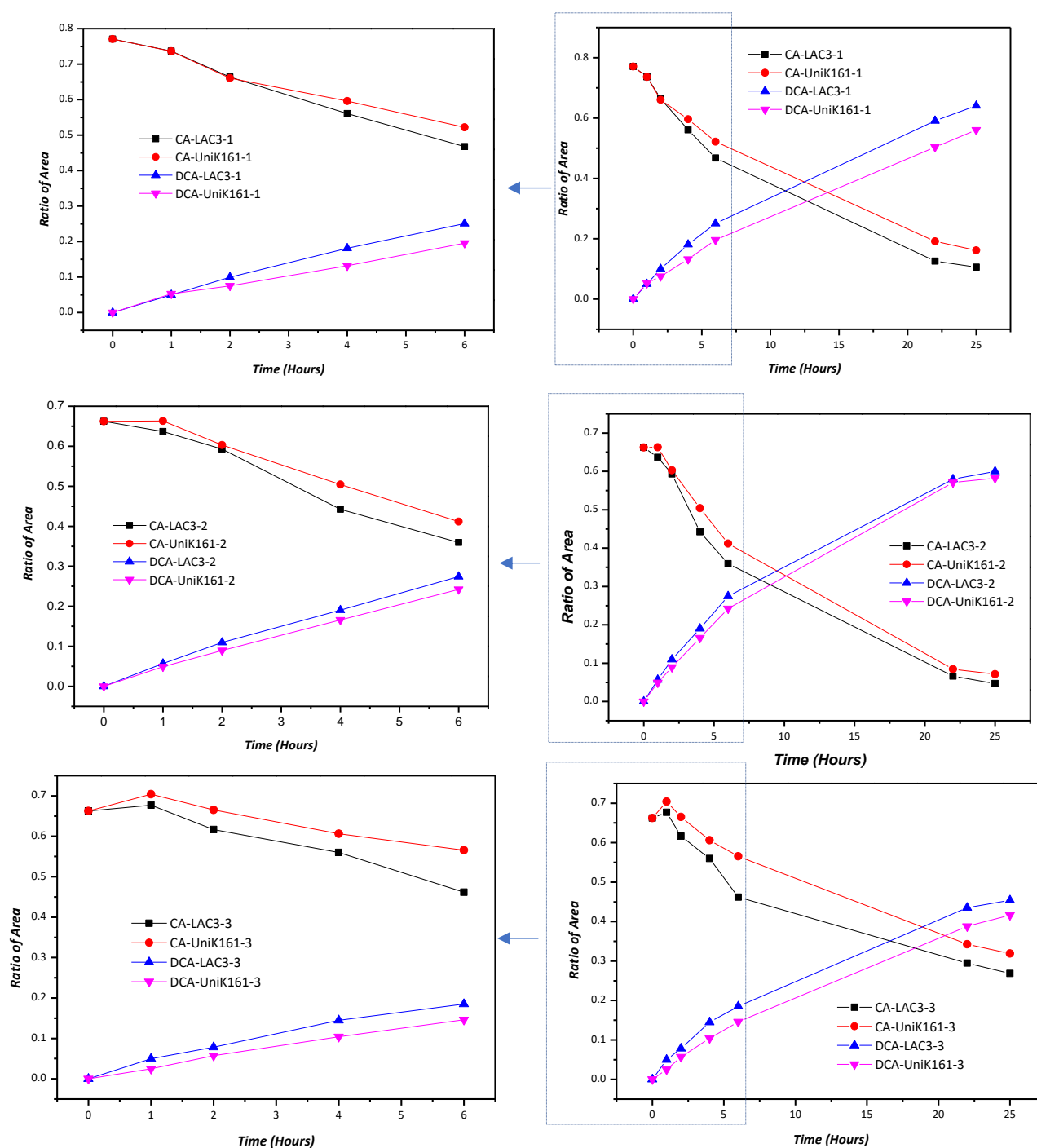


Fig. III-2-22 Oxidation of coniferyl alcohol catalyzed by immobilized laccases. Experiments were incubated in 0.1M pH=5,5 Acetate buffer, at 30°C in a thermomixer at 1000rpm, for maximum 25 hours, in a final volume of 500 μ L and CA concentration of 1.6 mM. The ordinate is the ratio of the area of the peak corresponding to the reactant on the HPLC chromatogram to the area of the peak corresponding to the reference benzophenone. Three groups of immobilized laccases were tested and the amount of laccase used is as follows: Group 1: 554 ng immobilized enzyme; Group 2: 695 ng immobilized enzyme; Group 3: 250 ng immobilized enzyme in the total reaction system. CA: coniferyl alcohol; DCA: dehydroconiferyl alcohol.

Then the oxidation of CA was carried out by immobilized laccases (three independent graftings) under the same conditions as control experiments. Consumption of the substrate coniferyl alcohol (CA) and production of the major product dehydroconiferyl alcohols (DCA) over time are seen on **Fig. III-2-22**.

Note that in order to better monitor the formation of dimer products and avoid polymerization, the amount of laccase was maintained as low as 1 U/L (ABTS activity) on purpose. At this laccase concentration, a 25-h window allows comparing the consumption of 1.6 mM substrate by the two immobilized enzymes LAC3 and UniK₁₆₁.

As can be seen from the figures, the difference in enzyme efficiency between the immobilized LAC3 and the immobilized UniK₁₆₁ is rather small, appearing only after 6 hours of reaction. However, as this trend is reproduced in the three independent experiments, we performed it seems to be significant. This result is the opposite of that obtained in the control experiments in which CA was oxidized by free laccase. In addition to the synthetic substrate ABTS, this inversion of efficiency points out that the effect of directional immobilization of the laccase on its activity is observable with phenolic substrates like CA as well.

Table III-2-6 Normalized value of the consumed substrate [(initial CA area/benzo area) – (remaining CA area/benzo area)] of the free and immobilized laccase at the 6th hours. Area represent the peak area on the HPLC chromatogram

Commercial Aldehyde Particles (C21)	Consumed substrate [(initial CA area/benzo area) – (remaining CA area/benzo area)]	Amount of Laccase (ng)	Consumed substrate /Amount of Laccase (1/mg)	Ratio* of LAC3/UniK161
Free LAC3	0.548	6.8	80603	0.87
Free UniK161	0.652	7.0	93074	
LAC3-1	0.303	554	547	1.22
UniK161-1	0.249	554	449	
LAC3-2	0.303	695	436	1.21
UniK161-2	0.251	695	361	
LAC3-3	0.201	250	803	2.07
UniK161-3	0.097	250	387	
Average Ratio* after immobilization (LAC3/UniK₁₆₁):				1.50

A LAC3/UniK₁₆₁ ratio (Ratio^{*}) can be defined as quantitatively express the effect of the oriented immobilization on the oxidative properties of laccase. First, because the area of a peak on the HPLC chromatogram is proportional to the amount of the compound that is present, so the ratio of CA/benzophenone on the HPLC chromatogram can be regarded as the amount of substrate left in the reaction mixture. Second, according to the calculation of the first point, after a period of reaction, the amount of residual substrate in the reactions respectively catalyzed by LAC3 and UniK₁₆₁ is calculated. Then, the amount of residual substrate is normalized to each unit of enzyme by dividing the amount of laccase used. And the normalized values can be regarded as Specific Activity (SA) of laccase towards coniferyl alcohol. Eventually, the SA ratio (Ratio^{*}) of the two enzymes represents the relative efficiency of the two enzymes.

Calculations of the Ratio^{*} after oxidation of 6 hours are found in **Table III-2-6**. It can be seen that: with the free laccases systems, the Ratio^{*} is 0.87, meaning that the amount of substrate consumed in the reaction mixture after reaction 6 hours with free UniK₁₆₁ is slightly higher than that with free LAC3. While, in the immobilized laccase oxidation system, the Ratio^{*} is climb to 1.5 (mean value), which is about 2 times of that for free laccase. This difference between the two systems (free vs grafted) is consistent with what we observed with ABTS as substrate. More importantly, it illustrates a similar behavior of the immobilized enzymes regarding synthetic and phenolic substrates. It seems indeed that bringing the oxidation center at the interface between the enzyme and the MNP bead surfaces (in the case of UniK₁₆₁) reduces ABTS as well as CA oxidation.

2.3 Conclusions

In this subsection, commercial aldehyde particles were used as support materials to study the influence of oriented immobilization on the activity of laccase. Two substrates (ABTS and Coniferyl alcohol) were studied to achieve this goal. From the study of these two substrates, it is concluded that the immobilization near the active site (in the case of UniK₁₆₁) and the immobilization far away from the active site (in the case of LAC3) can be differentiated on the basis of the activity of laccase.

For ABTS, the ratio of the specific activities of LAC3 and UniK₁₆₁ is increased from 0.82 before immobilization to 1.5 after immobilization. This clearly supports an inhibitory effect on ABTS oxidation when bringing the oxidation site close to the aldehyde functionalization layer. For coniferyl alcohol, a similar trend is observed: the ratio of the specific activities of LAC3 and UniK₁₆₁ as immobilized enzymes is about 2 times greater (1.5) than that as free enzymes (0.87). This supports that the aldehyde functionalization layer nearby the enzyme's oxidation site is also affecting the phenolic substrate oxidation. Therefore, bringing the enzyme's oxidation site at the interface with

the particle's functional shell leads apparently to a global decrease of the activity that could be reasonably associated to a physical limitation (hindrance) to access the active site.

Although modestly, orientation of the enzyme during immobilization affects laccase activity. Is this universal? In other words, will it be observed when other particles are used as carriers? To what extend? Can it be used to modulate the activity? In order to answer these questions, custom-made aromatic aldehyde particles were used for immobilization experiments, under the same experimental conditions as the commercial aliphatic aldehyde ones.

3 Custom-made aldehyde particles (H23) immobilization

3.1 Information of the custom-made aldehyde particles

The custom-made aldehyde particles (MNPs $g\text{-Fe}_2\text{O}_3\text{@SiO}_2\text{@Lin-CHO}$, number as H23) were synthesized by Hongtao Ji a PhD student working under the supervision of Dr. Karine Heuzé from the University of Bordeaux. Compared to the commercial aldehyde particles previously used in chapter III section 2, although the shells of H23 is also coated with silica, this silica is not linked to the aldehyde group by a 21 carbon long aliphatic linker, but attached via an aromatic core (**Fig. III-3-1**).

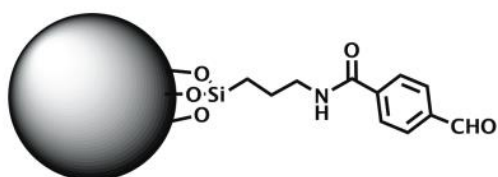


Fig. III-3-1 Schematic diagram of custom-made aldehyde particles H23

In the report of Jesse M. McFarland and Matthew B. Francis in which numerous aldehydes have been screened for immobilization on lysozyme (which has six lysines), the conclusion is that simple alkyl aldehydes generally exhibit lower levels of reactivity, while substrates possessing aromatic groups afford higher levels of product conversion. This is likely due to the enhanced stability of the imine intermediates arising from hydrophobic interactions between these groups and the proteins and/or catalyst.² So, aromatic aldehyde particles were synthesized and investigated here with the expectation that higher difference in activities could be observed between different orientations the enzyme through its immobilization.

Because aldehyde is still used as the surface functional group in H23, the immobilization reaction (reductive alkylation) is the same as the one used with the commercial particles (introduced in details in the previous section, chapter III section 2.1). Since most of the experimental conditions (including the preparation of particle suspensions, the measurement of enzyme loadings) were established for the commercial aldehyde particles, the content of the study in this section will be simplified. Only the initial enzyme concentration was examined prior to the formal immobilization. The rest of the parameters are referred to the conditions used for C21 immobilization: the reaction was carried out in a thermomixer at 30°C with a rotating speed of 1000 rpm, the concentration of the particles was 2 mg/ml, final volume 200µL; Iridium catalyst used equals 10 times the enzyme concentration (for the detailed protocol, please refer to Experimental Methods section in this manuscript).

3.2 Results and discussion

3.2.1 Relationship between initial laccase and activity

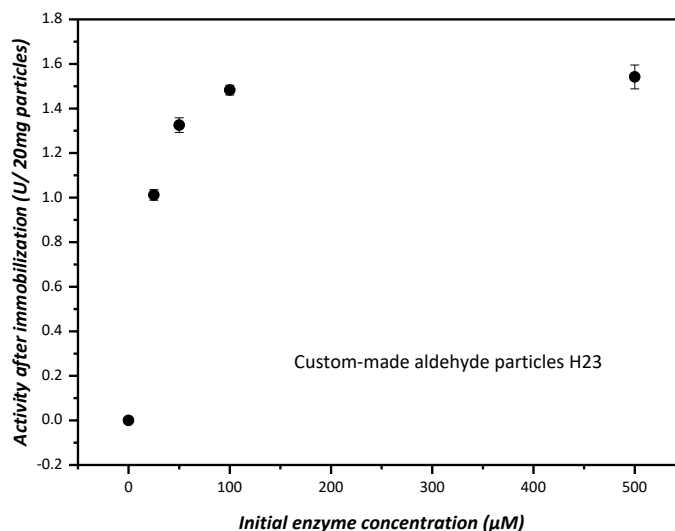


Fig. III-3-2 Relationship between the initial laccase concentration and the immobilized laccase activity for the custom-made aldehyde particles H23. LAC3 was used as model protein in these cases. Particles concentration 2mg/mL. Reaction temperature: 30°C. Rotating speed: thermomixer 1000 rpm. The maximum activity point for the grafted LAC3 appears for an initial enzyme concentration of 100 μM .

As previously demonstrated, the initial concentration of laccase is a very important factor influencing laccase activity after immobilization. Because the initial laccase concentration affects the enzyme loading which in turn could influence the enzyme activity due to diffusional limitations or conformation changes when a multilayer of enzyme occurs. In order to be able to compare the effect of the orientation on laccase activity, the influence of other factors should be avoided. So, the concentration contributing to the maximum activity of immobilized laccase should be set as the concentration in the immobilization experiments.

The relationship between the initial laccase concentration and the immobilized laccase activity was studied using LAC3 as the model protein (**Fig. III-3-2**). UniK₁₆₁ immobilization is considered to have the same consequence as for LAC3, as the two enzymes are actually the same laccase (but for position 161), and it has been confirmed that site-directed mutagenesis has no effect on the specific activity of the laccase (at least on ABTS).¹ It can be seen that in the low concentration range, the activity of the immobilized enzyme increases as the initial concentration of laccase increases, this is likely due to the increased enzyme loading. After the initial enzyme concentration exceeds a certain value, laccase activity is stable or slightly reduced as a result of saturation or due to diffusional limitations caused by the formation of a multilayer of enzymes. Altogether, the relationship between the initial enzyme concentration and the activity of the immobilized enzyme is similar to the picture

obtained for the commercial aldehyde particles. The maximum activity point of the H23 grafted LAC3 particles is appearing at the initial enzyme concentration of 100 μ M. Therefore, in the following immobilization experiments on H23 particles, the initial laccase concentration was set to this value.

3.2.2 Enzyme loading

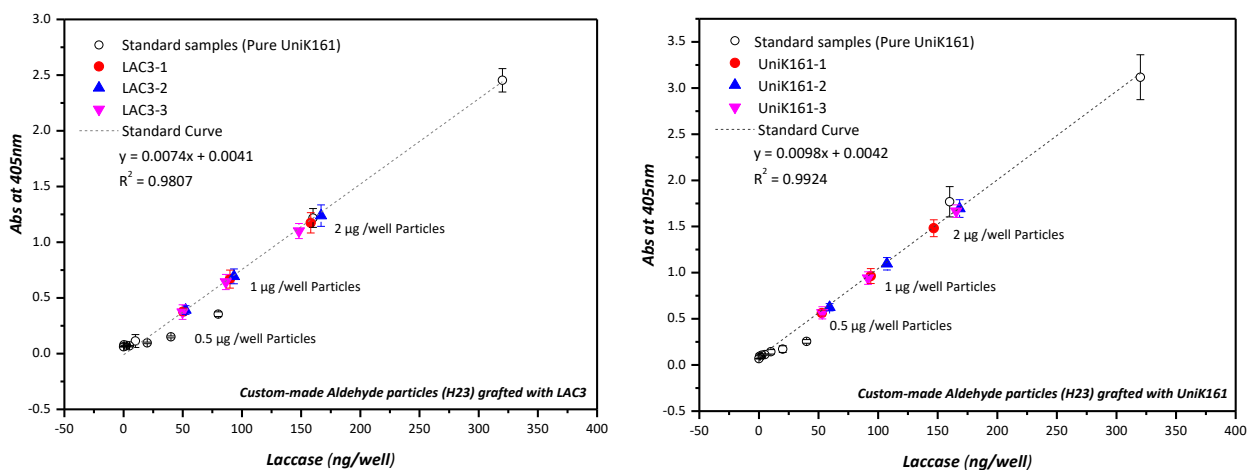


Fig. III-3-3 Enzyme loading tested by ELISA for the custom-made aldehyde particles. Three independent immobilizations were performed separately under the same conditions: particles concentration: 2mg/mL, immobilization buffer: 50 mM phosphate contains 0.1M sodium formate, pH 7.4. Initial laccase concentration: 100 μ M. Total system volume: 200 μ L. Ir catalyst: 10 eq [E]. Reaction temperature: 30 $^{\circ}$ C. Thermomixer rotation set at 1000rpm. 2 μ g, 1 μ g and 0.5 μ g particles immobilized with different laccase were triplicated in the microwell for measurements. The points on the graph are representing the average value of the triplicate tests in the microwell. A and B are the enzyme loading of LAC3 and UniK₁₆₁ respectively. Error bar were less than 12% for the immobilized samples.

As before, three independent immobilizations were performed. For each group, enzyme loading was tested by ELISA following the procedure described previously (refer to the Experimental Methods section of the appendix in this manuscript for the detailed protocols). Dilutions of the freshly produced UniK₁₆₁ (batch 2018.04) were used for establishing calibration curves. For each immobilization, different amounts (2 μ g, 1 μ g and 0.5 μ g) of particles were used for verification, and the corresponding amount of bare particles was used as a blank control. Both the standard samples and the particle samples (particles immobilized with different laccase) were tested in triplicate in microplates. Results are displayed in **Fig. III-3-3**.

From the figure, it can be seen that: first, calibration curves have good linearity and samples values are all located within the working range of the curve. Therefore, the results are considered to be reliable. Second, regarding the enzyme loading, only small variations among the three independent immobilizations were observed. Therefore, it can be considered that the immobilization

experiment is stable and repeatable. Also, for both laccases, the enzyme loading represented by the absorbance value is basically at the same level.

The detected absorbance value increased with the increase of the particle amount, the two being proportionally linked. As it has been confirmed that the particles have no effect on the absorbance (Chapter III section 2.2.5.1), this increase is a result of an increased amount of enzyme immobilized onto the particles. Incidentally, this highlights that laccase is successfully immobilized on the particles.

Table III-3-1 Enzyme loading calculations for self-produced aldehyde particles immobilization

Samples	Particles used ($\mu\text{g}/\text{well}$)	Enzyme loaded (ng/well)	Enzyme Loading ($\mu\text{g}/\text{mg}$)	Average enzyme Loading ($\mu\text{g}/\text{mg}$)	STEDV
H23 immobilized LAC3-1	2	158	79	90	10.50 (12%)
	1	90	90		
	0.5	50	100		
H23 immobilized UniK161-1	2	147	74	91	16.43 (18%)
	1	94	94		
	0.5	53	106		
H23 immobilized LAC3-2	2	167	84	94	10.26 (11%)
	1	93	93		
	0.5	52	104		
H23 immobilized UniK161-2	2	168	84	103	17.35 (17%)
	1	107	107		
	0.5	59	118		
H23 immobilized LAC3-3	2	148	74	87	13.01 (15%)
	1	86	86		
	0.5	50	100		
H23 immobilized UniK161-3	2	166	83	94	11.59 (12%)
	1	92	92		
	0.5	53	106		

The calculation of the enzyme loading is presented in **Table III-3-1**. Variations in enzyme loading from different particle amounts are within a range of 11-18 % (the last column in the table). This deviation may be caused by the agglomeration of the particles during the measurement and the heterogeneity of the particles. So, to minimize errors, the average value of the measurements with different amounts of particles was taken as the enzyme loading for each grafted particle.

For LAC3 and UniK₁₆₁, enzyme loadings for the three immobilizations are respectively 90, 94, 87 μg and 91, 103, 94 μg of laccase per mg particles. The difference in enzyme loading between the two laccases are small. As already mentioned, the moderate deviation observed could result from the heterogeneous nature of the supporter materials.

3.2.3 Activity and Specific Activity evaluation of free and immobilized laccase towards ABTS

The measurement of the activity and the calculation of the specific activity were carried out as described in chapter III section 2.2.5.2. The activity of immobilized laccases is shown in **Fig. III-3-4**. For all the three immobilization sets, LAC3 demonstrated a higher activity than its UniK₁₆₁ counterpart. The observed difference between the two immobilized enzymes (more than 2 times) is larger than when using commercial aldehyde particles.

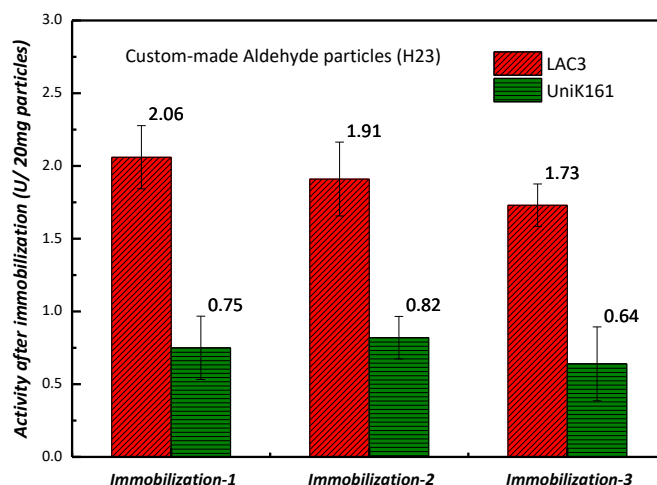


Fig. III-3-4 Activity of self-produced aldehyde particles immobilized laccase towards ABTS, at pH 5.5, 30°C

Calculated specific activities (activity normalized to U per mg enzymes) for free and immobilized laccases are shown in **Table III-3-2**. Influenced by mass transfer restrictions and potential deleterious conformational changes of the protein during covalent immobilization, the specific activity of immobilized laccase is decreased dramatically compared to the free enzymes (more than 200 times decrease at the maximum extent for UniK₁₆₁-3. This decline is consistent with the results obtained for commercial aldehyde particle immobilization.

The effect of orientation on laccase activity is evaluated through the comparison of the ratios of specific activities of LAC3 and UniK₁₆₁. It can be seen that prior immobilization, the ratio of the specific activity of the two enzymes is about 1, meaning that free LAC3 and UniK₁₆₁ have the same efficiency towards ABTS substrate. However, after immobilization, the ratio changed to above 2.5 for all the three independent immobilizations, indicating that, as expected, LAC3 has a higher catalytic efficiency on ABTS than UniK₁₆₁ in their immobilized forms. Since most of the other factor (over-loading caused mass-transfer limitations, inaccurate enzyme loading) are excluded, such changes can be attributed to be resulting from the orientation of the enzyme.

Table III-3-2 Specific Activity of free and immobilized laccase for self-produced aldehyde particles (H23)

Custom-made Aldehyde Particles (H23)	Enzyme Loading ($\mu\text{g}/\text{mg}$)	Activity after Graft (ABTS; U/20mg grafted particles)	Specific Activity (ABTS; U/mg laccase)	Ratio of SA: (LAC3/UniK161)
Free LAC3	--	--	73	1.03
Free UniK161	--	--	71	
LAC3-1	90	2.06	1.144	2.78
UniK161-1	91	0.75	0.412	2.55
LAC3-2	94	1.91	1.016	
UniK161-2	103	0.82	0.398	2.92
LAC3-3	87	1.73	0.994	
UniK161-3	94	0.64	0.340	
Average ratio of SA after immobilization (LAC3/UniK₁₆₁):				2.75

The effect of the orientation on laccase activity is marked here when using the custom-made aldehyde particles as support materials. Indeed, specific activities ratios of LAC3/UniK₁₆₁ are varying from 1.03 to 2.75 (the average ratio of the three immobilizations), a window significantly larger than that obtained with the commercial C21 particles (0.8 to 1.5). Since the grafting function (i.e. aldehyde) is identical for the two particles, this increased effect (almost a factor 2) could be a consequence of either the nature of the linker (aliphatic for C21, aromatic for H23) or its length more or less removing the enzyme away from the silica shell or a combination of these two parameters.

3.2.4 Coniferyl alcohol biotransformation with H23 immobilized laccase

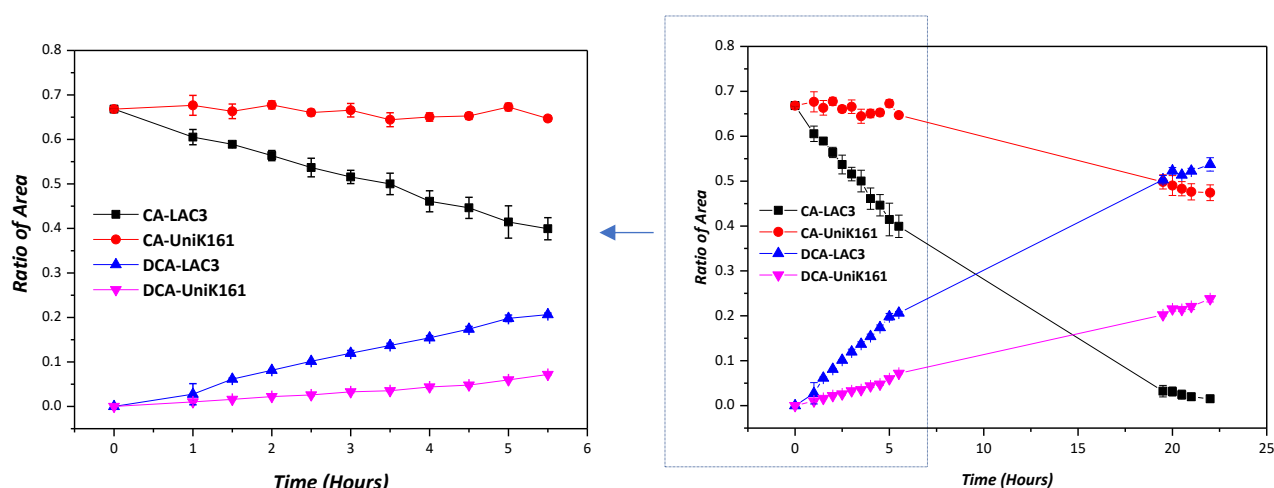


Fig. III-3-5 Oxidation of coniferyl alcohol catalyzed by immobilized laccases. The experiments were performed in 0.1M pH=5.5 Acetate buffer, at 30°C in a thermomixer set at 1000rpm, for maximum 22 hours, in a final volume of 500 μL and CA concentration of 1.6mM, 340 ng immobilized enzyme. The ordinate is the ratio of the area of the peak corresponding to the reactant on the HPLC chromatogram to the area of the peak corresponding to the reference benzophenone.

Oxidation of CA by laccases immobilized on H23 particles was carried out under the same conditions with the C21 immobilized laccases (chapter III section 2.2.5.3). The consumption of the substrate coniferyl alcohol (CA) and the production of the major product dehydroconiferyl alcohols (DCA) as function of time are shown in **Fig. III-3-5**. A pronounced difference in enzyme efficiency between the immobilized LAC3 and the immobilized UniK₁₆₁ was observed, LAC3 exhibiting a markedly higher efficiency than UniK₁₆₁ throughout the whole oxidation process. The fast substrate consumption and major products generation rates were opposite to those in the control experiments. Overall, similar to the results obtained with C21 particles (activity affected by a directional immobilization), it should be noted that the difference between the two opposite orientations is here particularly exacerbated.

Table III-3-3 Normalized value of the consumed substrate [(initial CA area/benzo area) – (remaining CA area/benzo area)] of the free and immobilized laccase at the 6th hours. Area represent the peak area on the HPLC chromatogram

Self-Produced Aldehyde Particles (H23)	Consumed substrate [(initial CA area/benzo area) – (remaining CA area/benzo area)]	Amount of Laccase (ng)	Consumed substrate /Amount of Laccase (1/mg)	Ratio* of LAC3/UniK161
Free LAC3	0.548	6.8	80603	0.87
Free UniK ₁₆₁	0.652	7.0	93074	
LAC3-Immobilized	0.288	340	848	12.4
UniK ₁₆₁ -Immobilized	0.023	340	68	

Calculation of the defined ratio (Ratio*, refer to chapter III section 2.2.5.3) after oxidation at 6 hours are shown in **Table III-3-3**. As described previously, the ratio poises the relative values of the substrate remaining in the mixture of the reaction during the oxidation by LAC3 and UniK₁₆₁ respectively.

From 0.87 with the the free laccases systems, the Ratio* climbs to 12.4 with the immobilized laccases systems. The evolution observed here is consequent and reflects a real difficulty of the UNIK₁₆₁-H23 system for the oxidation of the phenolic substrate. Consequently, if bringing the oxidation center at the interface between the enzyme and the MNP bead surfaces reduces both ABTS and CA oxidation, the bias observed towards CA oxidation suggests that, from the grafted C21 and to the grafted H23, the system acquired some selectivity through the orientation of the enzyme and through the modulation of the functional layer. One plausible explanation for this drastic change may reside in the aroma-linked portion of the custom-made particle: closely resembling to the laccase substrate phenol, a free grafting function could occupy the oxidation site acting as an inhibitor.

3.3 Conclusions

Custom-made aromatic aldehyde particles were used as support materials to study the influence of orientation on the activity of immobilized laccases. As already done for commercial aliphatic aldehyde particles the oxidation of two substrates (ABTS and coniferyl alcohol) was studied.

For ABTS, the ratio of LAC3 and UniK₁₆₁ specific activities is increased from 1.03 before immobilization to 2.75 after immobilization. For coniferyl alcohol, the ratio of LAC3 and UniK₁₆₁ specific activities for the free laccases is increased from 0.87 before immobilization to 12.4 after immobilization, about 15 times greater than that of free laccases.

These results are fully consistent with those obtained previously with the aliphatic aldehyde C21-laccase functionalized particles. Again, they clearly support a selective effect of the enzyme orientation on substrate oxidation: both phenolics and ABTS oxidation are affected when bringing the laccase oxidation site close to the aldehyde functionalization layer. Hindrance appears more important in the UniK₁₆₁-H23 system, possibly because of the chemical nature or the length or a combination of both the nature and the length of the linker used compared to UniK₁₆₁-C21 systems.

Most importantly, compared to the immobilization on commercial aliphatic aldehyde particles, ratios obtained on CA oxidation with laccases immobilized on custom-made aromatic aldehyde are spectacularly larger. Besides their differences in the density of aldehyde function at the particle surface, in the reactivity of aldehydes (aromatic *vs* aliphatic) a possible explanation may lie in the different microenvironments brought around the active site of the immobilized laccase. In particular, the structural proximity of the benzaldehyde moiety of the functionalization shell with a phenolic substrate is invoked. The evolution on almost one order of magnitude of the performance of the different configurations of the catalyst supports an acquisition of a form of selectivity and validates our initial hypothesis.

In order to verify the above trend and assumption, we studied commercial particles with a functionalization different from aldehyde. In the following section, grafting of azide particles was studied given that the azide groups offer not only a different possibility for a covalent reaction (cycloaddition instead of reductive alkylation), but also a potential different chemical microenvironment for the enzyme's oxidation site.

4 Immobilization on commercial azide particles

4.1 Information on azide particles

Azide beads used in this experiment were purchased from Aldrich. The particles are made of purely metallic nanoparticles (metallic cobalt core) coated with a thin (ca. 2 nm) graphene-like carbon layer, which is then functionalized with azide groups (extent: ≥ 0.1 mmol/g). Other important beads properties are: average diameter ≤ 50 nm; spec. surface ≥ 15 m²/g, carbon content of this beads is less than 4 wt.%, magnetizations ≥ 120 emu/g.¹⁰

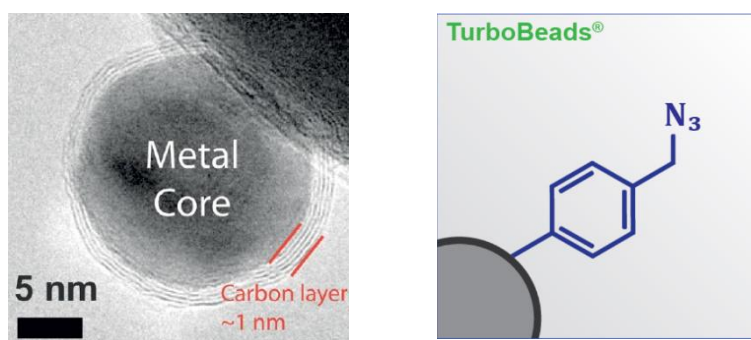


Fig. III-4-1 The inner core and outer shell of commercial azide particles (pictures are from <http://www.turbobeads.com/>)

Coupling laccases onto the commercial azide beads requires two steps a) the formation of a laccase-alkyne hybrid by reductive alkylation (**Fig. III-4-2 A**) and b) the immobilization of the laccase-alkyne hybrid on azide beads using Huisgen cyclo addition (click chemistry) (**Fig. III-4-2 B**).

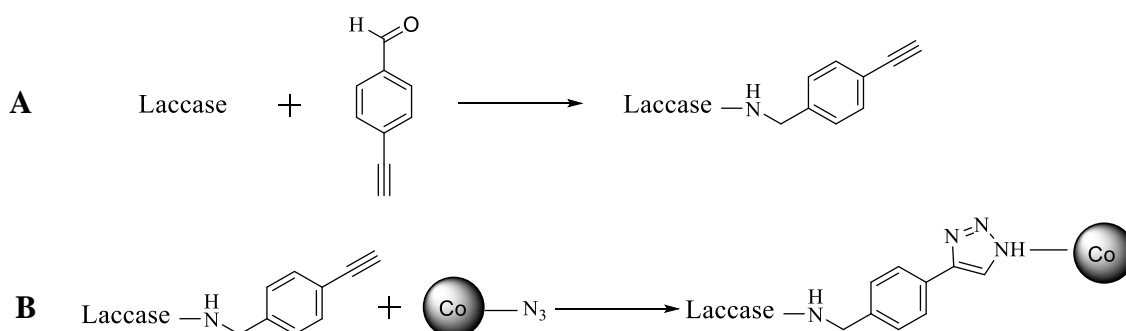


Fig. III-4-2 Schematic illustration of the immobilization of laccase onto the azide particle surface. A: reductive alkylation; B: Huisgen cycloaddition

Reaction conditions (including initial enzyme concentration, particles amount, pretreatment of the particles) were optimized before performing the final immobilization experiment. Details about reaction settings can be found in the Experimental Methods section in the appendix of this manuscript.

4.2 Optimization of immobilization reaction conditions

4.2.1 Effect of initial enzyme concentration on activity

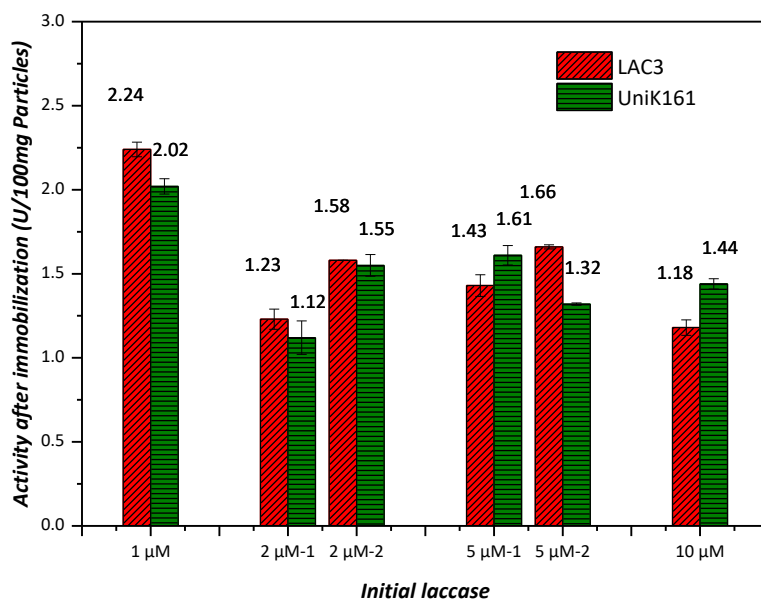


Fig. III-4-3 Relationship between the initial laccase concentration and the activity of the immobilized laccase for the commercial azide particles. Particles concentration 10mg/mL. Reaction temperature: room temperature. Rotating speed: thermomixer 1000rpm, final volume 1mL. Laccase activity were tested with ABTS as substrate in 0.1M acetate buffer pH 5.7 at 30°C. The maximum activity point of the grafted laccase appears at the initial enzyme concentration of 1 μ M.

Dependence of the (laccase-particles) hybrid activity as function of the initial laccase concentration were determined for an initial laccase concentration ranging from 1.0 to 10.0 μ M (**Fig. III-4-3**). The maximum activity for both LAC3 and UniK₁₆₁ was observed for a concentration of 1 μ M. Increasing laccase input does not improve activity of the hybrid but rather slightly reduces it. It has been reported that at higher enzyme concentration, agglomeration may take place and the active site becomes less accessible to the substrate, which lowers the enzyme catalytic activity.¹¹ This results with commercial azide beads is consistent with our previous results on aldehyde particles.

4.2.2 Effect of particles amount on activity

The commercial azide particles have a tendency to agglomerate and sediment due to their small particle size (~20 nm). Consequently, weighing particles is difficult, especially when a small amount (1 mg) is needed. Apparently, using 10 mg/mL particles the activity of immobilized laccases is \approx 2 times higher than using 1 mg/mL (**Fig. III-4-4**). So, the amount of particles used in the immobilization experiments and the initial laccase concentration were respectively set to 10 mg/mL and 10 μ M.

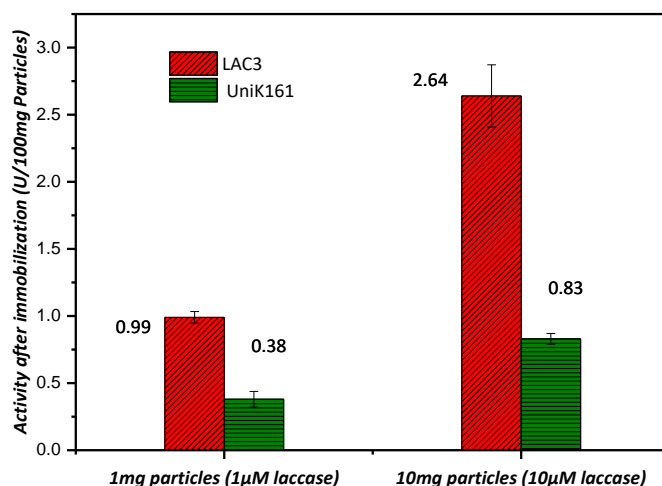


Fig. III-4-4 Relationship between particles amount and the activity of the immobilized laccase. The final volume of the reaction system is 1mL; particles were tested at 1mg/mL and 10mg/mL, and the initial enzyme concentration used is 1μM and 10μM respectively to keep the ratio of surface functional groups and laccase (the stoichiometric ratio) unchanged. Reaction temperature: room temperature. Rotating speed: thermomixer 1000rpm. Laccase activity was tested with ABTS as substrate in 0.1M acetate buffer pH 5.5 at 30°C.

4.2.3 Effect of particle pretreatment method on activity

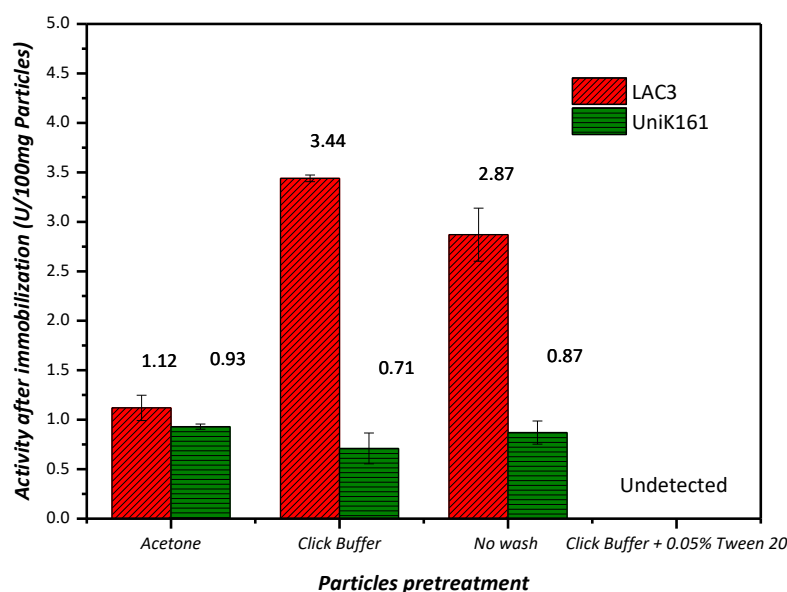


Fig. III-4-5 Effect of particle pretreatment on the immobilized laccase activity. Particles concentration 10mg/mL. The initial enzyme concentration is 10μM. Reaction temperature: room temperature. Rotating speed: thermomixer 1000rpm. The final volume of the reaction system is 1mL. Laccase activity were tested with ABTS in 0.1M acetate buffer pH 5.7 at 30°C.

The commercial azide particles were washed prior immobilization as residual reactants or stabilizers used during the production of azide particles may affect the performance of laccase. Different washing solutions were tested and the results are shown in **Fig. III-4-5**.

No activity was detected after washing the particles simply with the click buffer (50mM phosphate pH=7.5) containing 0.05% Tween 20. The typical cleaning solvent acetone advised by the manufacturer gave the lowest activity. Compared with no washing, click buffer (without Tween 20) showed a slightly better effect, so, it is beneficial to wash the azide particles by the click buffer before immobilization.

4.3 Results and discussion

4.3.1 Enzyme loading

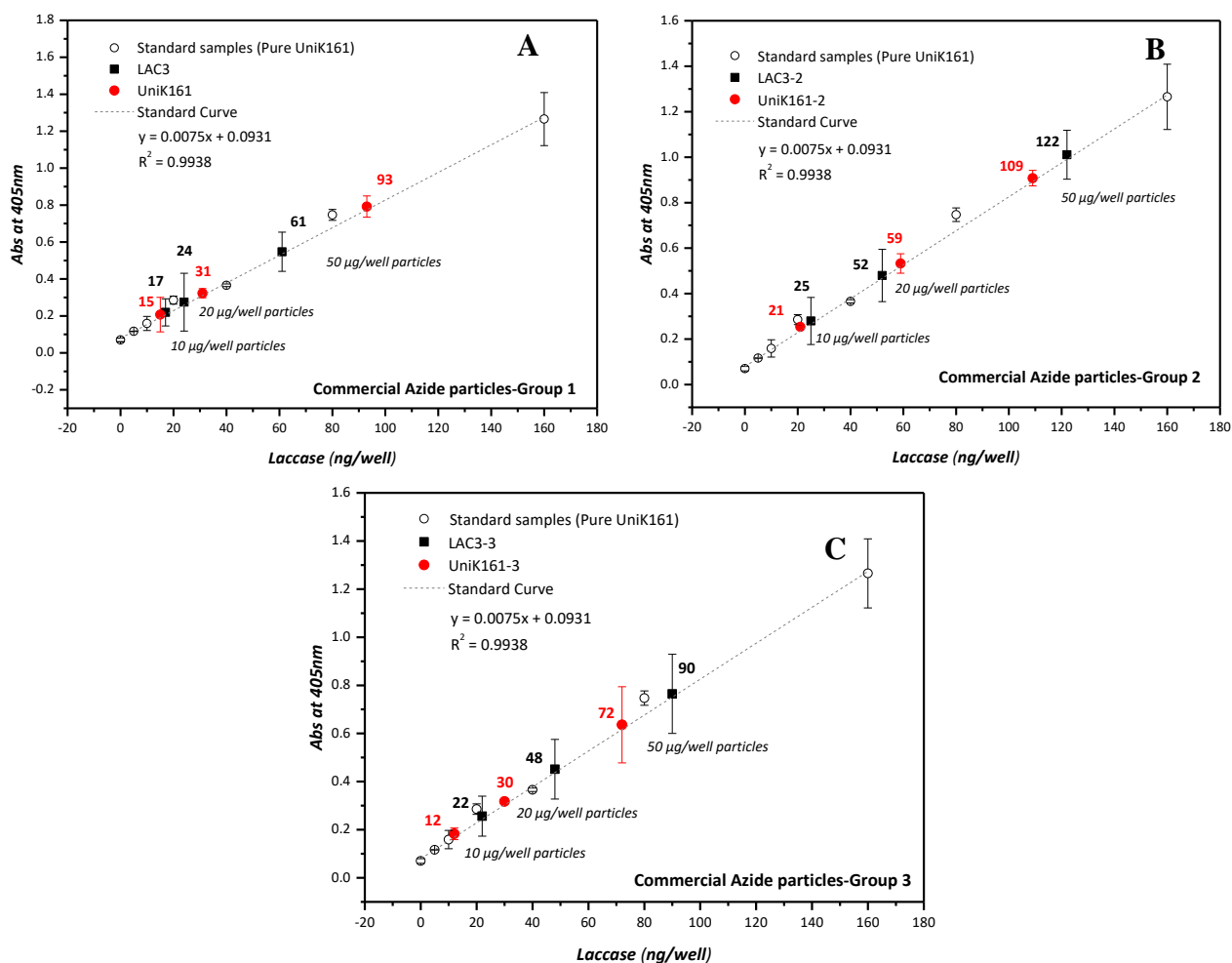


Fig. III-4-6 Enzyme loading tested by ELISA for the commercial azide particles. Three independent immobilizations were performed separately for each enzyme (A, B and C). 10µg, 20µg and 50µg particles immobilized with each laccase were triplicated in the microwell for measurement. The points in the graph are the average value of the triplicated tests in the microwell.

As before, three independent immobilizations were performed separately for each enzyme. The enzyme loading was tested by ELISA following the procedure described previously (refer to the Experimental Methods section of the appendix in this manuscript for the detailed protocols). UniK₁₆₁ (batch 2018.04) was used as standard enzyme for making calibration curves. For each measurement,

different amounts (50 μ g, 20 μ g and 10 μ g) of particles were used, and the same amount of bare particles were used as blanks. Both the standard samples and the particle samples (particles immobilized with different laccase) were tested in triplicate in a microwell plate. Results are displayed in **Fig. III-4-6**.

First, the calibration curves have good linearity and samples values are all located within the working range of the curve. In addition, similarly to the trend observed previously (chapter III, section 2.2.5.1 and section 3.2.2), the absorbance value increased linearly with the increase of the particle amount. Since the particles themselves have been shown to have no effect on absorbance (Chapter III section 2.2.5.1) this can be attributed to an increase amount of enzyme successfully immobilized onto the particles.

Second, except for the second group, the difference of enzyme loading between LAC3 and UniK₁₆₁ is apparently large (the black square and red circles in the figure have scattered absorbance values in **Fig. III-4-6**) a variability in click reaction yields between experiments. This may be due to the nature of the particles. As mentioned, the commercial azide particles used in these experiments are small in size and are less prone to form stable suspensions, inevitably tending to agglomerate during the immobilization process. Such an uncontrollable aggregation may be the source of variations between experiments.

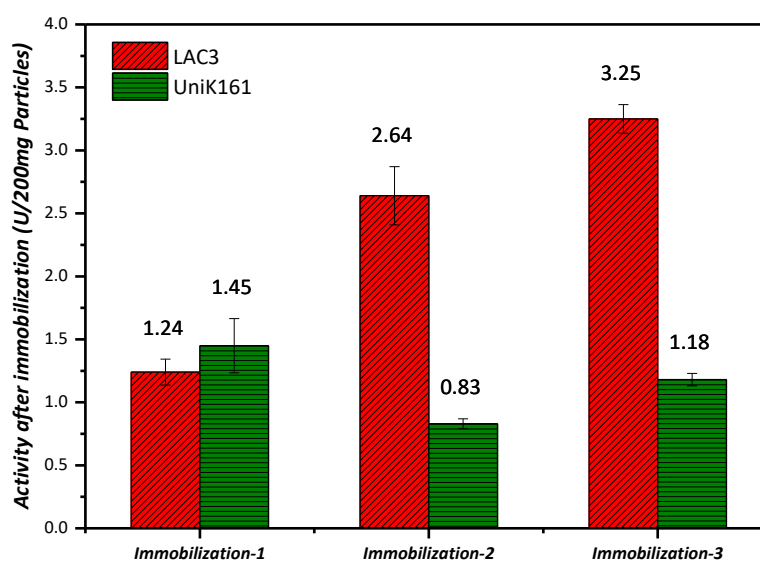
Calculation of the enzyme loading presented in **Table III-4-1** reflect the variations of enzyme loading obtained for different particle amounts (range 3-21% , see last column in **Table III-4-1**).

To minimize the effect of these variations, enzyme loading values obtained with different amounts of particles were averaged. Enzyme loadings for the three immobilizations were 1.37; 2.51; 2.13 and 1.64; 2.41; 1.38 μ g laccase per mg particles respectively for LAC3 and UniK₁₆₁.

Table III-4-1 Enzyme loading calculations for commercial azide particles immobilization

Samples	Particles used ($\mu\text{g}/\text{well}$)	Enzyme loaded (ng/well)	Enzyme Loading ($\mu\text{g}/\text{mg}$)	Average enzyme Loading ($\mu\text{g}/\text{mg}$)	STEDV
Azide immobilized LAC3-1	50	61	1.22	1.37	0.283 (21%)
	20	24	1.20		
	10	17	1.70		
Azide immobilized UniK161-1	50	93	1.86	1.64	0.195 (12%)
	20	31	1.55		
	10	15	1.50		
Azide immobilized LAC3-2	50	122	2.44	2.51	0.081 (3%)
	20	52	2.60		
	10	25	2.50		
Azide immobilized UniK161-2	50	109	2.18	2.41	0.469 (19%)
	20	59	2.95		
	10	21	2.10		
Azide immobilized LAC3-3	50	90	1.80	2.13	0.306 (14%)
	20	48	2.40		
	10	22	2.20		
Azide immobilized UniK161-3	50	72	1.44	1.38	0.159 (12%)
	20	30	1.50		
	10	12	1.20		

4.3.2 Evaluation of Specific Activity for free and immobilized laccase towards ABTS

**Fig. III-4-7** Activity of laccases immobilized on commercial azide particles towards ABTS, at pH 5.57, 30°C

Activity measurements and calculation of the specific activity were carried out as described in chapter III section 2.2.5.2. The activity of the three sets of independently immobilized laccases is shown in Fig. III-4-7. In the first set, LAC3 and UniK₁₆₁ grafted particles showed similar activities. In the other two sets, LAC3 grafted particles demonstrated a significantly higher activity than UniK₁₆₁ grafted particles.

Specific activities of the free and immobilized laccases are shown in Table III-4-2. As previously observed, the specific activity of immobilized laccases decreased dramatically as compared to the free enzymes (~100 times decrease at the maximum extent for the immobilized UniK₁₆₁-2). As discussed before, this significant decrease may be associated to mass transfer restrictions and potential conformational changes deleterious to the activity occurring during the covalent immobilization.

Table III-4-2 Specific Activities of free and immobilized laccases for commercial azide particles

Commercial Azide Particles	Enzyme Loading (µg/mg)	Activity after Graft (ABTS; U/200 mg grafted particles)	Specific Activity (ABTS; U/mg grafted laccase)	Ratio of SA: (LAC3/UniK ₁₆₁)
Free LAC3	--	--	170	0.98
Free UniK ₁₆₁	--	--	173	
LAC3-1	1.37	1.24	4.53	1.03
UniK ₁₆₁ -1	1.64	1.45	4.41	3.04
LAC3-2	2.51	2.64	5.26	
UniK ₁₆₁ -2	2.41	0.83	1.73	1.68
LAC3-3	2.13	3.25	7.64	
UniK ₁₆₁ -3	1.30	1.18	4.54	
Average ratio of Specific Activity after immobilization (LAC3/UniK₁₆₁):				1.92

As for the previous hybrids constructions (i.e. aldehyde grafted particles) ratios of SA of LAC3 over UniK₁₆₁ were calculated to evaluate the effect of enzyme orientation on its activity. Prior immobilization, the ratio LAC3/UniK₁₆₁ is close to 1, meaning that both the free LAC3 and the free UniK₁₆₁ have the same efficiency towards ABTS substrate before immobilization. After immobilization, the ratio is about 2 (average value), suggesting that LAC3 has a higher catalytic efficiency than UniK₁₆₁ when immobilized. Like for the two previous examples of immobilization on aldehyde particles, such an acquired asymmetry seems to be attributable to the different preset orientations of the enzyme at the particle surface.

However, comparing ratios of SA of free and immobilized laccases for the three different particles used in this study (Fig. III-4-8) the picture appears slightly more complex. Laccases grafted on azide particles are globally exhibiting the lowest ratio values among the three types of particles compared. In other words, azide-based particles appear to have retained the most laccase activity compared to the two aldehyde type particles which seem otherwise to behave the same way.

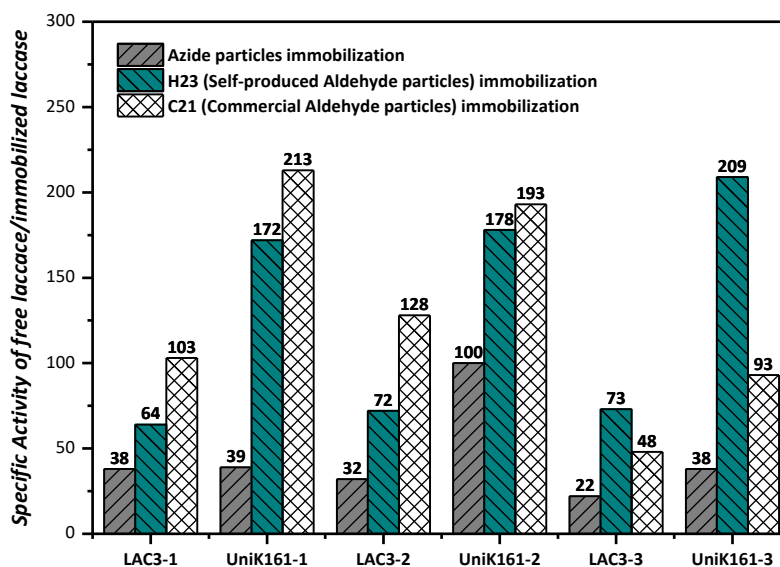


Fig. III-4-8 Ratios of specific activities of free and immobilized laccase for different particles

This “better” retention of initial activity of azide-grafted particles appears to be fairly well shared by the two types of grafting: LAC3-azide particles and UniK₁₆₁-azide particles. Whereas grafting reactions (reductive alkylation and click chemistry) in solution have proved to have little influence on laccase activity^{1,3} it seems however that globally laccases are more active on grafted azide particles for an unknown reason at the moment. On the other hand, comparing grafting on azide particles vs aldehyde particles leads to focus on a structural difference at the interface particles/enzyme.

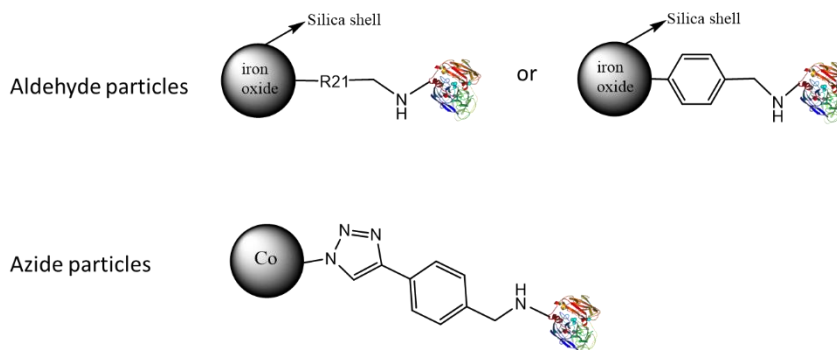


Fig. III-4-9 Schematic diagram of aldehyde particles immobilization (reductive alkylation reaction) and Azide particles immobilization (reductive alkylation reaction plus Click chemistry).

Indeed, for the two aldehyde particles (aliphatic and aromatic) the reductive alkylation reaction eventually results in the formation of a simple amine bond connecting the particle and the enzyme whereas for the azide particle the reaction of the ethynyl benzaldehyde moiety of the enzyme with the azido benzene moiety of the particles results in a benzo-triazole “spacer” (Fig. III-4-9). Moving the enzyme farther away from the functionalization surface might explain the low bias observed between the two orientations of the laccase at the azide particle surface as well as the variability of SA ratios for the three independent graftings.

4.3.3 Coniferyl alcohol biotransformation with laccase immobilized on azide particles

The oxidation of coniferyl alcohol (CA) by the azide immobilized laccases was carried out under conditions similar to those used for the two previous hybrids tested (C21 particles, chapter III section 2.2.5.3 and H23 particles chapter III section 3.2.4). Small adjustments of parameters (e.g. the final reaction volume, the incubation speed and the amount of particles used) were made according to the desired condition.

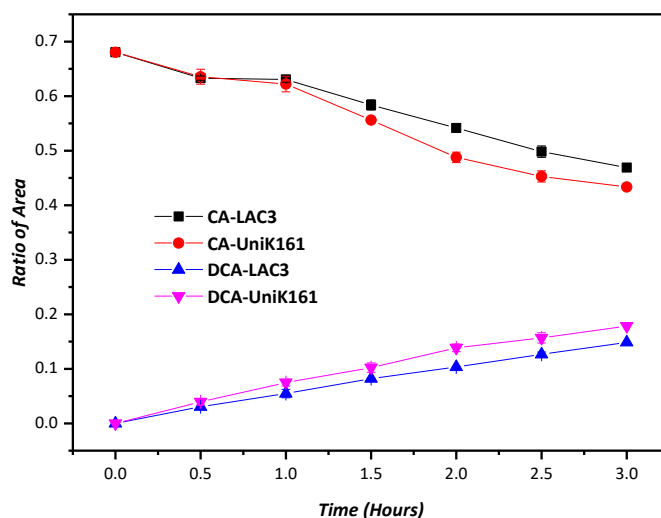


Fig. III-4-10 Oxidation of coniferyl alcohol catalyzed by laccases immobilized on azide particles. Hybrids were incubated in 0.1M acetate buffer, pH=5,7 at 30°C on thermomixer 1000rpm, for a maximum of 3 hours, in a final volume of **1mL** and CA concentration of 1.6mM, 323ng immobilized enzyme. The ordinate is the ratio of the area of the peak corresponding to the reactant on the HPLC chromatogram to the area of the peak corresponding to the reference benzophenone.

The consumption of the substrate CA and the production of the major product dehydroconiferyl alcohols (DCA) was initially followed during the first 3 hours (Fig. III-4-10). UniK₁₆₁-azide particles appear as efficient or slightly more efficient as LAC3-azide particles

regarding CA biotransformation (as shown by the slightly faster substrate consumption and the main products generation rate). Interestingly, this result is opposite to that was obtained with ABTS as substrate, and also is contrary to the trend previously obtained with laccases immobilized on aldehyde particles (both C21 and H23). It is worth mentioning that, when repetitions of the experiments with small parameter changes (e.g. increase of the incubation speed or the reaction volume) were performed similar results were always obtained. Unfortunately, for a time limitation reason, the experiment was not conducted on 24h period like for the previous systems. We are aware that interpretations given below may reflect this fact.

Calculation of the defined ratio (Ratio^{*}, refer to chapter III section 2.2.5.3) after oxidation at 3 hours are shown in **Table III-4-3**. As described previously, the ratio poises the relative values of the substrate remaining in the mixture of the reaction during the oxidation by LAC3 and UniK₁₆₁ respectively. It can be seen that the efficiency of the two immobilized enzymes was nearly identical for both free (0.87) and immobilized (0.86) laccase, which indicates that CA oxidation is apparently not influenced by the orientation of laccase immobilized on the commercial azide particles.

One may argue about the inconsistent state of particle aggregations, because of the heterogeneity characteristic of the small size particles. Indeed, azide magnetic particles are highly susceptible to aggregate during the reaction process. However, there is no reasonable argument to think that such a phenomenon would apply specifically to CA oxidation and not to ABTS oxidation for which **SA** ratios of laccase-azide systems are similar to those of laccase-aldehyde systems. This asymmetry in the behavior of the laccase-azide system towards the two substrates was not observed with the previously used laccase-aldehyde systems. This asymmetry, if confirmed, could reflect a form of selectivity of the laccase-azide system towards CA (phenolics) oxidation.

Table III-4-3 Normalized value of the consumed substrate [(initial CA area/benzo area) – (remaining CA area/benzo area)] of the free and immobilized laccase at the 6th hours. Area represent the peak area on the HPLC chromatogram

Commercial Azide Particles (H23)	Consumed substrate [(initial CA area/benzo area) – (remaining CA area/benzo area)]	Amount of Laccase (ng)	Consumed substrate /Amount of Laccase (1/mg)	Ratio* of LAC3/UniK161
Free LAC3	0.548	6.8	80603	0.87
Free UniK ₁₆₁	0.652	7.0	93074	
LAC3-Immobilized	0.211	323	654	0.86
UniK ₁₆₁ -Immobilized	0.247	323	765	

4.4 Conclusions

In this subsection, commercial azide particles were used as support materials to study the influence of immobilization orientations on the activity of laccase. Two substrates (ABTS and coniferyl alcohol) were studied to achieve this goal.

For ABTS, the ratio of the specific activity of LAC3 and UniK₁₆₁ is increased from 0.98 before immobilization to 1.92 after immobilization, showing again that the immobilization near the active site influence the activity of laccase towards ABTS.

For coniferyl alcohol oxidation, immobilized UniK₁₆₁ and LAC3 are apparently equally efficient. This trend is opposite to that observed for ABTS. It may reflect a form of selectivity that has to be confirmed with new experiments.

In the mean time, these additional results seem to confirm the trend of a modulation of the laccase activity through a manipulation of the microenvironment around the laccase active site.

Besides, an evidence that the microenvironment around the laccase could influence the laccase activity was obtained.

In order to further validate the conclusions obtained so far and achieve more evidences for the effect of orientations on the laccase activity, another surface-functionalized particles, the amino particle will be studied in the next section.

5 Amino particles immobilization of laccase

5.1 Information of amino particles

Amino particles are widely used magnetic particles for protein immobilization. Normally, surface amino modification is the primary step to start an immobilization. When magnetic particles are modified with amino groups at their surface, they can be activated by homobifunctional linkers, for the coupling of proteins.

The amino particles used in this section were produced in our lab. Fe_3O_4 particles were first synthesized by chemical co-precipitation technique according to the following reaction equation: $2\text{Fe}^{3+} + \text{Fe}^{2+} + 8\text{OH}^- \rightarrow \text{Fe}_3\text{O}_4 + 4\text{H}_2\text{O}$. Then the above custom-made magnetic particles were directly reacted with ethylenediamine to obtain the amino surface modified particles **MNP-NH₂** (Fig. III-5-1 eq.1).

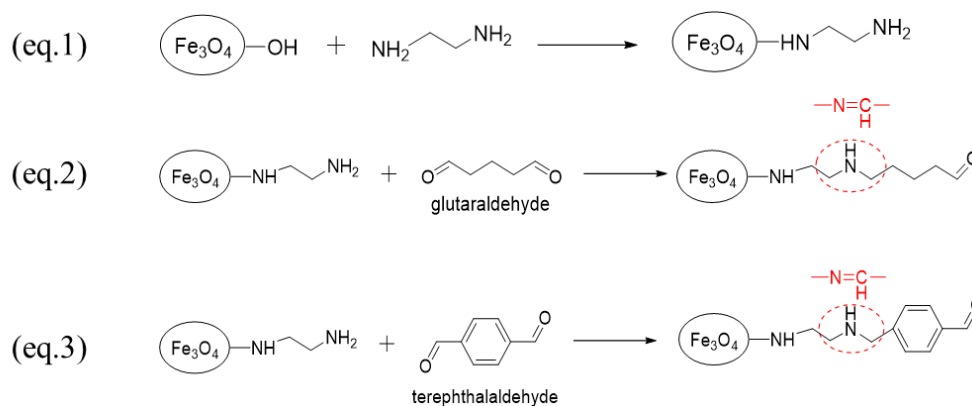


Fig. III-5-1 Surface modification of the custom-made magnetic particles

Prior to perform laccase immobilization, **MNP-NH₂** were activated with glutaraldehyde (Fig. III-5-1 eq.2) or terephthalaldehyde (Fig. III-5-1 eq.3), to display aldehyde functional groups on the surface of the particles. After activation, the two kinds of particles were designated as **MNP-CHO-GLU** and **MNP-CHO-TER** and used immediately for laccase immobilization, to avoid oxidation of aldehyde groups.

All synthesized amino particles were investigated for the oriented immobilization of laccases., **MNP-NH₂** particles being investigated as a control group. Characterization of the particles were performed by microscopy, zeta potential measurement and FT-IR by Dr. Karine Heuzé at the University of Bordeaux. Alongside, commercial amino particles (**MNP-NH₂ Sigma**) from Sigma Aldrich¹² were used for comparison during the characterization. Some of the reaction parameters were optimized before the final immobilization.

5.2 Results and discussion

5.2.1 Characterization of the Amino particles (MNP-NH₂)

5.2.1.1 Morphological characterization

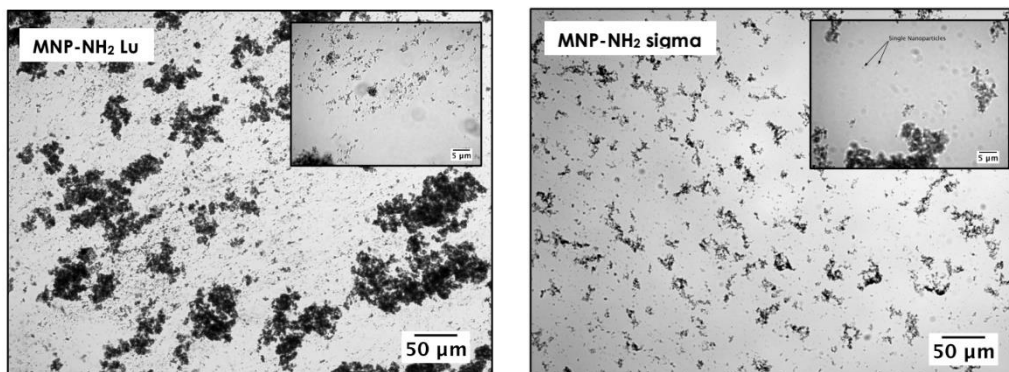


Fig. III-5-2 Microscopic morphology of amino particles

Optical Microscopy was performed on ZEISS Axiolab microscope in transmitted light mode. MNP-NH₂ and MNP-NH₂ Sigma samples were prepared in pure water. Both samples were sonicated for 10 seconds. Optical images were recorded and are shown in Fig. III-5-2. For both MNP-NH₂ and MNP-NH₂ Sigma samples, large aggregates are observed. The general size of the aggregates is 50~100 µm and 20~50 µm respectively. Additionally, single particles are also present in both cases.

5.2.1.2 Zeta potential measurement for the surface charge state of MNPs

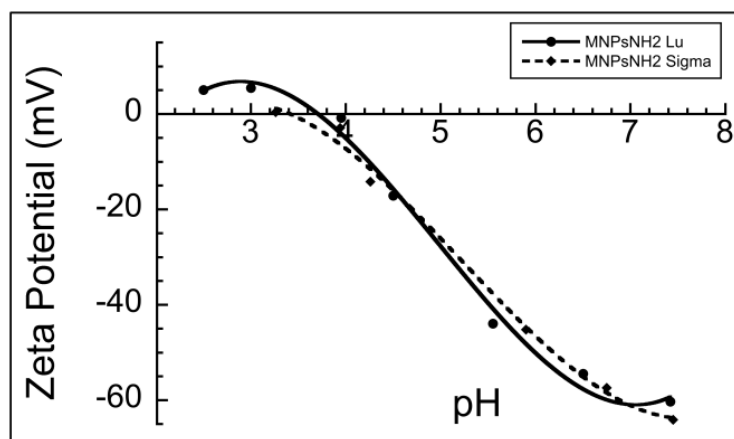


Fig. III-5-3 Effect of pH on the surface charge of amino particles

The effect of pH on the surface charges were studied by measuring zeta potentials of suspensions of MNPs in pure water by varying pH from 2.5 to 7.5. Both samples MNP-NH₂ and MNP-NH₂ Sigma have similar behaviors with IEP (isoelectric point) close to 3.5 (Fig. III-5-3). The curves also show that MNPs have a stable colloidal state in water for solutions with pH over than 5 (when zeta potential is inferior to -30 mV).

5.2.1.3 Qualitative characterization of the surface functional groups

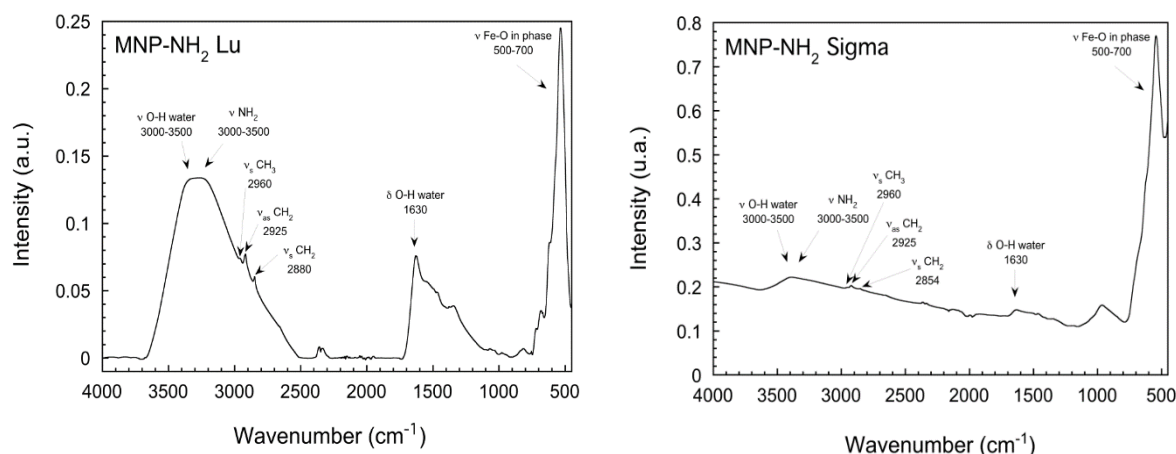


Fig. III-5-4 FT-IR spectrum of amino particles

IR-ATR spectroscopy has been performed to qualitative characterization of the surface functional groups on FTIR. For both samples of MNP-NH₂ and MNP-NH₂ sigma, the presence of ν Fe-O (500~700 cm⁻¹) vibration bands as well as ν NH₂ (3000~3500 cm⁻¹, more or less intense) vibration bands were observed. ν CH₂ vibration bands of ethylenediamine were also detected.

5.2.2 Optimization of immobilization reaction conditions

5.2.1.1 Immobilization of laccase onto MNP-NH₂ with different buffers

Different kinds of buffers were used as reaction medium to observe the influence of buffers on the immobilization reaction. Then, the best reaction buffer was selected for further experiments, the results can be seen in **Table III-5-1**:

Table III-5-1 Influence of buffers on immobilization reaction

No.	React with glutaraldehyde	Immobilization with enzymes (50 μ M)	Grafted ratio (to enzymes)
1		LAC3	--
2	0.1M phosphate pH 7.5	UniK161	--
3		LAC3	--
4		UniK161	--
5		LAC3	--
6	0.1M MES pH=6.0	LAC3	36%

It can be seen from the data that: using 0.1M MES buffer pH=6.0 as reaction medium afforded 36% enzyme grafted onto the particles (measured by Bradford as described in Chapter III section 2.2.1) while it was not possible to measure differences in supernatants before and after reaction when

other buffers as solvents were used. So, 0.1M MES buffer pH=6.0 was used for both the activation and immobilization steps.

5.2.1.2 Immobilization of different amounts of laccase onto MNP-CHO-GLU

From previous experimental results, it was known that a high initial concentration of laccase does not necessarily relate to a higher efficiency of immobilization. Therefore, in order to know the appropriate concentration of laccase for the immobilization, the effect of the initial laccase concentration on immobilized laccase activity was investigated and results are shown on **Fig. III-5-5**.

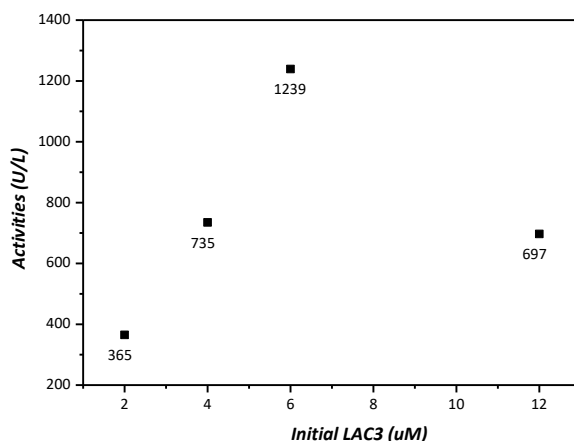


Fig. III-5-5 Effect of initial laccase concentration on activities of immobilized laccase

It can be seen from the figure that when the initial concentration of laccase is higher than 6 μM, the activity of the corresponding (MNPs-laccase) hybrid decreased. So for the MNP-NH₂ particles, it is better to keep the initial laccase concentration below 6 μM in a total reaction system of 1ml with 500 μL particles corresponding to 8.5mg as determined by drying the suspension in an oven.

5.2.3 Immobilization of laccase onto MNPs

Having determined the reaction medium and the initial concentration of laccase, immobilization of laccases on different magnetic particles were performed. Since the aldehyde particles (MNP-CHO-GLU or MNP-CHO-TER) were produced from MNP-NH₂ (by the reaction between amino groups and one of the aldehyde between glutaraldehyde or terephthalaldehyde), amino particles MNP-NH₂ were used as control experiments.

The detailed experimental process of immobilization is notified in the Experimental Methods section as an appendix to this manuscript. Experimental results are shown in **Table III-5-2**.

Table III-5-2 Immobilization of LAC3 on different magnetic particles

No.		1	2	3	4
Samples		MNP-NH ₂		MNP-CHO-GLU	
	Initial LAC3 (μM)	2.5	5	2.5	5
Graft	LAC3 after reaction (μM)	0	0	0	2.1
	Grafted ratio	100%	100%	100%	58%
	Wash 1 by MES PH=6 vortexing	--	--	--	--
	Wash 2 by MES PH=6 vortexing	--	--	--	--
Leak or not	Wash 3 by MES PH=6 vortexing	--	--	--	--
	Wash 4 by Acetate PH=5.7 vortexing	--	--	--	--
	Resuspended and sonication 30 mins	--	--	Leak	Leak
	Activities (U/L) ABTS	6408	17975	7632	14153

--" means no LAC3 was detected in the washing solutions.

Surprisingly, amino functionalized particles apparently display 100% immobilization whatever the initial concentration of material used (2.5 μM or 5 μM LAC3). Moreover, no laccase was released during the subsequent washing procedure (**Fig. III-5-6**). In contrast, for the aldehyde particles (MNP-CHO-GLU), when the initial concentration of LAC3 was 5 μM , the grafted ratio reached was only about 60% and there was also some leaching during the washing procedure. It is also surprising that for the MNP-CHO-GLU sample grafted with 5 μM initial concentration of laccase (**Table III-5-2**, No.4), although the graft ratio was only ca 60%, the corresponding activity (14153U/L) was almost two times higher than that of the MNP-CHO-GLU grafted with 2.5 μM initial concentration of laccase (7632U/L) and similar to the MNP-NH₂ in which all the 5 μM LAC3 were apparently grafted onto the particles.

In order to make sure that laccase was immobilized onto MNPs by covalent bond, a leaching test was performed by adding the laccase substrate syringaldazine (SGZ) to the supernatants. Since the oxidation of SGZ by laccase can be visually seen by the appearance of a pink colored product, a leak of enzyme from the particles would be easily visualized. Wash supernatants were discarded and 1mL storage buffer was added (0.1M acetate buffer, pH=5.7), the suspension mixed by vortexing and sonicated for different times. Particles were magnetically separated, supernatants were transferred in a new vessel containing the substrate SGZ and visually inspected. Pictures are shown in **Fig. III-5-6**.

For the MNP-NH₂, no leakage was observed after vortexing and ultrasonic treatments, indicating that the connection between the custom-made MNP-NH₂ and laccase is stable and robust. MNP-NH₂-GLU particles showed a different behavior. After washing three times with the coupling buffer, no enzyme was detected in the supernatant. After 30 minutes of bath sonication, leakage was observed in the supernatants for both 2.5 μM (Table III-5-2 and Fig. III-5-6 Sample No.3) and 5 μM (Table III-5-2 and Fig. III-5-6 Sample No.4) initial enzyme concentration. For the latter (Table III-5-2 and Fig. III-5-6 Sample No.4), the leakage did not stop still appearing after bath-sonication for 3 hours. This suggests that immobilized laccases are not all covalently bound and that may explain the aforementioned higher laccase activity for particles with a lower grafted amount of enzyme.

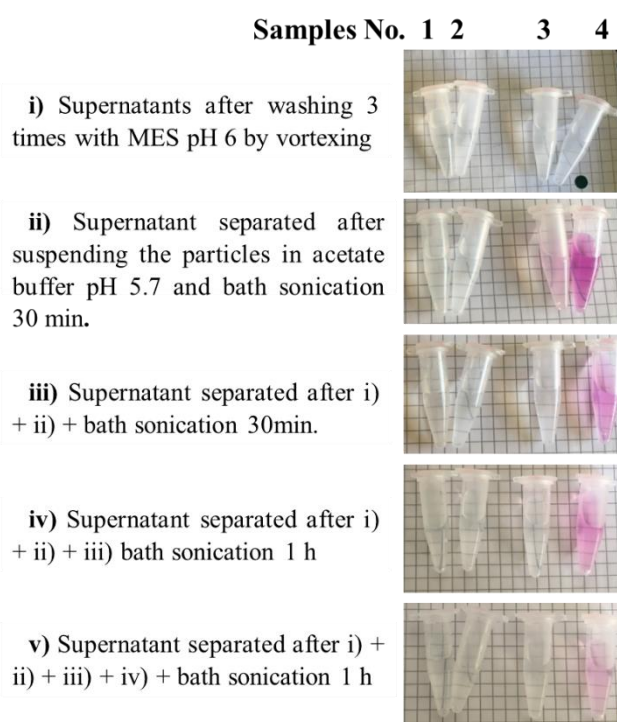


Fig. III-5-6 Enzyme leaking in the supernatant after washing

To conclude, despite the good grafting performance of MNP-NH₂ particles, a study of the orientation of laccase on those particles is not possible. Indeed, when amino groups at the particle surface are not completely converted to aldehyde groups (in fact, it is very difficult to achieve 100% conversion), the remaining amino groups may react with laccase (aldehyde or ketone are easily obtained from sugar residues of glycoprotein so amino particles also have ability to react with laccase (glycosylated) by Schiff base formation) resulting in a non-directional immobilization. Since orientated covalent binding is the basis of our research, this kind of non-directional immobilization will cause interferences. So amino particles are not suitable as a carrier in this study, unless some workarounds are found.

On the other hand, a desorption or reversible formation of imines is a possible explanation for the leaching observed. From our knowledge, the isoelectric point (IEP) of laccase is about 4 and IEP of particles is about 3.5, so when pH of the reaction medium is 6, electrostatic adsorption is less likely to occur, because both of the laccase and particles are negatively charged. Therefore, a physical adsorption can be excluded. For the reversible formation of imines, Ir catalysts or NaBH₄ could be applied to reduce imines into more stable amines (Fig. III-5-7).

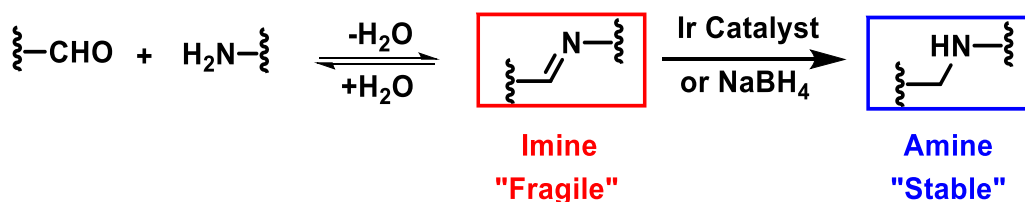


Fig. III-5-7 Methods for preventing the leakage of immobilized laccase on MNPs

Although amino particles were proved to be ineffective for the purpose of this study (oriented immobilization), experiments for preventing a leakage were further conducted. The experimental procedure is the same than in the previous experiment, except that strong reductants (Ir catalysts or NaBH₄) which are capable of reducing the imine obtained in the first step to more stable secondary amine were added. Results are shown in Table III-5-3.

It can be seen from Table III-5-3 (a) and (b) that all the immobilized LAC3 did not leak after sonication 30min when adding the Ir catalyst (0.1~0.05 equivalent to LAC3) or NaBH₄ (~10 equivalent to LAC3) to the reaction system. The grafted ratios were almost stable, and laccase activity after immobilization was almost at the same level as compared to the previous experiments. This is indicating that the addition of a catalyst is effective in preventing laccase leakage.

Table III-5-3 Immobilization of LAC3 on MNPs with reductive agent

(a) 100 mM MES PH=6 +100 mM HCOONa + Ir catalysts (15μL of 14 μM in total volume 1mL)					
samples:		MNP-NH ₂		MNP-CHO-GLU	
Graft	initial lac3 (μ M)	1.7	4.5	1.7	4.5
	Lac3 after reaction (μ M)	0.2	0.4	0	0
	grafted ratio	88%	91%	100%	100%
Leak or not	wash 1 by MES PH=6 vortexing	--	--	--	--
	wash 2 by MES PH=6 vortexing	--	--	--	--
	wash 3 by MES PH=6 vortexing	--	--	--	--
	wash 4 by Acetate PH=5.7 vortexing	--	--	--	--
	reuspended and sonication 30 mins	--	--	--	--
	Activities (U/L) ABTS	8246	21024	8084	24909
	(b) 100mM MES PH=6 +NaBH₄ (10μL of 5M in total 1mL volume)				
Samples		MNP-NH ₂		MNP-CHO-GLU	
Graft	Initial lac3 (μ M)	3.0	4.2	3.0	4.2
	LAC3 after reaction (μ M)	0	0.5	0	0
	Grafted ratio	100%	88%	100%	100%
Leak or not	Wash 1 by MES PH=6 vortexing	--	--	--	--
	Wash 2 by MES PH=6 vortexing	--	--	--	--
	Wash 3 by MES PH=6 vortexing	--	--	--	--
	Wash 4 by Acetate PH=5.7 vortexing	--	--	--	--
	Resuspended and sonication 30 mins	--	--	--	--
	Activities (U/L) ABTS	5831	11976	5438	10201

Glutaraldehyde is commonly used as bifunctional linker to activate amino functionalized particles and display at the surface of magnetic particles the aldehyde groups needed for a further coupling with biomolecules. Besides that, terephthalaldehyde was also investigated in this section since from literature and our own experience, aromatic aldehyde groups react more easily than aliphatic ones. Considering the solubility of terephthalaldehyde, the use of ethanol as reaction media was needed before and after reaction. After functionalization, particles were washed 3 times with ethanol to remove the excess of terephthalaldehyde then washed by MQ water several times before coupling with LAC3. Other processes were the same standard steps as described in previous experiments. The results are listed in the following table (**Table III-5-4**):

Table III-5-4 Immobilization of LAC3 on different magnetic particles with terephthalaldehyde as bridge

Particles	MNP-NH ₂	MNP-TER	MNP-NH ₂	MNP-TER	MNP-NH ₂	MNP-TER
Conditions	Only buffer		Ir catalysts (15μL of 14μM)		NaBH ₄ (10μL of 5M)	
Initial LAC3 (μM)	3	3	3	3	2.8	2.8
LAC3 after reaction (μM)	0	0	0	0	0.1	0
Graft ratio	100%	100%	100%	100%	96%	100%
Leaking	No leak after wash and sonication (30mins)					
Activities ABTS (U/L)	19479	17206	14340	16556	14164	17119

Using terephthalaldehyde as a bridging agent led to higher grafting ratios with no enzyme leaching (even without the addition of reducing agents). It means beside glutaraldehyde, terephthalaldehyde is also reliable for introducing aldehyde groups at the surface of amino functionalized particles.

5.3 Conclusion

Through the experiments of this section, it seems that a random immobilization of laccase is difficult to avoid with custom-made amino particles. Anyway, the following picture can be drawn for the immobilization with laccase the custom-made amino particles: (1) 0.1M MES buffer pH=6.0 is the best reaction medium; (2) initial laccase concentration should be maintained below 6μM (total reaction system 1ml, 500μL beads); (3) need the use of reducing agents: Ir catalysts (0.1 equivalent to LAC3) or NaBH₄ (~10 equivalent to LAC3) to achieve stable immobilization laccase onto MNPs ; (4) both glutaraldehyde and terephthalaldehyde can be used as bridge to display aldehyde groups at the MNP-NH₂ beads surface.

6 Conclusions

In this chapter, several particles were used for the oriented immobilization of laccase, and two substrates ABTS and Coniferyl alcohol were studied. Evolution of SA ratios for free and grafted enzymes are reported in the table below:

Particles Substrates	C21		H23		Azide	
	ABTS	CA	ABTS	CA	ABTS	CA
Free LAC3/UniK ₁₆₁	0.82	0.87	1.03	0.87	0.98	0.87
Grafted LAC3/UniK ₁₆₁	1.5	1.5	2.75	12.4	1.92	0.86

The first type of particles studied are bearing an aldehyde function, whether it is the commercial aldehyde particles (aliphatic aldehyde) or the custom-made aldehyde particles (aromatic aldehyde). The oriented immobilization of laccases on these particles yield a consistent result: the orientation of the enzyme at the particle surface influence its activity. The two laccase-particles systems follow the same trend, i.e. the catalytic efficiency of the enzyme is decreased when the enzyme is grafted close to its active site. This probably reflect a hindrance modifying the active site accessibility. Most importantly, ratios obtained on CA oxidation with laccases immobilized on aromatic aldehyde are spectacularly larger than those obtained with laccases immobilized on aliphatic aldehyde. The evolution on almost one order of magnitude of the performance of the different configurations of the catalyst supports an acquisition of a form of selectivity.

Globally, azide-based particles retain more laccase activity compared to aldehyde particles and that despite two successive functionalization reactions (reductive alkylation + click). As opposed to the previous aldehydes particles, results on CA and ABTS oxidation are found asymmetric: whereas the SA of UniK₁₆₁ towards ABTS decreases upon functionalization its SA towards CA remains apparently unaffected by the orientation. This preliminary study suggests that the selectivity of the laccase-particle system can be modulated through a variation of the chemical landscape around the enzyme's active site.

Performances of the MNP-NH₂ particles we synthesized are not those expected. These particles react non-specifically with laccase and this results in a non-directional immobilization. Therefore, these amino particles are not suitable as carrier in this study. Nevertheless, properties of these particles (easy measurement of the enzyme loading, high activity after immobilization, selectable bi-functional linker) make them perfectly suited for a generic immobilization of laccase. It is probably worth exploring ways to solve issues and make them suitable for the oriented immobilization.

Appendix: Materials and Methods chapter III

1 General

1.1 Laccase

Laccase used in this study (CA or CA analogues oxidation) is LAC3 from *Trametes* sp C30, which is produced in *Aspergillus niger* and purified in our lab.¹³

1.1.1 Concentration determination

Laccase concentration was estimated by UV-visible spectroscopy (Cary 60, Agilent Technologies, USA) using an $\epsilon_{610\text{ nm}} = 5600\text{ M}^{-1}\cdot\text{cm}^{-1}$ for the T1 copper site.

1.1.2 Activity measurement

Laccase activity was assayed using 2,2'-azino-bis (3-ethylbenzthiazoline-6-sulphonic acid) (ABTS) as substrate. Oxidation of ABTS was detected by following the absorbance at 420 nm ($\epsilon_{420\text{ nm}} = 36000\text{ M}^{-1}\cdot\text{cm}^{-1}$) during 2 min with a spectrophotometer (Cary 60, Agilent Technologies, USA). The reaction mixture (1 mL) contained 10 μL of appropriately diluted enzyme sample, 890 μL of acetate buffer (100 mM pH 5.7) and 100 μL of 50mM ABTS in Milli Q[®] Water at 30°C. The ABTS was added to initiate the reaction. One unit (U) of laccase was defined as one micromole of substrate oxidized per minute in these described conditions.

1.2 Zetametry measurements

Zetametry measurements for the surface charge state of the commercial aldehyde particles were performed on a NanoPartica SZ-100 apparatus.

1.3 FT-IR

IR-ATR spectroscopy has been performed on FTIR Nicolet iS50 spectrometer by Dr. Karine Heuzé at the University of Bordeaux.

1.4 HPLC test

CA oxidation products were separated by reverse phase HPLC on a RP-18 column. The mobile phase was composed of a mixture of water - acetic acid 3% (solvent A) and acetonitrile (solvent B) with the following gradient 90% A 10 % B for 5 min then 10% solvent B to 50% in 20 min then plateau 50% solvent B for 2 min then back to 10% solvent B for 2 min.

2 Immobilization

2.1 Aldehyde particles immobilization

(1) Weigh and transfer a certain number of Magnetic beads (2mg normally) to a centrifuge tube. Resuspend the beads by adding 1 ml RA (Reductive Amination) Buffer (50 mM aqueous phosphate with 0.1M sodium formate, pH 7.4) and mix the beads by vigorously vortexing for 1-2 minutes, if some beads aggregated after suspending them, sonicate mildly for 2 to 5 minutes. (2) Place the tube on the magnetic separator for 1-3 minutes. Remove the supernatant while the tube remains on the separator. Remove the tube from the separator and resuspend the beads with 1 ml RA buffer by pipetting. (3) Repeat step-2 once. (4) Add the enzymes solutions and Iridium catalysts (calculate the volume added in advance) to the beads. Resuspend the magnetic beads and mix very well by pipetting. Incubate the reaction with continuous rotation at 30°C overnights. (5) After reaction, place the tube on the magnetic separator for 1-3 minutes, take out of the supernatant by pipette carefully to new tube for test. (6) Wash the beads several times with 1 ml coupling buffer as described at step (2). (7) Resuspend the beads in Store Buffer (0.1M acetate buffer pH=5.7), store at 4°C until use.

2.2 Azide particles immobilization

(1) Prepare enzymes: change buffer of lac3 and unik161 to RA (Reductive Amination) buffer (50mM phosphate buffer pH=7.4 containing 100mM sodium formate); then measure their concentrations. (2) Preparation of 3mM 4-ethynylbenzaldehyde solution: 0.0039g 4-ethynylbenzaldehy, are dissolved into 1000 μ L DMSO, then dilute 10times with RA (100 μ L initial solution + 900 μ L buffer). (3) Calculate amount of reactants for being in the following conditions: Total volume: 2.5 mL; enzyme concentration [E]:50 μ M; 4-ethynylbenzaldehyde 10 equiv. respect to [E], Ir catalysts=10 equiv. respect to [E]. (4) Fix two round-bottom flask into iron support, mark them respectively as lac3 and unik161. (5) Add the reactants: enzymes, 4-ethynylbenzaldehyde, Iridium catalysts (14mM) RA buffer. (6) Seal with a rubber stopper, and react under magnetic stirring for 72 hours. (7) After reaction, the enzymes are recovered using PD MiniTrap G-25 columns and concentrated by centrifuge with 30kD VIVASPIN 2. (8) Measure concentrations of the collected enzymes by UV-Vis spectrum. (9) Prepare CuSO₄/Ascorbic acid/bathophenanthrolinedisulfonic: Weigh ①0.024g CuSO₄·H₂O ②0.059g bathophenanthrolinedisulfonic and ③0.0176g Ascorbic acid dissolved in 1ml MQ water respectively, then take out of 500 mL each in the order of ①②③ and mix well. (10) Calculate amount of reactants at conditions of: Total volume: 500 μ L; [E]=10 μ M, Azide particles 10mg, CuSO₄/ Ascorbic acid/bathophenanthrolinedisulfonic=30 equivalence=1.5mM. (11) Prepare particles: 10mg azide particles are suspended in 1mL MQ water by the use of an ultrasonic bath for 20 min. (12) Remove the supernatant by magnetic separation,

add the Click buffer (50mM Phosphate buffer pH=7.5) for washing, then magnetic separation and discard the supernatant, repeat 3 times. (13) Add reactants sequentially to the particles and mix well. (14) The mixture was stirred on a thermomixer (1000rpm/min) at 30°C overnights. (15) After reaction, the supernatant was magnetically separated and extracted. (16) Wash beads 3 times with 1 mL Click buffer at each time. (17) Resuspend the beads in 1ml acetate buffer pH=5.7, store at 4°C until use.

2.3 Amino particles immobilization

(1) Weigh 500 μ L of MNP-NH₂ particles (stored in MQ water), discard the supernatant by magnetic separation. (2) Resuspend by vortexing and wash 3 times using corresponding buffer, discard the supernatant by magnetic separation. (3) Add aldehyde-containing reagents (500 μ L 40mM terephthalaldehyde or 500 μ L 25% glutaraldehyde in total volume 1500 μ L ethanol or in total volume 1500 μ L buffer), incubate at room temperature for 3 hours. (4) Wash 6 times using corresponding buffer after incubation. (7) Add certain amount of enzymes (diluted by the corresponding buffer, total volume: 1mL), blend well and incubate at room temperature overnight. (8) Collect the supernatant after reaction for measurement. (9) Wash several times and collect the washed solutions for measurement. (10) Resuspend the beads in acetate buffer PH=5.7, store at 4°C until use.

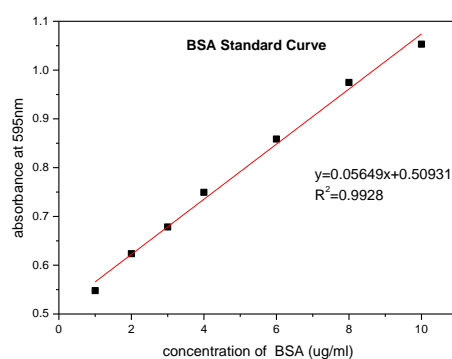
3 Enzyme loading measurement

For UV-visible spectrophotometry and Bradford method, the amount of enzyme immobilized on the magnetic particles (enzyme loading) corresponds to the difference between the initial amount of d enzyme engaged in the reaction and the amount of enzyme remaining in the supernatant after reaction (**enzyme loading = (enzyme added)- (enzyme left in the supernatant after reaction)**).

3.1 Enzyme loading measurement by UV-visible spectrophotometry

The supernatants after immobilization were first subjected to gel filtration (Sephadex G-25 in PD-10 Desalting Columns) to separate the enzyme from other reactants and to allow a re-oxidation of the enzyme. Concentration of the re-oxidized supernatant (laccase) is determined spectroscopically (UV/vis) and is based on the evaluation of the CuII T1 absorbance at 610 nm ($\epsilon=5600 \text{ L}\cdot\text{mol}^{-1}\cdot\text{cm}^{-1}$). Volume of the supernatant after gel filtration and concentration were determined by pipetting.

3.2 Enzyme loading measurement by Bradford Protein Assay



(1) 0.05 g BSA (bovine serum albumin) was weighed and dissolved into 50ml distilled water to prepare an initial 1 mg/ml solution; then diluted it with MQ water to final concentrations of 10, 20, 30, 40, 60, 80, 100 μ g/ml as standard samples. (2) Respectively add 700 μ l of MQ water, 200 μ l Coomassie Blue, and 100 μ l each of the above standard samples into 1cm Vis Cuvettes and mix them by inversion, wait 10 minutes. (3) Measure absorbance of the standard samples at wavelength 595nm, absorbance of [800 μ l MQ water plus 200 μ l Coomassie Blue] as concentration 0. (4) Plot the Standard Curve (the corresponding concentrations 0,1, 2, 3, 4, 6, 8, 10 μ g/ml respectively with considering the dilution of the protein in cuvette). (5) Measure absorbance of the laccase (supernatants) samples. (6) Calculate their concentrations using the prepared Calibrate Curve (see above).

3.3 Enzyme loading test by ELISA (Enzyme-Linked ImmunoSorbent Assay)

Materials: Coating buffer: (0.2 M sodium carbonate/bicarbonate, pH 9.4) 13.608g NaHCO₃ and 4.028 g Na₂CO₃ dissolve into 1 L MQ water, adjust pH to 9.4; Washing buffer: (0.1 M phosphate, 0.15 M sodium chloride, pH 7.2 containing 0.05% Tween 20) 3.864g NaH₂PO₄·H₂O, 10.224g Na₂HPO₄ and 8.76g NaCl dissolve into 1L MQ water, adjust pH to 7.2; add 0.05% (500 μ L) Tween 20; Blocking buffer: (2% (w/v) Bovine Serum Albumin (BSA) in Washing Buffer) 1g BSA dissolve into 50mL Washing buffer; Substrate solution: 1 tablet of PNPP (5mg) dissolve into 10mL glycine buffer (see instructions of the substrate).

Procedure: (1) Prepare a series of standard samples: dilute the standard enzyme to the appropriate concentrations in coating buffer at the plate in triplicate, allowing sufficient volume of 100 μ L in each well ; (2) Add 300 μ L blocking buffer to the other well which will be used to put the particles samples; (3) Cover plate, incubate at room temperature for 2 hour or at 4 °C overnight. (4) Remove the blocking buffer (not the standard enzymes) and add a series of particles at different concentration to the well which pre-incubated by blocking buffer in triplicate. (5) Remove all the solutions and wash the plate (including particles, using magnetic) with 200 μ L washing buffer 3 times, 5minutes each. (6) Add 300 μ L blocking buffer to each well, cover the plate and incubate on a thermomixer at 600rpm for 1 hour at room temperature. (7) Remove the blocking buffer. (8) Dilute the biotinylated

detection AC 5000×with blocking buffer, add 100 μL diluted biotinylated detection AC to each well. (9) Cover the plate and incubate at room temperature for 1 hour. (10) Remove the solution and wash 5 times with 200 μL washing buffer, 5 minutes each time. (11) Dilute the enzyme conjugate AP-streptavidin 1000×with 200 μL washing buffer, add 100 μL diluted AP-streptavidin to each well, cover the plate and incubate at room temperature for 1 hour. (12) Remove the solution and wash 7 times, 5 minutes each with washing buffer. (13) Add 100 μL substrate solutions to each well, wait until the desired color is reached. (14) Measure absorbance at 405nm. (15) Calculate the enzyme loading.

4 Fluorescence Qualitative Experiment

(1) 0.0012g dansylhydrazine was dissolved into 200 μL DMF+800 μL acetate buffer, 20mM, pH=5.7 to make a 1ml 4.2 $\mu\text{mol}/\text{mL}$ dansylhydrazine initial solution. (2) Then 100 μL of the 4.2 $\mu\text{mol}/\text{mL}$ dansylhydrazine solution was added to 900 μL of acetate buffer, 20mM, PH=5.7 to prepare the 0.42 $\mu\text{mol}/\text{mL}$ dansylhydrazine; produce two identical solutions using this way, one is for reacting with the magnetic particles, the other one is used for blank contrast. (3) Added 1ml the above 0.42 $\mu\text{mol}/\text{mL}$ dansylhydrazine solution to the prepared 1mg particles. (4) Incubate the reaction with continuous rotation at room temperature for 30 minutes. (5) After reaction, place the tube on the magnetic separator for separation, keep for a longer time to ensure that the separation is carried out adequately. (6) Take out of 100 μL the supernatant by pipette carefully to new tube, then add 900 μL acetate buffer, 20 mM, PH=5.7 for dilution(10 times), this 10 times dilution as sample supernatant. (7) Dilute the blank sample 10 times in the same way as sample blank. (8) First scan the sample blank at the UV spectrophotometer from 200 to 800 nm, find out the peak wavelength. (9) Use this value as the start excitation wavelength at the spectrofluorometer to debug test parameters (Excitation wavelength, Emission wavelengt, slit). (10) Test the fluorecence intensity of the above samples with FLUORMAX-4 spectrofluorometer (HORIBAJOBIN YVON, France) and recorded the data.

5 Biotransformation of Coniferyl Alcohol

(1) Prepare coniferyl alcohol solutions: 0.0036 g coniferyl alcohol dissolved in 100 μL ethanol and 900 μL 0.1 M pH=5,7 Acetate buffer to make 20 mM solutions. (2) Test free and immobilized enzyme activity and calculate enzyme amount. (3) Add the reactants to a 1 ml centrifuge tube and incubate at thermomixer at 30 $^{\circ}\text{C}$ 1000 rpm. (4) take 50 μL of the sample at a certain reaction time (for example 1 h, 2h...), add 50 μL of reference Benzophenone (0.0072 g benzophenone dissolved in 20mL Acetonitrile), mix well and remove the supernatant by magnetic separation. (5) Add 50 μL the above samples to the HPLC machine for testing. (6) Calculate the results.

Reference

- (1) Robert, V.; Monza, E.; Tarrago, L.; Sancho, F.; De Falco, A.; Schneider, L.; Npétag Ngoutane, E.; Mekmouche, Y.; Pailley, P. R.; Simaan, A. J.; et al. Probing the Surface of a Laccase for Clues towards the Design of Chemo-Enzymatic Catalysts. *ChemPlusChem* **2017**, *82* (4), 607–614. <https://doi.org/10.1002/cplu.201700030>.
- (2) McFarland, J. M.; Francis, M. B. Reductive Alkylation of Proteins Using Iridium Catalyzed Transfer Hydrogenation. *J. Am. Chem. Soc.* **2005**, *127* (39), 13490–13491. <https://doi.org/10.1021/ja054686c>.
- (3) Lalaoui, N.; Rousselot-Pailley, P.; Robert, V.; Mekmouche, Y.; Villalonga, R.; Holzinger, M.; Cosnier, S.; Tron, T.; Le Goff, A. Direct Electron Transfer between a Site-Specific Pyrene-Modified Laccase and Carbon Nanotube/Gold Nanoparticle Supramolecular Assemblies for Bioelectrocatalytic Dioxygen Reduction. *ACS Catal.* **2016**, *6* (3), 1894–1900. <https://doi.org/10.1021/acscatal.5b02442>.
- (4) Aldehyde magnetic beads | Bioclone <http://www.bioclone.us/aldehyde-terminated-magnetic-beads-particle-resin-matrix.html> (accessed Sep 3, 2019).
- (5) Jiang, J.; Oberdörster, G.; Biswas, P. Characterization of Size, Surface Charge, and Agglomeration State of Nanoparticle Dispersions for Toxicological Studies. *J. Nanoparticle Res.* **2009**, *11* (1), 77–89. <https://doi.org/10.1007/s11051-008-9446-4>.
- (6) Yan, B.; Li, W. Rapid Fluorescence Determination of the Absolute Amount of Aldehyde and Ketone Groups on Resin Supports. *J. Org. Chem.* **1997**, *62* (26), 9354–9357. <https://doi.org/10.1021/jo9712512>.
- (7) TR0065-ELISA-guide <https://www.thermofisher.com › sfs › brochures › TR0065-ELISA-guide> (accessed Sep 9, 2019).
- (8) Cruz, J. C.; Pfromm, P. H.; Tomich, J. M.; Rezac, M. E. Conformational Changes and Catalytic Competency of Hydrolases Adsorbing on Fumed Silica Nanoparticles: I. Tertiary Structure. *Colloids Surf. B Biointerfaces* **2010**, *79* (1), 97–104. <https://doi.org/10.1016/j.colsurfb.2010.03.036>.
- (9) Monza, E.; Lucas, M. F.; Camarero, S.; Alejaldre, L. C.; Martínez, A. T.; Guallar, V. Insights into Laccase Engineering from Molecular Simulations: Toward a Binding-Focused Strategy. *J. Phys. Chem. Lett.* **2015**, *6* (8), 1447–1453. <https://doi.org/10.1021/acs.jpcllett.5b00225>.
- (10) TurboBeads™Azide 742627
<https://www.sigmaaldrich.com/catalog/product/aldrich/742627> (accessed Sep 17, 2019).

- (11) Arsalan, A.; Younus, H. Enzymes and Nanoparticles: Modulation of Enzymatic Activity via Nanoparticles. *Int. J. Biol. Macromol.* **2018**, *118*, 1833–1847.
- (12) Micro particles, magnetic, amino functionalized 53572 <https://www.sigmaaldrich.com/catalog/product/sigma/53572> (accessed Sep 22, 2019).
- (13) Simeng, Z.; Rousselot-Pailley, P.; Lu, R.; Charmasson, Y.; Dezord, E. C.; Robert, V.; Tron, T.; Mekmouche, Y. Production and Manipulation of Blue Copper Oxidases for Technological Applications. *Methods Enzymol.* **2018**, *613*, 17–61.

General Conclusion

The main target of this research work was to develop effectors for laccase catalyzed reaction, with the aim to introduce some selectivity (e.g. chemical, regio or stereo) or any kind of control to the laccase catalytic system which is not selective per se. Specifically, we focused our interest on *At*DIR6, a plant dirigent protein as a natural model of laccase effector and on a bio-inspired system consisting in Magnetic NanoParticles (MNPs) functionalized with oriented laccases.

The recombinant *At*DIR6 protein we purified is known to change the fate of laccase-catalyzed bioconversion of coniferyl alcohol towards the exclusive formation of a single 8-8' dimer: the (-)-pinoresinol. During this work, we obtained evidences of *At*DIR6 activity on ferulic acid (FA), coniferyl acetate and coniferyl azide, all being natural or synthetic analogues of coniferyl alcohol with variations on the allylic chain. This represents the first indication that the specificity of *At*DIR6, and by analogy that of all (-)-pinoresinol forming DPs as well as probably that of the enantio complementary (+)-pinoresinol forming DPs, is not limited to CA itself, layering new ground for research in biocatalysis.

In our laboratory, it has been previously shown that *At*DIR6 stabilizes the CA^{+•} radicals prior to direct their coupling towards the formation of the (-)-pinoresinol. We know from our new room temperature EPR studies in solution that *At*DIR6 stabilizes the fugacious radicals of the CA analogues as well. Radical signals varying in intensity from substrate to substrate, observations from this work open unique possibilities for structure-function relationships studies.

Prior performing the stereoselective radical coupling reaction, how is a dirigent protein stabilizing (interacting with) these highly reactive species? Previous investigations in our laboratory on the reactivity of *At*DIR6 with the generic ABTS^{+•} radical used as a probe have revealed protein-radical adducts formation, in particular with tyrosines located in the CA binding cavity. Unprecedented, our preliminary MALDI TOF mass spectrometry differential analysis of *At*DIR6 prior to and after reaction with CA^{+•} radicals suggest that, during the coupling reaction, part of the protein may be eventually labelled through the formation of two stable adducts. The identification of such adducts could be a breakthrough in understanding the role of amino acids in the selective coupling of CA radicals.

In summary, we progressed towards the understanding of the elusive mechanism of radical coupling promoted by dirigent proteins, laying down the following landmarks: i) allylic hydroxyl group of coniferyl alcohol is not an essential part for substrate recognition by DP. Carboxylic, aceto and azido groups at least can substitute for the hydroxyl group of CA and are therefore selectively introduced in new neo-lignan structures; ii) substrate radicals are stabilized by DP prior coupling; iii) CA radicals form adducts with DP, potentially labelling residues critical for the reaction. Our results

not only provide new support information on a perfectly controlled radical coupling reaction, but also open new possibilities for the use of DP in the field of green synthetic chemistry.

The idea of the construction of an artificial effector of laccase activity is bioinspired from DPs function. Schematically, DPs provide different chemical environments out of the substrate oxidation centre of laccase. As a model, we choose MNPs with various surface functional groups a performed covalent immobilization of laccases precisely controlling the enzyme's orientation. The specific orientation of the enzyme's substrate oxidation center towards the MNP surface, in a close proximity to the functionalization shell, constitutes an original way to study the impact of different physicochemical environment on laccase activity.

Particles bearing long aliphatic or short aromatic aldehydes can both serve as platforms for a reductive alkylation of laccases surface through a lysine group strategically located either next to or diametrically opposed ($>30 \text{ \AA}$ away) to the CuII T1 copper center (i.e. oxidation site). The use of any of these laccase-functionalized particles for the oxidation of model synthetic (ABTS) or natural (CA) substrates leads to the same consistent observation: bringing the enzyme's oxidation center in the vicinity of the functionalization shell affects laccase activity. It is probable that the physical proximity of the enzyme's oxidation center with the particles surface is structurally limiting the accessibility of the active site to the substrates. However, beyond obvious considerations, a side by side examination of these different catalysts and their free counterparts points a discrimination of the phenolic substrate CA by a laccase, the oxidation site of which is exposed to aromatic aldehydes. Although the fact that benzaldehyde acts as a competitive inhibitor of CA remains to be independently established (i.e. in solution), the evolution on almost one order of magnitude of the performance of the different configurations of the catalyst supports an acquisition of a form of selectivity and validates our initial hypothesis.

The robustness of the enzyme allows performing two successive functionalization reactions to access azide environment via click chemistry. Changing chemical functions from aldehyde to azide seems to be accompanied by an effect on the phenolic substrate recognition. This effect might be more important than it first appears as it seems to partly compensate the structural effect linked to the creation of an interface between the enzyme oxidation center and the particle's shell otherwise significant on the synthetic substrate ABTS. As preliminary as end of project's experiments can be, the catalysts's behavior that they presently reflect would confirm the modulation of the acquired selectivity we initially postulated.

Recently cyclodextrines have been used in our laboratory in a first attempt to control the evolution of CA oxidation products.¹ CDs, somehow mimicking the DPs cavity, protect the neo-formed dimers from a further oxidation whereas they have no influence on CA oxidation itself. The

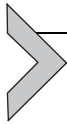
comparative study of the three different laccase-grafted MNPs systems presented here is a first approach to the modulation of laccase activity through a variation of chemical functions in the immediate vicinity of the substrate oxidation site.

Prior to this work, immobilization technologies were mainly used for the acquisition of stabilization and recyclability properties and to the best of our knowledge no research have focused on the oriented immobilization of enzymes and the effect of the microenvironment on their activity after immobilization. Beyond the modulation of laccase activity linked to the control of the orientation of the enzyme at the material's surface, our results argue for a careful construction of a structured chemical landscape around the substrate oxidation site. Combined to molecular evolution of the enzyme this could help to obtain a controllable laccase catalytic system in the future.

Reference

- (1) Tarrago, L.; Modolo, C.; Yemloul, M.; Robert, V.; Rousselot-Pailley, P.; Tron, T. Controlling the Polymerization of Coniferyl Alcohol with Cyclodextrins. *New J. Chem.* **2018**, *42* (14), 11770–11775.

Appendix



Production and manipulation of blue copper oxidases for technological applications

Simeng Zhou, Pierre Rousselot-Pailley, Lu Ren, Yolande Charmasson, Elise Courvoisier Dezord, Viviane Robert, Thierry Tron, Yasmina Mekmouche*

Aix Marseille Université, CNRS, Centrale Marseille, iSm2, Marseille, France

*Corresponding author: e-mail address: y.mekmouche@univ-amu.fr

Contents

1. Introduction	19
2. Heterologous production of fungal laccases	22
2.1 Cloning	23
2.2 Transformations	26
2.3 Screening for laccase secreting transformants in <i>S. cerevisiae</i> and <i>A. niger</i>	33
2.4 Fermentation in <i>A. niger</i>	40
3. General purification procedure and characterization	41
3.1 Purification procedure	41
4. Applications	47
4.1 General procedure for an oriented covalent grafting of the laccase surface	49
4.2 Hybridization with materials	55
5. Conclusions	56
Acknowledgment	56
References	56
Further reading	60

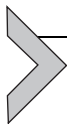
Abstract

Fungal laccases are robust multicopper oxidoreductases. Perfectly amenable to synthetic evolution, the fungal laccase scaffold is a potential generic for the production of tailored biocatalysts, which, in principle, can be secreted at substantial levels in industrially relevant organisms. In this chapter, the strategy we have developed for the rapid production of hundreds of milligram of laccase variants is detailed. It is based on the use of two heterologous expression hosts: the yeast *Saccharomyces cerevisiae* for a rapid upstream screening and the fungus *Aspergillus niger* for downstream production.

Methods for screening active and nonactive laccase variants, convenient setups for enzyme production in both organisms as well as a methodology for efficient purification of large amounts of recombinant enzymes are given. The general procedure for developing new materials for artificial catalysis is also described.

Abbreviations

AA	amino acid
Ab-LAC	polyclonal anti-lac3 antibody
ABTS	2,2'-azino-bis(3-ethylbenzothiazoline-6-sulfonic acid)
ABTS^{•+}	ABTS stable radical cation
AIP	alkaline phosphatase
ATA	aurin tricarboxylic acid ammonium salt
Bp	base pair
BSA	bovine serum albumin
DEAE	diethylaminoethanol
DNA	deoxyribonucleic acid
DTT	dithiothreitol
ELISA	enzyme-linked immunosorbent assay
FPLC	fast protein liquid chromatography
GRAS	generally regarded as safe
MWCN	multiwall carbon nanotube
MWCO	molecular weight cut off
PBST	phosphate buffer saline with tween 20
PCR	polymerase chain reaction
PEG	polyethylene glycol
PES	polyethersulfone
pNPP	4-nitrophenyl phosphate disodium salt hexahydrate
PPD	<i>p</i> -phenylenediamine
rpm	rotation per minute
RT	room temperature
SD	synthetic defined
SDS-PAGE	sodium dodecyl sulfate-polyacrylamide gel electrophoresis
SGZ	syringaldazine
SN	supernatant
sp	signal peptide
ss	single strand
STC	sodium tris chloride
TFA	trifluoroacetic acid
TFF	tangential flow filtration
TNC	trinuclear cluster
UF	ultrafiltration
UNIK	single lysine LAC3 variant
UV-vis	ultraviolet-visible
YPD	yeast extract-peptone-dextrose
<i>ε</i>	molar extinction coefficient



1. Introduction

New technologies for a more sustainable society are urgently needed (Kates, 2017). Considering the needed change of paradigm from fossil to renewable feedstock, a selective and efficient conversion of bioresources is crucial and will have a real impact on the sustainability of our developed society (Armstrong & Blundell, 2007). A number of current industrial processes feature catalytic methods for aerobic oxidation. However, their long-term use is condemned as reagents such as metal-oxide or chlorine-based oxidants are often required, generating organic and heavy metal wastes with safety concerns (Anastas & Warner, 1998). As an oxidant, dioxygen (O_2) is available at no cost and produces no environmentally hazardous by-products. Therefore, catalytic systems capable of selective oxidation reactions driven by clean dioxygen reduction with no by-products represent an important asset to progress toward sustainability.

Nowadays, the principle of using enzymes for large-scale industrial processes is well established (Kirk, Borchert, & Fuglsang, 2002; Meyer et al., 2013; Nestl, Hammer, Nebel, & Hauer, 2014). Limitations to the use of these excellent (enantio) selective and renewable catalysts, such as good operational stability or high production costs remain, but are progressively overcome thanks to the availability of constantly improving molecular evolution, fermentation, and immobilization methodologies.

Laccase (EC 1.10.3.2 from plant, fungi, or bacteria) is a particularly robust and well-studied biocatalyst. This copper-containing enzyme (four copper ions) couples the oxidation of a wide range of substrates to the neat reduction of one molecule of dioxygen to two water molecules. In the past 2 decades, a significant number of reports have illustrated the potential of this enzyme in technological and bioremediation processes (e.g., bleaching, clarification of beverages, detoxification, sensors) (Zucca, Cocco, Sollai, & Sanjust, 2016), focusing on its stability and efficiency (Alcalde, Ferrer, Plou, & Ballesteros, 2006; Couto & Toca-Herrera, 2006, 2007), as well as on its adaptability (plasticity) to different reaction conditions (e.g., tolerance to different organic solvents) (Kunamneni et al., 2008). Recent reviews address the use of laccases in these different fields (Cannatelli & Ragauskas, 2017; Mate & Alcalde, 2017) as well as in organic synthesis (Cracknell, Vincent, & Armstrong, 2008; Mikolasch & Schauer, 2009; Riva, 2006; Witayakran & Ragauskas, 2009) and in biofuel cells, in which they are wired

on solid support and serve as the cathodic catalyst reducing dioxygen to water (Fernández-Fernández, Sanromán, & Moldes, 2013; Gutiérrez-Sánchez, Pita, Vaz-Domínguez, Shleev, & De Lacey, 2012; Jones & Solomon, 2015; Lalaoui et al., 2016; Le Goff, Holzinger, & Cosnier, 2015; Milton & Minter, 2017; Pistone et al., 2016; Pita et al., 2011, 2014; Qiu et al., 2009; Shleev et al., 2005; Shleev, Pita, Yaropolov, Ruzgas, & Gorton, 2006). Recently, the potential of laccases for the development of molecular hybrid catalysts has been demonstrated (Lazarides et al., 2013; Mekmouche et al., 2015; Schneider et al., 2015; Simaan et al., 2011; Tarrago et al., 2018).

Genes encoding laccases from different origins have been heterologously expressed with various successes in bacteria, yeasts, filamentous ascomycetes, basidiomycetes, or plants reaching expression levels of up to a gram per liter (Alves et al., 2004; Kiiskinen et al., 2004; Record et al., 2002). Both variation of the cultivation conditions and mutagenesis in a given host can be used to tune production (Bulter et al., 2003; Mate et al., 2010; Rodgers et al., 2010). In addition, well-established protein engineering methodologies are available for modulating enzyme properties such as redox potential, pH tolerance, and thermostability (Mate & Alcade, 2015). However, it is noteworthy that a complex posttranslational maturation of the enzyme is influencing expression of laccases genes as well as the diversity obtainable among synthetic variants. The two copper-containing redox centers of laccases—a blue copper site located near the surface (oxidation of substrates) and an embedded trinuclear copper center (O₂ reduction) (Fig. 1) (Jones & Solomon, 2015; Riva, 2006; Solomon et al., 2014; Solomon, Szilagyi, DeBeer George, & Basumallick, 2004; Tron, 2013)—need to be precisely inserted within the three cupredoxin domains that are typical of proteins from the multicopper oxidase family. Moreover, fungal laccases are secreted, a process involving both enzymatic decorations of the enzyme surface with sugar moieties (glycosylation) and of the signal sequence by specific peptidase(s) during secretion. Thus, maximizing the production of fungal laccase variants requires a careful selection of the initial sequences, highly secreting hosts and a simple and straightforward selection procedure. Since the “perfect” host (allowing both selection and production at the same time) does not exist, best performances are obtained by splitting the process into two steps: (1) selection of variants (from sequences initially propagated in *Escherichia coli*) and (2) production of selected variants, involving each a specialized heterologous expression host (e.g., yeasts for step 1 and filamentous fungi for step 2).

We have forged our own experience in large-scale production of recombinant laccases from the study of isoenzymes originating from the fungus

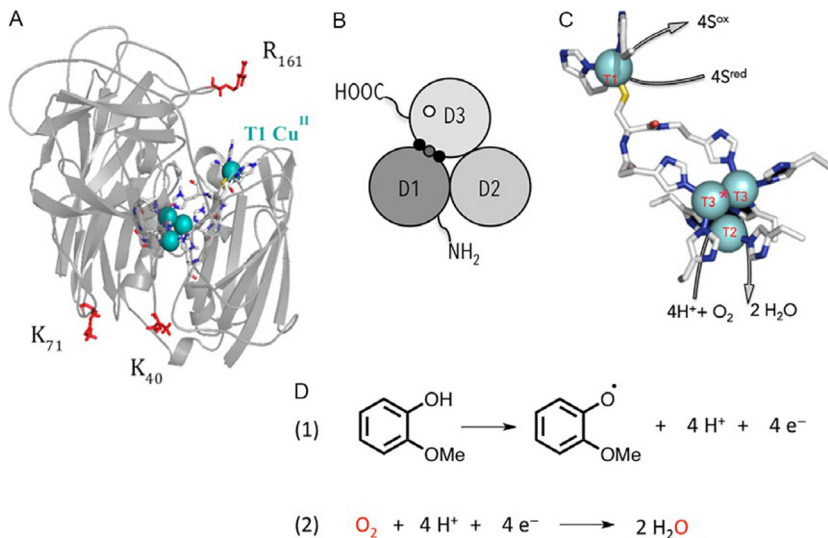


Fig. 1 Structure and function of laccase. (A) Structural model (*ribbon*) of LAC3 from *Trametes* sp. C30 with amino acids subjected to mutagenesis colored in *red*; Cu(II) ions are depicted as *blue spheres*. (B) Cartoon of the three cupredoxin domains (D1, D2, and D3) in the laccase structure; *white circle*, T1 copper ion; *gray circle*, T2 copper ion, *black circle*, T3 copper ions. (C) Close-up of the copper-active sites; *blue spheres*: copper ions annotated T1, T2, and T3. * This sign stands for the presence of a hidden histidine residue coordinated to the T3 copper site. (D) Overall outcome of the catalytic reaction.

Trametes sp. C30 (Robert, Mekmouche, Rousselot-Pailley, & Tron, 2011). The isoenzyme LAC3, which is the enzyme pivotal to all of our studies since 2005, has been selected from a functional screen of the yeast *Saccharomyces cerevisiae* transformants. LAC3, and several of its variants are produced in the yeast *S. cerevisiae* in the milligram per liter range (Balland et al., 2008; Cusano, Mekmouche, Meglec, & Tron, 2009; Klonowska et al., 2005; Liu et al., 2014). Further, recombinant laccase production has recently been scaled up to levels of nearly 1 g L^{-1} , through the transformation and subsequent optimization of fermentation conditions in the GRAS ascomycete *Aspergillus niger* (Mekmouche et al., 2014). Altogether, these works highlight the potential of combining a generic laccase sequence with yeast and fungal expression systems for the generation and large-scale production of variants. Demonstrations of the practical use of this combination can be found in our most recent works on the production and use of robust laccase-based hybrids catalysts (Lalaoui et al., 2016; Mekmouche et al., 2015; Robert et al., 2017; Schneider et al., 2015).

In this chapter, we will detail our methodologies to produce large-scale synthetic laccases with desired properties for the purpose of developing new

offers possibilities: (i) to overcome the production of several isoenzymes resulting from the coexpression of multiple laccase-encoding genes usually found in parental organisms; (ii) to produce laccases from genes poorly expressed in parental organisms; (iii) to engineer a laccase by random or rational mutagenesis to improve its properties (e.g., stability vs pH, $T^{\circ}\text{C}$, solvents). Recent reviews covering laccase engineering are available (Alcalde, 2015; Mate & Alcade, 2015; Pardo & Camarero, 2015; Rodgers et al., 2010).

As mentioned, our reference enzyme is LAC3, a laccase from *Trametes* sp. C 30. Cloning and heterologous expression of laccase *Trametes* sp. C 30 cDNAs has been undertaken to select enzymes with high oxidative capacities. In particular, *clac3* (GenBank accession number AY397783), which encodes a laccase isoform previously undetected in fungal cultures, has been isolated and successfully expressed in the yeast *S. cerevisiae* (Klonowska et al., 2005).

2.1 Cloning

Laccase-encoding sequences (cDNA, synthetic genes) are fused to bacteria/yeast shuttle vectors that are either commercially available (ex. Gateway™ pYES-DEST52 Vector) or custom (ex. pAK145, a constitutive yeast expression vector the construction of which is detailed in Klonowska et al., 2005) and are propagated in *E. coli* strain DH5 α (F⁻ Δ 80lacZ Δ M15 Δ (lacZYA-argF)U169 deoR recA1 endA1 hsdR17(rk⁻, mk⁺) phoA supE44 thi-1gyrA96 relA1 λ ⁻) using standard techniques (Sambrook, Fritsch, & Maniatis, 1989). Note that the secretion signal (encoding the signal peptide) to be fused to the sequence encoding the mature peptide is a matter of tuning. Heterologous peptides like the yeast alpha factor sp (Camarero et al., 2012; Mate et al., 2010) or that of the yeast invertase (Klonowska et al., 2005) are often chosen to replace the native laccase sp although in our hand the latter was found to lead to LAC3 secretion as well (Klonowska, unpublished results). In addition, improvements in the secretion (and therefore the production) of laccases have been linked to the accumulation of mutations in the sp during molecular evolution rounds (Bulter et al., 2003; Camarero et al., 2012; Mate et al., 2010). We sought both cloning methods to produce recombinant laccases and variants, i.e., a rational and a random method (Fig. 3).

2.1.1 Site-directed mutagenesis

Site-directed mutagenesis (Fig. 3A) is the basis for structure and function studies (Mate & Alcade, 2015). In this view, a 3D structure of the favorite

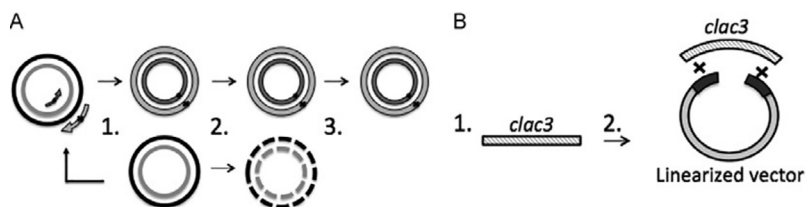


Fig. 3 Selected methods for producing variants of laccase. (A) Rational-directed mutagenesis: (1) mutant strand synthesis containing the targeted mutation; (2) digestion of template; and (3) transformation of mutated molecule into competent cells. (B) Gap repair technique: (1) gene of interest and (2) yeast transformed with vector and insert and homologous recombination to repair the gap.

enzyme or, failing that, a robust model (easily obtainable from web-based protein modeling platforms like SwissProt, PMP, Modeller, etc.) is highly recommended. Through site-directed mutagenesis, we have challenged the plasticity of our favorite enzyme (Klonowska et al., 2005; Liu et al., 2014), as well as its robustness in electrocatalysis (Balland et al., 2008; Lalaoui et al., 2016) or in chemo-enzymatic catalysis involving electron transfer from a transition metal catalyst (Mekmouche et al., 2015; Schneider et al., 2015) or from photosensitizers (Robert et al., 2017) (see Table 1). Replacement of selected sequences or codons in the *lac3* original coding sequence was obtained using a commercial kit (QuikChange[®], Stratagene[™]). Mutated laccase sequences were constructed by designing the appropriate primers and following the recommendation of the manufacturer (Stratagene).

Recently, we started the construction of single lysine laccase variants of LAC3 with the intention of obtaining genetically defined, single surface-located, primary amino group variants amenable for posttranslationally site-directed chemical modification. A three-step semiempirical strategy was used in order to achieve the following aims: (i) To replace the only two lysine residues (K_{40} and K_{71}) naturally present in the mature sequence of LAC3 (Fig. 1A). Libraries of sequences coding $K_{40}Q$, M or I and $K_{71}H$, A , R , E (representing natural variations found at positions 40 and 71) were constructed from which the variant K_0 ($K_{40}M$, $K_{71}H$) devoid of lysine was selected: (ii) To replace a chosen surface accessible residue by a lysine, for example, in the UNIK₁₆₁ ($R_{161}K$) variant (Lalaoui et al., 2016; Robert et al., 2017).

2.1.2 Yeast recombination

In vivo gene cloning or gap repair is a very efficient and fast method by which to assemble recombinant DNA in the yeast *S. cerevisiae* (Fig. 3B). This method produces, in a single step, propagatable circular DNA by homologous recombination between a linearized vector (gap) and a linear

Table 1 Variants of LAC3 engineered by site-directed mutagenesis

Study	Characterization	Main Results	References
Functional expression in yeast	E° T1; EPR spectroscopy; activity	Characterization of recombinant enzyme and comparison with homologous LAC1 and LAC2 from <i>Trametes</i> sp. C30	Klonowska et al. (2005)
Immobilization of LACCASE on electrode	Electrocatalysis; activity; spectroscopy	Characterization of a self-assembled monolayer immobilized laccase. Redox-mediated electrocatalysis	Balland et al. (2008)
Functional expression of C- and N-terminus modified laccases	Activity	Characterization and comparison of C-terminal modified laccases: depleted or/and His-tagged. Effect of glycosylation pattern on activity	Liu et al. (2014)
Oriented immobilization of LAC on electrodes to maximize direct electron transfer	Molecular biology; spectroscopy; activity; electrocatalysis	Efficient direct electron transfer for reduction of dioxygen using nanostructured electrodes modified with a site-specific surface modification laccase (single covalently bound pyrene group close to the T1 center)	Lalaoui et al. (2016)
Controlled orientation of a graft at the surface of a fungal laccase	Spectroscopy; activity; molecular biology; covalent docking; molecular dynamics simulations	Engineering of laccase variants with unique surface accessible lysine residues and orientated covalent grafting of a photosensitizer to promote photocatalysis. Simulation studies fit well with observed reactivity	Robert et al. (2017)

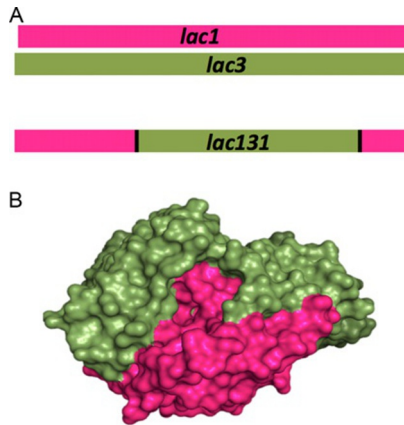


Fig. 4 Construction of laccase chimeras through yeast homologous recombination of *Trametes* sp. strain C30 laccase cDNAs sharing 65%–71% identity. (A) Schematic view of intermolecular recombination events between the *lac1* and *lac3* parental genes and the resulting hybrid *lac131* gene. Genes are represented by rectangles of variable lengths and recombinant junctions are represented by vertical black bars. (B) Molecular models of LAC131 hybrids constructed using the structure of the laccase 2HRG from *Trametes trogii* as template. The surface of LAC3 is colored in green; that of LAC1 is colored in pink. Adapted from Cusano, A. M., Mekmouche, Y., Meglecz, E., & Tron, T. (2009). Plasticity of laccase generated by homeologous recombination in yeast. *FEBS Journal*, 276, 5471–5480.

overlapping DNA fragment (insert) cotransformed in yeast (Oldenburg, Vo, Michaelis, & Paddon, 1997; Orr-Weaver, Szostak, & Rothstein, 1983). The recombination occurs within short homologous sequences between the vector and the insert. Laccase-encoding sequences sharing 65%–71% identity (*lac1*, *lac2*, *lac3*, and *lac5*) have been shuffled in vivo by homologous recombination in yeast using a *lac3* PCR fragment as the repair sequence. In recombinant sequences, junctions have been found to map within short stretches of identity varying from 5 to 45 base pairs. Three chimeric laccases (LAC131, LAC232, and LAC535) have been isolated and characterized (Fig. 4). This single random mutagenesis step has led to the generation of variants having extended pH tolerance toward alkaline conditions (Cusano et al., 2009).

2.2 Transformations

2.2.1 *S. cerevisiae*

The yeast *S. cerevisiae* W303-1A (*MATa* {*leu2-3,112 trp1-1 can1-100 ura3-1 ade2-1 his3-11,15*}) is transformed with recombinant DNA materials using either a lithium acetate/ss DNA carrier/PEG protocol (Gietz & Woods,

2002) or electroporation (Becker & Guarente, 1991). After transformation, cells are spread on selective media and plates are incubated at 28°C for 4 days. Below is a brief description of: (i) the preparation of electrocompetent cells; (ii) electroporation; and (iii) plating.

Equipment

1. Temperature-controlled orbital shaker set at 30°C.
2. Stationary incubator at 30°C.
3. Electroporation cuvette (sterile).
4. Electroporator (e.g., Eppendorf Eporator[®]).
5. Floor centrifuge.
6. UV-vis spectrometer.

Buffers and reagents

Sterilization is performed by autoclaving unless otherwise specified. Standard recipes can be found in *Methods in Enzymology*.

1. YPD (1% yeast extract, 2% peptone, 2% dextrose) medium.
2. 1 M sorbitol in sterile distilled water.
3. Yeast strain (e.g., *S. cerevisiae* W303-1A).
4. Synthetic dextrose (SD) medium agar.

Example: YNB without AA, 0.67%; dextrose, 2%; adenine, 30 mgL⁻¹; casein hydrolysate, 0.5%; tryptophan, 40 mgL⁻¹; CuSO₄, 100 μM; 50 mM succinate buffer pH 5.3; 15 gL⁻¹ Agar. Sterile (filtered through Ø0.2 μm filter) adenine, tryptophan, and guaiacol solutions are added postautoclave. Note that the composition of this medium has been optimized for the selection of uracyl prototrophs (*URA3* marker as part of the expression plasmid) secreting laccase.

Procedure

- Electrocompetent cells
 1. A fresh culture is prepared by growing 5 mL of *S. cerevisiae* strain in YPD in a 50 mL conical tube at 30°C, at 160 rpm overnight in order to reach an OD₆₀₀ = 1.3–1.5. The preparation can be started directly from a plate.
 2. The cells are centrifuged at 1500 × g for 5 min at 4°C in a precooled rotor, the pellet is retained and the supernatant is discarded. This step allows for concentrating the cells.
 3. The pellet is resuspended with 5 mL of *ice-cold* sterile water, vortexing the cells if necessary.
 4. The cells are centrifuged as in step 2, the pellet is resuspended with 2.5 mL of *ice-cold* sterile water.
 5. The cells are centrifuged as in step 2, the pellet is resuspended in 1.5 mL of *ice-cold* 1 M sorbitol.

6. The cells are centrifuged as in step 2, then the pellet is resuspended in 0.1 mL of *ice-cold* 1 M sorbitol to a final volume of approximately 0.15 mL. *The cells are kept on ice for immediate use, not stored.*
- Electroporation
 7. Yeast suspension (50 μ L) from step 6 is mixed with 2 μ g of plasmid (in 5 μ L sterile water) in a sterile Eppendorf tube.
 8. The mixture is transferred to an ice-cold 0.2 cm sterile electroporation cuvette.
 9. The cuvette is placed on ice for 5 min.
 10. The cells are pulsed according to the parameters for *S. cerevisiae* as suggested by the manufacturer of the specific electroporation device used.
 11. Ice-cold 1 M sorbitol (1 mL) is added immediately to the cuvette using a sterile pipette. After mixing gently, the cuvette contents are transferred to a 15 mL sterile tube.
 12. The tube is incubated at 30°C without shaking for 1 h.
- Plating
 13. Aliquots (200 μ L) of the transformation (either LiAc or electroporation) are plated on SD plates. Transformants are selected for the appropriate prototrophy resulting from the complementation of one of the auxotrophies of *S. cerevisiae* W303-1A after transformation (corresponding to the selection marker present on the plasmid).
 14. Plates are incubated for 2–3 days at 30°C until colonies form.
 15. 10–20 colonies are chosen and streaked onto fresh SD plates. It is possible to screen for laccase activity/extracellular production by plating on an activity plate (i.e., containing guaiacol or ABTS), as will be further discussed in [Section 2.3.2](#).

2.2.2 *A. niger*

Efficient expression in *A. niger* requires multiple integrations of the heterologous sequence to the genome. We are routinely using the strain D15#26 [(*pyrG*⁻) (*prtT*) (*phmA*)] ([Gordon et al., 2000](#)) and plasmids pAN52-4 (EMBL accession number Z32750) for laccase sequence subcloning and pAB4-1 harboring *pyrG* as selection marker ([van Hartingsveldt, Mattern, van Zeijl, Pouwels, & van den Hondel, 1987](#)) all obtained from Peter Punt's laboratory. The following procedures have been adapted from previously published works ([Mekmouche et al., 2014](#); [Punt & van den Hondel, 1992](#); [Record et al., 2002](#)).

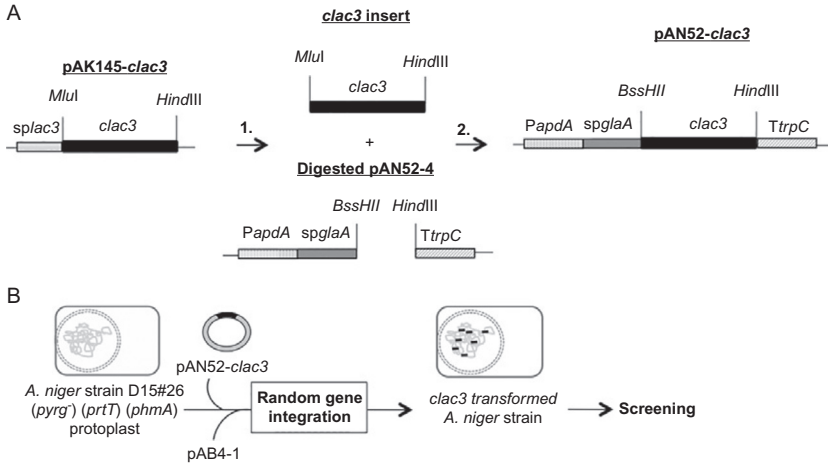


Fig. 5 (A) Description of the gene expression vectors for LAC3 plasmid pAK145-*clac3* for *S. cerevisiae* expression and plasmid pAN52-*clac3* for *A. niger* expression. The cloning restriction sites are annotated and signal peptides are indicated as sp (*splac3* for pAK145-*clac3* and *spglaA* for pAN52-*clac3*). The constitutive promoter is the untranslated region *PgdpA*. The terminator gene is *trpC*. (B) Schematic description of pAN52-*clac3* and pAB4-1 transformation of *A. niger* [strain D15#26 (*pyrg⁻*) (*priT*) (*phmA*)]. (i) The host strain is sensitive to the antibiotic; (ii) preparation of protoplasts competent for DNA integration and subsequent regeneration; and (iii) selection procedures for optimal transformation frequencies. From Punt, P. J., & van den Hondel, C.A. (1992). Transformation of filamentous fungi based on hygromycin B and phleomycin resistance markers. *Methods in Enzymology*, 216, 447–457.

a. Construction of a pAN52-laccase expression plasmid

The sequence encoding a laccase of interest (a *MluI/HindIII* PCR fragment encompassing the sequence coding for the mature LAC3 in our case) is easily inserted at the *BssHIII/HindIII* sites of the pAN52-4 vector and is known as pAN52-*clac3* (Fig. 5). In the recombinant molecule, the sequence encoding the mature laccase is fused to a synthetic signal sequence (from the glucoamylase gene) and flanked by the 5' untranslated region of the glyceraldehyde-3-phosphate dehydrogenase gene (constitutive promoter) and the terminator region of the *trpC* gene from *A. nidulans*. The plasmid is propagated in *E. coli* (ampicillin resistance) (Fig. 5).

Site-directed mutagenesis can be directly performed on this expression vector. *K₀*, a variant of LAC3 devoid of lysine was constructed starting from pAN52-*clac3* expression plasmid (unpublished).

b. Transformation of *A. niger*

A. niger D15#26 is transformed by the pAN52-*lac* plasmid along with the pAB4-1 plasmid that houses the auxotrophic marker *pyrG* (cotransformation) as described by Punt and van den Hondel (Punt & van den Hondel, 1992; van Hartingsveldt et al., 1987). Stable *pyrG*⁺ transformants resulting from recombination at the *pyrG* locus are selected for uridine prototrophy. Cotransformants with multiple random integration of the laccase-encoding sequence in the *A. niger* genome are selected for laccase activity.

Equipment

1. Malassez cell counting chamber.
2. Microscope.
3. Temperature-controlled orbital shaker.
4. Ø90 mm Petri dish plates.

Buffers and reagents

1. *A. niger* [strain D15#26 (*pyrG*⁻) (*prtT*) (*phmA*)].
2. Trace elements (1000×) solution: 76 mM ZnSO₄, 178 mM H₃BO₃, 25 mM MnCl₂, 18 mM FeSO₄, 7.1 mM CoCl₂, 6.4 mM CuSO₄, 6.2 mM Na₂MoO₄, 174 mM EDTA.
3. Complete medium: 70 mM NaNO₃; 3.7 mM KCl, 11 mM KH₂HPO₄, 2 mM MgSO₄, glucose 1% (w/v), trace elements (1×), 10 mM uridine; 2 gL⁻¹ casaminoacid; 5 gL⁻¹ yeast extract.
4. Solid minimum medium: 70 mM NaNO₂, 3.7 mM KCl, 11 mM KH₂HPO₄, 2 mM MgSO₄, glucose 1% (w/v), trace elements (1×) 15 gL⁻¹ agar. Make the final solution 50 mgL⁻¹ CuSO₄, 5H₂O, and 0.2 mM ABTS from sterile stock solutions prior to gelification (hardening) if a laccase activity detection is desired.
5. Vector pAB4-1 containing the *pyrG* selection marker.
6. STC buffer: 1.2 M sorbitol; 10 mM Tris-HCl, pH 7.5, 50 mM CaCl₂·2H₂O, 35 mM NaCl.
7. CaCl₂ buffer: 0.27 M CaCl₂·2H₂O; 0.6 M NaCl.
8. PEG buffer: 60% PEG 4000; 10 mM Tris-HCl, pH 7.5; 50 mM CaCl₂·2H₂O.
9. pAN-52-*lac*.
10. Glucanex from Sigma (L1412).
11. ATA (aurin tricarboxylic acid ammonium salt, 10–20 mM, MERCK).
Trace elements stock solution: 76 mM ZnSO₄, 178 mM H₃BO₃, 25 mM MnCl₂, 18 mM FeSO₄, 7.1 mM CoCl₂, 6.4 mM CuSO₄, 6.2 mM Na₂MoO₄, 174 mM EDTA.

12. Minimum medium: 70 mM NaNO₃, 7 mM KCl, 200 mM Na₂HPO₄, 2 mM MgSO₄, 50 gL⁻¹ glucose, 50 mgL⁻¹ CuSO₄, 5H₂O. Then add 1‰ of trace element stock solution and adjusted to pH 5 with a 1 M citric acid solution.
13. Tween 80–water: 10 drops of tween 80 in 10 mL of water.
14. Sterile 1 M citric acid.

Procedure

- Generation of protoplast

Protoplasts generation is generally the basis for fungal transformation: it is followed by a PEG/CaCl₂-mediated DNA uptake.

1. 250 mL of complete medium is inoculated in a 1 L conical flask at a final concentration of 2×10^6 spores mL⁻¹ (described in [Section 2.2.2](#), Mass production of spores) and incubated with shaking at 150 rpm (24 h) at 30°C.
 2. The spent medium is filtered through sterile miracloth. The collected mycelium is washed with CaCl₂ buffer, resuspended in CaCl₂ buffer (5 g mycelium in 50 mL buffer) containing Glucanex (500 mg)^a and incubated at 30°C for 2 h in an orbital shaker (80 rpm) ([Li, Tang, Lin, & Cai, 2017](#)).
 3. The protoplast suspension is then filtered through sterile miracloth, gently resuspended in the same volume of cold STC buffer and centrifuged at $1026 \times g$ at 4°C for 15 min. Protoplasts should be visualized as a small white strip at the bottom of the tube.
 4. The supernatant is carefully decanted and the protoplasts are resuspended in 25 mL of cold STC buffer. The suspension is then centrifuged at $1478 \times g$ at 4°C for 10 min.
 5. After removing the supernatant the protoplasts are resuspended in 1 mL of cold STC buffer, and kept on ice. At this stage, the number of protoplasts (with an appropriate dilution) is estimated by counting them with a Malassez cell counting chamber under a microscope. The count should be between 10×10^7 and 10×10^8 protoplast mL⁻¹.
- Transformation of protoplasts
 6. In a cell culture tube, 1 μL ATA, 10 μg of pAN-52-lac, 2 μg of pAB4-1 and 150 μL of protoplasts are mixed well and incubated for 30 min at RT.

^a The enzyme mix used for cell wall digestion originally used in the reference publication is no longer available. Satisfactory results have been obtained with the Glucanex preparation from Sigma that is therefore used as replacement.

7. PEG buffer (850 μL) is added, mixed well, and the suspension is incubated at RT for 20 min.
 8. After adding 10 mL STC buffer, the suspension is centrifuged at $1864 \times g$ at 4°C for 10 min and the supernatant is removed.
 9. The protoplasts are resuspended in 1 mL of STC buffer.
- Plating and selection
 10. About 50 μL of solution from step 9 are plated on solid selective minimum medium (\varnothing 90 mm Petri dish plates) and incubated for 4 days at 30°C . Note that it is possible (and easy) to screen for laccase-secreting transformants already at this stage by plating transformants on ABTS-containing plates. See [Section 2.3.2](#) for further details.
 - Mass production of spores

It is necessary to obtain spores (from the parental strain or from transformants) for conservation (storage) as well as for the initiation of further steps of screening and enzyme production.

Equipment

1. Stationary incubator set at 30°C .
2. Large (\varnothing 150 mm) Petri dish plates.
3. Miracloth filter.
4. Malassez cell counting chamber.
5. Microscope.

Buffers and reagents

1. Solid minimum medium: the same composition as above is used for transformants selection.
2. 500 mL physiological water supplemented with 10 drops of tween 80.
3. 1 L of sterile water in a 1 L Erlenmeyer flask.

Procedure

1. Minimum medium agar plates are prepared. About 15 large plates should be necessary for generating enough spores to inoculate 8 L of culture in a bioreactor.
2. Plating is carried out, using about 50 μL of spores stock solution per plate, and these are incubated for 10 days at 30°C to allow vegetative growth and a subsequent sporulation. A 1-L Erlenmeyer flask full of sterile water is placed in a top bench incubator chamber to maintain a humid atmosphere and prevent plates from drying out over time.
3. After 10 days, the dark spores are collected with 10 mL of saline/tween 80 solution per plate and filtered through a sterile film (Miracloth) to eliminate traces of agar and mycelium debris.

4. A few microliters of a known dilution of the sample is introduced to a Malassez cell counting chamber, and the number of spores is estimated under a microscope.
5. The spores can be stored in 15% of glycerol saline solution and kept at -80°C until further use.

2.3 Screening for laccase secreting transformants in *S. cerevisiae* and *A. niger*

Clone-to-clone variations in expression and/or secretion levels are high both in *S. cerevisiae* and in *A. niger*. It is therefore important to reach transformation frequencies allowing screening on a sufficient number of clones (typically a few tens to several hundred in the case of libraries) in order to select the best secretors. Laccase secretors are selected either for their ability to oxidize a laccase substrate (e.g., using an activity test with ABTS or guaiacol) or for their specific reaction with an antilaccase antibody (immunodetection is especially useful in the case of production of nonactive enzyme, such as a T1-depleted enzyme). Screening tests can be performed on activity plates (primary screening) and thereafter on liquid cultures of isolated clones for both organisms. Deep-well plates and microtiter plates are adapted to the cultivation of *A. niger* and *S. cerevisiae* transformants, respectively.

2.3.1 Screening of clones from deep-well or microtiter plate cultures

This is a convenient method for rapid screening of a large number of parallel liquid cultures of transformants from both *S. cerevisiae* and *A. niger*.

- a. Cultivation of *S. cerevisiae* transformants in microtiter plate

Equipment

1. Floor centrifuge (equipped with microplate holder).
2. Rotary incubator.

Buffers and reagents

1. Sterile SD medium (see [Section 2.3.1](#)).

Procedure

1. A 96-well microtiter plate is filled with 300 μL of SD medium.
2. Each yeast colony is inoculated with a sterile toothpick.
3. Cells are grown for 3 days at 30°C .
4. An aliquot of 10 μL of this cell suspension is taken and inoculated 300 μL of fresh SD medium.
5. The culture is grown for 24 h at 30°C .

6. Cells are pelleted at 3000 rpm for 2 min, and the supernatant (SN) is retained in a clean microtiter for measuring activity and protein concentration (see [Section 2.3.3](#)).

b. Cultivation of *A. niger* transformants in deep-well plates

Equipment

1. Polypropylene 24 deep-well plates (Whatman INC, Piscataway, USA).
2. Breathable sterile sealing film (Breathseal, Greiner Bio-One).
3. Shaking incubator.
4. Malassez cell counting chamber.
5. Microscope.

Buffers and reagents

1. Trace elements stock solution (see [Section 2.2.2](#), part b).
2. Minimum medium: 70 mM NaNO₃, 7 mM KCl, 200 mM Na₂HPO₄, 2 mM MgSO₄, 50 g L⁻¹ glucose, 50 mg L⁻¹ CuSO₄, 5H₂O. Then add 1‰ of trace element stock solution adjusted to pH 5 with a 1 M citric acid solution.
3. Tween 80–water: 10 drops of tween 80 in 10 mL of water.
4. Sterile 1 M citric acid.

Procedure

1. Samples of stored spores, prepared according to the protocol of [Section 2.2.2](#) (mass production of spores), are thawed.
2. Each well of a 24 deep-well plate (containing 3 mL of sterile minimum medium) is inoculated at final concentration of 1×10^6 spores mL⁻¹, and 100 μL of sterile tween 80–water is added to each well to avoid adhesion of spores.
3. The deep-well plate is covered with a breathable sterile sealing film.
4. Incubation is carried out for 6 days at 30°C with orbital shaking set at 200 rpm. The pH is adjusted daily to 5.0 with 1 M citric acid. White balls of mycelium start to be visible after 3 days of culture ([Fig. 6](#)).
5. At the end of the culture, 1 mL of culture medium is filtered and analyzed for activity of production.
6. All cultures and analysis are carried out in triplicate.

2.3.2 Screening of laccase producing transformants on petri dish plates

Activity plate screening is based on the oxidation of chromogenic phenolic or nonphenolic laccase substrate. A colored halo (brownish and greenish for guaiacol and ABTS oxidation, respectively) developing with time around isolated colony attests for the secretion of active laccases ([Fig. 7](#)).



Fig. 6 Deep-well plate culture of laccase producing *A. niger* transformants. (A) View of the breathable film covering the plate during cultivation. (B) Aspect of a 3 mL culture of *A. niger* in minimum medium supplemented with glucose and oligoelements after 6 days of growth at 30°C. Each well corresponds to the growth of a single transformant. The presence of *white balls* attests for the development of the fungus.

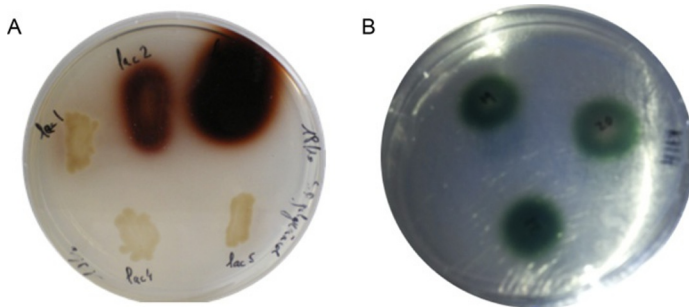


Fig. 7 Activity plates: guaiacol oxidation by yeast laccase producing variants (A) and ABTS oxidation by *A. niger* laccase producing variants (B).

This procedure is a particularly powerful primary screen applicable to a large number of clones at the same time directly on transformation plates, as the chromogenic substrates included in the selective media (ABTS or guaiacol) is nontoxic to transformants. Moreover, for colonies of similar size, both the extent of the halo and the color depth are indicative of differences in secretion levels and/or in specific activities (library screening).

Equipment

1. Stationary incubator set at 30°C.
2. Regular Petri dish plates.

Buffers and reagents

1. Solid minimum medium for *A. niger*. Same composition as above for transformants selection. Make the solution 50 mg L⁻¹ CuSO₄, 5 H₂O, and 0.2 mM ABTS final from sterile stock solutions prior to gelification (hardening).
2. Solid SD medium for *S. cerevisiae*: YNB without AA, 0.67%; galactose, 2%; adenine, 30 mg L⁻¹; casein hydrolysate, 0.5%; tryptophan, 40 mg L⁻¹; CuSO₄, 100 μM; 15 g L⁻¹ agar; 50 mM succinate buffer pH 5.3. Add 500 μL L⁻¹ guaiacol prior to gelification (hardening).

Procedure

1. Activity ABTS minimum medium plate is used for the selection of *A. niger* transformants. About 50 μL of transformants solution are applied per plate, followed by incubation for 4 days at 30°C. Development of a green halo around a colony, visible to the eye, attests for active laccase secretion.
2. SD medium plates are used for the selection of *S. cerevisiae* transformants. 200 μL of transformants are spread per plate, which are incubated for 2–3 days at 30°C until colonies form. Development of a green halo around a colony attests for active laccase secretion.

2.3.3 Screening of activity on 96-well plate

96-Well ABTS plate screening is an easy way to follow laccase activity.

Equipment

1. Three 96-well microtiter plates.
2. Microtiter plate reader.

Buffers and reagents

1. Buffer A: ABTS solution (5 mM final) freshly prepared in any buffer compatible with laccase activity and ABTS stability. We routinely use 100 mM acetate buffer pH 5.7 or Britton and Robinson buffer for extended pH studies.

Procedure

1. The ABTS activity assay is based on the rate of production of the chromophoric radical cation ABTS^{•+} at 414 nm ($\epsilon = 3.5 \times 10^4 \text{ L mol}^{-1} \text{ cm}^{-1}$ at pH 6.0).
2. The enzyme concentration is determined by the method of Bradford colorimetric assay on microtiter plates (protocol from furnisher).

Generally, Bradford assays are performed on 150 μL of nondiluted SN. The laccase protein concentration is estimated from a standard curve obtained from BSA solution (bovine serum albumin from 0 to 80 $\mu\text{g mL}^{-1}$).

3. Supernatants are diluted with buffer A (dilution factors are SN/20 and SN/40).
4. 20 μL of SN at an appropriate dilution is added to 180 μL of buffer A solution to initiate the reaction (final volume 200 μL). The specific activity of the laccase enzyme is calculated from the initial rate of the absorbance increase at 414 nm within 5 s of shaking, at 30°C. Kinetics are followed for 1 h within 30 s intervals with a microtiter plate reader (Fig. 8).
5. The specific activity of laccase toward ABTS is described as the number of micromoles of ABTS oxidized per minute per milligram of enzyme.

Note

1. This test is perfectly amenable for determining the enzymatic parameters of pure laccase as previously exemplified (Cusano et al., 2009).

2.3.4 ELISA screening

Sandwich ELISA, a variant of ELISA, is a highly sensitive technique for sample antigen detection. It allows quantification of the antigen between two layers of antibody molecules: the capture layer and the detection layer. An immobilized polyclonal anti-LAC3 antibody (multiepitope recognition) is used to capture the antigen. The same polyclonal biotinylated anti-LAC3

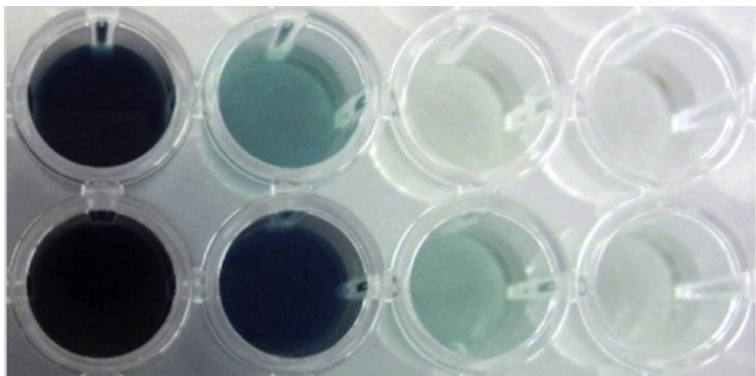


Fig. 8 Microtiter plate assay for laccase-mediated ABTS oxidation. The *green color* attests for laccase activity. Adapted from Cusano, A. M., Mekmouche, Y., Meglecz, E., & Tron, T. (2009). Plasticity of laccase generated by homeologous recombination in yeast. *FEBS Journal*, 276, 5471–5480.

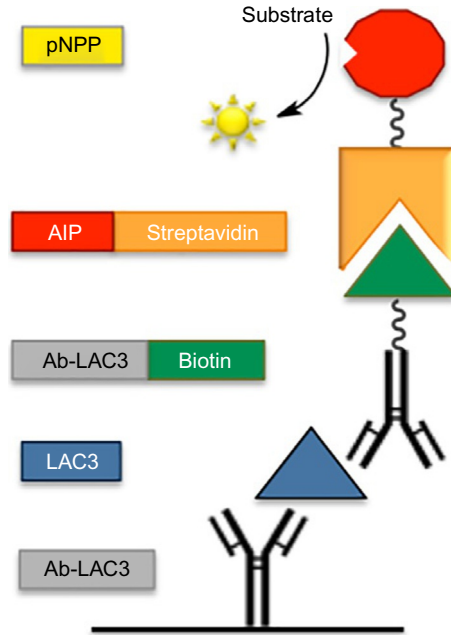


Fig. 9 Scheme of the “Sandwich ELISA” technique. The coated polyclonal antibody anti-LAC3 (Ab-LAC3) captures the antigen (LAC3). The secondary antibody, the same polyclonal biotinylated anti-LAC3 antibody (Ab-LAC3-biotin) serves for detection. The detection is made possible with the enzyme conjugate AIP-Streptavidin. The substrate pNPP (4-nitrophenyl phosphate disodium salt hexahydrate) is hydrolyzed into a colorimetric product detected at 405 nm.

antibody serves for the detection (Fig. 9). This method is particularly suited to the detection of low-activity or inactive laccase variants. The advantage of this method is that the antigen does not need to be purified before analysis.

Equipment

1. 96-Well microplates coated for ELISA.
2. Any microplate reader.
3. Multichannel precision pipettes.

Buffers and reagents

1. Coating buffer: 0.2 M sodium carbonate/bicarbonate, pH 9.4.
2. Capture antibody: antilaccase antibody Ab-LAC (Thermo Fisher) diluted in coating buffer.
3. PBST washing buffer: 0.1 M phosphate, 0.15 M sodium chloride, pH 7.2 containing 0.05% tween 20.
4. Blocking buffer: 2% (w/v) BSA in PBST washing buffer.
5. Standard dilution buffer: purified laccase diluted in blocking buffer.

6. Detection antibody: biotinylated polyclonal Ac-LAC antibody.
7. Biotin-secondary antibody.
8. Enzyme conjugate: Streptavidin Alkaline Phosphatase (Jackson Immuno Research).
9. Substrate: pNPP (Sigma S0942).
10. Glycine buffer: 0.1 M glycine, pH 10.4, with 1 mM MgCl₂ and 1 mM ZnCl₂.

Procedures

The steps are as follows:

- Antibodies preparation (capture and detection)
 1. Purification of Ab-LAC: following procedure from manufacturer (Thermo Scientific 89952).
 2. Biotinylation of Ab-LAC: following the protocol of a Biotin Protein Labeling Kit (Sigma Aldrich).
 3. Dilute to 2 mgmL⁻¹, adding an equal volume of glycerol (final concentration: 50%), and store at -20°C.
- Surface preparation
 4. The capture antibody is diluted (20,000 ×) in coating buffer.
 5. 100 μL of diluted capture antibody is added to each well; the microplates are then covered and incubated overnight at 4°C.
 6. Discarding the solution, the plates are washed three times with 200 μL per well of PBST washing buffer.
 7. 200 μL of blocking buffer is added per well, the plates are then covered and incubated for 1 h at RT.
- Antigen capture
 8. The blocking buffer is discarded and 100 μL of sample or standards (100–2000 pg) is added. The plates are incubated for 1 h at RT.
 9. The solution is discarded and the plate washed three times with 200 μL per well of PBST washing buffer.
 10. The biotinylated detection antibody is diluted 5000-fold in blocking buffer.
 11. To each well is added 100 μL of diluted biotinylated detection antibody, the plate is then covered and incubated for 1 h at RT.
 12. The solution is discarded and the plate is washed five times with 200 μL per well of PBST washing buffer.
- Detection and quantification
 13. The enzyme conjugate AIP-Streptavidin is diluted 1000-fold.
 14. 100 μL of the diluted AIP-Streptavidin is added to the plate, which is then covered and incubated for 1 h at RT.

15. After removing the solution, the plate is washed seven times with 200 μL per well of PBST washing buffer.
16. The substrate solution is prepared: one tablet of pNPP (5 mg) is used in 10 mL of glycine buffer.
17. The plate is incubated at RT until the desired color intensity is reached. Ideally, a clear gradient is obtained with the variable concentrations of standard used.
18. The absorbance at 405 nm is recorded with a plate reader to estimate the amount of bound antigen from the standard curve established from different concentrations of pure LAC3 antigen.

2.4 Fermentation in *A. niger*

As stated earlier, the production of laccase and variants is carried out in 5 or 10L bioreactors following production procedures already described (Mekmouche et al., 2014; Record et al., 2002). Prior to the fermentation, it is necessary to produce a sufficient stock of spore allowing an inoculum of 2×10^6 spores mL^{-1} for 10L culture: this is described below.

2.4.1 Preparation of spore inoculum and storage

See Section 2.2.2.

A stock of stored spores is thawed to prepare the inoculum, and as many plates as necessary for a 10L culture are prepared. Usually, 15 plates are necessary to inoculate a 10L fermentor.

2.4.2 Production in bioreactor and growth parameters

The initial growth parameters are presented in Table 2. Parameters such as agitation or addition of antifoam are adjusted daily. Specific activity, O_2 consumption, and protease activity are measured routinely (Mekmouche et al., 2014).

Growth conditions in a 10L bioreactor have been described previously (Mekmouche et al., 2014). The recombinant enzyme is the major secretion

Table 2 Typical growth parameters for heterologous expression of fungal laccase in *A. niger*

Parameters	Aeration (VVM)	Inoculum Size		pH	Glucose (gL^{-1})	Rotation (rpm)
		Spore (mL^{-1})				
	1.2	2×10^6		5.5	50	200–600

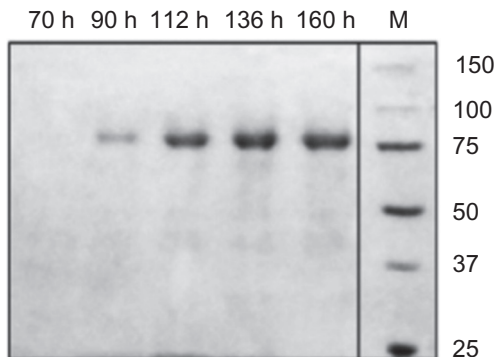


Fig. 10 Time course of laccase production during up-scaled fermentation. SDS-PAGE (7.5%) is stained with Coomassie blue. 10 mL of culture supernatant were loaded per well as a function of cultivation time (from 0 to 184 h); *M*: molecular weight markers in kDa. Adapted from Mekmouche, Y., Zhou, S., Cusano, A. M., Record, E., Lomascolo, A., Robert, V., et al. (2014). Gram-scale production of a basidiomycetous laccase in *Aspergillus niger*. *Journal of Bioscience and Bioengineering*, 117, 25–27 with permission.

product: it is therefore possible to follow the time course of production of the enzyme simply by loading an SDS-PAGE with extracellular culture medium (Fig. 10).

3. General purification procedure and characterization

Purification of laccase variants can be obtained easily following a protocol adapted from Cusano et al. (2009) based on four steps: (1) filtration to eliminate the mycelium, (2) concentration, (3) capture (anionic exchange), and (4) polishing (gel filtration), altogether allowing for a satisfactory level of homogeneity (Fig. 11).

3.1 Purification procedure

3.1.1 Assay procedures

Although several substrates are regularly used for laccase activity determination, we will here describe only the syringaldazine (SGZ) colorimetric assay for volumetric activity determination and an electrophoretic colorimetric assay based on phenylenediamine (PPD) oxidation (zymogram).

a. SGZ assay procedure

Equipments

1. UV–vis spectrophotometer.
2. Disposable cuvettes of 1.5 mL.

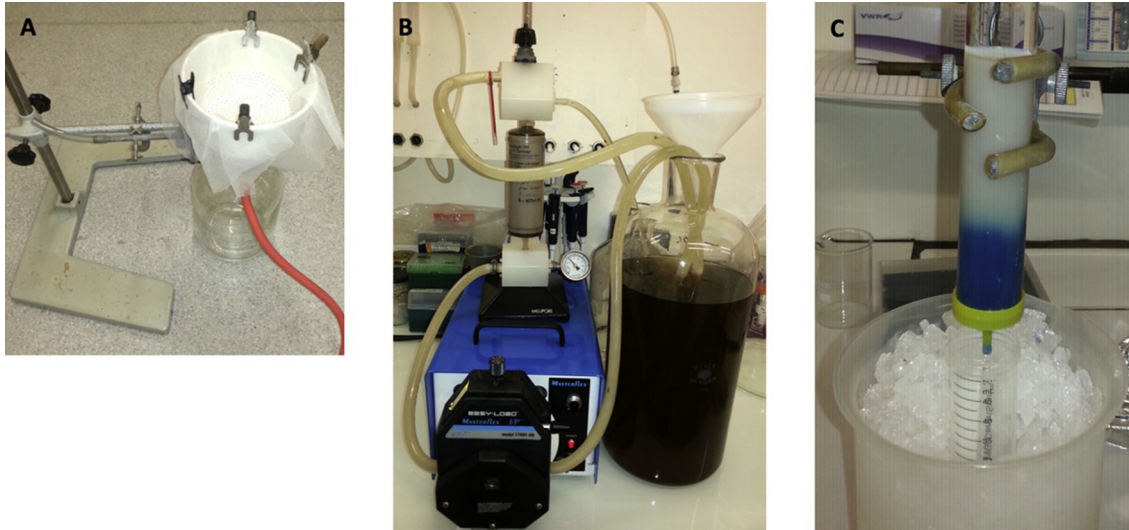


Fig. 11 Initial steps for the purification of recombinant laccases produced in *A. niger*. (A) Setting for the filtration of the cultivation medium through a Separ (SEFAR MEDIFAB 30-170/54) filter allowing for the elimination of the mycellium; (B) tangential ultrafiltration and concentration of 10 L of cultivation medium (UF cartridge regenerated cellulose cutoff 30 kDa from Millipore); and (C) NaCl gradient elution of laccase on a DEAE column ($2.5 \times 25 \text{ cm}^2$) loaded with the ultrafiltrate.

Buffers and reagents

1. Syringaldazine stock solution: 8 mg mL^{-1} in MeOH.
2. Buffer A: 100 mM sodium acetate pH 5.7.
3. Bradford reagent (Millipore).

Buffers and reagents

1. The SGZ activity assay is based on the rate of production of the corresponding quinone at 525 nm ($\epsilon = 65,000 \text{ L mol}^{-1} \text{ L cm}^{-1}$) (Bauer & Rupe, 1971).
2. The laccase concentration is determined by two colorimetric methods. The first method is the Bradford colorimetric assay (Bradford, 1976) and the second one is based on oxidized T1 absorption (when enzyme is purified) at 610 nm ($\epsilon = 5600 \text{ L mol}^{-1} \text{ L cm}^{-1}$) (Simaan et al., 2011).
3. For routine assay a working concentration of $88 \mu\text{M}$ of syringaldazine is used. Laccase is added at an appropriate concentration to buffer A solution in the disposable cuvette to a final volume of $970 \mu\text{L}$.
4. The addition of $30 \mu\text{L}$ of SGZ initiates the reaction. The volumetric activity of the laccase enzyme is calculated from the initial rate measurement of the absorbance increase at 525 nm , followed over the time course of 2 min.
5. The specific activity of laccase toward SGZ is described as the number of micromoles of SGZ oxidized per minute per milligram of the laccase.

b. Zymogram assay procedure

It may be convenient to visualize laccase distribution in protein samples throughout purification. Beside (or in addition to) protein staining and immunodetection, laccase conversion of chromogenic substances to colored compounds is sensitive and quick. Laccase activity is easily detectable *in gel* after protein separation on a regular PAGE-SDS gel, providing any denaturation of the protein sample is avoided prior to loading the gel (i.e., no reducing agent is present in the loading buffer and no heat treatment has been used).

Equipment

1. SDS-PAGE gel (e.g., 7.5%).
2. Electrophoresis apparatus.

Buffers and reagents

1. Modified Laemmli sample buffer: 4% SDS, 20% glycerol, 0.004% bromophenol blue, and 0.125 M Tris-HCl, pH approx. 6.8.
2. Buffer A: 20 mM acetate buffer pH 3.6.
3. *p*-Phenylenediamine.
4. Buffer B: 100 mM phosphate buffer pH 7.5.

Procedure

1. Protein samples are diluted in modified Laemmli sample buffer (no reducing agent) and then loaded onto a PAGE SDS: it is important not to heat the protein sample.
2. The PAGE-SDS gel is run under appropriate conditions.
3. The gel is soaked in buffer A for 10 min.
4. The gel is rinsed three times with buffer A.
5. The gel is soaked in a freshly prepared solution of PPD (2 mg mL^{-1} in buffer A) until color is developed. The reaction is quenched by soaking the gel in buffer B.
6. Rinse the gel three times with buffer B.
7. Extensively wash with water prior to (short-term) storage.

3.1.2 Laccase purification procedure

Equipment

1. Vacuum filtration setting (e.g., 110 mm Büchner funnel + 5 L flask + vacuum pump).
2. Filters (SEFAR MEDIFAB 30-170/54).
3. High speed floor centrifuge, centrifuge tube.
4. Ultrafiltration apparatus (e.g., Prep/Scale Spiral-Wound Ultrafiltration Modules: TFF-2. MWCO 30 kDa 150 mL working volume).
5. High flow rate peristaltic pump (e.g., Cole Palmer Masterflex I/P Easy-Load Pump).
6. Empty glass gravity chromatographic column $2.5 \times 25\text{ cm}^2$ (e.g., Econo-Column[®] Bio-Rad).
7. Size-exclusion chromatographic column (e.g., HiPrep[™] 26/60 Sephacryl[®] S-300 HR, GE Healthcare).
8. Centrifugal concentrator 30,000 MWCO PES (e.g., Vivaspin 20 Sartorius).
9. Stirred-cell ultrafiltration apparatus (e.g., Amicon) with 30,000 MWCO PES membranes.
10. UV-vis spectrophotometer.
11. FPLC apparatus equipped with double wavelength detection 280 and 610 nm (e.g., Äkta purifier 10, GE Healthcare).

Buffers and reagents

1. Buffer C: 20 mM phosphate buffer pH 6.0.
2. Buffer D: 20 mM phosphate buffer pH 6.0, 300 mM NaCl.
3. Buffer E: 20 mM phosphate buffer pH 6.0, 200 mM NaCl.
4. Syringaldazine stock solution: 8 mg mL^{-1} in MeOH.

5. ABTS solution: buffer containing 5 mM ABTS, freshly prepared. It is possible to use any buffer compatible with laccase activity and ABTS stability. We generally use 100 mM acetate buffer pH 5.7 or Britton and Robinson buffer for pH studies.

Procedure

1. Filter the *A. niger* dark brown fermentation medium (typically 10 L) on a Büchner funnel equipped with a low porosity filter (SEFAR MED-IFAB 30-170/54) under vacuum. Wash the mycelium several times (three to five times) with a minimum volume of buffer A (for a total volume representing 10% of the initial cultivation volume).
2. Concentrate the filtered medium using an ultrafiltration apparatus equipped with a MWCO 30 kDa membrane down to the minimal volume (depends on apparatus and membrane specifications, usually ≈ 200 mL for a 2.3 sq. ft. membrane) at a flow rate compatible with the maximum operated pressure recommended by the membrane manufacturer (flow rate of $\approx 3 \text{ L min}^{-1}$). At this stage, most of the dark brown material goes to the permeate tank and the intensity of the blue-green color of the retentate visually translates laccase production.
3. Add 50 mL of DEAE-Sepharose resin previously equilibrated with buffer C to the retentate (batch process). Allow binding under slow magnetic stirring for 1 h at 4°C.
4. Pour the DEAE slurry into an empty glass chromatographic column $2.5 \times 25 \text{ cm}^2$ and pack it by gravity.
5. Wash the resin with 250 mL buffer C. Depending on the laccase variant the resin should be more or less intensely blue colored.
6. Connect the column to a low flow peristaltic pump and elute laccase by sharply raising the ionic strength of the buffer. Laccases derived from LAC3 produced in our laboratory elute usually with 50–75 mL of buffer D (containing 300 mM NaCl) at a flow rate of 2 mL min^{-1} . The presence of colorless laccase variants (e.g., delta T1) may be confirmed by immunodetection.
7. Protein concentration is evaluated by Bradford assay and laccase concentration is determined by UV-vis spectroscopy ($\epsilon_{610\text{nm}} = 5600 \text{ L mol}^{-1} \text{ cm}^{-1}$).
8. If necessary the protein concentration of the sample is adjusted to maximize loading of size-exclusion chromatography.
9. An appropriate volume of sample is applied to the top of a preequilibrated (buffer E) $2.6 \times 60 \text{ cm}^2$ Sephacryl S-300 HR column (or equivalent) connected to a FPLC system. Gel filtration is carried

out at a flow rate of 1 mL min^{-1} (buffer E) collecting 5 mL fractions. Progress is followed with detectors set at 280 and 610 nm. Repeated injections are necessary given the size of the sample obtained after DEAE. Fractions with a ratio between $14 < \lambda_{280\text{nm}}/\lambda_{610\text{nm}} < 16$ and an activity within 20% of the peak fraction are pooled (Fig. 12).

10. Pooled fractions are exchanged with buffer A to remove NaCl using a 30-kDa cutoff ultrafiltration membrane in a stirred-cell filtration unit (e.g., Amicon). The sample is concentrated to 10 mg mL^{-1} and 10% of glycerol (v/v) is added to the solution.
11. The sample is filtered under a sterile atmosphere using a $0.2 \mu\text{m}$ filter; $500 \mu\text{L}$ is then dispensed to 1 mL aliquots in cryotubes which are then stored at -20°C for long-term storage.

Representative yields for several laccase variants are presented in Table 3. Yields and catalytic properties for LAC3 and UNIK variants (unique lysine variants) are twofold higher than those of the K_0 variant (no lysine). Eventually, yields are markedly higher than those obtained in *S. cerevisiae* (about 40 times for LAC3 heterologous production) (Table 3).

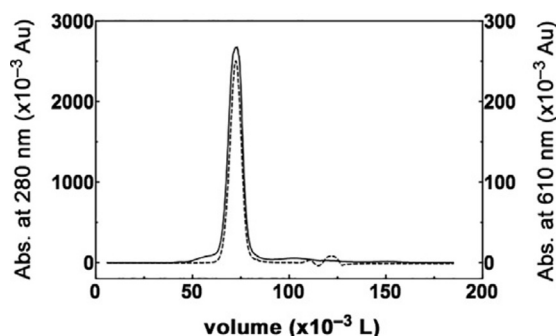


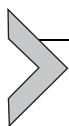
Fig. 12 Typical S300 chromatogram obtained for LAC3. Two wavelengths (280 nm solid line, 610 nm dashed line) are selected to follow the elution.

Table 3 Typical purification yields obtained for various LAC variants

	LAC3	UNIK ₁₆₁	UNIK ₁₅₇	K_0
Production	8 L	8 L	8 L	8 L
	$40,000 \text{ UL}^{-1}$	$28,000 \text{ UL}^{-1}$	$25,000 \text{ UL}^{-1}$	8900 UL^{-1}
Purification	900 mg	700 mg	600 mg	400 mg
	170 U mg^{-1}	160 U mg^{-1}	160 U mg^{-1}	90 U mg^{-1}

Notes

1. Filtration of the cultivation medium may lead to a rapid browning of the solution. This is probably a manifestation of laccase activity consecutive to a reoxygenation of the solution during the elimination of the O₂-consuming *A. niger* mycelium.
2. After ultrafiltration (step 2), the volume of the retentate is the minimal one that can be obtained, as it is constrained by the volume of the cartridge and tubings. It is usually necessary to rinse the system one or two times with a minimal volume of 200 mL. This variation of the volume does not affect the capture of the enzyme on an anionic exchanger.
3. At each step of the purification process, a small aliquot is taken out to load on SDS-PAGE, measure the protein concentration (Bradford assay and T1 absorbance for the last step) and the specific activity.



4. Applications

Over the past few years, efforts have been made to investigate alternative routes for the oxidation of organic compounds and to perform selective catalytic chemical transformations. To date, these reactions are highly important at an industrial level and the current processes are among the most polluting ones. Appearing as highly promising sustainable alternatives to traditional catalysts, artificial enzymes often combine a transition metal catalyst moiety with a protein environment (Diéguez, Bäckvall, & Pàmies, 2018; Schwizer et al., 2018). Inspired from this new field, we recently engaged ourselves in studying interactions between laccase and devices or materials. We study three types of interactions: (i) bimolecular; (ii) oriented covalent; and (iii) oriented supramolecular (Fig. 13).

We have recently described the first examples of catalytic systems combining the O₂-reducing power of a laccase with the catalytic power of inorganic moieties represented either by a palladium-based water-soluble catalyst (aerobic oxidation of veratryl alcohol) or a ruthenium-based complex (photo-induced oxidation of styrene compounds) (Fig. 14). In both cases, substrate is oxidized under mild conditions by the inorganic moiety probably redox cycling, via the enzyme, with the four-electron reduction of dioxygen into water. In these hybrid systems, the enzyme and the inorganic catalysts form functional bimolecular systems and O₂ acts as a renewable, cheap, and clean oxidant.

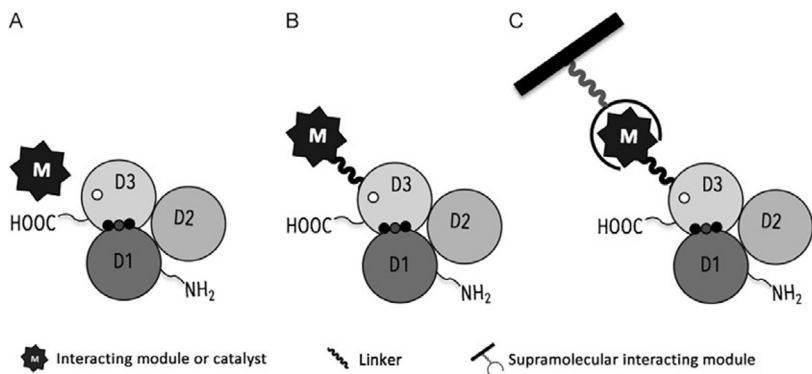


Fig. 13 General strategy for producing hybrid catalysts. Three cupredoxin domains (D1, D2, and D3) represent the laccase structure. *White circle*, T1 copper atom; *gray circle*, T2 copper atom; and *black circle*, T3 copper atoms. (A) Bimolecular interaction; (B) oriented covalent interaction; and (C) oriented supramolecular interaction between laccase and heterogeneous material.

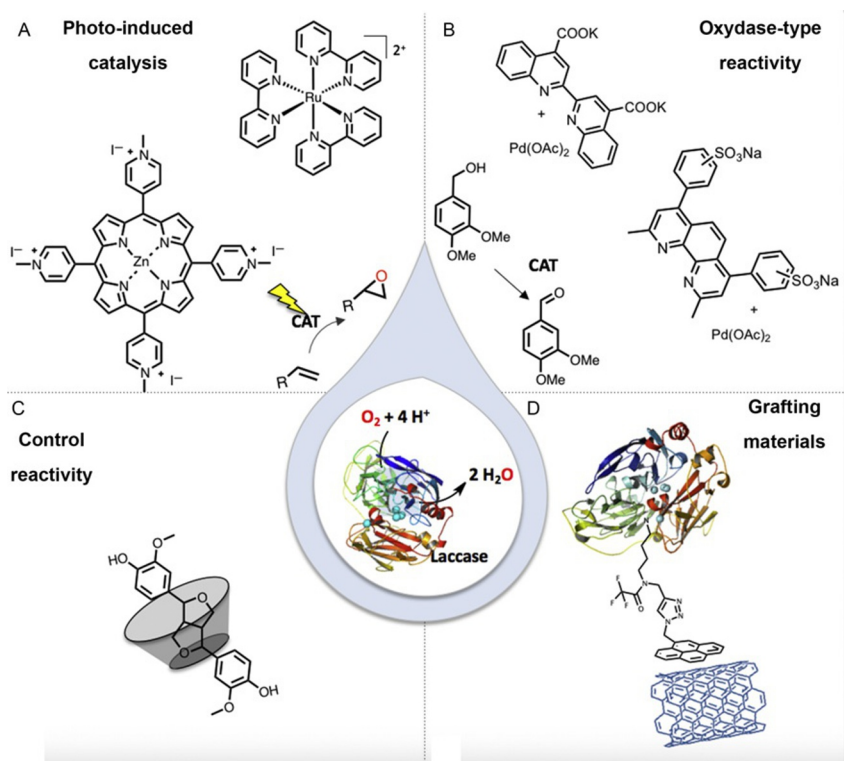


Fig. 14 Hybrid catalysts combining inorganic or organic moieties with the powerful oxidoreductase laccase. (A) Interaction of small photosensitizers with laccase to promote photo-induced oxidation of alkenes to epoxides; (B) laccase as a palladium oxidase. Primary alcohol oxidation mediated by the Pd/laccase/O₂ system under mild conditions; (C) controlled polymerization of coniferyl alcohol mediated by β -cyclodextrin with fungal laccase; and (D) supramolecular interaction of a pyrene-grafted laccase and MWCNT electrode to promote oriented direct electron transfer.

4.1 General procedure for an oriented covalent grafting of the laccase surface

4.1.1 Preparation of laccase variants for single-site anchoring

The well-known topography of laccases makes them easy material for surface-targeted modification. The design of variants for surface-targeted AA functionalization is addressed in [Section 2.2.1](#). Briefly, a single lysine (K) residue is precisely positioned at the surface of a lysine-less variant through site-directed mutagenesis. The variants created this way are designed UNIK.

4.1.2 Reductive amination of lysine

Highly selective modifications of primary amino groups present at the surface of proteins can be obtained under mild conditions. The chemical modification of UNIK variants is adapted from the procedure described by [McFarland and Francis \(2005\)](#). The primary amino group of lysine present at the surface of UNIK is reacted with an aldehyde-containing molecule under reducing conditions. Two recent publications from our group describe a strategy for achieving a controlled orientation in the grafting of the surface of a fungal laccase ([Lalaoui et al., 2016](#); [Robert et al., 2017](#)). The grafting procedure of two molecules is detailed hereafter. The first molecule is an original 2,2,2-trifluoro-*N*-(4-oxo-butyl)-*N*-(1-pyren-4-ylmethyl-1*H*-[1,2,3]triazol-4-ylmethyl)-acetamide reactant (compound **1**, [Fig. 15](#)) synthesized to favor the anchoring of laccase variants on carbon nanotubes containing electrodes through supramolecular interaction. This molecule features: (i) an aldehyde moiety for reductive amination and (ii) a pyrene moiety favoring interaction with the electrode material. [Fig. 14A](#) summarizes a schematic view of this multifunctional platform.

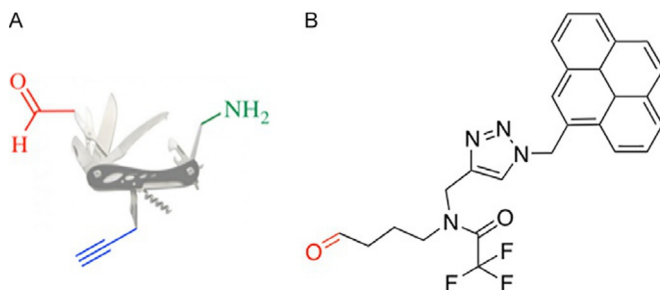


Fig. 15 (A) Artistic view of a multifunctional molecule as a graft for laccase. (B) Structure of the 2,2,2-trifluoro-*N*-(4-oxo-butyl)-*N*-(1-pyren-4-ylmethyl-1*H*-[1,2,3]triazol-4-ylmethyl)-acetamide reactant (compound **1**).

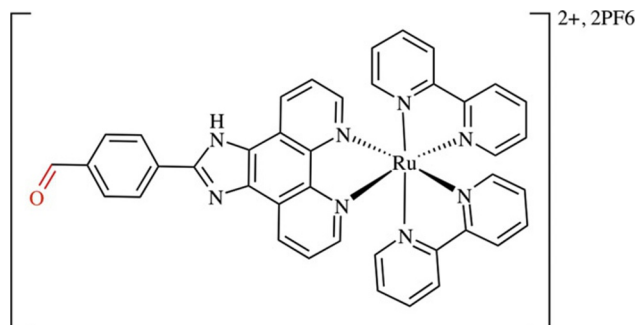


Fig. 16 Structure of compound **2** $[(\text{bpy})_2\text{Ru}(\text{fimbzl})][\text{PF}_6]_2 \cdot 2\text{H}_2\text{O}$ (fimbzl = 4 ([1,10] phenanthroline[5,6-*d*]imidazol-2-yl)benzaldehyde).

The second molecule is an original heteroleptic ruthenium(II)–polypyridine-type complex with one of the bipyridine ligands containing a fused imidazole motif and a benzaldehyde (compound **2**, Fig. 16).

This complex has been selected for the following reasons: (i) its ability to photoreduce laccases upon visible light excitation (Schneider et al., 2015; Simaan et al., 2011); (ii) its intense absorption band in the visible spectrum at $\lambda_{\text{max}} = 450 \text{ nm}$ ($\epsilon_{450\text{nm}} = 14,500 \text{ L cm}^{-1} \text{ mol}^{-1}$) (Kalyanasundaram, 1982) which does not overlap the $\lambda_{\text{max}} = 605 \text{ nm}$ of the T1 Cu(II) site of laccases; and (iii) its fluorescence properties ($\lambda_{\text{ex}} = 450 \text{ nm}$, $\lambda_{\text{em}} = 600 \text{ nm}$).

Equipment

1. $1.5 \times 150 \text{ cm}^2$ glass chromatography column.
2. Sephadex[®] G-25 fine (GE Healthcare).
3. Peristaltic pump (e.g., Gilson).
4. Centrifugeable ultrafiltration devices, 30,000 MWCO PES (e.g., Vivaspin 20, Sartorius).
5. Floor centrifuge and centrifuge tubes.
6. UV–vis spectrometer.

Buffers and reagents

1. Buffer A: 20 mM sodium phosphate buffer pH 6.0 containing 10% glycerol.
2. Buffer B: 25 mM sodium phosphate buffer pH 7.4 containing 100 mM sodium formate.
3. Buffer C: 50 mM sodium acetate buffer pH 5.5, 100 mM NaCl.
4. Buffer D: 50 mM sodium acetate buffer pH 5.5.
5. Custom aldehyde–donor molecule (e.g., compound **1** or compound **2**). Prepare a 3 mM stock solution in buffer A. This solution can contain up to 30% DMSO to solubilize the molecule of interest.

6. Water-stable $[\text{Cp}^*\text{Ir}-(\text{bipy})(\text{H}_2\text{O})]\text{SO}_4$ complex (Ir catalyst) synthesized as previously described (McFarland & Francis, 2005). Prepare a 14 mM stock solution in deionized water, aliquot, and store at -20°C .

Procedure

1. A 200 μM stock solution of laccase is prepared in buffer B, the concentration being based on the oxidized T1 absorption at 610 nm.
2. In a 5-mL round bottom flask equipped with a Teflon magnetic stirring bar, 625 μL of laccase, 417 μL of the custom aldehyde-donor molecule, and 90 μL of Ir catalyst are combined, adjusting to a final volume of 2.5 mL with buffer A. The reaction is carried out for 72 h with permanent stirring at RT. The solution is then concentrated to 1 mL with a centrifugeable ultrafiltration device.
3. The 1 mL mixture is loaded onto a G-25 gel filtration column preequilibrated with buffer C (5 CV) for desalting and buffer exchange. Elution is carried out with a linear flow of 1 mL min^{-1} of buffer C, collecting 500 μL fractions. Fractions containing laccase are identified with a colorimetric assay (ABTS or SGZ oxidation), pooled, and concentrated to 250 μL with an ultracentrifugation device (Vivaspin 20, 4500 rpm).
4. The concentrated protein solution is exchanged with buffer D (to remove NaCl) prior to analysis.

Notes

1. During the grafting procedure, laccase is solubilized at neutral to basic pH. In these conditions, laccase is reversibly inactivated and easily reduced by the formate-containing solution as testified by the loss of the characteristic blue color of the oxidized T1 copper site. The G25 column allows for the elimination of the excess of unreacted aldehyde and reduction catalyst and thus a progressive reoxidation of laccase (reapparition of the blue color) can be observed as elution progresses.
2. For photosensitive molecules, the desalting column (G25) and the 5-mL balloon are covered with a piece of black plastic to avoid any light-induced processes.

4.1.3 Evaluation of the grafting

The efficiency of grafting can be evaluated simply by use of UV-vis spectrophotometry, providing the graft absorbs at a wavelength clearly distinct from the transition at $\lambda_{\text{max}} = 605$ nm characteristic of the T1 Cu(II) site of laccases. For example, compounds **1** and **2** have each an intense absorption band at, respectively, $\lambda_{\text{max}} = 345$ nm ($\epsilon_{350\text{nm}} = 37,500 \text{ L mol}^{-1} \text{ cm}^{-1}$) and

$\lambda_{\max} = 450 \text{ nm}$ ($\epsilon_{450\text{nm}} = 14,500 \text{ L mol}^{-1} \text{ cm}^{-1}$). Therefore, the $A_{\lambda_{\max}} \text{ graft}/A_{\lambda_{\max}} \text{ laccase}$ ratio reflects well the grafting efficiency. With transition metal-containing complexes (like compound **2**) the metal/Cu ratio in the grafted enzymes (therefore the efficiency of the grafting) can be deduced from inductively coupled plasma mass spectrometry (ICP-MS) analysis. Compounds **1** and **2** being also fluorescent molecules, their grafting to the laccase surface can be visualized after electrophoresis on an SDS-PAGE gel under appropriate irradiation. However, this method is not quantitative. Ultimately, confirmation of the grafting location can be obtained by mass spectrometry analysis of peptides produced by trypsin digestion of the grafted laccase and separated by HPLC (UV-vis or fluorescence detection). A potential grafting at the amino terminus can be evaluated by AA sequencing (Edman degradation).

Equipment

1. RP-C18 HPLC column (150/4) (e.g., Nucleosil Macherey Nagel).
2. Desalting columns (e.g., PD-10 Amersham).
3. HPLC equipped with UV/fluorescence detector.
4. UV-vis spectrometer.
5. 7.5% SDS-PAGE gel.
6. Electrophoresis apparatus.
7. Thermomixer (e.g., Eppendorf).
8. Digital gel imaging system (e.g., UVITEC Cambridge).

Buffers and reagents

1. Buffer A: Britton and Robinson buffer pH 5.0.
2. Buffer B: 250 mM Tris-HCl, 4 mM EDTA, 6 M guanidine, pH 8.5.
3. Dithiothreitol (60-fold molar excess over disulfide bridges) in buffer F.
4. 2-Iodoacetamide.
5. Buffer C: 125 mM of NH_4HCO_3 pH 8.0.
6. Trypsin.
7. HPLC solvent A: water 0.1% TFA.
8. HPLC solvent B: acetonitrile 0.1% TFA.

Procedure

- UV-vis spectrometry analysis
 1. Solutions of both unreacted and functionalized laccases are prepared in buffer A at a convenient concentration ($\approx 50 \mu\text{M}$). The spectra of both laccase solutions (Fig. 17) are recorded. The number of grafted molecules per laccase can be deduced from the $A_{345\text{nm}}/A_{605\text{nm}}$ and $A_{450\text{nm}}/A_{605\text{nm}}$ ratios for compounds **1** (Fig. 15) and **2** (Fig. 16), respectively.

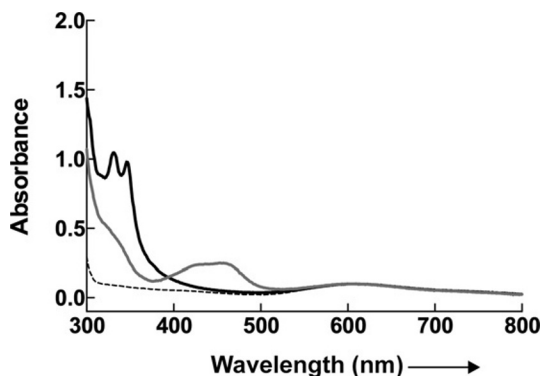


Fig. 17 UV-vis spectra of unreacted and grafted laccases. *Dashed line*, unreacted LAC3; *solid dark line*, UNIK grafted with compound **1**; and *solid gray line*, UNIK grafted with compound **2**. Adapted from Lalaoui, N., Rousselot-Pailley, P., Robert, V., Mekmouche, Y., Villalonga, R., Holzinger, M., et al. (2016). Direct electron transfer between a site-specific pyrene-modified laccase and carbon nanotube/gold nanoparticle supramolecular assemblies for bioelectrocatalytic dioxygen reduction. *ACS Catalysis*, 6, 1894–1900; Robert, V., Monza, E., Tarrago, L., Sancho, F., De Falco, A., Schneider, L., et al. (2017). Probing the surface of a laccase for clues towards the design of chemo-enzymatic catalysts. *ChemPlusChem*, 82, 607–614.

- SDS-PAGE analysis

This method is qualitative and highlights the grafting of a fluorescent probe at the surface of the enzyme. Under the conditions of electrophoretic migration, unbound molecules will not follow the same profile as laccase because compound **1** is uncharged and compound **2** is positively charged.

1. A 7% SDS-PAGE gel is prepared.
2. Samples are heat denatured according to standard SDS-PAGE electrophoresis protocol.
3. The gel is loaded with unreacted enzyme and grafted laccase samples (5 μg /well).
4. After electrophoresis, the gel is examined under irradiation at the appropriate wavelength to excite the fluorophore. Thereafter, the gel is stained with Coomassie Blue and examined under white light irradiation. An example of analysis of samples subjected to reductive alkylation with compound **2** is given in Fig. 18.

- Mass spectrometry analysis

In case the graft is a transition metal complex the exogenous metal (graft)-to-laccase ratios can be confirmed by analyzing the metal content of the grafted enzymes by ICP-MS. Eventually, the precise location of the graft at the surface of enzymes can be confirmed by MALDI-TOF-MS

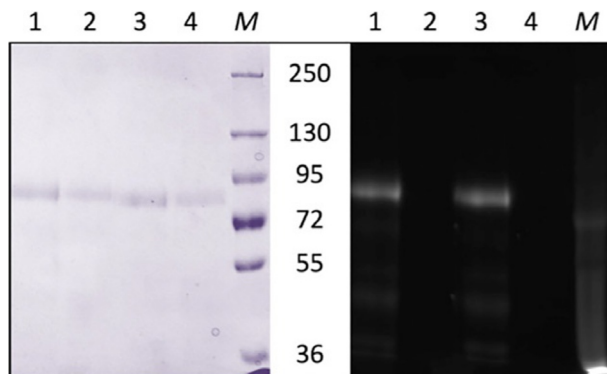


Fig. 18 Representative separation of grafted enzymes on a 7% SDS-PAGE gel. *Left panel:* white light irradiation (Coomassie blue staining); *right panel:* UV irradiation (360 nm). *M:* molecular weight markers. Apparent masses are expressed in kDa. Lane 1: 1–UNIK161 (5 mg); lane 2: UNIK161 (5 mg); lane 3: 1–LAC3 (5 mg); and lane 4: LAC3 (5 mg). *Adapted from Robert, V., Monza, E., Tarrago, L., Sancho, F., De Falco, A., Schneider, L., et al. (2017). Probing the surface of a laccase for clues towards the design of chemo-enzymatic catalysts. ChemPlusChem, 82, 607–614.*

analysis of trypsin peptides. Samples are prepared according to a procedure adapted from [Kharrat et al. \(1998\)](#).

1. The modified enzyme solution at a desired concentration is placed in a 1-mL microtube.
2. Prior to digestion, the protein is reduced with an excess of dithiothreitol (DTT) (60-fold molar excess over disulfide bridges) in buffer B for 20 h at 40°C, under nitrogen and in the dark.
3. S-alkylation of the protein is carried out by adding an excess of 2-iodoacetamide (threefold molar excess over DTT). This mixture is maintained under constant gentle stirring at room temperature for 20 min using a thermomixer.
4. The S-alkylated protein is desalted on a PD-10 column preequilibrated with buffer C.
5. The alkylated protein is digested with trypsin (5%, w/w) for 20 h in buffer A at 37°C.
6. The resulting peptides are purified by HPLC equipped with a RP-C18 column.
7. Example of conditions: injection of 50–100 μ L of sample; elution is monitored both by UV-vis ($\lambda = 280$ and 450 nm) and by fluorescence ($\lambda_{\text{ex}} = 450$ nm) with the following elution program ([Table 4](#)). Peaks displaying fluorescence are collected and submitted to MALDI-TOF analysis (Microflex II (2008) Bruker).

Table 4 Elution conditions for the separation of peptides digested from modified laccase

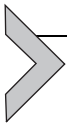
Time (min)	Solvent A	Solvent B	Flow Rate (mL min ⁻¹)
0	100	0	1
45	50	50	1
50	50	50	1
55	0	100	1
60	0	100	1

4.2 Hybridization with materials

The development of new processes for a sustainable chemistry lies at the heart of the great challenges for tomorrow. In heterogeneous catalysis or supported catalysis, major breakthroughs are expected in terms of functionalization and surface modification as well as in the development of nanocatalysts. Along with these developments, immobilization of enzymes on solid supports for various applications (biosensors, medical fields, biocatalyst carriers, biofuel cells, etc.) has gained a spectacular growing interest as judged by the number of reviews published in this field (Bernal, Rodríguez, & Martínez, 2018; Bezerra, de Farias Lemos, de Sousa, & Gonçalves, 2015; Górecka & Jastrzębska, 2011; Hartmann & Dirk Jung, 2010; Milton & Minter, 2017; Singh, Tiwari, Singh, & Lee, 2013; Zhou & Hartmann, 2013). As for synthetic catalysts, many advantages arise from immobilization, such as improved stability, reusability, and localization. Additionally, the architecture, the chemical nature, and mechanical properties of the solid support can be tuned to improve enzyme efficiency. Indeed, there is growing interest in achieving a comprehensive view of processes that control all mechanistic aspects related to stability, efficiency, and selectivity of reactions catalyzed by these systems that are often much less controlled than in homogeneous catalysis. Molecular biology has also facilitated strategies of enzyme immobilization (Bernal et al., 2018), techniques that include entrapment, encapsulation, physical adsorption, ionic binding, affinity and, most recently, covalent attachment. Covalent binding of an enzyme to appropriately functionalized surfaces can prevent leaching. The ultimate aim is to understand fundamental synthesis and processing concepts in order to tailor materials fully controlling all involved mechanistic aspects.

We aim at developing such materials. Enzyme electrodes for example represent promising electrocatalytic biomaterials for bioenergy conversion.

By combining methodologies described above (i.e., large production of a site-directed variant of laccase followed by an oriented postfunctionalization of the enzyme surface), we have obtained a homogeneous population of pyrene-functionalized laccase π -stacked at a MWCNT material. The resulting biocathode is robust and operates at high catalytic current densities (up to 3 mA cm^{-2}). Compared to our previous attempt based on His-tagged laccases (Balland et al., 2008), the precise control of the orientation of our fungal laccase during its immobilization on an electroactive surface has helped to maximize the rate of direct electron transfer between the electrode and the enzyme (Lalaoui et al., 2016). We are also studying the effect of the orientation of the enzyme grafted at the surface of superparamagnetic particles on particles activity (Lu Ren, unpublished data).



5. Conclusions

Fungal laccases are known to be particularly robust catalysts. A significant number of reports have focused on the application of this eco-friendly enzyme in many applications. Improving the productivity of heterologous systems is a challenging task from fundamental to practical points of views. In this chapter, an overview of the large-scale production of laccase variants, their purification, and their use in different applications has been given. Exploring the plasticity of laccase through mutagenesis and expression in the yeast *S. cerevisiae*, it is efficient to use the GRAS organism *A. niger* for mass production of chosen variants. Precisely controlled chemical postfunctionalizations of the enzyme surface are leading to new biohybrid catalysts or materials with unprecedented performances regarding laccase function.

Acknowledgment

We thank the Plateforme Analyse et Valorisation de la Biodiversité (AVB-AMU) for help in producing the recombinant enzyme. This study was supported by grants from the Agence Nationale de la Recherche (ANR-09-BLANC-0176 and ANR-15-CE07-0021-01).

References

- Alcalde, M. (2015). Engineering the ligninolytic enzyme consortium. *Trends in Biotechnology*, 33, 155–162.
- Alcalde, M., Ferrer, M., Plou, F. J., & Ballesteros, A. (2006). Environmental biocatalysis: From remediation with enzymes to novel green processes. *Trends in Biotechnology*, 24, 281–287.

- Alves, A. M. C. R., Record, E., Lomascolo, A., Scholtmeijer, K., Asther, M., Wessels, J. G. H., et al. (2004). Highly efficient production of laccase by the basidiomycete & *Pycnoporus cinnabarinus*. *Applied and Environmental Microbiology*, *70*, 6379–6384.
- Anastas, P. T., & Warner, J. C. (1998). *Green chemistry: Theory and practice*. UK: Oxford University Press.
- Armstrong, F., & Blundell, K. (2007). *Energy...beyond oil*. Oxford, UK: Oxford University Press.
- Balland, V., Hureau, C., Cusano, A. M., Liu, Y., Tron, T., & Limoges, B. (2008). Oriented immobilization of a fully active monolayer of histidine-tagged recombinant laccase on modified gold electrodes. *Chemistry—A European Journal*, *14*, 7186–7192.
- Bauer, R., & Rupe, C. O. (1971). Use of syringaldazine in a photometric method for estimating “free” chlorine in water. *Analytical Chemistry*, *43*, 421–425.
- Becker, D. M., & Guarente, L. (1991). High-efficiency transformation of yeast by electroporation. *Methods in Enzymology*, *194*, 182–187.
- Bernal, C., Rodríguez, K., & Martínez, R. (2018). Integrating enzyme immobilization and protein engineering: An alternative path for the development of novel and improved industrial biocatalysts. *Biotechnology Advances*, *36*, 1470–1480.
- Bezerra, C. S., de Farias Lemos, C. M. G., de Sousa, M., & Gonçalves, L. R. B. (2015). Enzyme immobilization onto renewable polymeric matrixes: Past, present, and future trends. *Journal of Applied Polymer Science*, *132*, 42125.
- Bradford, M. M. (1976). A rapid and sensitive method for the quantitation of microgram quantities of protein utilizing the principle of protein-dye binding. *Analytical Biochemistry*, *72*(1), 248–254.
- Bulter, T., Alcalde, M., Sieber, V., Meinhold, P., Schlachtbauer, C., & Arnold, F. H. (2003). Functional expression of a fungal laccase in *Saccharomyces cerevisiae* by directed evolution. *Applied and Environmental Microbiology*, *69*, 987–995.
- Camarero, S., Pardo, I., Cañas, A. I., Molina, P., Record, E., Martínez, A. T., et al. (2012). Engineering platforms for directed evolution of laccase from *Pycnoporus cinnabarinus*. *Applied and Environmental Microbiology*, *78*, 1370–1384.
- Cannatelli, M. D., & Ragauskas, A. J. (2017). Two decades of laccases: Advancing sustainability in the chemical industry. *The Chemical Record*, *17*, 122–140.
- Couto, S. R., & Toca-Herrera, J. L. (2006). Industrial and biotechnological applications of laccases: A review. *Biotechnology Advances*, *24*, 500–513.
- Couto, S. R., & Toca-Herrera, J. L. (2007). Laccase production at reactor scale by filamentous fungi. *Biotechnology Advances*, *25*, 558–569.
- Cracknell, J. A., Vincent, K. A., & Armstrong, F. A. (2008). Enzymes as working or inspirational electrocatalysts for fuel cells and electrolysis. *Chemical Reviews*, *108*, 2439–2461.
- Cusano, A. M., Mekmouche, Y., Meglecz, E., & Tron, T. (2009). Plasticity of laccase generated by homeologous recombination in yeast. *FEBS Journal*, *276*, 5471–5480.
- Diéguez, M., Bäckvall, J.-E., & Pàmies, O. (2018). *Artificial Metalloenzymes and MetalloDNAzymes in catalysis: From design to applications*. Wiley-VCH Verlag GmbH & Co. KGaA.
- Fernández-Fernández, M., Sanromán, M. A., & Moldes, D. (2013). Recent developments and applications of immobilized laccase. *Biotechnology Advances*, *31*, 1808–1825.
- Gietz, R. D., & Woods, R. A. (2002). Transformation of yeast by lithium acetate/single-stranded carrier DNA/polyethylene glycol method. *Methods in Enzymology*, *350*, 87–96.
- Gordon, L., Khalaj, V., Ram, A. F. J., Archer, D. B., Brookman, J. L., Trinci, A. P. J., et al. (2000). Glucoamylase: Green fluorescent protein fusions to monitor protein secretion in *Aspergillus niger*. *Mutagenesis*, *146*, 415–426.
- Górecka, E., & Jastrzębska, M. (2011). Immobilization techniques and biopolymer carriers. *Biotechnology and Food Sciences*, *75*, 65–86.

- Gutiérrez-Sánchez, C., Pita, M., Vaz-Domínguez, C., Shleev, S., & De Lacey, A. L. (2012). Gold nanoparticles as electronic bridges for laccase-based biocathodes. *Journal of the American Chemical Society*, *134*, 17212–17220.
- Hartmann, M., & Dirk Jung, D. (2010). Biocatalysis with enzymes immobilized on mesoporous hosts: The status quo and future trends. *Journal of Materials Chemistry*, *20*, 844–857.
- Jones, S. M., & Solomon, E. I. (2015). Electron transfer and reaction mechanism of laccases. *Cellular and Molecular Life Sciences*, *72*, 869–883.
- Kalyanasundaram, K. (1982). Photophysics, photochemistry and solar energy conversion with tris(bipyridyl)ruthenium(II) and its analogues. *Coordination Chemistry Reviews*, *46*, 159–244.
- Kates, R. W. (2017). Sustainability science. In D. Richardson, N. Castree, M. F. Goodchild, A. Kobayashi, W. Liu, & R. A. Marston (Eds.), *The international encyclopedia of geography*. John Wiley & Sons, Ltd.
- Kharrat, R., Mansuelle, P., Sampieri, F., Crest, M., Oughideni, R., Van Rietschoten, J., et al. (1998). Maurotoxin, a four disulfide bridge toxin from *Scorpio maurus* venom: Purification, structure and action on potassium channels. *FEBS Letters*, *406*, 284–290.
- Kiiskinen, L. L., Kruus, K., Bailey, M., Ylösmäki, E., Siika-Aho, M., & Saloheimo, M. (2004). Expression of *Melanocarpus albomyces* laccase in *Trichoderma reesei* and characterization of the purified enzyme. *Microbiology*, *150*, 3065–3074.
- Kirk, O., Borchert, T. V., & Fuglsang, C. C. (2002). Industrial enzyme applications. *Current Opinion in Biotechnology*, *13*, 345–351.
- Klonowska, A., Gaudin, C., Asso, M., Fournel, A., Réglie, M., & Tron, T. (2005). LAC3, a new low redox potential laccase from *Trametes* sp. strain C30 obtained as a recombinant protein in yeast. *Enzyme and Microbial Technology*, *36*, 34–41.
- Kunamneni, A., Camarero, S., García-Burgos, C., Plou, F. J., Ballesteros, A., & Alcalde, M. (2008). Engineering and applications of fungal laccases for organic synthesis. *Microbial Cell Factories*, *7*, 32.
- Lalaoui, N., Rousselot-Pailley, P., Robert, V., Mekmouche, Y., Villalonga, R., Holzinger, M., et al. (2016). Direct electron transfer between a site-specific pyrene-modified laccase and carbon nanotube/gold nanoparticle supramolecular assemblies for bioelectrocatalytic dioxygen reduction. *ACS Catalysis*, *6*, 1894–1900.
- Lazarides, T., Sazanovich, I. V., Simaan, A. J., Kafentzi, M. C., Delor, M., Mekmouche, Y., et al. (2013). Visible light-driven O_2 reduction by a porphyrin-laccase system. *Journal of the American Chemical Society*, *135*, 3095–3103.
- Le Goff, A., Holzinger, M., & Cosnier, S. (2015). Recent progress in oxygen-reducing laccase biocathodes for enzymatic biofuel cells. *Cellular and Molecular Life Sciences*, *72*, 941–952.
- Li, D., Tang, Y., Lin, J., & Cai, W. (2017). Methods for genetic transformation of filamentous fungi. *Microbial Cell Factories*, *16*(1), 168.
- Liu, Y., Cusano, A. M., Wallace, E. C., Mekmouche, Y., Ullah, S., Robert, V., et al. (2014). Characterization of C-terminally engineered laccases. *International Journal of Biological Macromolecules*, *69*, 435–441.
- Mate, D. M., & Alcalde, M. (2015). Laccase engineering: From rational design to directed evolution. *Biotechnology Advances*, *33*, 25–40.
- Mate, D. M., & Alcalde, M. (2017). Laccase: A multi-purpose biocatalyst at the forefront of biotechnology. *Microbial Biotechnology*, *10*, 1457–1467.
- Mate, D., García-Burgos, C., García-Ruiz, E., Ballesteros, A. O., Camarero, S., & Alcalde, M. (2010). Laboratory evolution of high-redox potential laccases. *Chemical Biology*, *17*, 1030–1041.

- McFarland, J. M., & Francis, M. B. (2005). Reductive alkylation of proteins using iridium catalyzed transfer hydrogenation. *Journal of the American Chemical Society*, *127*, 13490–13491.
- Mekmouche, Y., Schneider, L., Rousselot-Pailley, P., Faure, B., Simaan, A. J., Bochot, C., et al. (2015). Laccases as palladium oxidases. *Chemical Science*, *6*, 1247–1251.
- Mekmouche, Y., Zhou, S., Cusano, A. M., Record, E., Lomascolo, A., Robert, V., et al. (2014). Gram-scale production of a basidiomycetous laccase in *Aspergillus niger*. *Journal of Bioscience and Bioengineering*, *117*, 25–27.
- Meyer, H.-P., Eichhorn, E., Hanlon, S., Lütz, S., Schürmann, M., Wohlgemuth, R., et al. (2013). The use of enzymes in organic synthesis and the life sciences: Perspectives from the Swiss Industrial Biocatalysis Consortium (SIBC). *Catalysis Science & Technology*, *3*, 29–40.
- Mikolasch, A., & Schauer, F. (2009). Fungal laccases as tools for the synthesis of new hybrid molecules and biomaterials. *Applied Microbiological and Biotechnology*, *82*, 605–624.
- Milton, R. D., & Minteer, S. D. (2017). Direct enzymatic bioelectrocatalysis: Differentiating between myth and reality. *Journal of the Royal Society Interface*, *14*(131), 20170253.
- Nestl, B. M., Hammer, S. C., Nebel, B. A., & Hauer, B. (2014). New generation of biocatalysts for organic synthesis. *Angewandte Chemie International Edition*, *53*, 3070–3095.
- Oldenburg, K. R., Vo, K. T., Michaelis, S., & Paddon, C. (1997). Recombination-mediated PCR-directed plasmid construction in vivo in yeast. *Nucleic Acids Research*, *25*, 451–452.
- Orr-Weaver, T. L., Szostak, J. W., & Rothstein, R. J. (1983). Genetic applications of yeast transformation with linear & gapped plasmids. *Methods in Enzymology*, *101*, 228–245.
- Pardo, I., & Camarero, S. (2015). Laccase engineering by rational and evolutionary design. *Cellular and Molecular Life Sciences*, *72*, 897–910.
- Pistone, L., Ottolina, G., De, S., Romero, A. A., Martins, L. O., & Luque, R. (2016). Encapsulated laccases for the room-temperature oxidation of aromatics: Towards synthetic low-molecular-weight lignins. *ChemSusChem*, *9*, 756–762.
- Pita, M., Gutierrez-Sanchez, C., Olea, D., Velez, M., Garcia-Diego, C., Shleev, S., et al. (2011). High redox potential cathode based on laccase covalently attached to gold electrode. *Journal of Physical Chemistry C*, *115*, 13420–13428.
- Pita, M., Mate, D. M., Gonzalez-Perez, D., Shleev, S., Fernandez, V. M., Alcalde, M., et al. (2014). Bioelectrochemical oxidation of water. *Journal of the American Chemical Society*, *136*, 5892–5895.
- Punt, P. J., & van den Hondel, C. A. (1992). Transformation of filamentous fungi based on hygromycin B and phleomycin resistance markers. *Methods in Enzymology*, *216*, 447–457.
- Qiu, H., Xu, C., Huang, X., Ding, Y., Qu, Y., & Gao, P. (2009). Immobilization of laccase on nanoporous gold: Comparative studies on the immobilization strategies and the particle size effects. *Journal of Physical Chemistry C*, *113*, 2521–2525.
- Record, E., Punt, P. J., Chamkha, M., Labat, M., van den Hondel, C. A. M. J. J., & Asther, M. (2002). Expression of the *Pycnoporus cinnabarinus* laccase gene in *Aspergillus niger* and characterization of the recombinant enzyme. *European Journal of Biochemistry*, *269*, 602–609.
- Riva, S. (2006). Laccases: Blue enzymes for green chemistry. *Trends in Biotechnology*, *24*, 219–226.
- Robert, V., Mekmouche, Y., Rousselot-Pailley, P., & Tron, T. (2011). Engineering laccases: In search for novel catalysts. *Current Genomics*, *12*, 123–129.
- Robert, V., Monza, E., Tarrago, L., Sancho, F., De Falco, A., Schneider, L., et al. (2017). Probing the surface of a laccase for clues towards the design of chemo-enzymatic catalysts. *ChemPlusChem*, *82*, 607–614.

- Rodgers, C. J., Blanford, C. F., Giddens, S. R., Skamnioti, P., Armstrong, F. A., & Gurr, S. J. (2010). Designer laccases: A vogue for high-potential fungal enzymes? *Trends in Biotechnology*, 28, 63–72.
- Sambrook, J., Fritsch, E. F., & Maniatis, T. (1989). *Molecular cloning: A laboratory manual* (2nd ed.). Cold Spring Harbor, NY: Cold Spring Harbor Laboratory.
- Schneider, L., Mekmouche, Y., Rousselot-Pailley, P., Simaan, A. J., Robert, V., Réglie, M., et al. (2015). Visible-light-driven oxidation of organic substrates with dioxygen mediated by a [Ru(bpy)₃](2+)/laccase system. *ChemSusChem*, 8, 3048–3051.
- Schwizer, F., Okamoto, Y., Heinisch, T., Gu, Y., Pellizzoni, M. M., Lebrun, V., et al. (2018). Artificial metalloenzymes: Reaction scope and optimization strategies. *Chemical Reviews*, 118, 142–231.
- Shleev, S., Christenson, A., Serezhenkov, V., Burbaev, D., Yaropolov, A., Gorton, L., et al. (2005). Electrochemical redox transformations of T1 and T2 copper sites in native *Trametes hirsuta* laccase at gold electrode. *Biochemistry Journal*, 385, 745–754.
- Shleev, S., Pita, M., Yaropolov, A. I., Ruzgas, T., & Gorton, L. (2006). Direct heterogeneous electron transfer reactions of *Trametes hirsuta* laccase at bare and thiol-modified gold electrodes. *Electroanalysis*, 18, 1901–1908.
- Simaan, A. J., Mekmouche, Y., Herrero, C., Moreno, P., Aukauloo, A., Delaire, J. A., et al. (2011). Photoinduced multielectron transfer to a multicopper oxidase resulting in dioxygen reduction into water. *Chemistry—A European Journal*, 17, 11743–11746.
- Singh, R. K., Tiwari, M. K., Singh, R., & Lee, J. K. (2013). From protein engineering to immobilization: Promising strategies for the upgrade of industrial enzymes. *International Journal of Molecular Sciences*, 14, 1232–1277.
- Solomon, E. I., Heppner, D. E., Johnston, E. M., Ginsbach, J. W., Cirera, J., Qayyum, M., et al. (2014). Copper active sites in biology. *Chemical Reviews*, 114, 3659–3853.
- Solomon, E. I., Szilagy, R. K., DeBeer George, S., & Basumallick, L. (2004). Electronic structures of metal sites in proteins and models: Contributions to function in blue copper proteins. *Chemical Reviews*, 104, 419–458.
- Tarrago, L., Modolo, C., Yemloul, M., Robert, V., Rousselot-Pailley, P., & Tron, T. (2018). Controlling the polymerization of coniferyl alcohol with cyclodextrins. *New Journal of Chemistry*, 42, 11770–11775.
- Tron, T. (2013). Laccases. In R. H. Kretsinger, V. N. Uversky, & E. A. Permyakov (Eds.), *Encyclopedia of metalloproteins* (pp. 1066–1070). New York: Springer.
- van Hartingsveldt, W., Mattern, I. E., van Zeijl, C. M., Pouwels, P. H., & van den Hondel, C. A. (1987). Development of a homologous transformation system for *Aspergillus niger* based on the pyrG gene. *Molecular Genetics & Genomics*, 206, 71–75.
- Witayakran, S., & Ragauskas, A. J. (2009). Synthetic applications of laccase in green chemistry. *Advanced Synthesis & Catalysis*, 351, 1187–1209.
- Zhou, Z., & Hartmann, M. (2013). Progress in enzyme immobilization in ordered mesoporous materials and related applications. *Chemical Society Reviews*, 42, 3894–3912.
- Zucca, P., Cocco, G., Sollai, F., & Sanjust, E. (2016). Fungal laccases as tools for biodegradation of industrial dyes. *Biocatalysis*, 1, 82–108.

Further reading

- Bessa, D., Pereira, F., Moreira, R., Johansson, B., & Queirós, O. (2012). Improved gap repair cloning in yeast: Treatment of the gapped vector with Taq DNA polymerase avoids vector self-ligation. *Yeast*, 29, 419–423.
- Lippard, S. J. (2006). The inorganic side of chemical biology. *Nature Chemical Biology*, 2, 504–507.

- Mezard, C., & Nicolas, A. (1994). Homologous, homeologous, and illegitimate repair of double-strand breaks during transformation of a wild-type strain and a rad52 mutant strain of *Saccharomyces cerevisiae*. *Molecular and Cellular Biology*, *14*, 1278–1292.
- Mezard, C., Pompon, D., & Nicolas, A. (1992). Recombination between similar but not identical DNA sequences during yeast transformation occurs within short stretches of identity. *Cell*, *70*, 659–670.
- Solomon, E. I., Baldwin, M. J., & Lowery, M. D. (1992). Electronic structures of active sites in copper proteins: Contributions to reactivity. *Chemical Reviews*, *92*, 521–542.
- Yang, J., Li, W., Bun, N. T., Deng, X., Lin, J., & Ye, X. (2017). Laccases: Production, expression regulation, and applications in pharmaceutical biodegradation. *Frontiers in Microbiology*, *8*, 832.
- Zumarraga, M., Camarero, S., Shleev, S., Martinez-Arias, A., Ballesteros, A., Plou, F. J., et al. (2008). Altering the laccase functionality by in vivo assembly of mutant libraries with different mutational spectra. *Proteins*, *71*, 250–260.

Effecteurs de la sélectivité dans les réactions catalysées par la laccase

Résumé: Les laccases sont des oxydases multi-cuivre produites par des champignons, des bactéries ainsi que des plantes et des insectes. Ces enzymes couplent la réduction du dioxygène à quatre électrons/quatre protons à l'oxydation de divers substrats, soit des molécules organiques, soit des ions métalliques. Largement utilisés dans diverses applications biotechnologique pour leurs propriétés rédox, les laccases sont, en retour, peu sélectives en ce qui concerne l'oxydation de leurs substrats. Dans cette étude, nous nous sommes concentrés sur les moyens d'apporter une certaine sélectivité dans les réactions catalysées par la laccase en utilisant des effecteurs. Une protéine dirigeante de plante (*AtDIR6*) a d'abord été étudiée comme modèle naturel. La DP *AtDIR6* a la capacité de diriger la biosynthèse stéréosélective du (-) - pinorésinol à partir d'un monolignol. Ici, nous avons exploré la spécificité de substrat de *AtDIR6* en utilisant des substrats analogues à l'alcool coniférylique avec des variations sur la chaîne allylique. La spectroscopie RPE a été utilisée pour sonder la stabilisation des radicaux par *AtDIR6*. Finalement, nous avons étudié la possibilité que le radical de l'alcool puisse former des adduits covalents avec *AtDIR6*. Nos résultats fournissent non seulement plus d'informations sur le mécanisme des DP, mais ouvrent également de nouvelles possibilités pour l'utilisation des DP dans le domaine de la chimie verte. Dans une seconde partie, des nanoparticules magnétiques (MNP) fonctionnalisées en surface ont été utilisées comme mimes bio-inspirés de DP. Deux variants de laccase offrant deux orientations opposées du site d'oxydation du substrat ont été immobilisées sur des MNP portant différents groupements fonctionnels (ex. un aldéhyde, un azide) à la surface des particules. L'activité des laccases orientées à la surface a été comparée à deux substrats modèles différents: l'ABTS et l'alcool coniférylique. A travers cette étude, nous apportons des preuves que l'activité d'une enzyme non sélective peut être fortement biaisée par le micro-environnement proposé autour de son site actif. Nos travaux peuvent constituer la base de nouvelles recherches visant à établir un système efficace d'oxydation contrôlées.

Mots-clés: laccase, protéine dirigeante, *AtDIR6*, nanoparticules magnétiques, immobilisation, sélectivité, effecteurs.

Effectors of selectivity in laccase catalyzed reactions

Abstract: Laccases are multicopper oxidases produced by fungi, bacteria as well as plants and insects. These enzymes are coupling the neat four electrons/four protons reduction of dioxygen to the oxidation of various substrates, either organic or metal ions. Widely used in a variety of biotechnology applications for their redox properties, laccase are, in return, poorly selective as regards their substrates oxidation. In this study we focused on ways to bring some selectivity in laccase catalyzed reactions using effectors. A plant dirigent protein (*AtDIR6*) was studied first as a natural model. *AtDIR6* has the ability to direct the stereoselective biosynthesis of the (-)-pinoresinol from a monolignol. Here, we explored the substrate specificity of *AtDIR6* using substrates analogue to coniferyl alcohol with variations on the allylic chain. EPR spectroscopy was used to probe the stabilization of radicals by *AtDIR6*. Eventually, we studied the possibility of the coniferyl alcohol radical to form covalent adducts onto *AtDIR6*. Our results not only provide more insights into DP mechanism, but also open new possibilities for the application of DP in the field of green chemistry. In a second part, surface functionalized magnetic nanoparticles (MNPs) were used as bio-inspired mimics of DPs. Two laccase variants offering two opposite orientations of the substrate oxidation site were immobilized onto MNPs harboring different chemical functional groups (e.g. aldehyde, azide) at the particles surface. The activity of the surface oriented laccases was compared with two different model substrates: ABTS and coniferyl alcohol. Through this study we bring evidences that the activity of a non-selective enzyme can be substantially biased by the micro-environment proposed around its active site. Our work can be the basis for new researches to establish an efficient system for controlled oxidations.

Keywords: laccase, dirigent protein, *AtDIR6*, magnetic nanoparticles, immobilization, selectivity, effectors